Université de Montréal

The Roles of TL1A and Pno1 in the Pathogenesis of Rheumatoid Arthritis

par
Xuehai Wang

Département de Médecine
Faculté de Médecine

Thèse présentée à la Faculté des études supérieures
en vue de l'obtention du grade de
Philosophiae Doctor (Ph.D.)
en Sciences Biomédicales

Octobre 2013

Université de Montréal

Faculté des études supérieures et postdoctorales

Cette thèse intitulée:

The Roles of TL1A and Pno1 in the Pathogenesis of Rheumatoid Arthritis

Présentée par :

Xuehai Wang

a été évaluée par un jury composé des personnes suivantes :

Dr. Mohit Kapoor	Président-rapporteur
Dr. Jiangping Wu	Directeur de recherché
Dr. Hongyu Luo	Codirectrice
Dr. Marie Sarfati	Membre du jury
Dr. Joyce Rauch	Examinateur externe
Dr. Muhammad Zafarullah	Représentant du doyen de la Faculté

RÉSUMÉ

La polyarthrite rhumatoïde (PR) est une maladie auto-immune chronique. Elle est caractérisée par une inflammation persistante touchant de multiples petites articulations, causant douleurs, rougeurs, gonflements et déformations. Des études menées auprès de patients et d'animaux ont démontré que certains auto-anticorps, cytokines et enzymes tissue-déstructives sont des médiateurs importants dans le développement de la PR. Au cours des deux dernières décennies, les traitements de fond (DMARDs en anglais) ont été démontrés très efficaces pour traiter la PR. D'autre part, des effets secondaires ont été rapportés pour ces traitements, par exemple l'augmentation du risque d'infections opportunistes. L'objectif de ce travail est d'acquérir des connaissances sur le rôle du TL1A (TNF-like molécule 1 A; TNFSF15) et son partenaire Nob1 (Pno1 ; YOR145c) dans la pathogenèse de la PR afin de découvrir de nouveaux médicaments contre ces molécules dans l'avenir.

TL1A est un membre de la famille du TNF. Il déclenche des signaux co-stimulateurs via le récepteur de mort 3 (DR3) et induit la prolifération ainsi que la production des cytokines pro inflammatoires par les lymphocytes. Des données multiples suggèrent l'implication de la cascade TL1A-DR3 dans plusieurs maladies auto-immunes. Donc, nous avons proposé les hypothèses suivantes:1) la production locale de TL1A dans les articulations est un composant d'un cercle vicieux qui aggrave la PR; 2) dans la PR, la production de TL1A dans les organes lymphoïde augmente la production d'auto-anticorps pathogénique. Au cours de ce travail, nous avons démontré que la TL1A aggrave la maladie chez les souris où l'arthrite a été induite par le collagène (AIC). Par ailleurs, nous avons constaté que l'expression de TL1A est élevée dans les tissus atteints de PR ainsi que dans les ganglions lymphatiques drainant de la souris AIC. Mécaniquement, nous avons découvert que la TL1A est induite par le TNF-α et IL-17 produits par les cellules T *in vitro*. Ces résultats montrent directement que les TL1A-DR3 jouent un rôle essentiel dans la pathogenèse de la PR. De plus, afin de poursuivre notre étude, la TL1A a été génétiquement supprimée dans les souris (TL1A KO). Nous avons montré que les souris TL1A KO n'ont aucune anomalie apparente et aucun dysfonctionnement du système immunitaire dans des conditions normales. Cependant, ces souris manifestent des AIC améliorées et une réduction significative des niveaux d'anticorps, anti-collagène du type II

dans le sérum. Nous avons trouvé que les ganglions lymphatiques de drainage (dLNs) de souris KO étaient plus petites avec une cellularité inférieure comparativement aux souris WT de 14 jours après l'immunisation. De plus, nous avons découvert que le DR3 a été exprimé par les cellules plasmatiques dans l'étape de la différenciation terminale et ces cellules surviennent mieux en présence de TL1A. La conclusion de cette étude apporte des nouvelles connaissances sur le rôle de TL1A qui amplifie les réponses humorales d'AIC. Nous avons suggéré que TL1A pourrait augmenter la réponse d'initiation d'anticorps contre collagène II (CII) ainsi que prolonger la survie des cellules plasmatiques.

Une autre molécule qui nous intéresse est Pno1. Des études antérieures menées chez la levure ont suggéré que Pno1 est essentielle pour la néogénèse du protéasome et du ribosome Le protéasome étant crucial pour la différenciation terminale des cellules plasmatiques pendant les réponses humorales chez les mammifères, nous avons donc supposé que Pno1 joue un rôle dans la production d'anticorps pathogenique dans la PR via la voie du protéasome. Nous avons donc généré des souris génétiquement modifiées pour Pno1 afin d'étudier la fonction de Pno1 *in vivo*. Cependant, une mutation non-sens dans le Pno1 provoque une létalité embryonnaire à un stade très précoce chez les souris. D'autre part, une réduction de 50% de Pno1 ou une surexpression de Pno1 n'ont aucun effet ni sur le fonctionnent des cellules T et B, ni sur les activités du protéasome ainsi que sur la réponse humorale dans l'AIC. Ces résultats suggèrent que Pno1 est une molécule essentielle sans redondance. Par conséquent, il n'est pas une cible appropriée pour le développement de médicaments thérapeutiques.

En conclusion, nos études ont révélé que la TL1A n'est pas essentielle pour maintenir les fonctions du système immunitaire dans des conditions normales. En revanche, il joue un rôle critique dans la pathogenèse de la PR en favorisant l'inflammation locale et la réponse humorale contre des auto-antigènes. Par conséquent, une inhibition de la TL1A pourrait être une stratégie thérapeutique pour le traitement de la PR. Au contraire, Pno1 est essentiel pour la fonction normale des cellules. Une délétion totale pourrait entraîner des conséquences graves. Il n'est pas une cible appropriée pour développer des médicaments de la PR.

Mots-clés: l'arthrite rhumatoïde, TL1A, DR3, inflammation, les cytokines, les cellules plasmatiques, Pno1, protéasome

ABSTRACT

Rheumatoid Arthritis (RA) is a chronic autoimmune disease characterized by persistent inflammation of multiple small joints, which manifests pain, redness, swelling, and deformation. Studies with patients and animal models have found that autoantibodies, cytokines and tissue-destructive enzymes are important mediators of the pathogenesis of RA. In the past two decades, biologic disease-modifying antirheumatic drugs (DMARDs) have achieved great success in the treatment of RA. On the other hand, they are also associated with adverse effect like increasing the chance of opportunistic infections. The aim of present work was to investigate the roles of TNF-like molecule 1A (TL1A; TNFSF15) and partner of Nob1 (Pno1; YOR145c) in the pathogenesis of RA for developing novel drugs based on these molecules in the future.

TL1A is a member of the TNF superfamily. It triggers costimulatory signals though death receptor 3 (DR3) and induces the proliferation and pro-inflammatory cytokine production in lymphocytes. Multiple lines of evidence suggest the implication of TL1A-DR3 signaling in several autoimmune diseases. Therefore, We hypothesized that 1) local TL1A production in the joints is a component of a vicious circle aggravating RA; 2) in RA, TL1A production in lymphoid organs enhances pathogenic autoantibody production. We demonstrated that the TL1A aggravates disease in murine collagen-induced arthritis (CIA). Moreover, we found elevated TL1A expression in RA-affected tissues, as well as in the draining lymph nodes (dLNs) of CIA mice. Mechanistically, we discovered that TL1A induces TNF-α and IL-17 production by T cells *in vitro*. These findings provided direct evidence that TL1A-DR3 signaling plays a critical role in the pathogenesis of RA. TL1A knockout (TL1A KO) mice were generated to further our study. We showed that TL1A KO mice have no visual anomaly, and no malfunction of immune system under a normal circumstance. However, they display ameliorated CIA and significantly reduced anti-Collagen II antibody levels in sera. We found that the draining lymph nodes (dLNs) from KO mice were smaller in size and lower in cellularity compared with their WT counterparts 14 days after immunization. Furthermore, we discovered that terminally differentiated plasma cells express DR3 and they survive better in the presence of TL1A. Our findings in this study present novel knowledge about the role of

TL1A promoting the humoral responses in CIA; we suggest that TL1A could elevate the initial Ab response against Collagen II (CII), as well as prolong the survival of plasma cells producing such pathogenic Abs.

Another molecule we were interested in present study is Pno1. Previous studies conducted in yeast suggest that Pno1 is essential to the proteasome and ribosome neogenesis. Since proteasome is crucial for the terminal differentiation of plasma cells during the humoral response in mammals, we hypothesized that Pno1 plays a role in the pathogenic Ab production in RA by affecting the proteasome assembly. For this purpose, we generated *pno1* gene-modified mice to investigate the function of Pno1 *in vivo*. However, null-mutation in *pno1* causes embryonic lethality in mice at a very early stage. On the other hand, a half amount reduction or overexpression of Pno1 is neither harmful nor useful to the T and B cell function, proteasome activities as well as humoral immune responses in CIA. These findings suggest that Pno1 is a vital molecule with no redundancy and is absolutely required for cell function, but animals can function normally with a small fraction of the normal Pno1 expression level. Thus, it might not be an appropriate target for developing therapeutic drugs.

In conclusion, our studies suggest that TL1A seems not essential in maintaining the immune functions under normal circumstances, but plays critical roles in the pathogenesis of RA by promoting local inflammation and humoral immune responses against autoantigens. Therefore, inhibiting TL1A could be a propitious therapeutic strategy for treating RA. In contrast, Pno1 is vital to the normal cell function, and its disruption could cause disastrous consequences. Thus, it might not be a good drug target for treating RA.

Keywords: Rheumatoid arthritis, TL1A, DR3, inflammation, cytokine, plasma cells, Pno1, proteasome

TABLE OF CONTENTS

LIST OF TABLES

CHAPTER 1

CHAPTER 4

APPENDIX

LIST OF FIGURES

CHAPTER 1

CHAPTER 2

CHAPTER 3

CHAPTER 4

APPENDIX

This thesis is dedicated to:

My parents and my wife, for their unconditional love and support.

ACKNOWLEGEMENTS

First of all, I would like to express my sincerest appreciation to my supervisor, Dr. Jiangping Wu and co-supervisor Dr. Hongyu Luo, for giving me the opportunity to further my study here and sharing their passion for science. My doctoral researches and this thesis could never have been done without their invaluable support, constant encouragement and untiring guidance.

I would also like to thank all my colleagues; Dr. Terra Rafik, Dr. Diep Pham, Dr. Hector Valderrama, Dr. Bing Han, Dr. Jianning Mao, Dr. Zenghui Wu, Wei Jin, Yujia Wang and Yan Hu, for their warmhearted help, suggestions and joyful crazy ideas in every lab meetings.

Many thanks to Dr. Jun Zhang, Dr. Hassan Fahmi, Dr. Martin Marcinkiewicz, Dr. Shijie Qi, Dr. Tao Wu, Dr. Alain Lamarre, Dr. Yaned Gatain, Dr. Maxime Bouchard, Dr. Michel Tremblay, Dr. Noriko Uetani, Dr. Silva Hanissian and all for their splendid collaborations.

Finally, I would like to extend my deepest gratitude to my jury members for evaluating this thesis and for their insightful comments.

Xuehai Wang, September 2013

STATEMENT OF AUTHORSHIP

Here is a statement regarding the contribution of coauthors and myself to the three papers included in this thesis.

Chapter 2:

Zhang J, **Wang X (Equal contributor)**, Fahmi H, Wojcik S, Fikes J, Yu Y, Wu J and Luo H. (2009) Role of TL1A in the Pathogenesis of Rheumatoid Arthritis. ***The Journal of Immunology*** 183, 5350–5357

Conceived and designed the experiments: JZ XW HL JW. Performed the experiments: JZ XW SW JF YY HL. Analyzed the data: JZ XW YY HL. Contributed reagents/materials/analysis tools HF Wrote the paper: XW JW. (XW conceived, designed, performed and analyzed all the experiments in Figure 4a, 4b, 5 and 6)

Chapter 3:

Wang X, Hu Y, Charpentier T, Lamarre A, Qi S, Wu J, Luo H. (2013) TNF-like ligand 1A (TL1A) gene knockout leads to ameliorated collagen-induced arthritis in mice: implication of TL1A in humoral immune responses. ***The Journal of Immunology*** 191, 5420-5429.

Conceived and designed the experiments: XW HL JW. Performed the experiments: XW YH TC SQ. Analyzed the data: XW AL WJ HL. Wrote the paper: XW JW.HL

Chapter 4:

Wang X, Wu T, Hu Y, Marcinkiewicz M, Qi S, et al. (2012) Pno1 Tissue-Specific Expression and Its Functions Related to the Immune Responses and Proteasome Activities. ***PLoS ONE*** 7: e46093.

Conceived and designed the experiments: XW HL JW. Performed the experiments: XW TW YH MM SQ HV HL. Analyzed the data: XW TW YH MM HV HL. Wrote the paper: XW JW.

Appendix-1:

Wang X, Marcinkiewicz M, Gatain Y, Bouchard M, Mao J, Tremblay M, Uetani N, Hanissian S, Qi S, Wu J, Luo H. (2013) Investigation of Tissue-Specific Expression and Functions of MLF1-IP during Development and in the Immune System. ***PLoS ONE*** 8:e63783

Conceived and designed the experiments: XW MB MT NU JW HL. Performed the xperiments: XW MM YG JM SQ. Analyzed the data: XW MM YG JM JW HL. Contributed reagents/materials/analysis tools: SH. Wrote the paper: XW JW HL.

Appendix-2:

Terra R, **Wang X (first co-author)**, Hu Y, Charpentier T, Lamarre A, Zhong M, Sun H, Mao J, Qi S, Luo H, Wu J. (2013) To Investigate the Necessity of STRA6 Upregulation in T Cells during T Cell Immune Responses. ***PLoS ONE*** 8:e82808

Conceived and designed the experiments: RT XW YH SH HL JW. Performed the experiments: RT XW YH JM SQ. Analyzed the data: RT XW AL MZ HS JM JW HL. Wrote the paper: RT XW YH HL JW. (XW conceived, designed, performed and analyzed all the experiments in Figure 2,4 and 5)

LIST OF ABBREVIATIONS

ACR	American College of Rheumatology
ACPA	Anti-cyclic citrullinated peptidea antibody
AIA	Antigen-induced arthritis
ADAMTS	A Disintegrin And Metalloproteinase with Thrombospondin Motifs
APRIL, TNFSF13	A proliferation-induced ligand
BAFF, TNFSF13B	B cell-activation factor
BCMA	B cell maturation Ag
BMDC	Bone marrow-derived dendritic cell
CD	Chron's disease
CFA	Complete Freund’s adjuvant
cFib	Citrullinated fibrinogen
CHOP	C/EBP homologous protein
CHX	Cycloheximide
CIA	Collagen-Induced Arthritis
CII	Collagen II
COX	Cyclooxygenase
CP	Core particle
CRP	C-reactive protein
CTLA4	Cytotoxic T-lymphocyte antigen 4
DCs	Dendritic cells
dLN	Draining lymph node
DMARDs	Disease-modifying anti-rheumatic drugs

DR3, TNFRSF25	Death receptor 3
DSS	Chronic-dextran sodium sulfate
EAA	Experimental allergic asthma.
EAE	Experimental Autoimmune Encephalomyelitis
EAMG	Experimental autoimmune myasthenia gravis
ER	Endoplasmic reticulum
ESR	Erythrocyte sedimentation rate
EULAR	European League Against Rheumatism
FADD	Fas-associated death domain-containing molecule
FDA	Food and drug administration
FDC	Follicular dendritic cell
FGL	Fibrinogen-like protein
FLICE	FADD-like ICE
FLIP	FLICE-inhibitory protein
G-CSF	Granulocyte-colony-stimulating factor
GAG	Glycosaminoglycans
GC	Germinal center
GPI	Glucose-6-phosphate isomerase
HUVEC	Human umbilical vein endothelial cell
HVEM	Herpesvirus entry mediator
IBD	Inflammatory bowel disease
IC	Immune complexes
ICE	Interleukin-1β-converting enzyme
IFA	Incomplete Freund’s adjuvant

iNOS	Inducible nitric oxide synthase
KO	Knockout
LAG	Lymphocyte activation gene
LCMV	Lymphocytic choriomenigitis
LIF	Leukemia inhibitory factor
LLPC	Long-lived PCs
LP	Lamina propria
LPMC	Lamina propria mononuclear cells
LT	Lymphotoxin
MCF	Mononuclear cell factor
MCMV	Murine cytomegalovirus
MCs	Mast cells
MDC	Monocyte-derived DC
mDC	Myeloid DCs
MM	Multiple myeloma
MMP	Matrix metalloproteinase
mRNA	Messenge RNA
mTOR	Mammalian target of rapamycin
MTX	Methotrexate
NASIDs	Non-steroidal anti-inflammatory drugs
NF-κB	Nuclear factor κB
NO	Nitro oxide
NTPDase-1, CD39	Triphosphate diphosphohydrolase-1
ODF	Osteoclast differentiation factor

OSM	Oncostatin M
PAC	Proteasome-assembling chaperones
PADI4	Encoding type IV peptidylarginine deiminase
pDCs	Plasmacytoid DCs
PDGF,	Platelet-derived growth factor
PNA	Peanut agglutinin
PG	Proteoglycan
PGE2	Prostaglandin E2
PGIA	Proteoglycan induced arthritis
PI	Proteasome inhibitors
PIGF	Placenta growth factor
PMN,	Polymorphonuclear
Pno1	Partner of Nob1
PTPN22	Protein tyrosine phosphatase, non receptor 22
RANKL	Receptor activator of NF-κB ligand
RF	Rheumatoid factor
RF	Rheumatoid factor
RIP	Receptor interaction protein
ROI	Reactive oxygen intermediate
RP	Regulatory particle
SF	Synovial fibroblast
SLPCs	Short-lived PCs
SNPs	Single nucleotide polymorphisms
STAT4	Signal Transducer and Activatorof Transcription protein 4

SUMO	Small ubiquitin-like modifier
SZW	Streptococcal cell wall
TACI	Transmembrane activator and calcium modulator ligand interactor
TCR	T cell receptor
TEC	Tubular epithelial cell
Tfh	T follicular helper cell
TL1A	TNF-like ligand 1A
TLR4	Toll-like receptor 4
TRADD	TNFR-1-associated death domain protein
UC	Ulcertive colitis
UMP1	Ubiquitin-mediated proteolysis 1
UPR	Unfolded protein response
VEGF	Vescular endothelial cell growth factor
VEGI	Vascular endothelial growth inhibitor
WT	Wild type

CHAPTER 1 INTRODUCTION

1.1 Overview of Rheumatoid Arthritis

Rheumatoid arthritis (RA) is the most common inflammatory arthritis, manifesting redness, swelling, tenderness and destruction of the joint tissues (Aletaha et al., 2010). It is caused by chronic immune system disorder, which primarily affects the joints and their surrounding tissues, but also affects many other parts of our body (Firestein, 2003). Tissues and organs involved in RA complications include: the skin (rheumatoid nodules, ulcers and rash), eyes (scleritis, Sjogren's syndrome), cardiovascular system (pericarditis, heart attack and stroke), circulation system (vasculitis, anemia, Felty's syndrome), kidney (renal amyloidosis) and lung (collapsed lungs, plural effusion and pulmonary hypertension). There is no cure for RA, but current treatment can delay the disease progression and prevent the joint damage (Upchurch and Kay, 2012).

1.1.1 Diagnosis and Classifications of RA

The original diagnostic criteria for RA were published by the Committee of the American Rheumatism Association in 1956, and quickly updated by a revised version after two years (Committee of the American Rheumatism Association, 2008; Ropes et al., 1957). The criteria was again revised and published in 1987, formulated from computerized analysis of RA patients and healthy controls, with fewer criteria, improved sensitivity and specificity (Arnett et al., 1988). In 2010, a joint group of American College of Rheumatology (ACR) and European League Against Rheumatism (EULAR) published new classification criteria, aiming to differentiate RA patients at early-stage (Aletaha et al., 2010). It is noteworthy that the criteria in this version were designed for better classification of RA patients for clinical studies, rather than for a diagnostic purpose (Aletaha et al., 2010). Several studies have compared them with the 1987 diagnostic criteria and found that the 2010 criteria are more robust and sensitive, but slightly less specific (Britsemmer et al., 2011; Radner et al.; Van der Linden and Knevel, 2011). More evidence remain to be collected to determine whether these new criteria are appropriate to be used for diagnosis.

Table 1.1 Comparison of 1987 and 2010 versions of RA criteria

Criterion	Versions	
	1987	**2010**
Joint involvement	Joint type and quantity	Joint type and quantity
Radiographic changes	Included	Included
Serology	RF	RF, ACPA
Acute-phase reactants	N/A	CRP, ESR
Duration of symptoms	N/A	Included
Rheumatoid nodules	Included	N/A

RF: rheumatoid factor; ACPA: anti-cyclic citrullinated peptide; CRP: C-reactive protein; ESR: erythrocyte sedimentation rate

1.1.2 Epidemiology of RA

RA occurs in 0.5-1% of the general population (Firestein, 2003). Several epidemiological studies have shown variations of disease incidence across populations. One half to 1.1% of the population in North America and Northern Europe are affected by RA, while lower prevalence of 0.3-0.7% is found in Southern Europe (Tobón et al., 2010). The prevalence of RA in East Asia is similar to those in Southern Europe. Developing countries in South Asia, Middle East and Africa have lowest prevalence of RA, which is around 0.38% (Hammoudeh et al., 2013; Tobón et al., 2010; Zeng et al., 2008). The low prevalence of RA found in developing countries may not reflect the actual situations due to the limited prevalence studies and incomplete data collection (Alamanos et al., 2006). Prevalence and incidence of RA also display a gender-specific disparity, with approximately 2-4 fold more RA patients and higher incidence among women than men in different populations (Alamanos et al., 2006; Hammoudeh et al., 2013). Multiple studies have suggested that the average onset age of RA is rising (Gabriel et al., 1999; Imanaka et al., 1997; O et al., 1996). At the same time, there are progressive decreases in both incidence and prevalence of RA across several different regions (Doran et al., 2002; Jacobsson et al., 1994; Kaipiainen-Seppanen et al., 1996; Kaipiainen-Seppanen and Kautiainen, 2006; O and K, 2000; Shichikawa et al., 1999). On the other hand, despite our better knowledge of pathogenic mechanisms and great improvement of the RA management, the mortality rate in RA patients seems not decreasing in the last few decades (Myasoedova et al., 2010).

1.1.3 Risk Factors of RA

1.1.3.1 Genetic Factors

Various evidence from migration studies, familial clustering studies and twin studies have indicated the importance of genetic factors to the susceptibility, severity and responsiveness to treatment of RA (Criswell et al., 1998; John and Worthington, 2001; Lin et al., 1999; Plant et al., 2011). From genetic association studies, growing numbers of RA genetic risk factors have been uncovered in the past decades (Huizinga, 2003; McInnes and Schett, 2007; van der Helm-van Mil et al., 2005). The first and most well-established disease locus is HLA-DRB1, alleles in HLA-DRB1 region containing "shared epitope" confer disease risk, and account up to one third of the total genetic risk of susceptibility of RA (Cornélis et al., 1998; Gregersen et al., 1987). To date, most potential risk genes are found in the genes encoding molecules important to immune regulations, such as NF-κB, PTPN22 (protein tyrosine phosphatase, non receptor 22), CTLA4 (cytotoxic T-lymphocyte antigen 4), STAT4 and CD40, as well as those encoding pro-inflammatory cytokines (IL-10, IL-1β, IL-2 and IL-21) (Begovich et al., 2004; Cantagrel et al., 1999; Daha et al., 2009; Eskdale et al., 1998; Li et al., 2012b; Orozco et al., 2010; Plenge et al., 2007; Remmers et al., 2007). Moreover, single nucleotide polymorphisms (SNPs) discovered in sequence encoding type IV peptidylarginine deiminase (PADI4), an enzyme believed to produce autoantigens by posttranslationally converting arginine residues to citrulline, are also reported to have association with susceptibility to RA(Suzuki et al., 2003). It is worth mentioning that many of risk genes listed above are also related to other autoimmune diseases, such as Type 1 diabetes and systemic lupus erythematosus (SLE), implicating the shared mechanisms in these common autoimmune disease (Begovich et al., 2004; Remmers et al., 2007). In addition, polymorphisms proved to be the risk factors in one population are not necessary to be the risk factors in other populations (Barton et al., 2004; Suzuki et al., 2003).

1.1.3.2 Gender and Hormonal Factors

Gender is probably the most important risk factors for RA. Since females have higher risk of developing RA, it is conceivable that sex hormones might also have a role in RA. Early study has found that RA patients have decreased levels of serum testosterone; the reduction of serum

testosterone levels occur prior to the onset of RA (Pikwer et al., 2013; Spector et al., 1988). The negative association of testosterone levels and risk of disease indicate the protective function of testosterone, and its potential to be a pre-clinical marker to predict the RA risk. No consensus has been achieved regarding to the effect of estrogen on RA. Serum levels of estrogen are normal in men with RA, but elevated local concentration of estrogen is discovered in Synovial Fluid (SF), which is believed to aggravate the disease (Cutolo et al., 2003). Interestingly, women who take oral contraceptives containing high concentration of estrogen have a moderate decrease of RA risk (Doran et al., 2004). A possible explanation could be the different biological functions of systematically administered exogenous estrogen versus local endogenous estrogen. Additionally, female patients could have a "temporary exemption" from RA during the pregnancy due to the hormones changes in that period (Silman et al., 1992)

1.1.3.3 Environmental Factors

Several studies have indicated that smoking has a strong association with RA incidence as well as the disease activity and severity (Papadopoulos et al., 2005). Besides smoking, other forms of bronchial stress, such as exposure to silica and traffic pollution have also been confirmed as novel environmental risk factors for RA (Hart et al., 2009; Yahya et al., 2013). Other environmental factors associated with RA include obesity, blood transfusion, virus infection and stress (Cutolo and Straub, 2006; Meron et al., 2010; Symmons et al., 1997). On the other hand, coffee, tea and caffeine consumption don't seem to be risk factors of RA, at least to women (Karlson et al., 2003; Mikuls et al., 2002).

The development of RA is believed to depend on the interactions between multiple risk factors. Substantial evidence indicated that the interaction between the genetic background and environmental factors could have synergistic effect that greatly increases the risk of RA. For example, individuals who are genetically susceptible and cigarette smoking at the same time are at higher risk to develop RA than those with either of these risk factors alone (Costenbader et al., 2008; Lundström et al., 2009; Padyukov et al., 2004; van der Helm-van Mil et al., 2007; Verpoort et al., 2007). Taken together, understanding the role of various risk factors and the

interactions among them could help us to have a better knowledge in etiology, pathogenesis, as well as prevention and the treatment of RA.

1.1.4 Management and Challenges in the Treatment of RA

The goals of RA management and the treatment are relieving the swelling and pain, slowing down the progression of the disease, and preventing joint deformity and other extra-articular complications (American College of Rheumatology Subcommittee on Rheumatoid Arthritis Guidelines, 2002; Wasserman, 2011). Current RA treatment mainly relies on medications. However, invasive measures such as joint replacement surgery is also carefully considered in patients with unacceptable pain, lost joint motions or end-stage joint damage (American College of Rheumatology Subcommittee on Rheumatoid Arthritis Guidelines, 2002; Scott et al., 2010). Medications adopted in RA treatment fall into two main classes: non-steroidal anti-inflammatory drugs (NASIDs) and disease-modifying anti-rheumatic drugs (DMARDs). In the first half of 19th century, NASIDs were first introduced to RA treatment for their symptomatic benefits as reducing the pain and stiffness of the affected joints. However, drugs of this class have limited impact on reducing disease activity and slowing down the disease progression (Upchurch and Kay, 2012). DMARDs were wildly accepted as the key therapeutic agents in the past two decades as they are able to modify the disease outcome such as, decelerating the progression of the disease, improving joints' functions and reducing the disability (Scott et al., 2010; Wasserman, 2011). DMARDs could be further divided into non-biologics and biologics. The first non-biologic DMARDs, gold salt, was reported on 1929, and many others were discovered thereafter (Hartung, 1943; Upchurch and Kay, 2012). Most of the early DMARDs are not recommended anymore for use today because of the high incidence of adverse events or poor tolerance (Saag et al., 2008). Currently, only five non-biologic DMARDs are included in the recommendations for the treatment of RA (Table 2) (Saag et al., 2008; Singh et al., 2012). The biologic DMARDs are antibodies and cell surface receptor inhibitors that target key cytokines and molecules regulating the inflammatory responses in RA (McInnes and Schett, 2007). According to clinical studies and meta-analysis, it is safe to conclude that these biologic DMARDs are generally effective and safe, but whether they are superior to the conventional DMARDs is still inconclusive (Aaltonen et al., 2012; Breedveld et al., 2005; Keystone et al., 2004). However, the combination use of biologics and MTX is better tolerated

and more efficacious than the use of either MTX or biologics alone (Aaltonen et al., 2012; Ash and Emery, 2012; Chen et al., 2006; Klareskog et al., 2004; Lipsky et al., 2000; Weinblatt et al., 1999). As immunosuppressive agents, elevated infection risk is the main adverse drug reaction observed in patients taking biologics to treat RA (Singh et al., 2011). There are currently five TNF-α blockers, one IL-1 receptor antagonist, one IL-6 blocker, one T cell co-stimulation blocker, and one B cell stimulation blocker, approved by FDA and recommended by ACR for treatment of RA (Table 2) (Saag et al., 2008; Scott, 2012; Singh et al., 2012; 2011).

Table 1.2 DMARDs recommended by ACR 2008 and ACR 2012

Drugs	ACR 2008	ACR2012	**Function or Targets**	**Adverse effects**
Conventional	Hydroxychloroquine	Hydroxychloroquine	Antimicrobial	Rare ocular toxicity
	Methotrexate (MTX)	Methotrexate (MTX)	Dihydrofolate reductase	Liver effects, teratogenesis, hair loss, oral ulcers
	Sulfasalazine	Sulfasalazine	Folate depletion	Anemia in G6PD deficiency, gastrointestinal effects
	Leflunomide	Leflunomide	Pyrimidine	Liver effects, gastrointestinal effects, teratogenesis
	Minocycline	Minocycline	Antimicrobial	Drug-induced lupus erythematosus, Clostridium difficile colitis
Biologic DMARDs	Abatacept	Abatacept	CD28	Opportunistic infection
	Rituximab	Rituximab	CD20	Infusion reaction, opportunistic infection, progressive multifocal leukoencephalopathy
		Tocilizumab	IL-6	Opportunistic infection
	Adalimumab	Adalimumab	TNF-α	TB, opportunistic infection
	Etanercept	Etanercept		
	Infliximab	Infliximab		
		Certolizumab pegol		
		Golimumab		

Adapted from Singh et al. and Wasserman et al. (Singh et al., 2012; Wasserman, 2011)

Historically, newly diagnosed RA patients were first treated with NSAIDs and followed by DMARDs. But growing evidence have suggested that the early intervention of RA by DMARDs achieves significant reduction of radiographic progression in RA patients (Finckh et al., 2006). Since the past decade, more aggressive strategy has been adopted to treat early RA

(Upchurch and Kay, 2012). The ACR suggests patients to start DMARDs therapy within 3 months of diagnosis, and with periodically reassessment of disease progression and update of treatment regimen accordingly (American College of Rheumatology Subcommittee on Rheumatoid Arthritis Guidelines, 2002). Single (monotherapy) or combination conventional with DMARDs (dual-therapy or triple therapy) is recommended to patients with different levels of disease and features of prognosis, regardless of disease duration. However, biologic DMARDs are used with more caution; early RA patients are not recommended to, except those one with high disease activity and poor prognosis; for established RA, biologic DMARDs are only considered after the failure of combination DMARDs therapy (American College of Rheumatology Subcommittee on Rheumatoid Arthritis Guidelines, 2002). In addition, tuberculosis has to be treated before using the biologic DMARDs (Saag et al., 2008; Singh et al., 2012).

1.2 Collagen-Induced Arthritis (CIA)

In 1977, Trentham et al. first reported that rat immunized with type II collagen in either complete Freund's adjuvant (CFA) or incomplete Freund's adjuvant (IFA) developes a chronic inflammatory arthritis, which they designated as Collagen-Induced Arthritis (CIA) (Trentham et al., 1977). A subsequent study hypothesized that there are two stages of disease development. In the first stage, as early as day 12 after the immunization, hyperplasia and fibrin deposition could be seen in the synovium; the second stage starts earliest on day19, it is characterized by the inflammatory cells infiltration, which form the pannus and cause the destruction of cartilage and bone eventually (Caulfield et al., 1982). Similar to the rat model, the CIA mouse model starts with edema and synovial hyperplasia, and is followed by infiltration of polymorphonuclear and mononuclear cells. As the disease progresses, pannus forms in the affected joins causing cartilage damage, and finally bone erosion (Courtenay et al., 1980).

Since CIA resembles many pathological features found in RA, it is still the most wildly used model for studying the pathogenesis of human RA in animals, as well as a gold standard for testing the therapeutic drugs for RA in the pharmaceutical industry (Brand et al., 2007). During the past three decades, CIA model made substantial contributions to understand the

role of individual cell types (T cells, B cells, master cells, etc) and cytokines (TNF-α, IL-1β, IL-17, etc) in RA (Brahn et al., 1992; Hom et al., 1992; Kadowaki et al., 1994; Morgan et al., 2005; Nakae et al., 2003b; Nigrovic and Lee, 2005; Tada et al., 1996; Yanaba et al., 2007). Furthermore, the arthritogenicity of autoantibody was also revealed by the fact that the arthritis could be transferred by serum from rodents immunized with Collagen II (Stuart et al., 1984). Of course, there are also certain discrepancies between CIA animal models and human RA. For example, vasculitis which often could be found in RA, is not presented in CIA; on the other hand, periostitis develops in CIA but not in RA(Stuart et al., 1984).

1.3 Mechanisms of RA

1.3.1 Synovial Architecture of Normal Joint

The synovial joints are the most common type of joints in our body, providing precise and smooth movement and maintain the stability and strength as well. The major components of synovial joints are synovial capsule and articulating bones; the outer layer of synovial capsule is a fibrous layer, uniting the articulating bones by attaching their periosteum linings; the inner layer is a one to three cell layer called synovial membrane which contains fibroblast-like synoviocytes and macrophages, secreting synovial fluid to fill up the synovial cavity. The synovial cavity is enclosed by the synovial capsule(Perlman and Pope, 2010). Synovial fluid contains high concentrations of hyaluronic acid and albumin; it absorbs shocks, and lubricates and nourishes the joint. The articulating bones are covered by a thin layer of connective tissue called cartilage, which is made up with a well-organized network of type II collagen fibers. These collagen fibers are produced by chondrocytes scattered in the cartilage. Importantly, there is no blood supply to articular cartilage, while its nourishment depends exclusively on synovial fluid. The synovial fluid also contains phagocytes which are responsible for cleaning up the tissue debris generated from wear and tear of cartilage in our daily life (Rogers, 2010).

1.3.2 Architecture Changes of RA Joint

The normal joint structure goes through a series of changes in RA. It involves synovial hyperplasia and lymphocyte infiltration. In RA, synovium increases its thickness, due to the synovial lining cell proliferation and blood-derived lymphocytes influx trough the vessel wall

into the synovium (Figure 1.1) (Konisti et al., 2012). Moreover, the increased cell numbers in the affected joint contribute to hypoxia and ischemia, posing a signal for angiogenesis; Neovessels exuberate the synovial inflammation by transporting more inflammatory cells and delivering nutrients and oxygen to the RA synovium (Marrelli et al., 2011). As inflammatory cells accumulate in the synovial membrane, where they protrude and form a unique structure called pannus. Pannus invades the cartilage and bone, and causes the cartilage degradation and bone erosion (McInnes and Schett, 2007; Neumann et al., 2010).

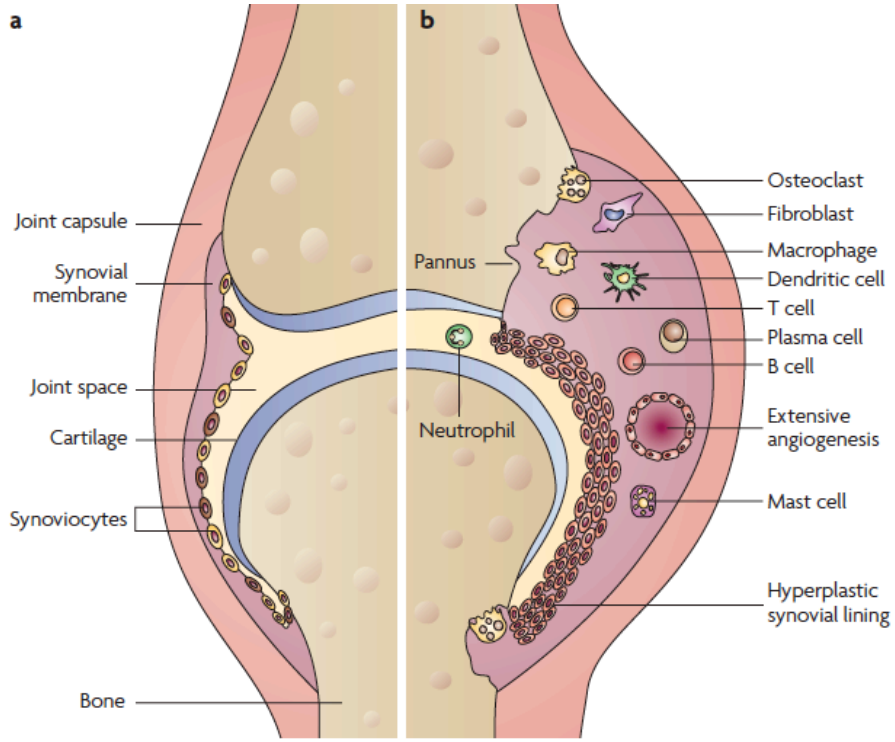

Figure 1.1. Synovial architecture joint. (a) normal joint; (b) joints affected by RA. Adapted from Strand V. et al. (Strand et al., 2007)

1.3.3 Autoantigens, Autoantibodies and B cells

The presence of autoantibodies in the serum and synovial fluids of RA patients has been known for a long time. Since the first description of "a factor" that agglutinate sheep blood cells (late designated as rheumatoid factor (RF)), growing number of autoantibodies have been discovered, and some of them are utilized in clinical diagnostics (Bläss et al., 1999; Waaler, 1940). While most attention to the autoantibodies is focused on their diagnostic value, less contemplation has been given to their role in the pathogenesis of RA. In fact, how those

normal molecules turn into “autoantigens”, and stimulate the production of autoantibodies is the fundamental question that needs to be answered. The followings are four most prominent pairs of autoantigen and autoantibodies related to RA.

1.3.3.1 Rheumatoid Factor

Rheumatoid factor (RF) was first discovered in 1940s and later identified as antibodies that bind the Fc region of Ig (FRANKLIN et al., 1957; Waaler, 1940).It was quickly included as a criterion for clinical diagnosis of RA in 1958, and remains the exclusive diagnostic autoantibody for more than 50 years (Aletaha et al., 2010; Arnett et al., 1988; Committee of the American Rheumatism Association, 2008). Healthy humans or animals are reported to produce a transient wave of RFs after vaccination or immunization, while 80% of RA patients have persistent increased level of RF in sera(Coulie and Van Snick, 1983; M J Welch, 1983; Nell et al., 2005). The physiological roles of RFs are 1) promoting complement fixation, 2) helping the clearance of immune complexes (IC), and 3) increasing the avidity and specific of functional antibodies(Carson et al., 1987). RF is believed to be pathogenic in RA as it induces the RA-related cytokines production. Early studies have shown that RF induces monocytes to produce prostaglandin E_2 and mononuclear cell factor (MCF), two potent stimulator of bone resorption (Gowen et al., 1983; Nardella et al., 1983). Moreover, IC formed by RF and immunoglobulin (Ig) from arthritic synovial tissue has been demonstrated to stimulate the production of TNFs from monocytes (Ishikawa et al., 1975; Mathsson et al., 2006).

1.3.3.2 Anti-Citrullinated Protein Antibody (ACPA)

Citrullination is a biological process of converting amino acid arginine into citrulline; it is conducted by peptidylarginine deminase enzymes (PAD), which have 5 isoforms (PAD1, 2, 3, 4/5 and 6)(Vossenaar et al., 2003). Many essential physiological activities require PADs, such as embryo development, electrical insulation in the nervous system and transcriptional control for DNA, and so on (Vossenaar et al., 2003). Citrullination may also occur under certain pathogenic conditions, notably in RA, producing autoantigens. Both PADs (2 and 4) and citrullinated protein (fibrinogen, fibronectin, vimentin and Collagen II) are found in affected RA joints, but not healthy joints (Baeten et al., 2001; Kinloch et al., 2008; Tabushi et al.; Vossenaar et al., 2004; Yoshida et al., 2006). Anti-citrullinated protein antibodies (ACPAs)

are antibodies against citrullinated proteins of various origins. They are present in around 70% of RA patients, and included in the RA classification criteria, due to their high specificity for RA (90-95% compare to 40-90% of RF) and strong association with a severe disease status (Aggarwal et al., 2009; Aletaha et al., 2010; Schellekens et al., 2000). Generally, citrullination of protein and their further conjugation with their autoantibodies increase their immunogenicity and arthritogenicity (Lundberg et al., 2005; Shelef et al., 2012; Sokolove et al., 2011). For examples, citrullinated fibrinogen (cFib) and myelin binding protein, but not their natural forms, are capable of activating basophils from $ACPA^+$ RA patients (Schuerwegh et al., 2010). Both cFib and cFib-IC are more potent in inducing TNF production from macrophages compared to the natural form of fibrinogen (Clavel et al., 2008; Sokolove et al., 2011). *In vivo*, immunizing rat with citrullinated Collagen II (cCII) in incomplete Freund's adjuvant (IFA) induces earlier arthritis with higher incidences than with natural CII (Lundberg et al., 2005). Immunization with cFib but not natural fibrinogen in CFA or intra-articular administration of cFib plus transferring of cFib-specific T cells induces arthritis in mice carrying a RA susceptible MHC-II allele (Hill et al., 2008). The ACPAs might not be pathogenic under a healthy condition, but they could play a role in aggravating the disease after the onset of arthritis (Kuhn et al., 2006). A novel study discovered that ACPAs could bind to the citrullinated vimentin on osteoclast precursor cells and promote their differentiation into osteoclasts, leading to the bone erosion and joint destruction (Harre et al., 2012).These results are in accordance with the clinical finding that the presence of ACPAs in serum is usually related to the more advanced bone erosion condition in RA (Aggarwal et al., 2009).

1.3.3.3 Anti-Collagen II (CII) Antibody

Type II collagen (collagen II, CII) is the major component of articular cartilage in joints. The association between RA and CII antibodies has been found in the several clinical studies. The presence of anti-CII antibodies in serum is observed in about 30% of RA patients with indications of an early inflammatory/destructive disease phenotype (Beard et al., 1980; Cook et al., 1996; Fujii et al., 1992; Mullazehi et al., 2007; 2012; Raza et al., 2007; S et al., 1988). Anti-CII antibodies are also found in the synovial fluids of some RA patients who are genetically HLA-DR4 positive (Rönnelid et al., 1994). Both CII and anti-CII antibody are

arthritogenic: immunization of CII emulsified with either IFA or CFA induces arthritis in rat and mice (Courtenay et al., 1980; Trentham et al., 1977; 1978). The pathogenic role of anti-CII antibodies has been demonstrated by successful induction of arthritis in naïve rats/mice passively transferred with anti-CII antibodies-containing sera from CIA rats/mice; it has been further confirmed by the fact that direct administration of combination of anti-CII monoclonal antibodies caused full-blown arthritis (HOLMDAHL et al., 1990; Stuart and Dixon, 1983; Stuart et al., 1982; Terato et al., 1992). Moreover, anti-CII antibodies have been reported to cause thickening, aggregation and disorganization of CII fibrils in newly synthesized extracellular matrix (ECM), as well as alter the secretion rate of matrix metalloproteinase (MMPs) in culture, by interfering chondrocytes (Takagi and Jasin, 1992). Furthermore, CII-ICs have been shown to activate PBMCs and induce RA-like disease pro-inflammatory cytokine (TNF-α, IL-1β and IL-8) production (Mullazehi et al., 2006).

1.3.3.4 Anti-Glucose-6-Phosphate Isomerase (GPI) Antibody

The pathogenic role of GPI and its antibody in RA was discovered by chance. When transgenic mice overexpressing the TCR that recognizes peptide of bovine pancreas ribonuclease (RNase) in the context of A^k (KRN TCR) are crossed with NOD mice which bear a unique MHC-II (I-Ag7), the transgenic offspring (K/BxN) exhibits spontaneous inflammatory arthritis (Kouskoff et al., 1996). GPI, a ubiquitously expressed enzyme converting glucose-6-phosphate into fructose-6-phosphate, is later identified as the autoantigen in this arthritis murine model (Matsumoto et al., 1999). In the joints of arthritic K/BxN mice, thick linings of GPI molecules, accompanied by the deposition of IgG and C3 complement fragments could be seen on the surface of cartilage, synovium and pannus (Matsumoto et al., 2002). Accordantly, extremely high level of anti-GPI antibody is presented in the serum of K/BxN mice (Matsumoto et al., 2002). The mechanistic study has revealed that the joint inflammation in this particular arthritic model is caused by the GPI-IC formed in the joints which triggers the alternative complement pathway activation (Maccioni et al., 2002; Matsumoto et al., 2002). In the clinical study, deposition of GPI molecules is also observed in the synovial tissues from RA patients. However, most studies have shown anti-GPI antibodies are either rarely or non-specifically detected in RA serum (Kassahn et al., 2002; Matsumoto et al., 2003; Schaller et al., 2001; Schubert et al., 2002). Collectively, although the anti-GPI

antibody is proved to be athrogenic in mice, whether it is involved in the initiation and development of human RA is still unclear.

1.3.3.5 Other Autoantigens and Autoantibodies

In addition to those mentioned above, many other autoantigens and autoantibodies have been found related to RA. Some of them have potential to be novel diagnostic markers, while others attract less attention due to the inconsistent data and low disease specificities. Some of them are listed in Table 1.3.

Table 1.3 Autoantigens and autoantibodies found in rheumatoid arthritis

Autoantigen	Target	Disease	Reference
Articular components	Chondrocyte membranes (CH65)	RA	(Bang et al., 1994; Steinert et al., 1985)
	HC gp39 (YKL-40)	OA, RA	(Hakala et al., 1993; JOHANSEN et al., 1996)
	Osteopontin	OA, RA	(Sakata et al., 2001)
Ubiquitous	Heterogeneous nuclear ribonucleoprotein A2 (Ra33 or hnRNP A2)	SLE, RA	(Hassfeld et al., 1989; 1995)
	Calpstatin	SLE, RA	(Mimori et al., 1995)
	BiP		(Bläss et al., 1995; 2001)
	α-enolase	Autoimmune retinopathy, RA	(Kurz et al., 2011; Saulot et al., 2002)
Cytokines	B7-H1 (PD-L1)	RA	(Dong et al., 2003)
	IL-1α	RA	(Hansen et al., 1994)
	IL-8	Myasthenia gravis, RA	(Burbelo et al.; Peichl et al., 1992)

In summary, there are three possibilities for the pathogenic roles of a pair of autoantigen and its autoantibody. First, autoantigen is pathogenic by itself. Natural or modified proteins could become autoantigens and involved in the pathogenesis of RA by inducing the pro-inflammatory cytokine production, angiogenesis and synoviocyte proliferation (Sokolove et al., 2011; Yoo et al., 2012). Importantly, these autoantigens are not necessarily to be the joint exclusive proteins. However it is crucial for them to be present in the joint tissues of individuals with certain genetic background, given that immunization of these autoantigens is only able to induce arthritis in mice with the susceptible genetic background. Second, free Abs could be pathogenic. Certain autoantibodies such as anti-CII or anti-calpastatin Abs are able to

interfere with the interactions among cartilage proteins in joints, and cause degradation of cartilage components (Amirahmadi et al., 2005; Ménard and el-Amine, 1996). Third, autoantigen and its autoantibody contribute to the RA by forming immune complexes (IC). Transferring sera (or IgG fraction but not IC fraction) from CIA or K/BxN arthritic mice to naive mice causes arthritis (HOLMDAHL et al., 1990; Korganow et al., 1999; Matsumoto et al., 1999; Stuart and Dixon, 1983; Stuart et al., 1982; Terato et al., 1992). In accordance, anti-GPI autoantibodies have been reported to locate to distal joints within minutes after intravenous injection, whereas preformed ICs have difficulties to get into the joints (Wipke et al., 2002). It is believed that the autoantibody penetrates into the joints, forms articular ICs with pre-deposited autoantigens (like GPI or cCII), and initiates the disease (Matsumoto et al., 1999). These ICs then bind to the FcγR on the surface of monocytes/macrophages and induce the production of TNF, IL-1β, and IL-8 (Mathsson et al., 2006; Mullazehi et al., 2006; Sokolove et al., 2011). Besides FcγR, ICs are also reported to interact with toll-like receptor 4 (TLR4), which works synergistically with FcγR and elevates the TNF production by macrophage (Sokolove et al., 2011). More detailed in vivo studies using knockout mice have revealed that FcγRI and FcγRIII are responsible for the successful induction of CIA or antibody-induced arthritis (AIA) (Kleinau et al., 2000; Nandakumar et al., 2003a).

1.3.3.6 Functions of B cells Other Than Producing Autoantibodies

In addition to producing autoantibodies, several novel roles B cells playing in RA have been discovered by recent studies. Firstly, B cell is able to serve as an APC for autoreactive T cells. In a proteoglycan induced arthritis (PGIA) model, when transferring T cells from proteoglycan (PG)-immunized Ig-deficient mice to SCID mice, only those T cells that received adequate priming from cognate B cells are able to elicit the disease (O'Neill et al., 2005). A later study from the same group has shown that CD80/CD86, two costimulatory molecules expressed on B cells, are essential for the activation of autoreactive T cells in PGIA (O'Neill et al., 2007). Accordant with animal studies, a human study has also reported that B cell is essential for the activation of synovial follicular T cells, since adoptively transferred follicular CD4 T cells fails to get activated and secret pro-inflammatory cytokines in SCID mice chimeras with human RA tissues lacking B cells (Takemura et al., 2001). Secondly, B cell could affect the pathogenesis of RA by secreting cytokines. The B cells are reported to secrete various

cytokines to promote inflammation (TNF, IL-1, IL-6, G-CSF, GM-CSF and IL-12) and angiogenesis (VEGF-A), two prominent features in RA (Angeli et al., 2006; Pistoia, 1997). On the other hand, a novel subset of B cells called B regulatory cells have been discovered to attenuate the harmful immune responses by secreting IL-10 and TGF-β (Mizoguchi and Bhan, 2006). Two studies have shown that regulatory B cells ameliorate CIA in DBA mice through the secretion of IL-10 (Evans et al., 2007; Mauri et al., 2003).

1.3.4 T cells

1.3.4.1 Th1 and Th2 Cells

Th1 cells produce IFN-γ, which primarily activates macrophages and mediates the immune responses against intracellular infections (Kindt et al., 2007; Szabo et al., 2000). Th2 cells secrete IL-4, 5, 10 and 13 and are responsible for humoral responses to protect against infections from extracellular pathogens (Kindt et al., 2007). Early studies on RA patients found mRNA expression of IL-12 and IFN-γ in RA synovial fluid mononuclear cells, and identified Th1 cells as the predominant T cell subsets in synovial fluid (SF) from RA patients (Bucht et al., 1996; Kusaba et al., 1998; Morita et al., 1998). Th2 cytokine-producing cells are also detectable in the synovial tissues and peripheral blood of RA patients, but at a significantly lower frequency comparing to cells producing Th1 cytokines (Kusaba et al., 1998; Morita et al., 1998; Yudoh et al., 2000). Messenger RNA levels of IL-4 and IL-10 in synoviocytes become significantly lower as RA progresses (Miyata et al., 2000). It was believed that Th1 responses are generally associated with inflammation, whereas Th2 responses are protective to some extent. Based on this belief and clinical findings, a Th1/Th2 imbalance hypothesis is proposed for the pathogenesis of RA. However, emerging evidence from animal studies have shown complicated role of Th1 and Th2 cells in RA.

IFN-γ receptor deficient mice are more susceptible to CIA, and this is accompanied by accelerated and exacerbated disease, but less anti-CII antibodies (Manoury-Schwartz et al., 1997; Vermeire et al., 1997). More detailed studies by the same group and other groups have been performed to understand the protective role of this cytokine. The possible mechanisms are as follows: 1) the presence of IFN-γ signaling suppresses the arthritogenic myelopoiesis of the splenic Mac-1^{+} cells elicited by the mycobacterial component of CFA (Matthys et al.,

2001). Using IFA instead of CFA for immunization or inhibition of CFA-induced splenic Mac-1^+ cell expansion abolishes the exacerbated CIA in IFN-γ receptor KO mice (Matthys et al., 1999). 2) It is suggested by the same group that deficiency in IFN-γ signaling diminishes the function of Treg cells by bringing down Foxp3 transcription levels in Treg, and also dampens the function of APC cells (Kelchtermans et al., 2005). This finding is in accordance with recent discovery of regulatory role of IFN-γ (Wood and Sawitzki, 2006). 3) Two studies using streptococcal cell wall (SCW)-induced arthritis in rat have shown IFN-γ inhibits leukocyte chemotactic migration to the synovium, and prostaglandin E2 (PGE2) production and synoviocytes proliferation, indicting IFN-γ could suppress the arthritis through suppressing the mesenchymal cells (Allen et al., 1991; Wahl et al., 1991). 4) IFN-γ suppresses the Th17 cells. It is known that IFN-γ suppresses the *in vitro* differentiation of IL-17-producing Th17 cells (Bettelli et al., 2008). *In vivo*, neutralization of IFN-γ in CIA increases circulating and articular levels of IL-17, which causes accelerated disease (Sarkar et al., 2009). IFN-γ knockout mice in antigen-induced arthritis (AIA) have similar phenotypes as IFN-γ receptor deficiency mice in CIA; Articular administration of IFN-γ or treatments with mAb neutralizing IL-17 alleviates the disease (Irmler et al., 2007). It is suggested that deficiency of IFN-γ releases the suppression of IL-17 and leads to the aggravated disease (Irmler et al., 2007). A controversial result has been reported recently showing reduced arthritis in IFN-γ receptor KO mice in glucose-6-phosphate isomerase (G6PI)-induced arthritis (Frey et al., 2011). Doodes et al. has shown similar results using IFN-γ KO mouse models of proteoglycan-induced arthritis model (Doodes et al., 2010). Although IFN-γ is implied to exacerbate the arthritis in their findings, the suppressions of IL-17 production by IFN- γ in these studies are still obvious and negatively correlate with the disease (Doodes et al., 2010; Frey et al., 2011). Collectively, either IFN-γ or IL-17 alone is pathogenic in RA. The latter is much more avid, but is negatively regulated by the former. When the disease condition is in favor of IL-17 production, IFN-γ exhibits a protective role. Otherwise, IFN-γ would be pathogenic for the disease.

Administration of exogenous IL-4 reduces the histological score, pathogenic anti-CII antibodies' level and pro-inflammatory cytokine secretion by joint tissues in CIA mice (Horsfall et al., 1997). Similar results are obtained when treating the mice with IL-4 or IL-10,

or both, in PGIA and SCW models (Finnegan et al., 2003; Lubberts et al., 1998). More specifically, either systemic administration or articular overexpression of IL-4 appears to protect against bone destruction of CIA (Joosten et al., 1999; Lubberts et al., 2000a). The protective effect of IL-4 against bone destruction is through the suppression of IL-6 and LIF, and inhibition of osteoclasts (Miossec et al., 1994). Conversely, depletion of IL-4 or IL-10 has caused elevated disease in several different arthritis models (Finnegan et al., 2003; 2002; Hata et al., 2004). The change of disease caused by adding or removal of IL-4 is closely associated with the levels of specific arthritogenic IgG2a, indicating the IL-4 may prevent the class switching towards the pathogenic IgG isotope (Brand et al., 2003; Finnegan et al., 2002; Horsfall et al., 1997; Joosten et al., 1999; Kim et al., 2001b; Myers et al., 2002). IL-10 also confers a protective role in RA. It reduces TNF-α and IL-1 secretion from cultured synovial membrane tissues of RA patients, and costimulatory molecule expression of synovial cells(Katsikis et al., 1994; Kawakami et al., 1997). A Korean group has reported that the IL-10 suppresses the arthritis by diminishing IL-17 expression and inducing the Treg cells generation (Heo et al., 2010). Furthermore, IL-10 has an additive effect, or even a synergistic effect with IL-4 on the inhibition of proinflammatory cytokine production by activated mononuclear cells from RA patients (van Roon et al., 1996). In the SCW arthritis model, administration of IL-10 with IL-4 reduces both IL-1β and TNF-α levels in the synovium, while IL-10 alone only brings down the latter cytokine (Lubberts et al., 1998). In addition, IL-10 and IL-4 were also reported to have additive effect on stimulating the cartilage proteoglycan synthesis (van Roon et al., 1996). While most studies acknowledge the protective role of IL-4 in RA, there is a recent study implying that IL-4 can be pathogenic. In the K/BxN model, IL-4 has been demonstrated to be essential in initiating the arthritis by activating B cells (Ohmura et al., 2005). This result indicates that different settings of the arthritis models and genetic backgrounds could change the disease phenotypes drastically.

1.3.4.2 Th17 Cells

Th17 is a T cell lineage, producing a distinct cytokine profile including IL-17, IL-21 and IL-22. It is the major source of IL-17 (Weaver et al., 2006). IL-17, also known as IL-17A, belongs to the IL-17 family, which contains 7 different members. It is a potent proinflammatory cytokine and plays an essential role in autoimmune diseases (Gaffen, 2008).

Elevated IL-17 levels are observed in sera and synovial fluids from RA patients (Hussein et al., 2008; Kotake et al., 1999; Ziolkowska et al., 2000). The target cells of IL-17 in RA include synovial fibroblasts, macrophages, chondrocytes and osteoblasts, all of which are directly related to the pathogenesis of RA (van den Berg and Miossec, 2009). IL-17 alone, or synergistically with IL-1β or TNF-α, induces the production of IL-6, IL-8, granulocyte-colony-stimulating factor (G-CSF), prostaglandin E2 (PEG2) and leukemia inhibitory factor (LIF) by synoviocytes (Chabaud et al., 1998; Fossiez et al., 1996). In a Th17 cell and synovial fibroblast co-culture system, IL-17 increases the secretion of matrix metalloproteinase-1, -3 (MMP-1, -3), as well as IL-6 and IL-8, by synovial fibroblasts. Synovial fibroblasts, on the other hand, increase autocrine IL-17 production by Th17 cells through the cyclooxygenase (COX)/PEG2 pathway. Together, they built up a proinflammatory loop contributing to the pathogenesis of RA (Paulissen et al., 2013; van Hamburg et al., 2010). In addition, IL-17 has been reported to promote the survival of synovial fibroblasts (Lee et al., 2013). A similar proinflammatory loop is suspected to exist between IL-17 and synovial macrophages too. IL-17 stimulates macrophages and upregulates their arthritogenic cytokine (such as IL-1β and TNF-α) production, and synovial macrophages could, in turn, support the generation of Th17 cells (Egan et al., 2008; Jovanovic et al., 1998). Moreover, IL-17 was also suggested to promote the migration of macrophages (Shahrara et al., 2009; 2010). Chondrocytes are believed to be the target of IL-17 in RA as well. Chondrocytes stimulated with IL-17 elevate the production of nitro oxide (NO), inducible nitric oxide synthase (iNOS) and COX-2, as well as IL-1β, IL-6 and stromelysin; NO and IL-1β then cause cartilage proteoglycan (PG) loss and inhibit its synthesis in chondrocyte (Lubberts et al., 2000b; Shalom-Barak et al., 1998). IL-17's function on osteoclastogenesis was first demonstrated by a mouse hematopoietic cell and primary osteoblast co-culture system. Adding IL-17 stimulates PEG2 synthesis and elevates osteoclast differentiation factor (ODF) mRNA levels of osteoblasts. This then promotes the differentiation of osteoclasts in a cell-cell contacting fashion (Kotake et al., 1999). Mechanistically, it was suggested that IL-17 breaks the balance of the receptor activator of NF-κB ligand (RANKL)/RANK pathway, leading to osteoclastogenesis (Lubberts et al., 2003). Various arthritis murine models have been used in the *in vivo* studies of the essential roles of IL-17 in RA. Intra-articular injection of IL-17 could induce cartilage degradation in naive mice (Chabaud et al., 2001). Articular-specific adenoviral overexpression of IL-17

exacerbates the disease in terms of joint inflammation, cartilage degradation and bone erosion in CIA mice (Lubberts et al., 2003). Conversely, knockout of IL-17 or treatment with IL-17 antagonist antibodies confers great protective effect to mice in experimental arthritis models (Bush et al., 2002; Lubberts et al., 2004; Nakae et al., 2003a).

IL-22, another Th17 cell cytokine, could also be produced by synovial fibroblasts and macrophages (Ikeuchi et al., 2005). A recent report have shown IL-22$^{-/-}$ mice are less susceptible to CIA and have decreased disease incidence and clinical score, and oddly, higher levels of anti-CII IgG_{2c} comparing to WT counterparts (Geboes et al., 2009). In vitro study in the same model has also revealed show that IL-22, similar to IL-17, could promote osteoclastogenesis (Geboes et al., 2009). Human studies have demonstrated that increased IL-22 serum levels are associated with the disease progression of RA, and its mRNA is detected in synovial tissues and macrophages from RA patients (Leipe et al., 2011). These findings indicate the potential role of IL-22 in RA.

IL-21 is a type I cytokine, produced by CD4 T cells and NKT cells. The most well known function of IL-21 is to drive B cells to differentiate into plasma cells (Spolski and Leonard, 2008). Besides its function on B cells, IL-21 could act as an autocrine to regulate Th17 cells and induce RANKL expression and enhance the osteoclastogenesis in RA (Kwok et al., 2012). Niu et al. have discovered that IL-21 promotes the proliferation of Th17 cells while suppresses Treg cells, and the levels of IL-21 in serum and synovial fluids from RA patients are correlated to the percentage of Th17 cells (Niu et al., 2010). IL-21 is also detected in cultured synovial membrane cells from RA patients, and blocking IL-21 signaling in this culture system significantly downregulates TNF-α, IL-6 and IL-1β productions in these cells (Andersson et al., 2008). Recent animal studies have also shown an elevated level of IL-21 in the serum and synovium of mice with CIA (Kwok et al., 2012).

1.3.4.3 CD4 Treg cells

$CD4^+$ Treg cells express cell surface marker CD25 and transcription factor forkhead box P3 (FoxP3). They are inhibitory in the immune system and prevent the autoimmunity (Bacchetta et al., 2006; Shevach, 2009; Wildin et al., 2001). Treg cells could work on a wide variety of immune cells including T cells, DCs, B cells, macrophage, osteoblasts, mast cells, NK cells,

NK T cells and so on. They suppress immune responses by 1) directly targeting on T cells, inducing cell cycle arrest and apoptosis, and inhibiting cytokine production (Gondek et al., 2005; Pandiyan et al., 2007; Taylor et al., 2006); or 2) indirectly, through antigen presenting cells (APCs), inhibiting their maturation and providing the costimulatory signals to the T cells(Borsellino et al., 2007; Liang et al., 2008; Sarris et al., 2008; Shalev et al., 2008; Shevach, 2009; Wing et al., 2008).

Treg cells play an active role in the mouse arthritis model. Mice depleted of Tregs have much severer CIA. Adoptive transfer of Treg to Treg-depleted or normal mice decreases clinical scores but not autoantibody levels, which might be a consequence of reduced serum levels of TNF and IL-6 (Kelchtermans et al., 2009; Morgan et al., 2005; 2003). Similar results have been obtained from antigen-induced arthritis (AIA) model as well (Frey et al., 2005). Studies focused on circulating Treg number changes in RA patients haven't reached a consensus(Chavele and Ehrenstein, 2011). Although the presence of Treg cells in the synovial tissue and peripheral blood of RA patients is well documented, mechanism studies of Treg cells on human RA yield mixed results. Several studies reported that $CD4^+CD25^+FoxP3^+$ Treg cells isolated from SF of RA patients show normal suppressive effect on the proliferation of CD4 T cells (Cao et al., 2003; Lawson et al., 2006; Möttönen et al., 2005), whereas others suggested that the suppressive effect of Treg cells from RA synovial tissue is compromised (Ehrenstein et al., 2004; Skapenko et al., 2005). One study has demonstrated that Treg cells from SF of RA patient show stronger suppressive ability compare to those from PB, but the synovial T effector cells are less susceptible for Treg suppression (van Amelsfort et al., 2004). Similarly, Ohata et al. have shown that effector T cells from a later stage of mouse CIA are more resistant to the suppression (Ohata et al., 2007). It has been suggested by another study that the resistance acquired by effector T cells is probably induced by IL-6 produced by DC (Pasare and Medzhitov, 2003). On the other hand, two studies have found that the Treg cells from RA PBMC are capable of suppressing the T cell proliferation, but are defective in suppressing proinflammatory cytokine production (Ehrenstein et al., 2004; Valencia et al., 2006). Mechanistically, the malfunction of CTLA-4 expression and recruitment to the immunological synapse may cause the abnormal Treg function in RA (Flores-Borja et al., 2008). Furthermore, a recent study has identified Ser418a, phosphorylation site of FoxP3,

which is dephosphorylated by the TNF-α-induced protein phosphatase 1(PP1) in the RA synovium. Dephosphorylation of Ser418 severely impairs the transcription of FoxP3, and consequently the function of Treg cells(Nie et al., 2013).

1.3.4.4 Tfh Cells

The description of Tfh first appeared around 2000, when several studies reported a T cell population from human tonsils expressing CXCR5 and capable of promoting the B cell antibody production (Breitfeld et al., 2000; Kim et al., 2001a; Schaerli et al., 2000). Tfh cells were reported to express high levels of ICOS and CD40L on their cell surface, and secrete various cytokines including IL-4, IL-5, IL-13, IL-17, IL-21 and IFN-γ(Crotty, 2011).

Although few studies have been conducted to investigate the pathogenic role of Tfh in RA, it is conceivable that the mechanism of Tfh in RA has to be related to the production of the autoantibodies. In mouse CIA, blocking B7RP-1, the ICOS ligand, significantly lowers down the disease incidence and clinical score due to the reduction of Tfh cells as well as anti-CII antibodies (Hu et al., 2009). Dysregulation of Tfh cells could break the immune tolerance by providing inappropriate helps to autoreactive B cells (Leavenworth et al., 2013; Lim et al., 2004; Vinuesa et al., 2005). For example, *Sanroque* mice, defective in ring-type ubiquitin ligase which playing suppressive role in regulating Tfh cells, gain features of lupus due to the excessive Tfh cells and GCs (Linterman et al., 2009). Elevated circulating Tfh cell percentages are also observed in a subset of SLE patient (Simpson et al., 2010). Similar finding in RA were reported by several Chinese groups showing a correlation between the increased frequencies of peripheral Tfh-like cells ($CXCR5^{+}PD\text{-}1^{+}CD4^{+}$) and serum level of IL-21 and ACPA, as well as disease active score (DAS28) (Liu et al., 2012; Ma et al., 2012; Wang et al., 2013). One of these studies further showed that the percentage of Tfh cells decreased significantly in the drug-responding patients after the treatment with DMARDs (Wang et al., 2013).

1.3.4.5 CD8 T Cells

CD8 T cell knockout in B10.Q mice shows negligible effects other than delaying the disease onset of CIA (Ehinger et al., 2001). In transgenic mice (B6/129 background) overexpressing human RA-susceptible gene HLA-DQ8, CD8 deficiency increases the incidence and severity,

as well as autoantibody levels (Taneja et al., 2002). CD8 T cell knockout mice in the DBA background have a significantly lower incidence of CIA than their heterozygous counterparts (Tada et al., 1996). Depletion of CD8 T cells in K/BxN mice ameliorates the spontaneous arthritis, whereas transfering SKG CD8 T cells to nude mice elicits arthritis (Raposo et al., 2010; Wakasa-Morimoto et al., 2008). The presence of CD8 T cell affects the pathogenesis of arthritis, but whether it protects or aggravates the autoimmune disease is still under debate. Recently, two studies found that CD8 regulatory T cells (CD8 Treg) in CIA mice showing strong inhibition of the disease by eliminating the autoreactive Tfh and Th17 cells (Leavenworth et al., 2013; Notley et al., 2010). On the other hand, two autoreactive CD8 T cell clones that able to kill syngeneic synovial cells are identified in the SKG mice mentioned above (Wakasa-Morimoto et al., 2008).

Similar situations are also observed in human studies. In synovial fluids from RA patients, $CD8^+$ T cells comprise around 40% of T cells (McInnes, 2003). One study has reported that 15.5% percent of synovial $CD8^+$ T cells from different patients recognize a single EBV epitope, and secrete proinflammatory cytokines upon stimulation of this peptide (Tan et al., 2000). Analysis of T cell subsets and cytokine production in RA patients has also reveled a direct correlation between synovial $CD8^+$ T cells and disease severity (Hussein et al., 2008). Based on the cytokine production profiles, $CD8^+$ T cells of human origin could be classified into 3 subsets: Tc1, producing IFN-γ and other cytokines but no IL-4; Tc0, producing IL-4, IFN-γ and other cytokines; and Tc2 producing IL-4 but no IFN-γ (Vukmanovic-Stejic et al.). A study showed that the RA patients have significantly higher percentage of Tc1 in their synovial fluid (SF), but not in their peripheral blood (PB). Interestingly, the percentage of IL-10-producing Tc2 cells in the SF is unregulated in the same group of patients(Berner et al., 2000). These Tc2 cells are generally believed to be human regulatory/suppressive CD8 T cells, and exhibit suppressive phonotype upon their specific peptide stimulation(Bodman-Smith et al., 2003). In addition to Tc0, Tc1 and Tc2, a special fraction of CD8 T cell exclusively localized in the synovial membranes is found to regulate the ectopic GC formation(Wagner et al., 1998). It is characterized by expressing CD40L and producing IFN-γ, but not having perforin, the pore-forming enzyme (Wagner et al., 1998). Depletion of these synovial CD8 T cells results in GC dissociation, disappearance of follicular dendritic cell

(FDC) and reduced Ig productions, although the detailed mechanisms are yet unknown(Kang, 2002; Wagner et al., 1998). Collectively, these results indicate that the total CD8 T cell pool might contain different subpopulations of CD8 T cells that play distinct roles. Thus, a plausible explanation to the discrepancies found in the animal studies as well as RA patients could be that different strains of animals and methods of arthritis induction may result in variation of the CD8 T cell pools. The composition of CD8 T cell pools would decide the net effect of total CD8 T cells.

1.3.5 Monocytes/Macrophages

Macrophages appear in RA joints at a very early phase of RA(Singh et al., 2004). The number of macrophages on the synovial lining and sub-lining is correlated with either early joint pain or later stage symptom like articular destruction (Mulherin et al., 1996; Tak et al., 1997). It has been suggested that most RA synovial macrophages are derived from infiltrated pre-activated monocytes from peripheral blood. These macrophages have prolonged survival and constitutive activation status, but less proliferation (Catrina et al., 2005; Ceponis et al., 1998; Huang et al., 2007). Synovial macrophages play a central role in RA. It affects every stage of disease progression by producing a broad spectrum of cytokines in the RA synovium (Kinne et al., 2000). Depletion of macrophages alleviates the experimental arthritis (Brühl et al., 2007; Li et al., 2012a; Misharin et al., 2012). The major cytokines produced by macrophage and their potential functions in RA are listed in Table 1.4.

Table 1.4 Monocyte/macrophage cytokines and their potential functions

Family	Cytokine	Target	Function
IL-1	IL-1α/β	SF	Activation, ↑ cytokine, chemokine, MMP, iNOS and PG release;
		MN	↑ cytokine, ROI and PG release, osteoclast activation
		CD	↓GAG synthesis,
		EN	iNOS, MMP and aggrecanase, adhesion molecule expression
	IL-18	EN	↑Angiogenesis (Koch, 2003)
		Th	↑Th1 differentiation
		NK	↑Activation, cytokine release and cytotoxicity
		CD	↓GAG synthesis, iNOS expression
		MN	↑Cytokine release and adhesion molecule expression
		PMN	↑Activation, cytokine release and migration
	IL-1Ra		↓inflammatory reaction

TNF	TNF-α	EN	↑Angiogenesis (Koch, 2003)
		MN	↑Activation, cytokine and PG release
		PMN	↑Priming, apoptosis and oxidative burst
		Th	↑↓Apoptosis, clonal regulation and TCR dysfunction
		EN	↑Adhesion molecule expression, cytokine release
		SF	↓proliferation and collagen synthesis
		AP	↑FFA release
	BAFF	B	↑Proliferation, Ab secretion, isotype switching and survival
		T	↑costimulating
	APRIL	B	↑Proliferation
IL-6	IL-6	B	↑Proliferation and Ab production
		T	↑Proliferation, differentiation and cytotoxicity
		MN	↑Cytokine release
			Activation (Gibbons and Hyrich, 2009)
	OSM	MK	↑Differentiation
		SF	↑TIMP, cytokine release and protease inhibitor
		MN	↓TNF release and IL-1 effector function
Type II IFN	IL-4	EN	↑Activation, adhesion molecule expression and Angiogenesis (Koch, 2003)
		Th2	↑Differentiation, maturation; ↓apoptosis
		B	↑Maturation; ↑isotype switch (IgE)
		EI	↑Migration; ↓apoptosis
	IFN-γ	SF	↑Collagen sythesis
		MP	↑Activation
		DC	↑APC function, MHC-II expression
		EN	↑Adhesion molecule expression
		T	Th1 response
			↓Bone resortpion
	IL-10	MP	↑Cytokine release, iNOS and soluble receptor, ROI
		T	↓cytokine release and MHC expression; ↑anergy
		Treg	↑suppressive function (Chaudhry et al., 2011), maturation
		DC	↓Activation and cytokine release
		SF	↓MMP and collagen release
		B	↑Isotype switching
IL-12	IL-12	Th1	↑Proliferation, differentiation, cytotoxicity
		NK	↑Cytotoxicity
		B	↑Activation
	IL-23	Th17	↑Expansion
	IL-27		↑↓Inflammation (Villarino and Hunter, 2004)
Growth	TGF-β	Th17	↑differentiation; ↓proliferation and function
		Treg	↑differentiation; ↓proliferation and function
		NK	↓proliferation and function
		MP	Activation then suppression; ↓iNOS expression

factor		LK	↑Chemoattractant, gelatinase and intergrin expression
		SF	Activation (Rico et al., 2010; Rosengren et al., 2010)
	FGF	MCY	↑Growth and differentiation
		EP	↑Growth and differentiation
		SF	Activation (Malemud, 2007)
	VEGF		↑Angiogenesis (Koch, 2003)
	G-CSF	PMN	↑Function
	M-CSF	MN	Activation and maturation

This table is adapted and updated from(Firestein et al., 2012; McInnes and Schett, 2007)
SF, synovial fibroblast; MN, Monocyte; MMP, matrix metalloproteinase; iNOS, inducible nitric-oxide synthase; PG, prostaglandin; ROI, reactive oxygen intermediate; GAG, glycosaminoglycans; EN, endothelial cell; Th1, T helper cell1; NK, Nature Killer cell; CD, Chondrocyte; PMN, polymorphonuclear; AP, adipocyte; FFA, free fatty acid; MP, Macrophage; Treg, regularly T cell; DC, dendritic cell; MK, Megakaryocyte; LK, leukocyte; EI, Eosinophil; COX, Cyclooxygenase; PLA, phospholipase A; OSM, Oncostatin M; BAFF, B cell activating factor; RANKL, receptor activator of nuclear factor-κB ligand.

In addition to modulating the pathogenesis process in the RA synovium through secreting cytokines, monocytes/macrophages are capable of differentiating into osteoclast-like cells, which are believed to be unique in RA, playing a direct role in the bone destruction (Fujikawa et al., 1996; Gravallese et al., 2000). Collectively, main functions of macrophages/monocytes related to RA pathogenesis include 1) cell recruitment; 2) cell differentiation, activation and proliferation; 3) helping the antigen presenting cells and inducing both cellular and humoral autoimmunity; 4) neovascularization and angiogenesis; 5) cartilage and bone destruction. It is worth noting that, although the net outcome is promoting the disease, not all these functions are restricted to the disease aggregating side. The RA synovium also benefits from the anti-inflammatory cytokines produced by monocytes/macrophages. Furthermore, certain cytokines such as IL-6 and TGF-β exhibit dual functions, and could play opposite roles in the different stages of disease.

1.3.6 Synovial Fibroblasts (SF)

SF is a key type of pathogenic cells in the cellular network in the RA synovium. In healthy joints, SF provides various substances for nourishment and lubrication of the joints. It also contributes to the matrix remodeling and wound healing (Neumann et al., 2010). In RA, SF acquires activated phenotype, and secrets proinflammatory factors and enzymes contributing to the joint inflammation and structure destruction (Neumann et al., 2010). The activation of SF was suggested to be depending on the inflammatory environment and could be detected

shortly after the display of clinical signs (Lefèvre et al., 2009). Multiple factors are able to activate SF. Matrix and necrotic cell components released from the cartilage degradation in the early RA stage activates SFs by increasing their production of proinflammatory factors and MMPs as well as inducing their long-range migration potential (Brentano et al., 2009; Lefèvre et al., 2009; Müller-Ladner et al., 2007). Growth factors, inflammatory cytokines and chemokines were also reported to activate SFs and induce their proliferation, and cytokines and destructive enzyme secretion (Malemud, 2007; Müller-Ladner et al., 2007; Rico et al., 2010; Rosengren et al., 2010). In addition to soluble stimuli, several studies have demonstrated that the SFs are able to be activated by cell-cell contacting with endothelial cells or T cells through adhesion molecules (McGettrick et al., 2009; Müller-Ladner et al., 2007). Activated SFs assume multiple roles in the disease progression of RA. Firstly, SFs in RA joints (RASFs) have an increased proliferation rate and are resistance to apoptosis. IL-17 has been shown to promote the proliferation of RASFs directly, whereas down-regulating the adhesion molecule N-cadherin on the surface of SFs contributes to the proliferation by reducing their cell contact inhibition (NONOMURA et al., 2009; Zhang et al., 2009b). On the other hand, increased expression of apoptosis inhibitor molecules such as sentrin, FLICE-inhibitory protein (FLIP) and small ubiquitin-like modifier (SUMO)-1 in RASFs dampen their sensitivities to the apoptosis signaling (Ahn et al., 2010; Franz et al., 2000; Meinecke et al., 2009; Schedel et al., 2002). Accumulated RASFs due to the dysregulation of proliferation and apoptosis would cause synovial hyperplasia followed by local hypoxia, which eventually induce neoangiogenesis. Secondly, RASFs cause the cartilage and bone destruction in RA. Similar to macrophages, RASFs act as a source of inflammatory factors in the pathogenesis of RA. It produces a great mount of MMPs and cathepsin, which contribute to cartilage invasion (Hou et al., 2002; 2001; Müller-Ladner et al., 2007). RASFs also express high levels of RANKL which is essential in the bone erosions (Kim et al., 2007). Thirdly, activated RASFs are able to produce proangiogenic factors such as angiogenin, angiogenin-1, FGF-2, placenta growth factor (PIGF) and VEGF (Gravallese et al., 2003; Lioté et al., 2003; Presta et al., 2009; Yoo et al., 2009). Moreover, Lefevre et al. recently discovered a very unique role of RASFs contributing to disease spreading in RA(Lefèvre et al., 2009). The study showed that RASFs could crawl out from RA-affected joints, travel a long distance to healthy joints through blood, and cause cartilage degradation (Lefèvre et al., 2009).

1.3.7 Mast Cell, Dendritic Cell and Neutrophil

In addition to those cells mentioned above, mast cells (MCs), dendritic cells (DCs) and neutrophils are also found to be enriched in the RA synovium (Maruotti et al., 2006). MCs consist approximately 5% of the total synovial cells in RA joints(Maruotti et al., 2006). They produce a variety of cytokines that activating macrophages and SFs, and chemokines recruiting the inflammatory cells migrating into the RA joints (Maruotti et al., 2006). A recent study pointed out that, instead of Th 17 cells, MCs are the primary source of IL-17 in RA synovium (Hueber et al., 2010). DCs are also implicated in the local joint inflammation in RA. Both myeloid DCs (mDCs) and plasmacytoid DCs (pDCs) are presented in the synovial fluid from RA patients, and contribute to autoantigen presentation and proinflammatory cytokine production (Jongbloed et al., 2006; Zvaifler et al., 1985). Moreover, DCs are suggested to help the T effector cell differentiation and antibody production in RA joints by providing costimulatory signals and cytokines to the local T and B cells (Khan et al., 2009). The importance of neutrophils in RA is more than expected, since deletion of neutrophils protects the mice against arthritis in several experimental arthritis models (Nandakumar et al., 2003b; Tanaka et al., 2006; Wipke and Allen, 2001). Similar to MCs, neutrophils secrete proinflammatory cytokines and participate in the autoantibody-mediated RA pathogenesis (Németh and Mócsai, 2012).

As discussed above, the pathogenesis of RA is a complicated process mediated by numerous types of cells, cytokines and matrix enzymes. Studies focusing on role of individual cell and molecule in RA help us to have a big picture of disease progression of RA, and answer three important questions: (1) How is the immune response initiated? (2) How does the immune response lead to local joint inflammation? (3) How does the inflammation cause cartilage and bone destruction. Two models were proposed to explain the initiation of RA: B cell centric and T cell centric. In the B cell centric model, the B cells break tolerance in the lymph nodes and start to produce pathological autoantibodies. Because the blood-tissue barrier in the joints, unlike other tissues, lacks a basal membrane, it allows autoantibodies to pass through and form immune complex (ICs) with autoantigens in the joints. ICs then activate synovial phagocytes (macrophages) and the complement cascade, which triggers the release of cytokines and chemokines that stimulate the proliferation of synoviocytes and recruit inflammatory cells into

the joints (Benoist and Mathis, 2000). The T cell centric model argues that the disease is initiated by the activation of autoreactive T cells against synovial specific antigens in the joints (Benoist and Mathis, 2000). The activated T cells then secrete inflammatory cytokines, which trigger the synovial fibroblasts- and macrophages-mediated inflammation as mentioned above (Benoist and Mathis, 2000). The answers to the third question are less controversial. Cartilage degradation is caused by matrix enzymes that break down cartilage components, such as matrix metalloproteinases (MMPs) and A Distintergin And Metalloproteinase with Thrombospondin Motifs (ADAMTS) (McInnes and Schett, 2007). As disease progresses, inflammatory cytokines in the RA joints promote cartilage destruction by inducing the release of these enzymes from synovial fibroblasts, neutrophils, chondrocytes and osteoclasts. Osteoclasts are able to reabsorb bone tissue by secreting acid and a collagenase. The inflammatory cytokine environment within RA joints tends to drive the differentiation of osteoclasts from their precursor cells, thus enhance the bone erosion (McInnes and Schett, 2007) (Figure 1.2).

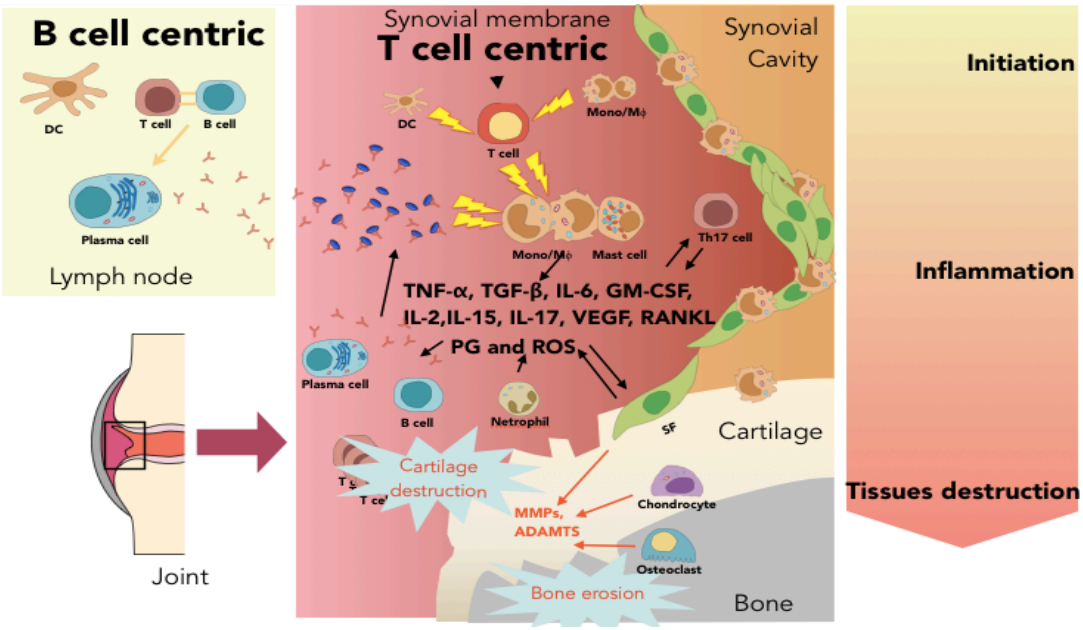

Figure 1.2. The pathogenesis of RA.

1.4 TNF-Like Ligand 1A and Death Receptor 3

TNF-like ligand 1A (TL1A), also known as TNFSF15 was first discovered in 2002. It binds to death receptor 3 (DR3, TNFRSF25) and Decoy receptor 3(DcR3, TR6). Interaction between

TL1A and DR3 triggers T cell proliferations and proinflammatory cytokine secretion. In the past ten years, emerging data have shown a strong relationship between TL1A and autoimmune diseases.

1.4.1 Characterization of DR3 and TL1A

DR3 (TNFRSF25, Apo3, WSL-1, TRAMP and LARD) was discovered in mid-90's with several papers published in high-profile journals. In 1996, Farrow and colleagues found a previously unknown protein which interacts specifically with the cytoplasmic portion of TNFR1 in HeLa cells based on the yeast two-hybrid assay, and designated it as WSL-1 (Kitson et al., 1996). The same protein was identified by several other groups at the same time though searching the cDNA libraries (Bodmer et al., 1997; Chinnaiyan et al., 1996; Marsters et al., 1996; Screaton et al., 1997). DR3 shares around 27% sequence identity to TNF-R1, and is by far a TNF family receptor most similar to TNF-R1 (Screaton et al., 1997). Mouse DR3 was later identified using labeled hDR3 cDNA as a probe (Wang et al., 2001). It shows great homology to its human counterpart (63% in total, and 94% in the death domain) (Wang et al., 2001). Both human and mouse full-length DR3s contain four cysteine rich domains (CRD), a transmembrane region and a death domain (Screaton et al., 1997; Wang et al., 2001). The crystal structure of DR3 has yet to be achieved. Shortened forms of DR3 are observed in both human and mice. There are at least 12 variants of human DR3 and 3 variants of murine DR3 (Figure 1.3) (Screaton et al., 1997; Wang et al., 2001). Variants missing one or more exon(s) would skip the transmembrane region or introduce an early stop codon before the transmembrane region. These variants become the secreted form of DR3 (hDR3-b, c, d, e, f, g, h, i and j; mDR3-b). Other variants such as hDR3-8 and mDR3-3 have intact transmembrane part and death domain, but lack one CRD in their extracellular domains (Screaton et al., 1997; Wang et al., 2001). Earlier attempts were failed to identify the ligand of DR3. However, these studies at least indicated that DR3 does not cross-react with other TNF family members other than its specific ligand (Bodmer et al., 2002; Marsters et al., 1996).

Human TL1A (hTL1A, 251aa) was first cloned and identified as the ligand of DR3 and TR6 (Migone et al., 2002). Like most of other TNF ligands, TL1A expresses on the cell surface, but also can be cleaved subsequently by metalloproteinase to become a soluble molecule. However, the cleavage of TL1A only happens on DC but not on T cells (Biener-Ramanujan et

al., 2010; Kim and Zhang, 2005; Migone et al., 2002). Prior to the discovery of full-length TL1A, a short form of hTL1A, TNF-like 1 (TL1;or vascular endothelial growth inhibitor, VEGI, 174aa) was discovered by two different groups using homology searches in the human umbilical vein endothelial cell (HUVEC) cDNA library (Tan et al., 1997; Zhai et al., 1999). Oddly, this TL1/VEGI does not have function unless the first 22aa from N-terminus are replaced with an IL-6 signal peptide (sVEGI), which converts it into a secreted protein. Later, several lines of evidence suggested that that the VEGI might be just a cloning artifact due to incompletely spliced nuclear RNA (Migone et al., 2002). In addition, VEGI-192 (192aa) and $TL1A_{V84\text{-}L251}$ were found and reported to induce cell growth arrest and apoptosis (Chew et al., 2002; Mück et al., 2010). The situation in the mouse is simple with no variant other than full-length TL1A (251aa) reported.

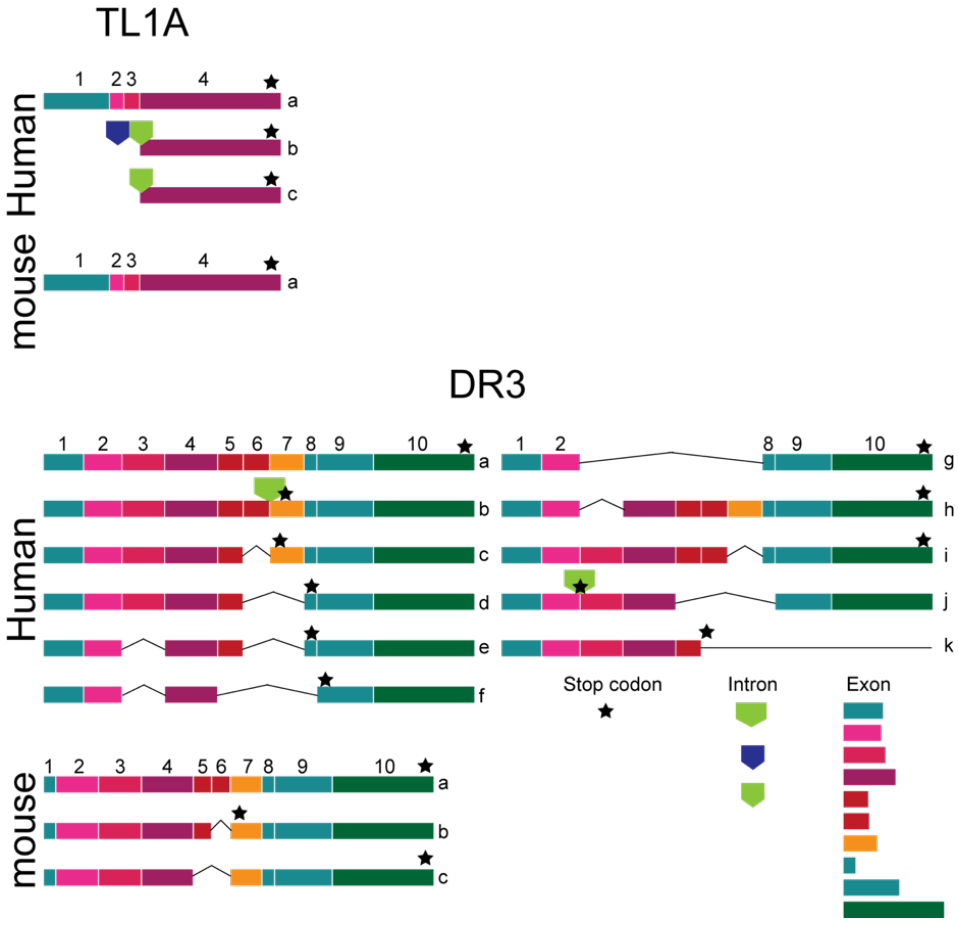

Figure 1.3. Isoforms of TL1A (upper panel) and DR3 (lower panel) in human and mouse. Adapted from Screaton et al. with modification (Screaton et al., 1997).

1.4.2 Expression of TL1A and DR3

Tissue-specific expression pattern of human DR3 was reported by several early studies with consistent results. There is an predominant 4kb transcript in the peripheral blood leukocytes (PBLs), spleen and thymus, and a mild expression in the intestine and colon in adults (Chinnaiyan et al., 1996; Kitson et al., 1996; Migone et al., 2002; Screaton et al., 1997). Additional larger transcripts at around 7 kb and 9 kb are observed in the brain, lung and kidney of the fetus (Marsters et al., 1996). Different expression patterns have been found between the human and mouse. There are three major transcripts (1.8 kb, 2.8 kb and 7.0 kb) in mice: two smaller transcripts are abundantly expressed in the spleen and thymus, and a bigger one is expressed in the brain, heart and kidney (Wang et al., 2001). Given that the DR3 transcriptions are found predominantly in the lymphoid organs, lymphocytes are analyzed for the expression of DR3 at the cell level. Screaton et al. detected DR3 mRNA in PBLs, B cells and CD4 or CD8 T cells, but not in macrophages and immortalized lymphocyte cell lines (Screaton et al., 1997). However, Bodmer et al. found DR3 proteins can also be detected in various human immortalized or tumor cell lines originated from epithelial, neuronal tissues (Bodmer et al., 1997). It is worth noting that although the total amount of DR3 mRNA in different types and status of lymphocytes might be the same, the splicing patterns could be remarkably different. For example, activated lymphocytes only express full-length DR3 (DR3-a) instead of short isoforms which are predominantly present in the resting lymphocytes (Screaton et al., 1997). Most of these short isoforms are secreted proteins, which are not able to transduce signals. It implies a potential mechanism to regulate the homeostasis of lymphocytes by expressing functional/non-functional isoforms of DR3.

TL1A mRNA is most abundant in the kidney, followed by the pancreas and prostate. Trace amount of transcriptions is found in the lung, intestine and thymus (Migone et al., 2002; Tan et al., 1997; Zhai et al., 1999). At the cellular level, only some endothelial cells (HUVEC and early passage of venous endothelial cells) and an erythroleukemic cell line TF1 cells were reported in early studies to express TL1A mRNA (Migone et al., 2002; Screaton et al., 1997; Zhai et al., 1999). Later studies revealed that monocytes/macrophages, dendritic cells, T cells and NKT cells also produce TL1A either upon stimulation or in the local inflammation sites (Bamias et al., 2006; Fang et al., 2008; Prehn et al., 2004; 2007; Takahashi et al., 2011).

1.4.3 Signaling Pathway of TL1A-DR3 Interaction

Before the ligand of DR3, TL1A, was identified, the downstream pathway of DR3 was already studied with ectopic expression systems. Signals through DR3 was found to be able to trigger activation of NF-κB and, at the same time, cell apoptosis (Bodmer et al., 1997; Chinnaiyan et al., 1996; Kitson et al., 1996; Marsters et al., 1996). Overexpression of DR3 in cell lines leads to apoptosis, while inhibiting the apoptosis made the effect of DR3 on NF-κB activation became more pronounced (Bodmer et al., 1997). As there is a high degree of homology between DR3 and TNFR1, TNFR1 downstream signaling molecules such as TRADD, RIP, FADD and ICE-like protease FLICE are potential candidates involved in the signaling pathways of DR3 (Baker and Reddy, 1998). Yeast-two hybrid studies showed that DR3 can form homodimers itself or heterodimers with TNFR1, but has very weak or no interaction with RIP, FADD or TRAFs (Bodmer et al., 1997; Chinnaiyan et al., 1996; Kitson et al., 1996). However, DR3, RIP and TRAF2 were found to be able to form a complex in the presence of TRADD, and induce NF-κB activation (Chinnaiyan et al., 1996). TRADD also serves as a bridge between the interaction of DR3 and FADD. FADD then recruits FLICE and triggers caspase activation and cell apoptosis (Chinnaiyan et al., 1996; Marsters et al., 1996). Unlike in the overexpression system, TL1A or DR3 agonistic antibody does not induce apoptosis of TF-1 cells that express endogenous DR3 at a physiological level. DR3 assembles the signaling complex containing the same adaptor protein as mentioned above, and triggers the NF-κB, ERK, JNK and p38-MAPK pathways, which play an anti-apoptotic role (Wen et al., 2003). On the other hand, DR3 has weaker associations with FADD, FLICE and caspase-8 in TF-1 cells compared to those cells overexpressing DR3 (Wen et al., 2003). Addition of TL1A-triggered anti-apoptotic protein c-IAP_2 expression, through activation of NF-κB, blocking the NF-κB activation or protein synthesis in TF-1 cell results in apoptosis (Wen et al., 2003).

1.4.4 Relationship Between TL1A-DR3 and Human Diseases

The expression of TL1A is mainly confined to the lymphoid organs, which suggest its essential role in the immune system. More importantly, in contrast to TNFR1, expression of TL1A is under tight regulations. In fact, accumulating evidence have suggested that increased expression of TL1A is related to the inflammation in certain autoimmune diseases.

Immunohistochemical analysis has shown the presence of intense signals of both DR3 and TL1A in surgical specimens from inflammatory bowel disease (IBD) patients. More specifically, TL1A is co-localized with lymphocytes and isolated LPMCs from Crohn's disease (CD) specimens, and with $CD138^+$ plasma cells of ulcerative colitis (UC) specimens (Bamias et al., 2003; Kamada et al., 2010). Circulating levels of TL1A in UC patients are also significantly higher than those in healthy controls (Bamias et al., 2010). Furthermore, It was reported that there is five-fold elevation of serum TL1A concentration in RA patients, with more pronounced increase seen in RF^+ patients or those having severe/terminal disease conditions (Bamias et al., 2008). TL1A is also expressed in RA synovium with similar distribution patterns of $CD68^+$ cells and $CD14^+$ cells, which surround the central area of fibrinoid necrosis; In accordance with Bamias's report, plasma cells expressing TL1A are occasionally presented in the RA synovial tissues (Cassatella et al., 2007). In acute cellular rejection specimens of renal allografts, upregulated DR3 and TL1A are observed in human renal tubular epithelial cells (TEC) and vascular endothelial cells (VEC), and in infiltrating mononuclear cells, respectively (Al-Lamki et al., 2003; 2008). Moreover, TL1A were reported to co-localize with monocytes/macrophages in the atherosclerotic plaques in carotid endoarteretomy tissues (Kang et al., 2005; Kim et al., 2008).

1.4.5 TL1A and T Cell Functions

T cells are known to express DR3 on their cell surface. They also produce a small amount of membrane TL1A but not its secreted form upon activation (Fang et al., 2008; Meylan et al., 2008; Papadakis et al., 2005; Prehn et al., 2004). Interestingly, TL1A elevation in T cells depends on the DR3 expression, as DR3 knockout T cells have defect in responding to TCR stimulation and producing TL1A (Meylan et al., 2008). TL1A affects T proliferation, cytokine secretion and differentiation through autocrine, but mainly paracrine signaling.

1.4.5.1 Proliferation

Exogenous TL1A has limited effect on the proliferation of T cells from human peripheral blood (PB) during activation. However, it enhances the expression of IL-2 receptors on these cells, and increases their responsiveness to IL-2-induced proliferation (Migone et al., 2002; Prehn et al., 2004). In contrast, murine T cells proliferate better in the presence of TL1A upon

suboptimal TCR stimulation (Meylan et al., 2008). TL1A can promote T effector cell as well as Treg cell proliferation *in vivo*, as transgenic TL1A expression in mice or TL1A-Ig administration to mice enhances the T cells expansion in lymphoid organs (Khan et al., 2013; Meylan et al., 2011a; Taraban et al., 2011). TL1A's costimulatory function in murine T cells is IL-2 dependent, and it is more pronounced on memory T cells(Bamias et al., 2006; Meylan et al., 2008).

1.4.5.2 Cytokine Production

TL1A increases the IFN-γ production in T cells from human peripheral blood or lamina propria mononuclear cells (LPMC) upon TCR stimulation (Migone et al., 2002; Prehn et al., 2004). TL1A was also reported to enhance the IFN-γ production in peripheral blood mononuclear cell (PBMC), and more significantly in isolated T cells, with the activation of IL-12 and IL-18 (Prehn et al., 2004). Later study revealed that two T cell subsets, $CCR9^{+}CD4^{+}$ and $CD161^{+}$ T cells, which resemble the gut T cell phenotypes, present increased production of IFN-γ upon activation in the presence of exogenous TL1A (Cohavy et al., 2011; Papadakis et al., 2005). Furthermore, $CCR9^{+}CD4^{+}$ T cells are able to express TL1A by themselves on the cell surface after stimulation, and this endogenous TL1A is enough to provide autocrine signaling to the cell surface DR3 in IL-12/IL-18-stimualted IFN-γ production (Papadakis et al., 2005). On the other hand, $CD161^{+}$ T cells only receive paracrine signaling of TL1A from monocyte and produce IFN-γ and IL-2, these T cells in turn promote the maturation of monocytes (Cohavy et al., 2011). TL1A has a similar effect on the induction of IFN-γ production in murine T cell (Bamias et al., 2006). However, TL1A only works in synergy with IL-12 for the induction of IFN-γ production in T cells, while its synergy with IL-18 is negligible (Bamias et al., 2006). Of note, secreted form of TL1A is more potent than its membrane form in terms of inducing IFN-γ production (Biener-Ramanujan et al., 2010; Kim and Zhang, 2005; Migone et al., 2002).

TL1A could also affect the cytokine production of NKT cells. It was reported that NKT cells from mouse lymph nodes express a high level of DR3， TL1A-DR3 could augment their Th2 cytokines produced in vivo; (Fang et al., 2008).

The T cell activation signal is critical in TL1A's costimulatory effect mentioned above. TL1A alone is not able to induce either proliferation or cytokine production of T cells. Memory T cell is, however, the exception due to its pre-deposited surface DR3. It is conceivable that cell activation contributes to TL1A's effect by upregulating its receptor expression levels on the target cell surface (Bamias et al., 2006; Cohavy et al., 2011; Papadakis et al., 2005). Interestingly, CD28 co-stimulation signal exhibit different effects on TL1A induced cytokine production of T cells. TL1A promotes the IL-4 production of murine T cells only under the condition with both anti-CD3 and anti-CD28 stimulations (Meylan et al., 2008). On the other hand, TL1A's effect on the upregulation of IFN-γ in T cells is diminished if T cells are activated by both CD3 and CD28 signalings, which give the cells the maximal stimulation (Meylan et al., 2008). Antigen-specific stimulation is a different story. In contrast to the antigen non-specific stimulation, the absence of TL1A-DR3 signaling in the OTII-Ova system results in less IL-2 and IL-4, but more IFN-γ production from the antigen specific T cells (Meylan et al., 2008).

1.4.6 TL1A and Macrophages

When DR3 was first identified, monocytes/macrophages were excluded from the cells expressing DR3 (Screaton et al., 1997). Later, *in vitro* studies showed DR3 was inducible in primary monocytes from peripheral blood (PB) upon either TNF-α or LPS stimulation (Kang et al., 2005). Furthermore, $CD14^+$ monocytes from human PB and two monocytic tumor cell lines (THP-1 and U937) were found constitutively expressing both DR3 and TL1A (Kang et al., 2005; Kim et al., 2008; Su et al., 2006). TL1A's effects on macrophages are mainly related to atherosclerosis. Treating THP-1 with agonistic anti-DR3 antibody or TL1A induced pro-atherogenic cytokines production, like TNF-α, IL-8, MMP-9 and monocyte chemoattractant protein (MCP)-1. In these cells, IFN-γ further increased the IL-8 production synergistically with TL1A (Kang et al., 2005; Su et al., 2006). A recent study further demonstrated, in both THP-1 cells and human monocyte-derived macrophages (HMDMs), that TL1A-DR3 signaling regulates key proteins governing the uptake and efflux of cholesterol, causing the imbalance in cholesterol homeostasis which eventually turns the macrophages into foam cells (McLaren et al., 2010).

In fact, monocytes/macrophages are more TL1A producers rather than TL1A responders. Stimulating monocytes from human PB with plate-bound IgG induce significant expression of TL1A mRNA and both soluble and membrane form of TL1A (Prehn et al., 2007). In line with this finding, Cassatella et al. showed that immune-complex, and precipitates from peripheral blood or synovial fluid of RF+/RA patients induced both membrane TL1A (mTL1A) and soluble TL1A (sTL1A) from cultured monocytes (Cassatella et al., 2007). Furthermore, IFN-γ or IL-4 promoted or abrogated the IC-simulated sTL1A production, respectively (Cassatella et al., 2007). Co-culture of monocytes and $CD4^+$ T cells primed with IL-12 and IL-18 produced more IFN-γ than $CD4^+$ T cells cultured alone; addition of IC significantly increased IFN-γ production in this system (Cassatella et al., 2007; Prehn et al., 2007). It was further demonstrated that the effect of the ICs on sTL1A production is through FcγrII and FcγrIII, but not FcγrI(Cassatella et al., 2007). Importantly, this IC-induced TL1A expression can be inhibited by TLR8 stimulation in an IFN-α independent manner (Saruta et al., 2009). Furthermore, many types of bacteria were reported to induced TL1A in monocytes and monocyte-derived DC partially through TLR, as a mechanism against enteric microorganisms (Shih et al., 2009). Macrophages from lamina propria (LP) affected by Crohn's disease (CD) upregulate membrane TL1A and IL-23 upon stimulation by commensal bacteria (Kamada et al., 2010; Uo et al., 2012). Mechanistically, LPS-induced TL1A expression in monocytes involves NF-κB-binding to the 5' flank region of *TL1A* (Endo et al., 2010).

1.4.7 TL1A and Dendritic Cells

Dendritic cell presents antigens and provides costimulatory signals to the T cell and it is the major source of endogenous TL1A. Human monocyte-derived DC (MDC) respond to stimulation of plate-bound IgG with rapid induction of TL1A mRNA, whereas LPS, Pam3CSK4, CBri1 flagellin and IFN-γ fail to induce TL1A in MDC (Prehn et al., 2007). Compared to the monocytes, human MDC express much less TL1A mRNA at peak of induction, but produce more soluble TL1A (Prehn et al., 2007). Accordantly, plate-bound Ig has similar effect on murine BMDC. TL1A mRNA of murine DC after stimulation reaches a peak level almost 200-folds higher than the basal level and that drops rapidly to the baseline (Meylan et al., 2008). In contrast to human MDC, murine BMDC also produce TL1A mRNA upon the stimulation of LPS, which acts through the TLR4/MyD88/TIRAP pathway (Meylan

et al., 2008). Expression of DR3 on DC is less known with Only one study reported a small subpopulation of CD11c+ cells from LN expressing DR3 (Fang et al., 2008)

1.4.8 TL1A Induced Apoptosis

Ectopic expression of DR3 in tumor cell lines, such as 293, MCF7 and 3T3 results in rapid apoptosis (Bodmer et al., 1997; Chinnaiyan et al., 1996; Kitson et al., 1996; Marsters et al., 1996). Addition of TL1A to TF-1 cells in the presence of cycloheximide (CHX) induces the activation of caspase and cell apoptosis. Surprisingly, primary activated T cells are resistant to TL1A-induced apoptosis in the presence or absence of CHX (Migone et al., 2002). Similar results are observed using IC-primed monocytes as the source of TL1A (Cassatella et al., 2007). Further study reveals that TL1A-induced NF-κB plays a counterbalanced role to TL1A-induced apoptosis, it increases the synthesis of anti-apoptotic molecule c-IAP2 that keeping TF-1 cells from apoptosis (Wen et al., 2003). The presence of protein synthesis inhibitor, CHX or NF-κB inhibitor breaks the balance and introduces apoptosis to TF-1 cells(Wen et al., 2003). Similarly, TL1A plays dual roles in tubular epithelial cells (TEC) in renal inflammation and injury. It activates NF-κB and upregulates TNFR2 to promote repairing the injury on one hand, and induces the caspase-3 activation and apoptosis of TEC on the other (Al-Lamki et al., 2008). Interestingly, the addition of TL1A in the cultured kidney of DR3 knockout mice fails to activate the NF-κB pathway and increase the apoptosis of TEC, but it is still able to induce TNFR2 (Al-Lamki et al., 2008). Furthermore, DR3 knockout TECs show elevated apoptosis under the cisplatin-induced renal injury, and TL1A could play a counter effect on TNF-induced apoptosis in TECs during renal injury (Al-Lamki et al., 2003).

1.4.9 TL1A-DR3 in Animal Disease Models

1.4.9.1 Inflammatory Bowel Disease

SAMP1/YitFc and $TNF^{\Delta ARE}$ mice develop spontaneous chronic ileitis resembling clinical features of human CD (Kontoyiannis et al., 1999; Rivera-Nieves et al., 2003). It was found that DR3 mRNA increases in terminal ileum of SAMP1/YitFc and $TNF^{\Delta ARE}$ mice with ileitis, and mucosal dendritic cells ($CD11c^{++}MHC\text{-}II^{+}$) are identified as a source of TL1A in the intestine of mice with spontaneous ileitis (Bamias et al., 2006).

Upregulated levels of TL1A and DR3 mRNA have been found in the mesenteric LN (mLN) and colon in the chronic DSS mice model. Stimulating $CD4^+$ T cells from mLN or LPMC with TL1A alone induce a significant amount of IFN-γ, IL-6 and IL-17, which is further increased in the presence of IL-12 or IL-23 (Takedatsu et al., 2008). Treatment before or after the onset of the disease with anti-TL1A antibody prevents or alleviates the clinical and pathological scores of DSS- and TNBS-induced colitis (Meylan et al., 2011a; Takedatsu et al., 2008).

1.4.9.2 Experimental Allergic Asthma

Meylan et al. showed TL1A-DR3 signaling was essential in developing experimental allergic asthma in mice(Meylan et al., 2008). Reduced disease severity was observed in DR3 knockout mice, accompanied by reduced number of T cells, NKT cells and eosinophils cells, and pathogenic Th2 cytokines in the lung (Meylan et al., 2008). They also pinpointed that the DR3 signaling in T cells was the critical requirement in this disease model (Meylan et al., 2008). Another group reported an antagonistic anti-DR3 antibody (L4G6) to prevent experimental allergic lung inflammation in mice by inhibiting the eosinophils exudation and pathogenic Th2 cytokine production (Fang et al., 2008). Although TL1A had been shown to be able to block IL-4, 5, 10 and 13 production in $CD4^+$ T cells from the lung, NKT cells were believed, in this study, to be the principle mediator of the TL1A blocking effect, as NKT-deficient mice adoptive transferred with DR3-domain negative transgenic NKT cells were resistant in the disease-transfer lung inflammation model (Fang et al., 2008). The same group later found an agonistic anti-TL1A antibody (4C12) strongly induced specific expansion of Treg cells *in vivo*. Treating mice before experimental allergic lung inflammation with 4C12 increased the ratio of Treg and T effector, suppressed the Th2 cytokine secretion and prevented the disease (Schreiber et al., 2010). They also showed that a format of recombinant TL1A with an Ig tag (TL1A-Ig) had similar effects (Khan et al., 2013). Since it appeared to be controversy that both agonist and antagonistic anti-DR3 antibodies were able to inhibit the allergic lung inflammation, the author claimed that the sequences of anti-DR3 treatment and immunization of OVA played a critical role (Schreiber et al., 2010).

1.4.9.3 Experimental Autoimmune Encephalomyelitis (EAE)

EAE is an experimental models for human multiple sclerosis (MS). It is also a very common model in mice to examine Th1 and Th17 immune responses (Constantinescu et al., 2011). EAE has been assessed in both TL1A knockout and DR3 knockout mice. DR3 knockout mice have drastically reduced clinical scores and fewer T cells, especially Th1 cells accumulated in CNS, compared to their WT counterparts (Meylan et al., 2008).

Roles of TL1A in the inflammatory responses were summarized in Figure 1.4.

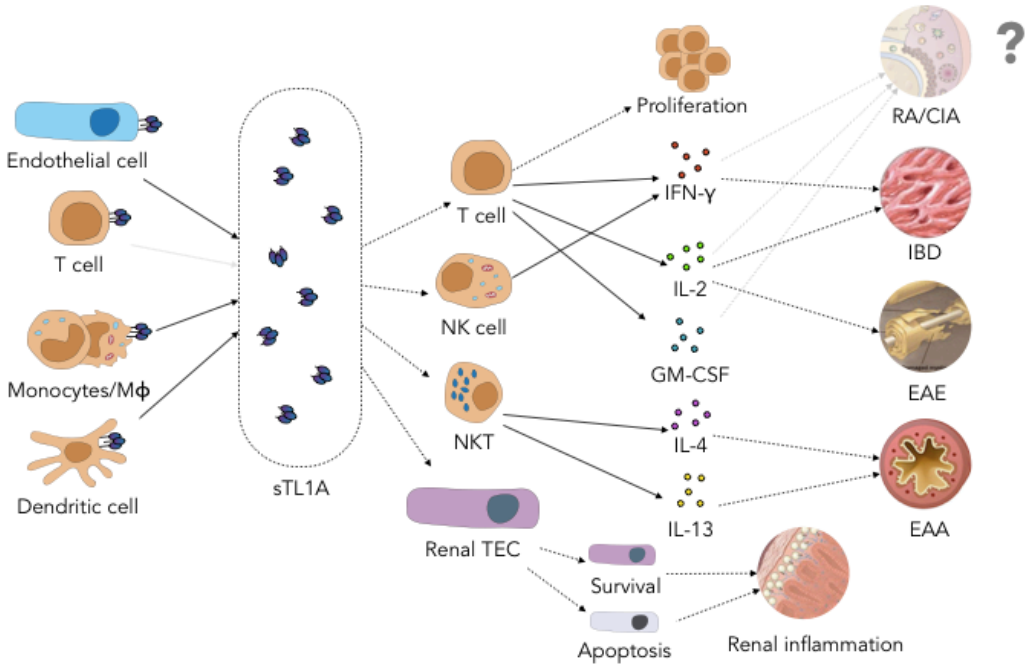

Figure 1.4. Role of TL1A in the inflammatory responses. RA: Rheumatoid Arthritis; CIA: Collagen indueced arthritis; IBD: Inflammatory Bowel Diesease; MS: Multiple sclerosis. EAA: Experimental allergic asthma.

1.5 Pno1

Pno1, also called Dim2, Yor145C and RPR20 in yeasts, was first described in 2002 as a binding partner of Nob1 in the maturation of proteasomes (Tone et al., 2000). Pno1 is highly conserved across different species. The mouse and yeast share 52% identity and 46.7% homology in protein sequence (Figure 1.4). Murine Pno1 mRNA contains a 746-nt open-reading frame with 7 exons; and Pno1 protein comprises 248 amino acid residues, with a molecule weight around 30kDa.

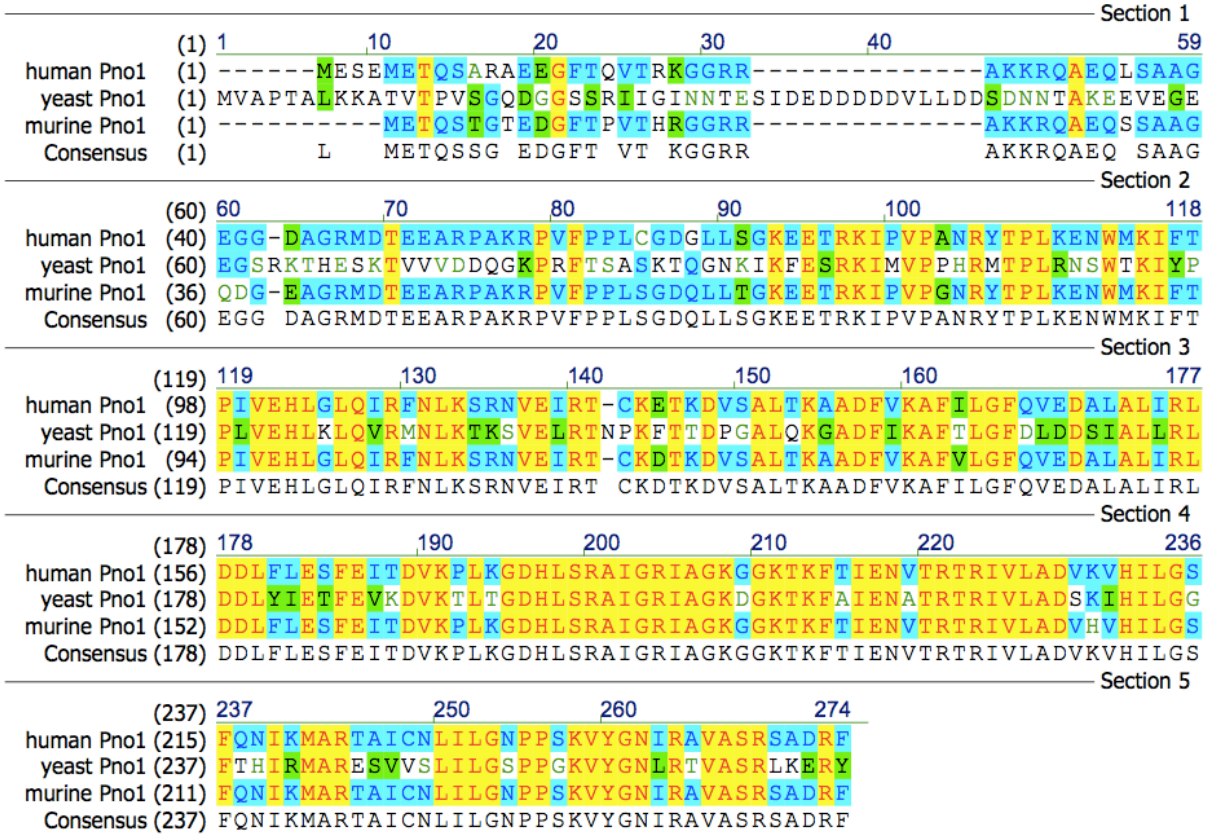

Figure 1.5. Comparison of yeast, human and mouse Pno1 amino acid sequences.

1.5.1 Subcellular Location

The subcellular location of Pno1 is highly dynamic but strictly regulated according to the cell growth phases (Vanrobays et al., 2004). It presents equally in both the nucleus and cytoplasm through the log growth phase, but is progressively trafficked into the nucleus at the transitional phase, and eventually is condensed into a small dot in the nucleus in the stationary phase (Vanrobays et al., 2004). Pno1 is quickly expanded to the cytoplasm and regain the equal distribution pattern once the cells transit to the log growth phase (Vanrobays et al., 2004). Additionally, the change of subcellular location of Pno1 is accompanied by its shifting in the sedimentation fractions (Vanrobays et al., 2004). It has been suggested that the dynamic distribution is due to the location transition in the process of small ribosomal RNA maturation (Vanrobays et al., 2004). Subsequent studies have indicated that the translocation of Pno1 to the nucleus is in response to nutritional, osmotic and oxidative stress controlled by the mammalian target of rapamycin (mTOR) pathway (Vanrobays et al., 2008).

1.5.2 Pno1 and Ribosome

Ribosome is one of the fundamental molecular machines in all the living cells as being the primary site for the protein synthesis. The eukaryotes ribosome comprises a small (40S) and a large (60s) subunit. During the protein translation process, 40S unit uses mRNA as templates matching the codon with specific tRNA, which carries the amino acid. In the large subunit, amino acid is then added to a growing polypeptide, which is eventually decorated and folded into protein. A mature ribosome has 4 RNAs (5.8S, 18S, 25S/28S and 5S) and around 80 ribosome proteins (Tschochner and Hurt, 2003).

Ribosome assembly is a multistep but highly regulated process involving as many as 200 assembly factors, many of which associate with the pre-RNA transiently or persist for certain period of time during the assembly, but are not present in mature ribosome (Tschochner and Hurt, 2003). Three rRNAs (5.8S, 18S and 25S/28S) are initially produced as a single transcript by RNA polymerase I (Pol I). There will be sequential cleavages at the 5' end of the single transcript at site A_0 and A_1, followed by a third cut at A_2 to release the 20S fragment into the cytoplasm. The remaining part eventually will be cleaved multiple times and mature into 5.8S and 25S/28S rRNA, which form 60S large subunit. The 20S will be cleaved again at site D close to the 3' end to generate 18S rRNA for 40S small subunit (Tschochner and Hurt, 2003).

The protein sequence of Pno1 has a KH domain, which is known to bind to RNAs (Gibson et al., 1993). As expected, Pno1 is found to be essential in the small ribosome subunit synthesis in the yeast (Senapin et al., 2003; Vanrobays et al., 2004). It is associated with Dim1p and ensures the correct cleavage and dimethylation in the early pre-RNA. Another study discovered that the KH domain of Pno1 is involved in the interaction between Pno1 and Nob1. It is suggested that the Pno1 could enhance the RNA binding ability of Nob1 and increase its cleavage activity at site D (Fatica et al., 2003; Lamanna and Karbstein, 2009; Pertschy et al., 2009; Woolls et al., 2011). In contrast, the interactions between Pno1 and Dim1 have been later proved to be indirect through kinases Rio2 (Campbell and Karbstein, 2011). Nevertheless, Pno1 is crucial to the ribosome assembly as deficiency of Pno1 in the yeast

abolishes 18S rRNA generation and lead to lethality (Senapin et al., 2003; Vanrobays et al., 2004; Woolls et al., 2011).

1.5.3 Pno1 and Proteasome

Proteasome is essential large protein complex responsible for ATP-dependent degradation of proteins tagged with ubiquitin. Every 26S proteasome contains a 20S proteolytic core particle (CP) and a 19S regulatory particle (RP). CP comprises 4 heptameric rings, stacking up to form a barrel-like structure. There are two identical inner rings (also called β ring) with 7 different β units of each, providing 6 catalytic sites in total (Groll et al., 1997). β1, β2 and β5 are those subunits contain catalytic sites with distinct proteolytic activities, referred as caspase-, trypsin- and chymotrypsin-like activities, respectively (Groll et al., 2005). The two outer rings share a similar structure as the β-ring, consisting 7 different α subunits. Regulatory particle (RP) is composed of more than 19 subunits. Its functions include recognition of ubiquitylated proteins, and unfolding and transporting those proteins into the 20S proteasome (Murata et al., 2009).

Assembly of proteasome requires help from different sets of chaperone proteins and consumes a great amount of energy. The assembly of CP is suggested to start from α-ring formation, and followed by β-ring. Four proteasome-assembling chaperones (PAC, Pba in the yeast) and ubiquitin-mediated proteolysis 1 (UMP1, Pomp in mammalian cells) are the major chaperone proteins assisting the assembly process (Murata et al., 2009). Four PACs form two heterodimeric chaperone complexes, known as PAC1-PAC2 and PAC3-PAC4. PAC1-PAC2 binds α5 and α7 to help α-ring formation and avoid aggregation of the two α-rings. PAC3-PAC4, however, is responsible of error checking, assuring the correct arrangement of each α-subunit. It is released from the α-ring during β-ring formation. β-ring formation is characterized by the existence of β subunit precursor peptides; and the precise sequential order of assembling, which is maintained by UMP1 (Gallastegui and Groll, 2010; Murata et al., 2009). In addition, UMP1 is required to initiate β-ring formation in mammal cells but not in yeasts. Once the β-ring formation is finished, two half-proteasomes (an α-ring plus a β-ring) dimerize into 20S proteasomes. UMP1 as well as PAC1-PAC2 are degraded at this step. RP contains a lid complex and a base complex, each of which is assembled individually and joint

together afterwards. Nas2, Nas6, Hsm3 and Rpn14 are four chaperone proteins required for the assembly of the base complex. Each chaperone protein binds to certain RP subunits and form three intermediates. These intermediates are subsequently joint together with two other RP subunits to complete the base complex assembly (Gallastegui and Groll, 2010). Similar to the base complex, two sets of lid subunits are formed independently and joint together with two additional RP proteins to generate the lid complex (Gallastegui and Groll, 2010). Lid and base complex then attach together through a regulatory particle non-ATPase 10(RPn10) to generate RP. Finally, RP is mounted on one or both end of 20S CP to form 26S proteasomes.

The role of Nob1 in rRNA maturation as a nuclease has been discussed above. In fact, Nob1 was first discovered to be able to interact with two subunits of regulatory particle of 26S proteasome, Rpn12 and regulatory particle triple-A protein1 (Rpt1), implicating its involvement in the proteasome activity (Tone et al., 2000). Subsequent study found Nob1's role in 26S proteasome assembly, as mutation of Nob1 causes the accumulation of precursors of β-subunits and defects of proteasome activity (Tone and Toh-E, 2002). Pno1 is proposed in this study to participate in the assembly of proteasome though its interaction with Nob1 (Tone and Toh-E, 2002). Mutation of Pno1 diminishes the integration of β2-subunit and β5-subunit into 20S CP, and causes the dislocation of α4-subunit (Tone and Toh-E, 2002).

1.5.4 Proteasome and Plasma Cells

Plasma cells are terminally differentiated B cells that participate in humoral immune responses by secreting a large amount of antibodies. There are two types of plasma cells: short-lived plasma cells (SLPC) and Long-lived plasma cells (LLPC). Certain antigen-stimulated B cells, with or without assistance from T cells, proliferate as plasma blasts in extra-follicular foci and differentiate into SLPC (MacLennan et al., 2003). SLPCs produce antigen specific IgM or IgG on site, and last for a few days up to a couple of weeks before going apoptosis (Smith et al., 1996). In contrast, LLPC could survive for several years or persist for a lifetime. Majority of LLPC are derived from B cells that go through the affinity maturation process in the germinal center. Interestingly, recent report has showed LLPCs can also be generated in the absence of germinal center (Bortnick et al., 2012; Sze et al., 2000).

The maturation of plasma cells is accompanied by down-regulation of typical B cell surface markers, such as Ig, B220, CD19, MHC-II and costimulatory molecule CD86, and up-regulation of CD138 (Oracki et al., 2010). B cells also go through dramatic morphological changes to become plasma cells. The size of individual cells is enlarged, especially the cytoplasmic part. Extensive Golgi apparatus and endoplasmic reticulum (ER) occupy the plasma cell cytosol, providing a physiological basis of producing large amounts of antibodies (Gass et al., 2004). To cope with the challenge of mass production of antibody, plasma cells acquire a unique unfolded protein response (UPR) (Gass et al., 2002). In regular cells, when there are overloaded unfolded or missfolded proteins in the ER, the UPR is activated to alleviate the ER stress by decreasing the protein folding load and increasing the folding capacity. Concomitantly, those misfolded protein failed in the re-folding process are retrogradely translocated from ER, and ubiquitylated and shredded in the 26S proteasome (Kostova and Wolf, 2003). If the stress cannot be mitigated overtime, the UPR signaling will eventually induce cell apoptosis (Walter and Ron, 2011). During the B cell differentiation to plasma cells, UPR is triggered before the large-scale antibody production rather than being induced by the ER stress. ER chaperone expression levels are enhanced to assist the protein folding, and the signaling in the plasma cells do not induce the expression of C/EBP homologous protein (CHOP), a transcription factor linked to apoptosis (Gass et al., 2002; van Anken et al., 2003; Wiest et al., 1990). At the molecular level, the initiation of plasma cells starts with the repression of PAX5 gene, and upregulation of transcription factor Blimp-1, a "master regulator" of plasma cells (Kallies et al., 2007). Blimp-1 blocks the B cells from entering the cell cycle, and activates XBP-1 production as well as ATF6 and IL-4 production (Lin et al.). XBP-1 rules the late stage of plasma cell differentiation, and it is crucial to the large scale antibody production machinery (Iwakoshi et al., 2003; Martins and Calame, 2008; Shaffer et al., 2004; Todd et al., 2009).

Proteasome inhibitors (PI) have been reported to be able to induce apoptosis of multiple myeloma (MM) cells, plasma cell tumors, regardless the elevated expression of UPR survival components in these cells (Lee et al., 2003; Obeng et al., 2006). The mechanisms have been elucidated by two research groups with different explanations. Glimcher's group has claimed that the PI increase the ER stress, but dampen the UPR through impairing the generation of an

active form of XBP-1 while sustaining the inactive form. Another group has suggested that the pro-apoptotic effect by PI is mediated by rapid induction of sets of terminal UPR components including Bax, PERK (a type 1 transmembrane serine/threonine protein kinase) and ATF4, which further induce the expression of CHOP, and lead to the ER stress-induced apoptosis (Harding et al., 2000; 1999; Meister et al., 2007; Obeng et al., 2006).

A later study has found that Bortezomib, a food and drug administration (FDA) proved PI to treat multiple myeloma, also induces apoptosis of normal plasma cells *in vitro*, and causes a transient reduction of plasma cells in bone marrow and alters alloantibody production and specificities (Perry et al., 2009). Furthermore, multiple studies have demonstrated the therapeutic roles of Bortezomib in autoimmune disease. Bortezomib is able to remove anti-dsDNA-Ab-producing autoantibody SLPC and LLPC in mice under two experimental lupus-like disease models, reducing the clinical symptoms and prolonging the survival of affected mice(Neubert et al., 2008). Similar effects are observed in rat with experimental autoimmune myasthenia gravis (EAMG) after Bortezomib treatment (Gomez et al., 2011).

1.6 Rational for Present Studies

RA is the most common from of inflammatory arthritis, which primarily affects the joints and their surrounding tissues. Great achievements have been made during the past two decades in understanding the pathogenic mechanisms of RA. Studies with patients and animal models have found that autoantibodies, cytokines and tissue-destructive enzymes produced by the infiltrating cells and local mesenchymal cells within the synovium are important mediators of the persisting synovitis and joint destruction. These findings helped us to design therapeutic strategies based on inhibiting these key molecules or removing the cells producing them. For examples, therapeutic drugs targeting TNF-α and IL-6, and B cell surface antigens CD20 have been accepted by the ACR as recommended biological DMARDS to treat RA. However, since these cytokines play vital roles in our immune system, blocking their activities often increase the chance of infections and malignancies. Treatment with drugs that eliminating B cells results similar side effects. Furthermore, current DMARDS sometimes fail or produce partial response in certain patients. Therefore, great efforts are still needed to keep looking for new molecular candidates to develop safer and more efficacious RA therapies. As discussed in

Section 1.4, multiple studies suggest the implication of TL1A in the autoimmune disease; however, its role in RA has not been previously investigated. In section 1.5, two recent studies have shown that proteasome inhibitors were effective in protecting mice from experimental autoimmune diseases. Since Pno1 is essential for the proteasome assembly, blocking its function might ameliorate the autoantibody production in RA by disrupting the proteasome assembly.

Here, we chose these two molecules from different categories to investigate their roles in the pathogenesis of RA in order to provide information for rational design of better therapeutic strategies based on these molecules.

CHAPTER 2 ARTICLE-1

As discussed in Section 1.3, TNF superfamily members play vital roles in the pathogenesis of RA. They are involved in the activation, survival, apoptosis and cytokine production of various types of cells implicated in RA. In section 1.4, we reviewed the research progress of TL1A, a novel TNF superfamily member. Multiple studies have suggested that this molecule plays a vicious role in the EAA, EAE and animal disease models of IBD. A recent study has further shown the presence of TL1A in synovial tissue of RA patients. However, direct evidence showing that TL1A promotes the pathogenesis of RA are yet to be established. In this part, *in vivo* studies using CIA mouse models were performed to confirm the pathogenic roles of TL1A in RA. Furthermore, *in vitro* approaches were used to investigate the mechanisms underlying the effect of TL1A.

This work has been published in ***The Journal of Immunology***.

Zhang J, **Wang X (Equal contributor)**, Fahmi H, Wojcik S, Fikes J, Yu Y, Wu J and Luo H. (2009) Role of TL1A in the Pathogenesis of Rheumatoid Arthritis. ***The Journal of Immunology*** 183, 5350–5357

2.1 Role of TL1A in the Pathogenesis of Rheumatoid Arthritis

[#]Jun Zhang[2], *Xuehai Wang[2], *Hassan Fahmi, [#]Susan Wolfe, [#]Jim Fikes, [+]Youhua Yu, *[+]Jiangping Wu, and *Hongyu Luo

From the [*]Research Center and [+]Nephrology Service, Centre hospitalier de l'Université de Montréal (CHUM), Notre-Dame Hospital, Montreal, Quebec, Canada; [#]Human Genome Sciences, Inc., Rockville, MD, USA; [+]Experimental Research Center, China Academy of Chinese Medical Sciences, Beijing, China

Address correspondence to: Dr. Jun Zhang, currently at the Department of Inflammation/Immunology, Pfizer Inc., 700 Chesterfield Parkway W. Chestfield, MO 63017, Telephone: (636) 247-4604; or Dr. Hongyu Luo, Laboratory of Immunology, Research Centre, CHUM, Notre-Dame Hospital, Pavillion DeSève, Room Y-5612, 1560 Sherbrooke Street East, Montreal, Quebec H2L 4M1, Canada, Telephone: (514) 890-8000 Ext. 27421, Fax: (514) 412-7596.

Running title: TL1A aggravates rheumatoid arthritis
Key words: TL1A, DR3, collagen-induced rheumatoid arthritis, synovial fibroblasts, IL-17

Footnotes

This work was supported by grants from the Canadian Institutes of Health Research (CIHR) to H.L. (MOP79565 and IMH 79565). It was also supported by grants from the CIHR (MOP57697, MOP69089, and PPP85159), the Kidney Foundation of Canada, the Heart and Stroke Foundation of Quebec, the Quebec Ministry of Economic Development, Innovation and Exportation (PSR-SIIRI-069) and the J.-Louis Levesque Foundation to J.W. It was supported in addition by a group grant from Fonds de la recherche en santé du Québec (FRSQ) for Transfusional and Hemovigilance Medical Research to J.W.

[2] J.Z. and X.W. contributed equally to this work.

Abstract

TL1A, a member of the TNF superfamily, is the ligand of DR3 and DcR3. Several types of cells, such as endothelial cells, monocytes/macrophages, dendritic cells and CD4 and CD8 T cells, are capable of producing this cytokine. In present study, we demonstrated that TL1A aggravated collagen-induced arthritis (CIA) in mice. It increased CIA penetrance and clinical scores as well as the severity of the pathological findings. TL1A administration led to the occurrence of multiple enlarged germinal centers in the spleen, and boosted serum anti-collagen Ab titers in vivo. In vitro, TL1A augmented TNF-α production by T cells upon TCR ligation, and greatly enhanced Th17 differentiation and IL-17 production. We further showed that, human RA synovial fluids had elevated TL1A titres, and human chrondrocytes and synovial fibroblasts were capable of secreting TL1A upon TNF-α or IL-1β stimulation. Taken together, these data suggest that and TL1A secretion in lymphoid organs might contribute to RA initiation by promoting auto-antibody production, and TL1A secretion stimulated by inflammatory cytokines in rheumatoid arthritis (RA) joints might be a part of a vicious circle that aggravates RA pathogenesis,

Introduction

Rheumatoid arthritis (RA) is a chronic autoimmune disease affecting mainly the small joints. It is characterized by persistent inflammation of multiple joints. Pathologically, the major finding is synovial hyperplasia, which is mainly composed of fibroblast-like synoviocytes combined with an infiltration of a large proportion of T lymphocytes and monocytes[1]. Antibodies appear to be important in causing synovitis[2]. In addition, the production of various cytokines within the synovium plays a crucial role in the inflammatory process. TNF-α and IL-1β are considered important mediators of inflammation and tissue destruction in RA[3]. Recently, it has been found that IL-17 plays a significant part in RA pathogenesis[4]. It induces local TNF-α, IL-1β and IL-6 production in the joints. These pathological changes in the joints lead to the eventual cartilage and bones damages and loss of mobility at a later stage of the disease[5-7].

TL1A, a member of the TNF superfamily of cytokines, is designated as TNFSF15. It is coded by the *TNFSF15* gene located on chromosome 9q32 in humans. TL1A is coded by all 4 exons of *TNFSF15*. Its mRNA is 2.02 knt in length, containing an open reading frame of 251 amino acids. However, the 3.3-kb continuous DNA sequence from the beginning of the 3rd exon until the end of the 4th exon of *TNFSF15* encodes a different protein called vascular endothelial growth inhibitor, or TL1[8]. X-ray crystallography shows that TL1A proteins form homotrimers in solution[9], like other TNF family members.

Initially, TL1A was believed to be produced only by endothelial cells, and its production was induced by TNF-α and IL-1β[s]. Further studies have shown that it is also secreted by monocytes/macrophages and dendritic cells upon immune complex stimulation, and constitutively expressed in NKT cells; it is also present in human synovial tissue and exudates[10-12]. In certain chronic inflammatory conditions, such as Crohn's disease, CD4 and CD8 T cells produce this cytokine [13]. A repertoire of all TL1A-producing cells has not yet been completed.

TL1A binds to two proteins, DcR3 and DR3, both of them being TNFR family members. DcR3 is a secreted protein. As such, it does not transduce signals into cells, but simply interferes with interactions between several ligands and receptors, such as FasL/Fas, LIGHT/LTβR, LIGHT/HVEM, and TL1A/DR3[8,14-16]. The *DR3* gene produces several alternative splicing variants, which can be membrane-bound as well as in secreted form[17,18]. DR3 is expressed on T cells and NK cells, and is upregulated upon their activation[17,19]. Its expression is induced by TGFβ1 and, hence, Th17 cells present especially high DR3 levels[20]. It is detectable in B cells, osteocytes and renal tubule epithelial cells[21-23]. In DR3 null mutant mice, thymocytes experience compromised negative selection[24]. T- and B-cell populations are normal in the periphery lymphoid organs of these mice, but detailed studies on the pathogenesis of various diseases have not been conducted.

Soluble TL1A increases IFN-γ and GM-CSF secretion in T cells with TCR ligation, and it synergizes with IL-12 to enhance IFN-γ production in T and NK cells[25]. TL1A enhances the ability of NKT cells to secrete IL-13. Mice receiving anti-TL1A Ab or transgenic mice with T cells/NK cells expressing dominant negative TL1A are resistant to lung inflammation[10]. TL1A also promotes adhesion of monocytes to endothelial cells, and presumably enhances their exudates to extravascular space[26]. Intracellular IL-17-positive CD4 cells are increased when TL1A is present in a condition favoring Th17 differentiation. Conversely, TL1A null mutant DC cells have a reduced capability of supporting Th17 cell differentiation[20]. Furthermore, TL1A null mutant mice are resistant to experimental autoimmune encephalitis induction, which requires Th17[20]. These in vitro and in vivo data have demonstrated that TL1A is an important mediator of inflammation.

In this study, we explored TL1A's role in RA pathogenesis. TL1A administration exacerbated collagen-induced arthritis (CIA) and augmented serum Abs against collagen in a mouse model. Further mechanistic experiments showed that fibroblast-like synoviocytes were capable of producing TL1A upon TNF-α and IL-1β stimulation, and TL1A, in turn, enhanced

the production of inflammatory cytokines, including TNF-α and IL-17, by T cells. The implications of these findings in RA pathogenesis are discussed.

Materials and methods

Reagents

Recombinant human TL1A (aa 72-251) was produced in CHO cells and subsequently processed to more than 95% purity, as described earlier[8]. Recombinant mouse IL-1β, TNF-α, TGF-β1, and IL-6 were purchased from R & D systems (Minneapolis, MN). Neutralizing mAbs against IFN-γ and IL-4 were obtained from R & D Systems. PE-conjugated anti-IL-17 mAb was from BD Biosciences (San Jose, CA).

Mouse CIA model

Eight to 10-wk-old DBA/1LacJ male mice (The Jackson Laboratory, Bar Harbor, ME) were used for this study. The Human Genome Sciences' Institutional Animal Care and Use Committee approved all experimental protocols used in this work.

The scheme of the mouse CIA model is depicted in Fig. 1A. Briefly, DBA/1LacJ mice were immunized at the base of the tail with 100 μg of bovine type II collagen (BTIIC; Chondrex, Redmond, WA), which was emulsified in equal volumes of Freund's complete adjuvant (2 mg/ml *Mycobacterium tuberculosis*, strain H37Ra; Difco, Detroit, MI) on day 0. Three groups of immunized mice were then injected i.p. daily with buffer (PBS), TL1A (1 mg/kg/day) or heat-denatured TL1A (HD-TL1A), respectively, from day 5 to 20. As a positive control, a fourth group was challenged on day 15 with a single s.c. injection of LPS (60 mg/mouse). The mice were examined for the development and severity of arthritis from day 5 to 50. Disease severity was scored on a scale from 0 to 3 by visual inspection of paws, and score criteria were as follows: 0.5, one or more swollen digits; 1.0, entire paw swollen; 2.0, deformity following acute edema; and 3.0, ankylosis, i.e., total loss of joint function. The scoring was done by two independent observers without knowledge of the experimental groups. The scores for each of four paws were added together to give a final score, such that the maximal severity score was 12 for a given mouse. The mice were considered as having arthritis if their clinical score was equal to or above 0.5.

Histology

After sacrificing animal on day 50, fore-paws and hind-paws (including the paw and ankle) were surgically removed and fixed in 10% buffered formalin. Following decalcification in 5% formic acid, the specimens were processed for paraffin embedding. Tissue sections (7 μm) that were stained with hematoxylin and eosin, were scored by a certified pathologist for mean inflammation, pannus formation, cartilage damage, and bone damage. The overall score was based on a set of three to four joints per animal and all were scored on a 0–5 scale, as previously described[27]. A mean score for each animal was determined for each parameter, and these were averaged to determine group means.

Chondrocyte culture

Human osteoarthritis (OA) cartilage samples from femoral condyles and tibial plateaus were obtained from OA patients undergoing total knee replacement (n = 4; mean ± SD of age: 64 ± 11 years). All OA patients were diagnosed according to the criteria developed by the American College of Rheumatology Diagnostic Subcommittee for OA[28]. At the time of surgery, the patients had symptomatic disease requiring medical treatment in the form of non-steroidal anti-inflammatory drugs or selective COX-2 inhibitors. Patients who had received intraarticular injections of steroids were excluded. The Clinical Research Ethics Committee of Notre-Dame Hospital approved the study protocol and the use of human articular tissues.

Chondrocytes were released from cartilage by sequential enzymatic digestion, as described previously [29][36]. In brief, this consisted of 2 mg/ml pronase for 1 h followed by 1 mg/ml type IV collagenase (Sigma, St. Louis, MO) for 6 h at 37°C in DMEM and antibiotics (100 U/ml penicillin, 100 μg/ml streptomycin). The digested tissue was briefly centrifuged and the pellet was washed. The isolated chondrocytes were seeded at high density in tissue culture flasks and cultured in DMEM supplemented with 10% heat-inactivated FCS. At confluence, the chondrocytes were detached, seeded at high density, and allowed to grow in DMEM, supplemented as above. The culture medium was changed every second day, and 24 h before the experiment, the cells were incubated in fresh medium containing 0.5% FCS. Only first-passage chondrocytes were used.

Synovial fibroblast (SF) culture

Human SF was isolated from synovial membranes obtained from OA patients undergoing total knee replacement as described above. They were released by sequential enzymatic digestion with 1 mg/ml pronase (Roche Applied Science, Laval, Quebec, Canada) for 1 h, followed by 6-h incubation with 2 mg/ml type IV collagenase (Sigma) at 37°C in DMEM supplemented with 10% heat-inactivated FCS, 100 U/ml penicillin and 100 μg/ml streptomycin. The cells were incubated for 1 h at 37°C in Primaria 3824 tissue culture flasks (Falcon, Lincoln Park, NJ), allowing the adherence of nonfibroblastic cells possibly present in the cell preparation. After removing the adherent nonfibroblastic cells, non-adherent cells were seeded in tissue culture flasks and cultured until confluence in DMEM supplemented with 10% FCS and antibiotics. Only cells between passages 3 and 7 were used.

Human synovial fluids

Normal human synovial fluids were obtained at necropsy, within 12 hours of death, from 4 donors (54 ± 8 years,) with no history of arthritic diseases. RA synovial fluids were obtained from 7 patients (57 ± 14 years, mean ± SD) undergoing total knee replacement. All patients were diagnosed on criteria developed by the American College of Rheumatology. Patients who had received intra-articular injections of steroids were excluded.

ELISA

For TL1A assays, flat-bottom 96-well plates (Costar EIA/RIA plate #3590, Fisher Scientific, Pittsburgh, PA) were coated with anti-TL1A capture mAb (15E09) (50 μl/well at 3 μg/ml) diluted in $NaHCO_3$ buffer (pH 9.0), and incubated overnight at 4^oC**.** After blocking for 1h at room temperature with 3% BSA in PBS, the plates were washed with washing buffer (0.05% Tween 20 in PBS). Samples (50 μl/well) were added to the wells and incubated overnight at 4^oC. After an extensive wash, 50μl/well of affinity-purified biotinylated-anti-TL1A rabbit polyclonal Ab at 0.1 μg/ml were added and incubated at room temperature for 2h. Fifty microliters/well of horseradish peroxidase-conjugated streptavidin (R & D Systems) diluted 1/200 in washing buffer were added after extensive washing. One hour later, the plates were washed, and 50 μl/well of tetramethylbenzidine (Sigma) were added and incubated for 30 min

at room temperature in the dark. Fifty microliters/well of 2N H_2SO_4 were added to stop the reaction, and optical densities were determined at 450 nm. Samples were assayed in duplicate.

To detect serum anti-bovine collagen Ab (total IgG and IgG_{2a}), mice were tail bled before being sacrificed on day 50. Serum samples were analyzed with ELISA kits from Chondrex following the manufacturer's instructions.

IFN-γ, TNF-α, IL-2 and IL-17 were measured by ELISA with kits from R & D Systems, according to the manufacturer's instructions. Samples were assayed in triplicate.

Reverse transcription-quantitative PCR (RT-qPCR)

Total RNA was isolated from chondrocytes, SF or mouse joints with the Trizol reagent. TL1A and DR3 mRNA in human chondrocytes, SF and mouse joints was measured by RT-qPCR. For human TL1A mRNA measurement, the forward primer 5'-AGGACAGGAGTTTGCACCTTCACA-3' and reverse primer 5'-AGTGCTGTGTGGGAGTTTGTCTCA-3' were employed to generate a 110-bp fragment. For mouse TL1A mRNA measurement, the forward primer 5'-TCATTTCCCATCCTCGCAGGACTT-3' and reverse primer 5'-TAATTGTCAGGTGTGCTCTCGGCT-3' were employed to generate a 166-bp fragment. For DR3 human mRNA measurement, the forward primer 5'-AAGGCGAAGAAGCACGAACGAATG-3' and reverse primer 5'-ACTCCGGCCGAGAAGTTGAGAAAT-3' were employed to generate a 66-bp fragment. The PCR conditions for these reactions were as follows: 2 min at 95°C, followed by 45 cycles of 10 s at 95°C and 15 s at 56°C, and 20 s at 72°C. Samples were in triplicate. β-actin mRNA levels was taken as internal controls, and the data were expressed as signal ratios of TL1A mRNA/β-acting mRNA and DR3 mRNA/β-actin mRNA.

In vitro Th1, Th2 and Th17 polarization

Th1 and Th17 populations were polarized from naïve DBA/1LacJ $CD4^+$ T cells, which were isolated from pooled splenocytes and lymph node cells using Naïve $CD4^+$ T Cells Isolation Kit (R&D Systems, Minneapolis, MN). The purity of naïve $CD4^+$ cells was routinely greater than 95%. Purified naïve T cells (0.25×10^6/well) were mixed with T-cell-depleted irradiated

(3000 Rads) DBA/1LacJ feeder splenocytes (1.25×10^6 cells/well), and cultured in 96-well plates in RPMI medium 1640 containing 10% FCS, 100 μg/ml streptomycin, 100 units/ml penicillin G, 1× nonessential amino acids, 1 μM sodium pyruvate, and 2.5 μM β-mercaptoethanol, and soluble anti-CD3ε mAb (clone 145-2C11, 2μg/ml. Th2 polarization was started with total $CD4^+$ T cells, which were purified with EasySep Mouse CD4 Positive Selection Kit (STEMCELL Technologies, Vancouver, BC, Canada). Purified total $CD4^+$ T cells (0.4×10^6/well) were mixed with irradiated (3000 Rads) T-cell-depleted DBA/1LacJ feeder splenocytes (0.2×10^6 cells/well), and cultured in 96-well plates in the same medium used for Th1 and Th17 polarization.

For Th1 polarization, 10 ng/ml rmIL-12 and 10 μg/ml anti-IL-4 mAb (clone 11B11) were added to the culture. For Th2 polarization, 20ng/ml rmIL-4 and 10 μg/ml of both anti-IL-12 mAb (10 μg/ml; BD Bioscience) and anti-IFN-γ mAb (10 μg/ml; R & D Systems) were added. For Th17 polarization, cultures were supplemented with recombinant mouse IL-6 (20 ng/ml; R & D Systems), recombinant human TGF-β1 (5 ng/ml; R & D Systems) and anti-IL-4 and anti-IFN-γ mAb (10 μg/ml; R & D Systems). Recombinant human TL1A was added at concentrations of 0, 40, 200, 1000 ng/ml.

For IL-17 assays, cells were washed and stimulated with 5 nM of PMA and 500 ng/ml of ionomycin in the last 4 hours of 3 days culture; the supernatants were then collected for cytokine analysis. For IFN-γ and IL-4 assays, the cells were kept in culture for 5 days, and then stimulated with 5 nM of PMA, 500 ng/ml of ionomycin and 50U/ml rhIL-2 in the last 12 hours, and the following steps are as same as that of IL-17.

Results

TL1A aggravated CIA in mice

With mouse CIA as a model, we investigated the roles of TL1A in disease development. DBA/1LacJ mice were immunized i.p. with BTIIC in CFA. A group was injected with PBS as negative controls, which did not develop any disease, as expected. Eighty percent of the BTIIC-immunized mice (CIA-PBS group) developed CIA within 50 days (Fig. 1B). Disease onset followed a slow kinetics, as CIA was not detected before day 24, and at day 40, only 35% of the mice showed CIA. As a positive control, a group of BTIIC-immunized mice was boosted with LPS (CIA-LPS group) on day 14, and it induced a rapid onset of arthritis within 2 days, i.e., on day 16, 80% of the mice became arthritic, and on day 20, 90%. When human recombinant TL1A (in all experiments of this study, the recombinant TL1A used was of human) was administered from day 5 to 20 (CIA-TL1A group), it significantly aggravated CIA induction. The disease started its manifestation earlier (day 20), compared to BTIIC immunization alone (day 24), and presented 100% penetrance on day 40, compared to only 35% for BTIIC immunization alone. On the other hand, BTIIC-immunized mice treated with heat-inactivated TL1A (CIA-HDTL1A group) showed disease development kinetics similar to that of BTIIC immunization alone. This ruled out the possibility that the aggravated CIA in TL1A-injected mice (CIA-TL1A group) was due to pyrogen contamination in the TL1A preparation, or due to its non-specific effect as a foreign antigen, as the recombinant human TL1A was used in our experiment.

The data are also presented in the form of clinical scores (Fig. 1C and 1D). Throughout the 50-day observation period, the BTIIC-immunized group did not present a mean clinical score above 2. Administration of heat-denatured TL1A from day 5 to 20 had no obvious effect (Fig. 1C). In the positive control group with LPS injection at day 15, the clinical score rapidly increased from 0 to a mean of 2.5 in 2 days. In the group that received TL1A for 15 days from day 5 to 20, the clinical score was significantly elevated, as its mean scores reached 3.0 on day 38 and 5.0 on day 50, compared to the CIA-PBS control group (Fig. 1C). At the end of the study on day 50, the score of this test group was significantly higher than that of the CIA-PBS group and the CIA-HDTL1A group ($p=0.0015$ and $p=0.004$, respectively) (Fig. 1D).

Representative histology sections of hind paws of CIA-PBS and CIA-TL1A mice at day 50 are illustrated in Fig. 2A. The left panel shows relatively normal histology of a CIA-PBS hind paw. The right panel is from a paw affected by TL1A-aggravated CIA. The pathological findings included obvious cartilage damage with synovial layer loss, severe pannus formation, and bone destruction and deformation. There were severe inflammatory changes including congestion, edema and significant cell infiltration within the articular space, and around or between joints. Diffused cell infiltration in the subcutaneous area was also observed. The histopathology of each treatment group was scored semiquantitatively, and the results were depicted in Fig. 2B. While CIA-PBS and CIA-HDTL1A groups showed no difference in their scores, the score of the CIA-TL1A group was significantly higher than that of these two groups.

It is to be noted that LPS-treated mice presented high clinical but low pathological scores. LPS triggers innate immune responses and inflammatory cytokine releases. It mainly causes swelling and loss of function of joints, but results in little cartilage and bone damage. Thus, LPS-treated mice showed high clinical scores, which were based on joint swelling and function. On the other hand, severe pathological scores were based on pannus formation, cartilage damage, and bone damage, which were absent in LPS-treated mice.

TL1A increased humoral immune responses in vivo

Collagen-specific auto-Abs are pathogenic in RA, and are directly disease-causative in CIA. Serum collagen-specific IgG and IgG_{2a} levels were measured at the end of the study on day 50 in mice receiving different treatments (Fig. 3). Naïve mice (naïve-PBS group) presented no anti-collagen IgG (Fig. 3A) and IgG_{2a} Abs (Fig. 3B). The CIA-PBS and CIA-HDTL1A groups had similar levels of collagen-specific IgG and IgG_{2a} Abs, but these Abs were elevated in the CIA-LPS group, as expected. In the CIA-TL1A group, levels of these Abs were significantly higher than those of the CIA-PBS group (for both IgG and IgG_{2a}, $p<0.05$ between the CIA-TL1A and CIA-PBS groups, and $p<0.01$ between the CIA-TL1A and CIA-HDTL1A groups).

Secondary lymphoid organs, such as the spleen, are the place where B cells undergo activation and differentiation, and become Ab-producing plasma cells. We examined the effect of TL1A

on spleen histology. As shown in Figure 3C, in the normal spleen (left panel), small germinal centers were occasionally present in the white pulp. However, in the spleen of mice treated with TL1A (3 mg/kg/day for 10 days without any additional immunization), there were many enlarged germinal centers displayed lightly stained areas, which might have been due to cell proliferation. This suggests that TL1A could promote humoral immune responses, and explains the significantly augmented anti-collagen Ab levels in mice with BTIIC-immunization followed by TL1A treatment.

TL1A expression in synovial fluids and cells in joints

Inflammatory cytokines locally produced in joints play an important role in RA pathogenesis. To test whether TL1A was produced locally in joints, we first assessed its presence in RA synovial fluids. As shown in Fig. 4A, TL1A was below the detection level in synovial fluids of 4 non-RA individuals. On the other hand, 5 out of 6 synovial samples from RA patients showed elevated TL1A levels.

We also tested TL1A expression in joints from CIA mouse joints, and found its mRNA level was significantly augmented, compared to that of joints of naïve mice (Fig. 4B), suggesting the involvement of local TL1A in CIA pathogenesis.

To identify the cell source of synovial fluid TL1A, human chondrocytes and SF were cultured in plain medium or in the presence of inflammatory cytokines IL-1β or TNF-α, and their TL1A mRNA levels were quantified by RT-qPCR. As shown in Figure 4C, chondrocytes in the resting state had barely detectable TL1A mRNA, but its expression increased in the presence of TNF-α but not IL1β after 24 h. SF presented higher constitutive TL1A mRNA level, and the expression increased slightly after IL1-β treatment, but significantly after TNF-α stimulation (Fig. 4C). Careful kinetic study revealed that TL1A mRNA was rapidly elevated in SF within 3-6 h after IL-1β stimulation, while it took 20 h to reach high levels after TNF-α stimulation (Fig. 4D). At the protein level, both IL-1β and TNF-α dose-dependently enhanced TL1A secretion by SF at 24 h after culture (Fig. 4E, top panel), and 48-h supernatants

contained more TL1A than 24-h supernatants (Fig. 4E, bottom panel). This result revealed that SF was a source of local TL1A, which might influence inflammation *in situ* in the joints.

On the other hand, neither chodrocytes nor SF showed apparent constitutive DR3 mRNA expression, nor did they upregulate DR3 expression after IL-1β and TNF-α stimulation (Fig. 4C), indicating that TL1A was unlikely to exert an autocrine effect on these cells. Indeed, TL1A did not affect proliferation of chondrocytes and SF, nor did it impact their apoptosis (data not shown). Therefore, chondrocytes and SF seemed not to be the intended targets of locally produced TL1A by SF.

TL1A expression in secondary lymphoid organs

In mouse CIA, systemic TL1A administration increased titres of anti-collagen Ab, which are pathogenic. In RA patients, particularly those rheumatic factor positive patients, their serum TL1A levels are increased [30].This implies that extra-articular TL1A might also be involved in pathogenesis of RA and mouse CIA. We assessed whether TL1A was produced in secondary lymphoid organs in our CIA model. We showed that TL1A expression was induced in MHC class $II^+/CD11c^+$ DC (Fig. 5A) and $F4/80^+$ macrophages/monocytes (Fig. 5B) in draining inguinal lymph nodes 2 weeks after tail base injection of CFA or of CFA plus collagen. CFA alone was sufficient to upregulate TL1A, and the presence of collagen alone with CFA further increased TL1A expression in these cells.

Effect of TL1A on lymphokine production

In RA, considerable T lymphocyte infiltration occurs in joints once the disease starts. What is the effect of local TL1A on these cells, which are known to express TL1A receptors, i.e., DR3? We assessed the influence of TL1A on lymphokine secretion by T cells, With TCR ligation, TL1A enhanced TNF-α production in a dose-dependent manner (Fig. 6A). Under a Th17-differentiation condition, the presence of TL1A in culture drastically increased IL-17 secretion (Fig. 6B). It is conceivable these local inflammatory cytokines, i.e., TNF-α and IL-17, triggered by TL1A could aggravate RA pathogenesis. On the other hand, under Th1 and

Th2 differentiation condition, the production of Th1 cytokine IFN-γ (Fig. 6C) and Th2 cytokine IL-4 (Fig. 6D) by T cells was not apparently influenced by the present of TL1A.

Discussion

In this study, we reported that TL1A aggravated RA in a mouse CIA model. Mechanistic investigation discerned that under stimulation of inflammatory cytokines, such as IL-1β and TNF-α, SF was capable of producing TL1A, which, in turn, could enhance the production of inflammatory cytokines, such as IL-17 and TNF-α. This study revealed a possible role of TL1A in RA pathogenesis.

In our CIA mouse model, the systemic administration of TL1A could have pathogenic effects on two fronts. One is in the joints locally. As demonstrated in our *in vitro* study, TL1A promoted T cells to secrete locally TNF-α, an established culprit in RA development[3]. It also promoted local IL-17 production, which has also been implicated in RA pathogenesis[4]. The second front is probably in the lymphoid organs, such as the spleen and bone marrow, where Abs are produced. TL1A drastically increased the size and number of germinal centers in the spleen, suggesting that it could drive B-cell activation and differentiation. Indeed, mice receiving TL1A showed heightened titers of serum anti-collagen Ab, which is pathogenic in both mouse CIA and RA patients[31]. The effect of TL1A on B cells is probably indirect via T cells, because B cells display almost no DR3[8], and we could not detect any direct effect of TL1A on B-cell activation and proliferation (data not shown).

Is TL1A a relevant factor involved in RA pathogenesis? In mouse CIA, we identified increased TL1A mRNA in inflammatory joints. In humans, we discovered elevated TL1A titres in RA synovial fluids, and found that SF under the influence of IL-1β and TNF-α could evoke TL1A secretion. This puts TL1A into a possible loop of a vicious circle that aggravates RA pathogenesis. Once RA is in progress, local IL-1β and TNF-α levels are increased in the joints, produced mainly by monocytes/macrophages[32]. In addition to their harmful effects in causing local inflammation[33,34], these cytokines could also trigger SF to produce TL1A, which could, in turn, augment TNF-α production by infiltrating T cells in the joints. The IL-17 induced by TL1A could be another detrimental factor ramified from this vicious loop, causing further local inflammation in the joints.

In a study that was published while our manuscript was under revision, Bamias et al. demonstrated that rheumatic factor-positive RA patients showed elevated serum TL1A titres[30]. The increased serum TL1A titres in RA patients suggest that TL1A outside the joints may also play a role in RA pathogenesis. We have shown that bacterial antigen stimulation in the form of CFA was sufficient to trigger TL1A expression in DC and monocytes/macrophages in draining lymph nodes. It is possible that under a pathophysiological condition, certain RA susceptible individuals have increased TL1A titres in secondary lymphoid organs upon environmental Ag stimulation; the augmented TL1A levels enhance the production of Ab, some of which might be autoreactive to joint tissues; this process then initiates RA pathogenesis.

In this regard, it is noteworthy that DR3 gene duplication in chromosome region 1p36.3 is prevalent in RA patients[35], raising the possibility that TL1A and DR3 interaction indeed plays a role in human RA pathogenesis.

In summary, we demonstrated that TL1A is a novel mediator involved in RA pathogenesis, and is a possible therapeutic target for this disease.

Note added in proof: While our manuscript was under review, Bull et al[36], reported that DR3 (the receptor of TLlA) gene knockout mice were resistant to antigen-induced arthritis (AIA). They further demonstrated that anti-TL1A mAb could reduce severity of both AIA and CIA in mice. These new findings support our conclusion that TL1A might have pathogenic roles in mouse CIA and human RA.

Reference

1. Scrivo, R., M. Di Franco, A. Spadaro, and G. Valesini. 2007. The immunology of rheumatoid arthritis. *Ann.N.Y.Acad.Sci.* 1108:312-322.

2. Mauri, C. and M. R. Ehrenstein. 2007. Cells of the synovium in rheumatoid arthritis. B cells. *Arthritis Res.Ther.* 9:205.

3. Firestein, G. S. 2003. Evolving concepts of rheumatoid arthritis. *Nature* 423:356-361.

4. Hirota, K., M. Hashimoto, H. Yoshitomi, S. Tanaka, T. Nomura, T. Yamaguchi, Y. Iwakura, N. Sakaguchi, and S. Sakaguchi. 2007. T cell self-reactivity forms a cytokine milieu for spontaneous development of IL-17+ Th cells that cause autoimmune arthritis. *J.Exp.Med.* 204:41-47.

5. Lubberts, E., M. I. Koenders, and W. B. van den Berg. 2005. The role of T-cell interleukin-17 in conducting destructive arthritis: lessons from animal models. *Arthritis Res.Ther.* 7:29-37.

6. Lundy, S. K., S. Sarkar, L. A. Tesmer, and D. A. Fox. 2007. Cells of the synovium in rheumatoid arthritis. T lymphocytes. *Arthritis Res.Ther.* 9:202.

7. Stamp, L. K., M. J. James, and L. G. Cleland. 2004. Interleukin-17: the missing link between T-cell accumulation and effector cell actions in rheumatoid arthritis? *Immunol.Cell Biol.* 82:1-9.

8. Migone, T. S., J. Zhang, X. Luo, L. Zhuang, C. Chen, B. Hu, J. S. Hong, J. W. Perry, S. F. Chen, J. X. Zhou, Y. H. Cho, S. Ullrich, P. Kanakaraj, J. Carrell, E. Boyd, H. S. Olsen, G. Hu, L. Pukac, D. Liu, J. Ni, S. Kim, R. Gentz, P. Feng, P. A. Moore, S. M. Ruben, and P. Wei. 2002. TL1A is a TNF-like ligand for DR3 and TR6/DcR3 and functions as a T cell costimulator. *Immunity.* 16:479-492.

9. Jin, T., F. Guo, S. Kim, A. Howard, and Y. Z. Zhang. 2007. X-ray crystal structure of TNF ligand family member TL1A at 2.1A. *Biochem.Biophys.Res.Commun.* 364:1-6.

10. Fang, L., B. Adkins, V. Deyev, and E. R. Podack. 2008. Essential role of TNF receptor superfamily 25 (TNFRSF25) in the development of allergic lung inflammation. *J.Exp.Med.* 205:1037-1048.

11. Prehn, J. L., L. S. Thomas, C. J. Landers, Q. T. Yu, K. S. Michelsen, and S. R. Targan. 2007. The T cell costimulator TL1A is induced by FcgammaR signaling in human monocytes and dendritic cells. *J.Immunol.* 178:4033-4038.

12. Cassatella, M. A., G. Pereira-da-Silva, I. Tinazzi, F. Facchetti, P. Scapini, F. Calzetti, N. Tamassia, P. Wei, B. Nardelli, V. Roschke, A. Vecchi, A. Mantovani, L. M. Bambara, S. W. Edwards, and A. Carletto. 2007. Soluble TNF-like cytokine (TL1A) production by immune complexes stimulated monocytes in rheumatoid arthritis. *J.Immunol.* 178:7325-7333.

13. Bamias, G., C. Martin, III, M. Marini, S. Hoang, M. Mishina, W. G. Ross, M. A. Sachedina, C. M. Friel, J. Mize, S. J. Bickston, T. T. Pizarro, P. Wei, and F. Cominelli. 2003. Expression, localization, and functional activity of TL1A, a novel Th1-polarizing cytokine in inflammatory bowel disease. *J.Immunol.* 171:4868-4874.

14. Bai, C., B. Connolly, M. L. Metzker, C. A. Hilliard, X. Liu, V. Sandig, A. Soderman, S. M. Galloway, Q. Liu, C. P. Austin, and C. T. Caskey. 2000. Overexpression of M68/DcR3 in human gastrointestinal tract tumors independent of gene amplification and its location in a four-gene cluster. *Proc.Natl.Acad.Sci.U.S.A* 97:1230-1235.

15. Pitti, R. M., S. A. Marsters, D. A. Lawrence, M. Roy, F. C. Kischkel, P. Dowd, A. Huang, C. J. Donahue, S. W. Sherwood, D. T. Baldwin, P. J. Godowski, W. I. Wood, A. L. Gurney, K. J. Hillan, R. L. Cohen, A. D. Goddard, D. Botstein, and A. Ashkenazi. 1998. Genomic amplification of a decoy receptor for Fas ligand in lung and colon cancer. *Nature* 396:699-703.

16. Zhang, J., T. W. Salcedo, X. Wan, S. Ullrich, B. Hu, T. Gregorio, P. Feng, S. Qi, H. Chen, Y. H. Cho, Y. Li, P. A. Moore, and J. Wu. 2001. Modulation of T-cell responses to alloantigens by TR6/DcR3. *J.Clin.Invest* 107:1459-1468.

17. Screaton, G. R., X. N. Xu, A. L. Olsen, A. E. Cowper, R. Tan, A. J. McMichael, and J. I. Bell. 1997. LARD: a new lymphoid-specific death domain containing receptor regulated by alternative pre-mRNA splicing. *Proc.Natl.Acad.Sci.U.S.A* 94:4615-4619.

18. Warzocha, K., P. Ribeiro, C. Charlot, N. Renard, B. Coiffier, and G. Salles. 1998. A new death receptor 3 isoform: expression in human lymphoid cell lines and non-Hodgkin's lymphomas. *Biochem.Biophys.Res.Commun.* 242:376-379.

19. Tan, K. B., J. Harrop, M. Reddy, P. Young, J. Terrett, J. Emery, G. Moore, and A. Truneh. 1997. Characterization of a novel TNF-like ligand and recently described TNF ligand and TNF receptor superfamily genes and their constitutive and inducible expression in hematopoietic and non-hematopoietic cells. *Gene* 204:35-46.

20. Pappu, B. P., A. Borodovsky, T. S. Zheng, X. Yang, P. Wu, X. Dong, S. Weng, B. Browning, M. L. Scott, L. Ma, L. Su, Q. Tian, P. Schneider, R. A. Flavell, C. Dong, and L. C. Burkly. 2008. TL1A-DR3 interaction regulates Th17 cell function and Th17-mediated autoimmune disease. *J.Exp.Med.* 205:1049-1062.

21. Bu, R., C. W. Borysenko, Y. Li, L. Cao, A. Sabokbar, and H. C. Blair. 2003. Expression and function of TNF-family proteins and receptors in human osteoblasts. *Bone* 33:760-770.

22. Craxton, A., G. Shu, J. D. Graves, J. Saklatvala, E. G. Krebs, and E. A. Clark. 1998. p38 MAPK is required for CD40-induced gene expression and proliferation in B lymphocytes. *J.Immunol.* 161:3225-3236.

23. Al Lamki, R. S., J. Wang, A. M. Tolkovsky, J. A. Bradley, J. L. Griffin, S. Thiru, E. C. Wang, E. Bolton, W. Min, P. Moore, J. S. Pober, and J. R. Bradley. 2008. TL1A both promotes and protects from renal inflammation and injury. *J.Am.Soc.Nephrol.* 19:953-960.

24. Wang, E. C., A. Thern, A. Denzel, J. Kitson, S. N. Farrow, and M. J. Owen. 2001. DR3 regulates negative selection during thymocyte development. *Mol.Cell Biol.* 21:3451-3461.

25. Papadakis, K. A., J. L. Prehn, C. Landers, Q. Han, X. Luo, S. C. Cha, P. Wei, and S. R. Targan. 2004. TL1A synergizes with IL-12 and IL-18 to enhance IFN-gamma production in human T cells and NK cells. *J.Immunol.* 172:7002-7007.

26. Yang, C. R., S. L. Hsieh, F. M. Ho, and W. W. Lin. 2005. Decoy receptor 3 increases monocyte adhesion to endothelial cells via NF-kappa B-dependent up-regulation of intercellular adhesion molecule-1, VCAM-1, and IL-8 expression. *J.Immunol.* 174:1647-1656.

27. Bendele, A. M., E. S. Chlipala, J. Scherrer, J. Frazier, G. Sennello, W. J. Rich, and C. K. Edwards, III. 2000. Combination benefit of treatment with the cytokine inhibitors interleukin-1 receptor antagonist and PEGylated soluble tumor necrosis factor receptor type I in animal models of rheumatoid arthritis. *Arthritis Rheum.* 43:2648-2659.

28. Altman, R. D. 1987. Criteria for the classification of osteoarthritis of the knee and hip. *Scand.J.Rheumatol.Suppl* 65:31-39.

29. Fahmi, H., J. A. Di Battista, J. P. Pelletier, F. Mineau, P. Ranger, and J. Martel-Pelletier. 2001. Peroxisome proliferator--activated receptor gamma activators inhibit interleukin-1beta-induced nitric oxide and matrix metalloproteinase 13 production in human chondrocytes. *Arthritis Rheum.* 44:595-607.

30. Bamias, G., S. I. Siakavellas, K. S. Stamatelopoulos, E. Chryssochoou, C. Papamichael, and P. P. Sfikakis. 2008. Circulating levels of TNF-like cytokine 1A (TL1A) and its decoy receptor 3 (DcR3) in rheumatoid arthritis. *Clin.Immunol.* 129:249-255.

31. Cho, Y. G., M. L. Cho, S. Y. Min, and H. Y. Kim. 2007. Type II collagen autoimmunity in a mouse model of human rheumatoid arthritis. *Autoimmun.Rev.* 7:65-70.

32. Chu, C. Q., M. Field, M. Feldmann, and R. N. Maini. 1991. Localization of tumor necrosis factor alpha in synovial tissues and at the cartilage-pannus junction in patients with rheumatoid arthritis. *Arthritis Rheum.* 34:1125-1132.

33. Arend, W. P. and J. M. Dayer. 1995. Inhibition of the production and effects of interleukin-1 and tumor necrosis factor alpha in rheumatoid arthritis. *Arthritis Rheum.* 38:151-160.

34. Feldmann, M., F. M. Brennan, R. O. Williams, J. N. Woody, and R. N. Maini. 2004. The transfer of a laboratory based hypothesis to a clinically useful therapy: the development of anti-TNF therapy of rheumatoid arthritis. *Best.Pract.Res.Clin.Rheumatol.* 18:59-80.

35. Osawa, K., N. Takami, K. Shiozawa, A. Hashiramoto, and S. Shiozawa. 2004. Death receptor 3 (DR3) gene duplication in a chromosome region 1p36.3: gene duplication is more prevalent in rheumatoid arthritis. *Genes Immun.* 5:439-443.

36. Bull, M. J., A. S. Williams, Z. Mecklenburgh, C. J. Calder, J. P. Twohig, C. Elford, B. A. Evans, T. F. Rowley, T. J. Slebioda, V. Y. Taraban, A. Al Shamkhani, and E. C. Wang. 2008. The Death Receptor 3-TNF-like protein 1A pathway drives adverse bone pathology in inflammatory arthritis. *J.Exp.Med.* 205:2457-2464.

Figure legend

Figure 1. TL1A aggravates CIA clinical scores in mice

A. Scheme of CIA induction and TL1A administration

B. RA incidence in mice receiving different treatments

Naïve-PBS: naïve mice received PBS i.p. from day 5 to 20; CIA-PBS: mice received BTIIC immunization on day 0, and PBS from day 5 to 20; CIA-LPS: mice received BTIIC immunization on day 0, and a single LPS (60 mg/mouse) injection s.c. on day 15; CIA-TL1A: mice received BTIIC immunization on day 0, and daily i.p. TL1A (1 mg/kg/day) injection from day 5 to 20; CIA-HDTL1A: mice received BTIIC immunization on day 0, and daily heat-denatured TL1A (1 mg/kg/day) injection i.p. from day 5 to 20. n=10 for each group.

C. RA clinical scores of mice receiving different treatments during 50 days of observation

Mice from Fig.1B were scored for their RA condition on the days indicated, and mean scores $\pm$ SEM were plotted.

D. *RA clinical scores of mice receiving different treatments on day 50 after initial BTIIC immunization*

Mice from Figure 1B were scored for their RA condition on day 50 after the BTIIC immunization. The horizontal lines represent mean scores of the group. Differences in scores between the CIA-TL1A and CIA-PBS groups, and between the CIA-TL1A and CIA-HDTL1A groups were highly significant ($p=0.0015$ and $p=0.004$, respectively; ANOVA t test).

Figure 2. Effect of TL1A on CIA histology

A. Histology of mouse joints

DBA/1LacJ mice were immunized with BTIIC to induce CIA in the absence or presence of TL1A injection. They were sacrificed on day 50 and the hind paws were sectioned and stained with H&E. The left panel shows a hind paw from a CIA-PBS mouse, and the right panel, a hind paw from a CIA- TL1A mouse.

B. Histopathological scores of mouse joints

Mice from Figure 1B were sacrificed on day 50, and joint histology was scored semi-quantitatively. The horizontal bars represent the mean scores of each group (n=10). The histopathological scores of the CIA-TL1A group are significantly higher than those of the

CIA-PBS and CIA-HDTL1A groups (p=0.0006 and p=0.002, respectively; ANOVA t test).

Figure 3. TL1A enhances humoral immune responses

A and B. Effect of TL1A on serum collagen-specific Abs

Sera from mice as described in Figure 1B were collected at the time of sacrifice (day 50 after initial BTIIC immunization). Collagen-specific IgG Ab (Fig. 3A) and IgG_{2a} Ab (Fig. 3B) were measured by ELISA. The data are expressed as unit/ml of 1:100 diluted sera. The horizontal bars represent the means of each group (n=20). Serum collagen-specific IgG and IgG_{2a} levels in the CIA-TL1A group are significantly higher that those in the CIA-PBS and CIA-HDTL1A groups (p values are indicated in the graphs; ANOVA t test).

C. TL1A drastically increases spleen germinal center formation

DBA/1LacJ mice were injected i.p. with TL1A (3 mg/kg/day) for 10 days, and spleen histology is shown. Left panel: normal spleen from a naïve mouse; right panel: spleen from a TL1A-injected mouse.

Figure 4. TL1A production in humans

A. Synovial fluid TL1A levels in patients with rheumatic diseases are elevated

Synovial fluids from RA joints (n=7) or from non RA joints (n=4) were assayed for TL1A by ELISA. Mean + SD of triplicate samples are shown. Each bar represents an individual patient. Non-RA synovial fluid TL1A levels were below the detection level of the assay.

B. Augmented TL1A mRNA expression in mouse CIA joints

RNA was extracted from skinless proximal interphalangeal joints of CIA (3 weeks after collagen/CFA injection) or naïve mice, and TL1A mRNA was quantified by RT-qPCR, using β-actin mRNA as internal control. The signal ratios of TL1A mRNA/β-actin mRNA are presented. Each symbol represents an individual mouse. Short horizontal bars represent mean signal ratios of each group. TL1A signals of the RA group is significantly higher than those of the naïve group ($p<0.01$, Student's *t* test)

C. TL1A and DR3 mRNA levels in human chondrocytes and SF

Human chondrocytes and SF were cultured in the presence or absence of IL-1β (200pg/ml_) and TNF-α (10 ng/ml). Samples were in duplicate. The cells were harvested from 45 min until 24 h after culture, and TL1A and DR3 mRNA levels were determined by RT-qPCR, using β-actin mRNA as internal control. The signal ratios of TL1A mRNA/β-actin mRNA are presented.

D. Kinetics of TL1A mRNA expression from 45 min to 20 h after culture

E. TL1A in SF culture supernatants

Human SF were cultured in the presence of various concentrations of IL-1β and TNF-α for 24 h (upper panel), or 24 h and 48 h (lower panel). Samples were in triplicate. Cytokine concentrations are indicated. TL1A in the supernatants were determined by ELISA. Means ± SD of TL1A concentrations in each sample are illustrated.

Data of Figs. 4C-4E are from representative experiments, and similar results were obtained in 2-3 independent experiments.

Figure 5. TL1A was upregulated in DC and macrophages/monocytes of inguinal lymph nodes of immunized mice

A. TL1A was upregulated in MHC-II and CD11c double positive DC cells

DBA/1J mice were immunized with CFA+PBS or CFA+BTIIC, and sacrificed on day 14. TL1A expression on inguinal lymph node DC cells was assessed by MHC-II, CD11c and TL1A 3-color staining followed by flow cytometry. The MHC-II and CD11c double positive DC cells were gated for TL1A expression analysis.

B. TL1A was upregulated in F4/80 positive monocytes/macrophages

Cells isolated from inguinal lymph nodes of immunized mice were also stained with Abs against F4/80 and TL1A, expression of TL1A was showed in histogram.

Figure 6. Effect of TL1A on lymphokine production

A. Effect of TL1A on TNFα secretion by anti-CD3-stimulated T cells

Purified T cells from DBA/1LacJ mice were stimulated by solid phase anti-CD3 (0.25 μg/ml for coating) in the presence or absence of TL1A (concentrations indicated). Samples were in triplicate. After 48 h, the culture supernatants were harvested and TNF-α concentrations were measured by ELISA. Means ± SD of a representative experiment are shown. Similar results were obtained in 3 independent experiments.

B. Effect of TL1A on IL-17 secretion under a Th17-differentiation condition

Naïve $CD4^+$ cells from DBA/1LacJ mouse spleens were cultured under a Th17-differentiation condition for 3 days. Samples were in duplicate. For the last 4 h of culture, the cells were stimulated with 10 nM PMA and 1 μg/ml ionomycin. The culture supernatants were then harvested and assayed for and IL-17 by ELISA. Means ± SD of a representative experiment are shown. Similar results were obtained in 3 independent experiments.

C and D. Effect of TL1A on INFγ and IL-4 secretion under Th1- and Th2-differentiation conditions, respectively

Naïve $CD4^+$ cells or total $CD4^+$from DBA/1LacJ mouse spleens were cultured under Th1- or Th2-differentiation conditions for 5-7 days. Samples were in duplicated. For the last 12 h of culture, the cells were washed and stimulated with 10 nM PMA and 1 μg/ml ionomycin. The culture supernatants were then harvested and assayed for IFN-γ and IL-4, respectively, by ELISA. Means ± SD of a representative experiment are shown. Similar results were obtained in 3 independent experiments.

Figures

Figure 2.1

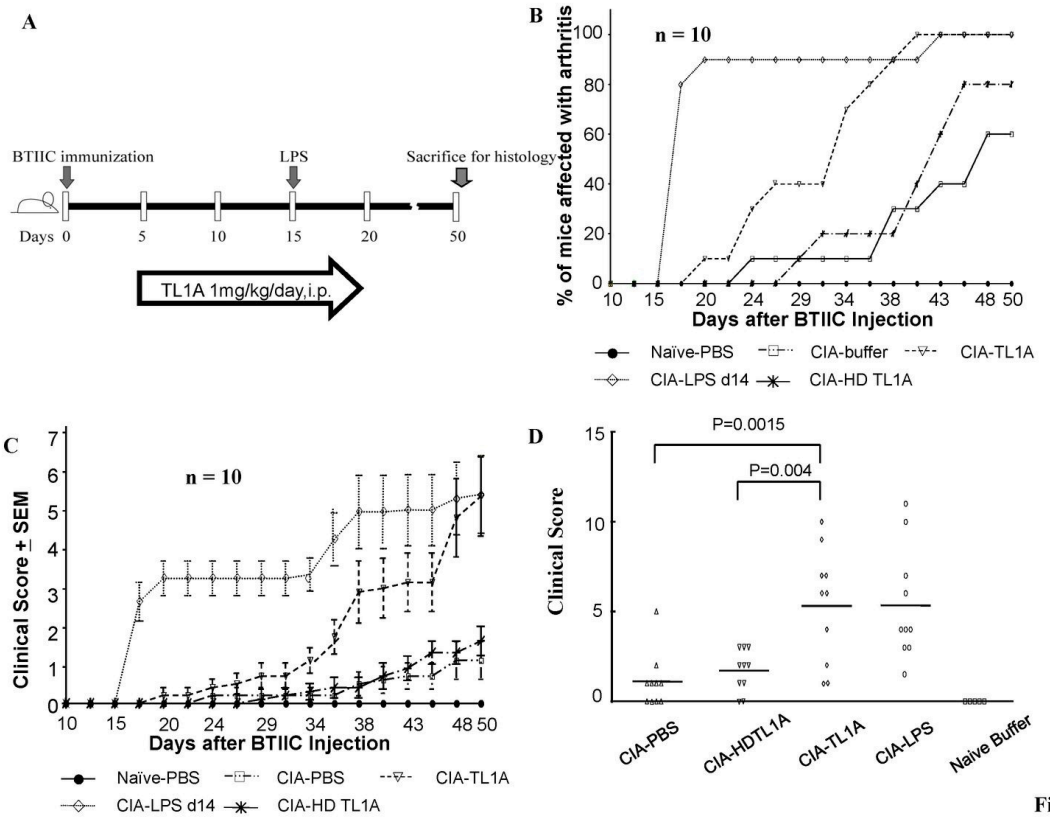

Fig. 1

Figure 2.2

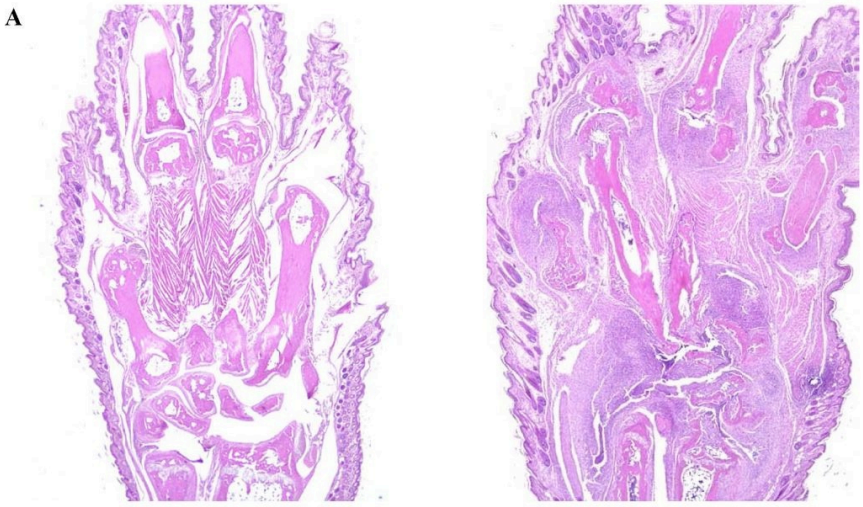
A

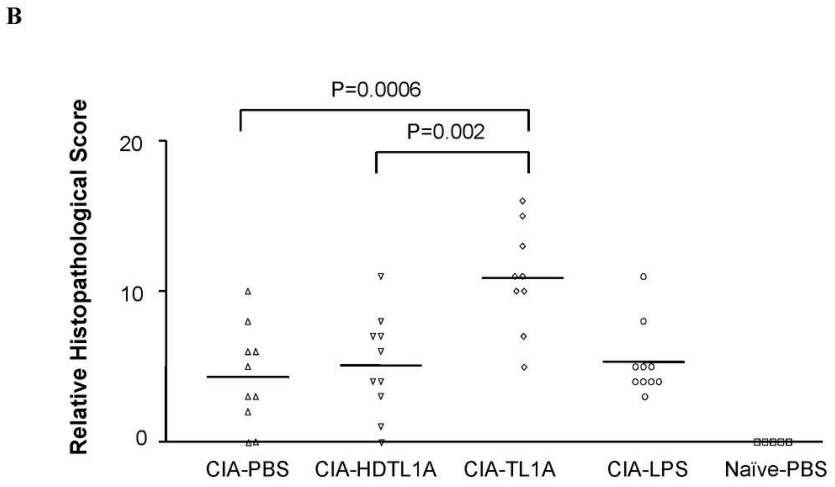
B
P=0.0006
P=0.002
Relative Histopathological Score
20
10
0
CIA-PBS
CIA-HDTL1A
CIA-TL1A
CIA-LPS
Naïve-PBS

Figure 2.3

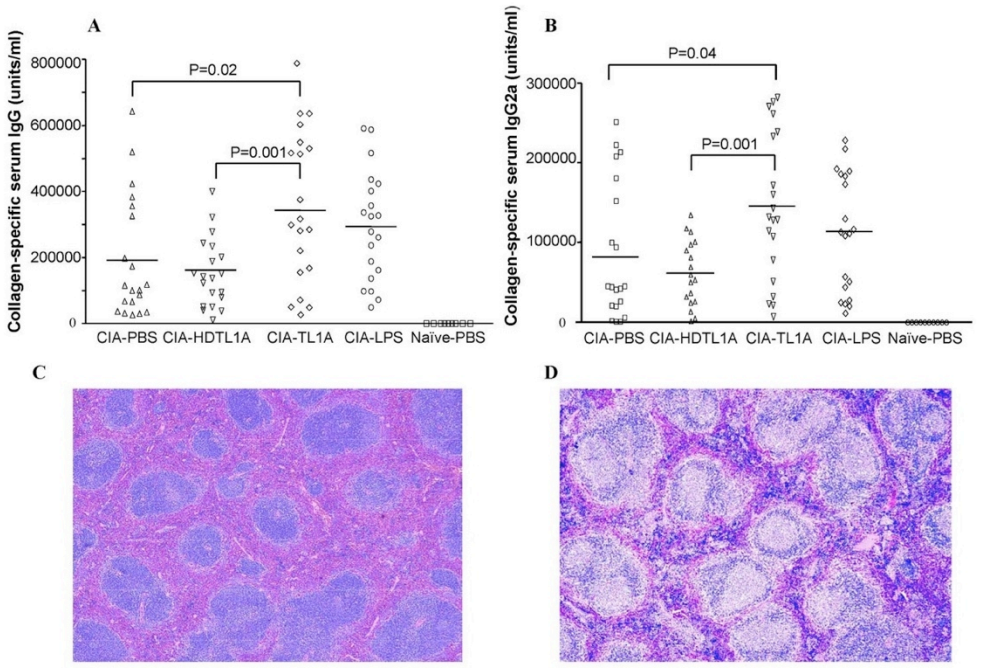

Fig. 3

Figure 2.4

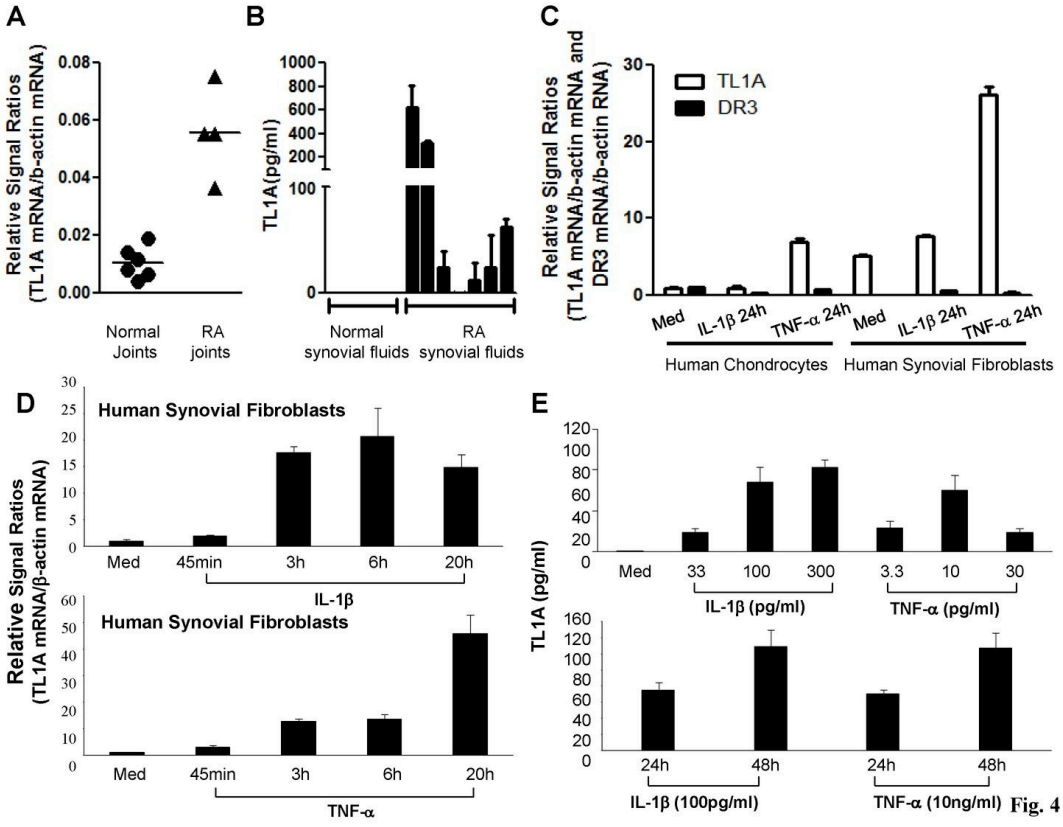

Fig. 4

Figure 2.5

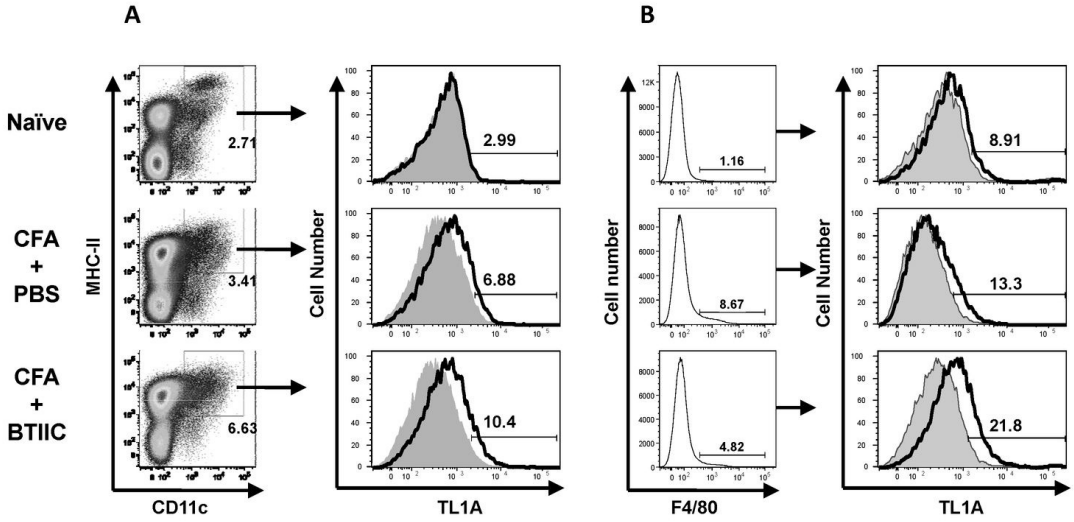

Fig. 5

Figure 2.6

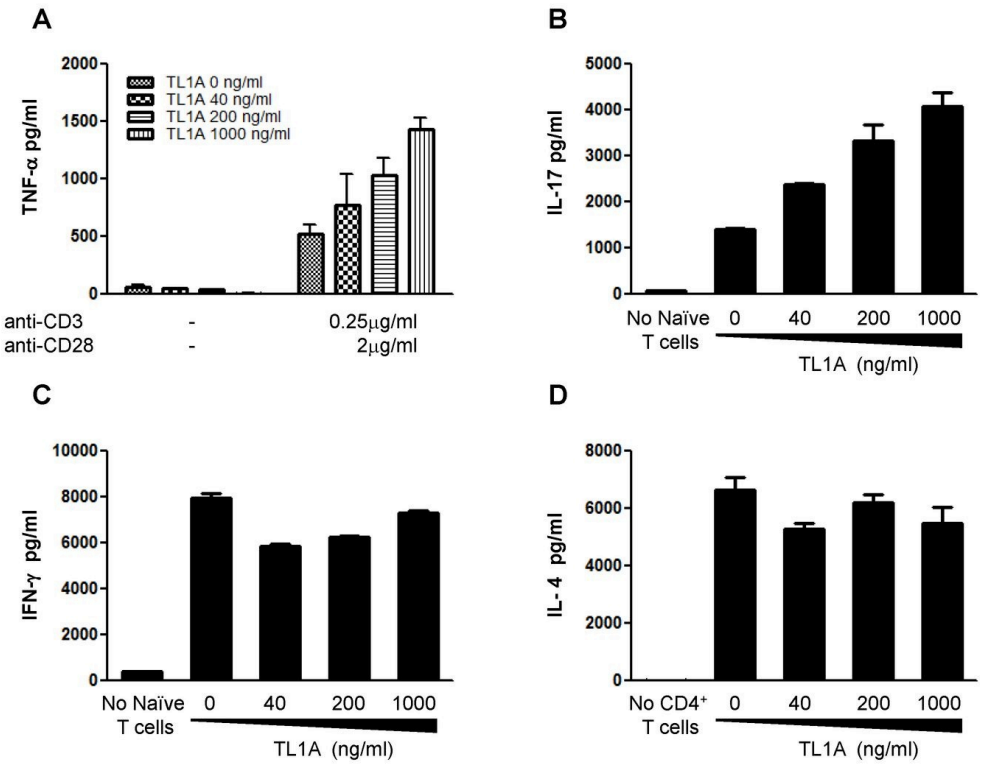

Fig. 6

CHAPTER 3 ARTICLE-2

Gene knockout mice were widely used to study the functions of certain molecules related to the human disease. As shown in Section 1.3, gene knockout mice in combination with animal models of arthritis provided us invaluable knowledge to understand the pathogenesis of RA. In this study, we generated TL1A KO mice in order to investigate whether CIA could be affected in absence of TL1A. We also evaluated the immune systems of TL1A KO mice with both *in vitro* and *in vivo* approaches. The information generated in this study might be helpful to predict the potential side effects of TL1A-targeting therapies.

This work has been published in ***The Journal of Immunology***.

Wang X, Hu Y, Charpentier T, Lamarre A, Qi S, Luo H, Wu J. (2013) TNF-like ligand 1A (TL1A) gene knockout leads to ameliorated collagen-induced arthritis in mice: implication of TL1A in humoral immune responses. ***The Journal of Immunology*** .191, 5420-5429

3.1 TNF-like ligand 1A (TL1A) gene knockout leads to ameliorated collagen-induced arthritis in mice: implication of TL1A in humoral immune responses

Xuehai Wang*, Yan Hu*, Tania Charpentier[#], Alain Lamarre[#], Shijie Qi*, Jiangping Wu*[+] and Hongyu Luo*

*From *Laboratory of Immunology and Nephrology Service, Centre de recherche, Centre hospitalier de l'Université de Montréal (CRCHUM) – Hôpital Notre-Dame, Montréal, Québec, Canada; [#]Institut national de la recherche scientifique (INRS) – Institut Armand-Frappier, Laval, Québec, Canada*

Address correspondence to:

Dr. Hongyu Luo or Dr. Jiangping Wu, Laboratory of Immunology, CRCHUM – Hôpital Notre-Dame, Pavillon DeSève, Room Y-5612, 1560 Sherbrooke Street East, Montreal, Quebec, Canada H2L 4M1; Telephone: (514) 890-8000 Extension 25319 (H.L.) or 25164 (J.W.); Fax: (514) 412-7596.

Running title: TL1A gene knockout leads to ameliorated CIA in mice

Footnotes

This work was supported by grants from the Canadian Institutes of Health Research (CIHR) to H.L. (MOP97829), J.W. (MOP69089 and MOP123389), and A.L (MOP89797). It was also supported by grants from the Heart and Stroke Foundation of Quebec, the Natural Sciences and Engineering Research Council of Canada (203906-2012) to J.W., and the Jean-Louis Levesque Foundation to J.W and A.L.

Abstract

TNF-like ligand 1A (TL1A), also known as TNFSF15, is a member of the TNF superfamily. Its known receptor is death receptor 3 (DR3). In humans, TL1A also binds to a secreted TNF family member called decoy receptor 3 (DcR3), which interferes with the interaction between TL1A and DR3. TL1A/DR3 signal has been implicated in several autoimmune diseases in animal models as well as in clinical conditions. We generated TL1A gene knockout (KO) mice to assess its role in collagen-induced arthritis (CIA), a mouse model of human rheumatoid arthritis. The KO mice were fertile and had no visible anomalies. Their lymphoid organ size and cellularity, T and B cell subpopulations, helper T cell and regulatory T cell development *in vivo* and *in vitro* and anti-viral immune responses were comparable to those of wild type mice. However, the KO mice presented ameliorated CIA in terms of clinical scores, disease incidence and pathological scores. The KO mice had reduced titres of pathogenic anti-collagen Abs in the sera. No apparent defect was found in the function of follicular helper T cells. We revealed that plasma cells but not B cells expressed high levels of DR3, and were direct targets of TL1A. In the presence of TL1A, they survived better and produced more pathogenic Ab. This study presented novel knowledge about the role of TL1A in humoral immune responses and its mechanism of action in CIA pathogenesis.

Introduction

TNF-like ligand 1A (TL1A), also called TNFSF15, is a member of the TNF superfamily. It was identified during homology searches in an endothelial cell cDNA library. It is produced by the endothelial cells(1), monocytes, dendritic cells, T cells, natural killer T cells (NKT), synovial fibroblasts and chondrocytes, either upon stimulation or *in situ* in inflammatory sites(2-6). Like other TNF superfamily members, TL1A can either be membrane-bound or soluble after being cleaved from the cell surface, but the cleavage happens on dendritic cells (DC) and not on T cells(1, 7). It was also discovered that the soluble form of TL1A was more potent in inducing IFN-γ production by T cells(8).

The receptor of TL1A death receptor 3 (DR3) is also called TNFRSF25, Apo3, WSL-1, TRAMP or LARD(9). In addition to the full length isoform, murine DR3 was reported to have two truncated variants: one secreted form displaying no transmembrane region and another lacking the fourth CRD in its extracellular sequence (10). A repertoire of all DR3-expressing cells has not yet been completed. DR3 is detectable on T cells, NK cells, NKT cells, osteocytes, renal tubule epithelial cells and *in vitro* plasma cells, but primary B cells express very low levels of DR3(3, 11-13). Previous studies of the immunological functions of TL1A and DR3 primarily focused on T cells, NK cells and NKT cells(3, 12, 14-16). In addition to DR3, DcR3 could also bind to TL1A in humans, and blocks the interaction between TL1A and DR3(1). Mice do not have a human DcR3 orthologue.

Earlier *in vitro* studies have shown that TL1A promotes T cell proliferation, Th17 differentiation and the production of pro-inflammatory cytokines by T cells (9), indicating its potential role in inflammatory autoimmune diseases. The presence of TL1A in diseased tissues, fluids and sera from patients of chronic colitis and rheumatoid arthritis (RA) corroborates the findings in animal models (2, 5, 17-19). *In vivo* studies of different animal models have provided direct evidence supporting the role of TL1A in autoimmune diseases. We have demonstrated that the administration of recombinant TL1A to mice with collagen-induced arthritis (CIA) aggravates the disease (5). Furthermore, overexpression of TL1A in transgenic mice results in spontaneous inflammatory bowel disease (IBD) as well as increased number of T helper cells (9, 20, 21). On the other hand, DR3 gene knockout (KO) mice have

reduced disease severity of allergic lung inflammation and antigen-induced arthritis and present less effective anti-viral and anti-bacterial immune responses(15, 22-25). Blocking DR3-TL1A interaction by TL1A-neutralizing Ab would partially protect the KO mice from CIA, lung inflammation, and 2,4,6-trinitrobenzene sulfonic acid (TNBS)- and dextran sodium sulphate (DSS)-induced colitis(3, 4, 9, 23). TL1A KO mice are less susceptible to experimental autoimmune encephalomyelitis (EAE) induction(22).

Rheumatoid arthritis (RA) is a chronic polygenic autoimmune disease characterized by chronic systemic inflammation that may affect various tissues and organs. Joints and their surrounding tissues are most frequently affected. Often, there is persistent synovitis and presence of auto-Abs leading to progressive destruction of cartilage and bone in the joints (26). The pathogenesis of RA is not fully understood with three primary, outstanding questions to be fully answered: (1) How is the immune response initiated by genetic and/or environmental factors? (2) How does the immune response lead to local joint inflammation? (3) How does the inflammation cause bone destruction. There are some findings from patients and animal models that have provided some partial answers to these questions(27-36).

In the current study, we generated *TL1A* knockout (KO) mice to study the role of TL1A in CIA pathogenesis. We found TL1A KO mice had significantly lower CIA clinical scores and incidence, and lower serum anti-collagen Ab titres than their wild type (WT) counterparts. Deletion of TL1A minimally affected T cell functions; however, TL1A could directly deliver survival signals to plasma cells as a way to promote pathogenic collagen-specific Ab production. Our findings revealed previously undocumented functions of TL1A in RA pathogenesis.

Materials and Methods

Generation of TL1A KO mice

A polymerase chain reaction (PCR) fragment amplified from the *TL1A* cDNA was used as probe to isolate genomic BAC DNA clone 112H6 from the 129/sv mouse BAC genomic library RPCI-22. The targeting vector was constructed by recombination and routine cloning methods using an 11-kb *TL1A* genomic fragment from clone 112H6 as the starting material (Fig. 1A) (37). The 2.05-kb ScaI-XhoI genomic fragment containing exon 1 was replaced by a 1.1-kb Neo cassette from pMC1Neo Poly A (Fig. 1A). The final targeting fragment was excised from its cloning vector backbone by Not I digestion and electroporated into R1 embryonic stem (ES) cells for G418 (38). The targeted ES cell clones were injected into C57BL/6 blastocysts. Chimeric male mice were mated with C57BL/6 females to establish mutated *TL1A* allele germline transmission.

Southern blotting with a probe corresponding to the 5' sequence outside the targeting region, as illustrated in Figure 1A (hatched rectangle) was used to screen gene-targeted ES cells and eventually for the confirmation of the gene deletion in mouse tail DNA. The targeted allele showed an 11.7-kb StulI/StulI band, and the WT allele, a 5.4-kb StulI/StulI band.

The *TL1A*-KO mice were subsequently backcrossed to the DBA/1LacJ for 8 generations for experimentation in this study. The littermate WT mice served as controls. In the beginning of the experiments, mice were on average 8 to 12 weeks of age.

PCR was adopted for routine genotyping of the targeted allele(s). The following PCR conditions were applied: 4 min at 94 ^{o}C, followed by 35 cycles of 30 s at 94 ^{o}C, 30 s at 68 ^{o}C, and 30 s at 72 ^{o}C with final incubation at 72 ^{o}C for 10 min. One forward primer and two reverse primers (forward primer 5'- TCC ACA GCC AAC ATA GGC AAG GA-3'; reverse primers 1: 5'- GTG TGG CTT GCA ACA GGA AAT GGA -3'; reverse primer 2 5'- ACC TGC GTG CAA TCC ATC TTG TTC-3') were included in the PCR which amplified a 581-bp fragment from the targeted allele and a 335-bp fragment from the WT allele. All mice were housed under specific pathogen-free conditions and studied according to protocols approved by the Institutional Animal Protection Committees of the CRCHUM and INRS-IAF.

Reverse transcription-quantitative PCR (RT-qPCR)

Murine TL1A and DR3 mRNA was measured by RT-qPCR. Total RNA was isolated from cells or tissues with Trizol reagent (Invitrogen, Carlsbad CA). For TL1A mRNA measurement, the forward primer 5'-TCA TTT CCC ATC CTC GCA GGA CTT-3' and reverse primer 5'-TAA TTG TCA GGT GTG CTC TCG GCT-3' were used to generate a 166-bp fragment. For measurement of mRNA of all 3 DR3 isoforms (the full length one, the one with transmembrane domain deletion and the one with deletion of the extracellular CRD domain), the forward primer 5'-AGA GGT ATG GCC CGT TTT G-3' and reverse primer 5'-AAG TGG TTG TCT CTG GTC AAG-3' were used to generate a 133-bp fragment. For mRNA of the full-length DR3 isoform, the forward primer 5'-TGC CTG GCT GGC TTC TAT ATA CGT G -3' and reverse primer 5'-ACA GAC AGC AGT GCA AGC CTT A-3' were used to generate a 92-bp fragment. The PCR conditions for both reactions were as follows: 2 min at 95^{o}C followed by 45 cycles of 10 s at 95^{o}C, 15 s at 56^{o}C and 20 s at 72^{o}C. Samples were in triplicates. β-actin mRNA levels was measured as described in our previous publication and taken as internal controls(5). The data were expressed as signal ratios of either TL1A mRNA/β-acting mRNA or DR3 mRNA/β-actin mRNA.

Flow cytometry

Single cell suspensions from the thymus, spleen and lymph nodes (LN) were prepared and stained immediately or after culture for 2-, 3-, 4- or 5-color flow cytometry. Mouse anti-mouse TL1A mAb (Tandys1a) was from eBioscience (San Diego, CA). Anti-PD-1 mAb; anti-GL7 mAb, anti-ICOS mAb, anti-CD40L mAb, anti-CXCR5 mAb, and anti-DR3 mAb were from BD Biosciences (Missisauga, ON, Canada) and eBioscience. The rest mAbs used in flow cytometry are described in our previous publications(39).

Cell culture and in vitro T help cells (Th) differentiation

In general, total spleen or LN cells, T cell subpopulations, B cell subpopulations or bone marrow cells were prepared, isolated with Miltanyii beads or sorted by flow cytometry as indicated and then cultured in RPMI1640 medium containing 10% FCS, 100 μg/ml streptomycin, 100 units/ml penicillin G, 1× nonessential amino acids, 1 μM sodium pyruvate,

2.5 μM β-mercaptoethanol and other supplements as indicated. In some cases, recombinant mouse TL1A (aa76-252; R & D systems, Minneapolis, MN) was added to the culture.

In vitro Th differentiation was conducted as follows. Naïve CD4 T cells ($CD4^+CD62L^+CD44^{low}$) were isolated from TL1A KO or WT mouse spleens with MagCellect Mouse Naïve $CD4^+$ T cell Isolation kits (R & D Systems). T cell-depleted TL1A KO or WT spleen cells were irradiated at 3000 Rad and used as feeder cells. The naïve CD4 cells (0.1×10^6/ well) were mixed with the feeder cells (0.5×10^6/well) and cultured in 96-well plates in the presence of soluble anti-CD3ε mAb (clone 145-2C11, 2 μg/ml; BD Biosciences). Cultures were supplemented with recombinant mouse IL-12 (10 ng/ml; R & D Systems) and anti-IL-4 mAb (10 μg/ml; R & D Systems) for the Th1 condition; recombinant mouse IL-4 (20 ng/ml; R & D Systems), anti-IL-12 mAb (10 μg/ml; BD Biosciences) and anti-IFN-γ mAb (10 μg/ml; R & D Systems) for the Th2 condition; recombinant mouse IL-6 (20 ng/ml; R & D Systems), recombinant human TGF-β1 (5 ng/ml; R & D Systems) and anti-IL-4 and anti-IFN-γ mAb (10 μg/ml; R & D Systems) for the Th17 condition; recombinant human TGF-β1 (5 ng/ml; R & D Systems), anti-IL-4 and anti-IFN-γ mAb (10 μg/ml; R & D Systems) for the Treg condition; and recombinant mouse IL-6 (20 ng/ml; R & D Systems), anti-IL-4 and anti-IFN-γ mAb (10 μg/ml) for the Tfh-like cell condition, without any supplement for the Th0 condition.

Mouse CIA model

Eight- to 12-week old TL1A KO mice and their WT littermates in the DBA/1LacJ background were used in the experiments. Details of the induction of CIA in these mice were previously described (5). Briefly, mice were immunized with single intradermal injection at the base of the tail with 100 μg of bovine type II collagen (BTIIC; Chondrex, Redmond, WA), which was emulsified in equal volumes of complete Freund's adjuvant (CFA; 4 mg/ml Mycobacterium tuberculosis, strain H37Ra; Difco, Detroit, MI) on day 0. The mice were examined for their development and severity of arthritis from day 20 to 50. Disease severity was scored on a scale from 0 to 4 by visual inspection of each paw according to methodology of Brand et al. with some modifications as follows: 0 = normal paw; 1 = erythema and mild swelling confined to two or more digits, or the tarsal, or the ankle joint; 2 = erythema and mild swelling

of any two regions of the metatarsal, tarsal or ankle joint; 3 = erythema and moderate swelling extending from the ankle to metatarsal joints; 4 = erythema and severe swelling encompassing the ankle, foot and digits, or ankylosis of the limb (40). The scores for each of four paws were added to give a final score, such that the maximal severity score was 16 for each mouse. The mice were considered as having arthritis, if their clinical score was equal to or above 1.

Histology

Mice immunized with BTIIC/CFA were sacrificed on day 50, and then their paws including ankles were surgically removed and fixed in 10% buffered formalin. Following decalcification in 5% formic acid, the specimens were processed for paraffin embedding. Tissue sections (7 μm) that were stained with hematoxylin/eosin and Safranin O (for cartilage staining) were scored according to three parameters, i.e., lining hyperplasia, bone erosion destruction and cell infiltration, in one-way blind fashion with the examiner not knowing the identity of the sections. Each parameter was scored on a 0–3 scale, as previously described, and all four paws (one section per paw) of each animal were scored. The overall score of an animal was the sum of the three parameters of the four paws(41).

Isolation of infiltrating cells of hematopoietic origin in paws

The mouse vascular system was perfused with 20 ml PBS under anaesthesia. The paws were then harvested, skinned and minced into small pieces, which was then digested with collagenase II (2 mg/ml, Chondrex, Redmont, WA) and dispase II (250 μg/ml, Roche Diagnostics, Indianapolis, IN) in 5 ml Hank's balanced salt solution at 37 ^{o}C for 40 min. The digested product was washed and passed through cell strainers (BD bioscience, San Jose, CA) of 70 μm in pore size, consecutively. Cells in the passing-through liquid was enumerated and stained with anti-CD45.2, CD11c, CD11b, Thy1.2 and B220 mAbs, and analysed and counted with flow cytometry.

Enzyme-linked immunoabsorbent assay (ELISA) for the titres of anti-BTIIC Abs

ELISA was used to measure the titres of mouse serum anti-BTIIC Abs. Flat-bottom 96-well plates (Costar EIA/RIA plate #3590, Fisher Scientific, Pittsburgh, PA) were coated with BTIIC in PBS (100 μl/well) overnight at 4 ^{o}C. After blocking for 1 h at room temperature with 3% BSA in PBS, the plates were washed with PBS containing 0.05% Tween 20. Samples in

duplicate were added to the wells (50 μl/well) and incubated overnight at 4 ^{o}C. After extensive washes, 50 μl horse radish peroixdase-conjugated goat anti-mouse IgG_1, IgG_{2a} and IgG_{2b} antisera (1:5000 dilution; Southern Biotechnology, Birmingham, AL) or rabbit anti-mouse IgG (1:5000 dilutions; GE healthcare life sciences, Little Chalfont, Bucks, United Kindom) were added to each well. Two hours later, the plates were washed, and tetramethylbenzidine (50 μl/well; BD Biosciences, San Jose, CA) was added followed by 10 min incubation at room temperature in the dark. Finally, 2N H_2SO_4 (50 μl/well) was added to the wells to stop the reaction, and optical densities were determined at 450 nm. The serum anti-BTIIC Ab titre of a WT with the highest level of anti-BTIIC Ab on day 28 after the BTIIC/CFA immunization was arbitrarily designated as a titre of one and used as a standard to determine the titres of all the serum samples.

ELISPOT for enumeration of anti-BTIIC Ab-producing cells

Multiscreen® filter plate (Millipore, Billerica, MA) was coated with BTIIC as described for ELISA. The wells were blocked with culture medium (RPMI1640 medium containing 10% FCS) for 2 h at 37 ^{o}C and then washed. Cells from draining LN (1×10^5 cells/100 μl/well) or bone marrow (BM; 5×10^5 cells/100 μl/well) in culture medium were added to the wells and incubated for 4 h at 37 ^{o}C. The plates were then washed, and biotin-Streptavidin conjugated AffiniPure F(ab')2 fragment of goat anti-mouse IgG Ab (Jackson ImmunoResearch, West Grove, PA) was applied. After overnight incubation at 4 ^{o}C, the plates were extensively washed. Alkaline-phosphatase conjugated-streptavidin (1:60 R&D systems) was added to the wells and incubated for 2 h at room temperature. The spots were visualized by adding 5-bromo-4-chloro-3-indolyl phosphate/nitro blue tetrazolium substrate (R&D systems). Pictures of each well were taken with an ELISPOT reader (C.T.L., Shaker Heights, OH) and spots were counted visually.

Results

Generation of TL1A KO mice and general features of their immune system

To understand the role of TL1A in immune responses, we generated TL1A KO mice. The targeting strategy was illustrated in Figure 1A. Germ-line transmission of targeted TL1A was confirmed by Southern blotting using tail DNA (Fig. 1B), and PCR was used for routine genotyping of KO, WT and heterozygous pups (Fig. 1C). TL1A deletion of KO mice at the mRNA level was verified by RT/qPCR as shown in Figure 1D. The deletion of TL1A protein in T cells from KO mice was demonstrated in Figure 1E according to flow cyotmetry. The KO mice were fertile and had no visible anomaly. Lymphoid organs such as the thymus, spleens and lymph nodes were of normal sizes and cellularity (data not shown). The CD4CD8 double-negative (DN), CD4CD8 double-positive, CD4 single-positive and CD8 single-positive subpopulations in the TL1A KO thymi were comparable to those in the WT thymi (Fig. 2A). The CD4 and CD8 T cell percentages (Fig. 2A) and B (Fig. 2B) cell percentages in the spleen and lymph nodes of TL1A KO mice were in the normal ranges. These results indicate that TL1A KO does not significantly affect T and B cell development.

We examined Th1, Th17 and Treg cell populations in the spleen and lymph nodes of TL1A KO and WT mice *ex vivo*, but no apparent differences were found (Fig. 2C). Th2 cells in the KO and WT spleens were below the reliable detection level (data not shown). We next assessed whether a lack of TL1A affected Th1, Th2, Th17 and Treg cell development *in vitro.* We compared WT and KO T cell-depleted splenocytes in their capacity to support the development of the said T cell populations, using naïve KO CD4 T cells as starting cells, which were used because they did not produce TL1A to confound result interpretation. The KO non-T splenocytes were capable of supporting the naïve KO CD4 T cells differentiating into Th1, Th2, Th17 and Treg cells in a similar fashion as were their WT counterparts in supporting of naïve KO CD4 T cells (Fig. 2D). This suggests that a lack of TL1A minimally affects Th1, Th2, Th17 and Treg development *in vitro*.

The anti-viral immune responses of TL1A KO mice were evaluated in a lymphocytic choriomeningitis virus (LCMV) infection model. As illustrated in Supplementary Figure 1A, the number of CD4 cells and CD8 cells in the spleens on day 8 post-infection (8 dpi) presented

no significant differences in WT and TL1A KO mice. The absolute numbers and relative percentages of LCMV-specific, tetramer-positive (gp_{33-41}^{+} and $np_{396-404}^{+}$) CD8 cells in virus-infected mice were all increased in comparison to uninfected control C57BL/6 mice (data not shown), but there were no significant differences between TL1A KO and WT mice with regard to these parameters (Supplementary Figs. 1B and 1C). The absolute number and relative percentages of LCMV-specific TNF-α-producing CD4 (gp_{61-80}^{+}) and CD8 cells (gp_{33-41}^{+}) (Supplementary Figs. 1D and 1E), and LCMV-specific IFN-γ-producing CD4 (gp_{61-80}^{+}) and CD8 cells (gp_{33-41}^{+}) (Supplementary Figs. 1F and 1G) in TL1A-KO mice were comparable to those in WT controls. This result indicates that TL1A is not essential in anti-LCMV immune responses.

TL1A KO mice presented ameliorated CIA

Our previous study demonstrated that administering recombinant TL1A aggravates CIA (5). Bull et al. demonstrated that neutralizing Ab against TL1A partially blocks antigen-induced arthritis (23). We wondered whether a total lack of TL1A would affect RA pathogenesis in the CIA model. TL1A KO and WT mice in the DBA/1LacJ background were immunized with BTIIC/CFA to induce CIA. The draining lymph nodes (dLN) of the immunized mice were assessed on day 14 after BTIIC/CFA immunization, a mid-term point between the starting of the immunization and a full-fledged CIA. The KO dLN were smaller in size (Fig. 3A, 1st panel) and lower in cellularity (2nd panel) compared to their WT counterparts. The absolute numbers of T cells and B cells in these KO dLN were significantly lower than those in the WT dLN (3rd and 4th panels). We assessed the size of the germinal centres (GC) and the percentage and absolute number of GC B cells in the dLN. As shown in Supplementary Figure 2A, TL1A KO dLN showed no abnormality in term of the size of the germinal centres. This is consistent with the fact that the percentages of GC B cells among the total dLNs cells were comparable between WT and KO (Supplementary Figure 2B). However, the absolute number of GC B cells in the dLNs was significantly lower in KO than in WT mice (Supplementary Figure 2C), due to a reduction of the cellularity of the KO dLNs.

The TL1A KO mice displayed slower onset of CIA and significantly lower clinical scores (Fig. 3B). Incidence of CIA in the TL1A KO mice was also lower compared to that amongst the WT controls before day 31 after the immunization, although all TL1A KO mice eventually developed CIA (Fig. 3C). At the end of the experiment, on day 50, the arthritic paws of the TL1A KO and WT groups were collected and then assessed histologically. As illustrated in Fig. 3D, the TL1A KO paws had less synovial membrane hyperplasia (asterisks), less immune cell infiltration and milder cartilage erosion (arrow heads). The pathological scores of the TL1A KO groups were significantly lower compared to the WT controls' (Fig. 3E). We isolated cells from paws on day 19 after BTIIC/CFA immunization, which was chosen because it was shortly before the onset of the disease and paws were still normal in appearance, so that the selection of the paws was in no way biased. The number of cells of the hematopoietic origin isolated from the paws was significantly smaller in TL1A KO mice than in WT mice, but the percentages of DC, neutrophils/macrophages/monocytes, T cells, and B cells among the total isolated cells from TL1A KO and WT paws showed no statistically significant differences (Fig. 3F).

These results clearly show that a lack of TL1A diminishes the severity of CIA.

TL1A KO mice had lower collagen-specific Ab titres after BTIIC/CFA immunization

The non-immunized TL1A KO and WT mice had comparable levels of total serum IgG, IgM, IgA, and IgG subtypes IgG_1, IgG_{2a} and IgG_{2b}, IgG_3 (Supplementary Fig. 3). Auto-Abs are pathogenic in RA (42, 43), and anti-collagen Ab is especially so in CIA. We measured the BTIIC-specific Ab during the course of CIA from day 14 to day 50 after BTIIC/CFA immunization. The BTIIC-specific total IgG titres in the KO mice were significantly lower than their WT counterparts at all time points starting from day 21 (Fig. 4A). Among the IgG isotypes, BTIIC-specific $IgG2_a$ and $IgG2_b$ but not IgG_1 titres in the TL1A KO mice were significantly lower than in the WT mice (Figs. 4B-D). The reduced titres of collagen-specific Abs titres, especially the $IgG2_a$ and $IgG2_b$ isotypes, which are major pathogenic Ab isotypes in CIA (44), is likely a relevant factor for the observed reduced CIA severity in the TL1A KO mice.

CIA-related T cell functions in TL1A KO mice

T cells are a major type of target cells of TL1A, and play vital role in RA pathogenesis including producing inflammatory lymphokines such as IFN-γ and IL-17 and providing help to B cells for pathogenic Ab production. We assessed the antigen-specific dLN T cells for their IFN-γ- and IL-17-production and proliferation upon *in vitro* collagen restimulation shortly before the onset of CIA on day 14 after the immunization, a time point these cells reportedly become detectable in this location (45, 46). However, no significant difference between TL1A KO and WT dLN was found (Supplementary Figures 4A and 4B). This finding is in agreement with a previous study concerning the role of TL1A in antigen-specific responses. In the OT-II system, deficiency of TL1A/DR3 signal does not affect Naïve T cells differentiation under antigen-specific stimulation, and DR3 KO dLN cells from EAE mice proliferate normally to the stimulation of MOG peptides *in vitro*(15). It is also compatible with the data of polyclonal T cell activation as shown in Figure 2.

CRCXR5$^+$/PD-1$^+$ follicle T help cells (Tfh) express CD40L and ICOS on the cell surface and produce IL-21, all of which are essential in B cell survival, differentiation and eventually Ab production. We examined Tfh in the dLN on day 18 after the immunization, shortly before the lower titres of BTIIC-specific Abs in the KO CIA mice became apparent. The TL1A KO and WT dLN harboured similar percentages of CRCXR5$^+$/PD-1$^+$ Tfh (Fig. 5A, left column); TL1A KO and WT Tfh cells expressed comparable levels of CD40L and ICOS (Fig. 5A, right column). Probably as a consequence, the Fas$^+$GL7$^+$ germinal centre B cells percentages in the dLN of TL1A KO and WT were not different (Fig. 5B). With that said, since the absolute number of T cells in the KO dLN was reduced (Fig. 3A), the absolute number of Tfh in the KO dLN was still smaller than that of WT dLN. We confirmed that undifferentiated CD4 T cells (Th0) did not expression DR3, but Th1, Th17 and Tfh cells all expressed DR3, providing a basis for them to respond to TL1A (Fig. 5C). *In vitro* differentiated Tfh cells from naïve TL1A KO and WT CD4 cells were all capable of produce high levels of IL-21, compared to KO Th0, Th1 and Th17 cells (Fig. 5D). Exogenous TL1A did not enhance IL-21 production by KO Tfh cells (Fig. 5D). The results of this section suggest that the deletion or exogenous

TL1A does not have significant effect on Tfh cells with regard to their B cell helper functions, such as their CD40L/ICOS expression and IL-21 production, although the diminished absolute number of Tfh in the KO dLN might be a factor contributing to the reduced level of collagen-specific Abs in KO CIA mice.

Plasma cells are direct target cells of TL1A

It is puzzling that in TL1A KO CIA mice, there was an obvious decrease in antigen-specific Ab production, yet T cell's B-cell-facilitating function showed no signs of compromise, with the exception of a decrease of absolute number of Tfh. To date, B cells and their derivative plasma cells are not known target cells of TL1A, as an earlier study demonstrate that B cells do not express or express very little DR3 (3, 13), although Pelletier et al. did reveal that in vitro generated human plasma cells express DR3 at the protein level(47). We confirmed that indeed, $B220^{+}CD138^{-}$ B cells did not express DR3, nor did $B220^{+}CD138^{+}$ plasmablasts (Fig. 6A, left and middle panel). However, we discovered that plasma cells from dLN of BTIIC/CFA-immunized WT mice expressed very high levels of DR3 (Fig. 6A, right panel). DR3 has a full-length isoform and also truncated isoforms (10). According to RT/qPCR, T cells and plasma cells expressed similar levels of the full-length DR3 isoform Fig. 6B, left panel), while the former expressed more isoforms with deletions (Fig. 6B, middle and right panels). The expression of the full length DR3 isoform on plasma cells provided a basis for them to respond to TL1A. We then interrogated the effect of TL1A on plasma cells. B cells and plasma cells from draining LN of KO mice 21 days after BTIIC/CFA immunization were negatively selected using B cell negative selection kit (STEMCELL Technologies) by eliminating T, NK, monocyte/macrophages and dendritic cells. The remaining B cells and plasma cells were cultured for six days in the presence of exogenous TL1A, as there was no endogenous TL1A in this system. In the presence of TL1A, significantly more plasma cells survived after the six-day culture (Fig. 6C, left panel) and there were higher levels of collagen-specific IgG secreted into the supernatants (Fig. 6C, right panel), compared to the culture without TL1A. In support of such *in vitro* results, on day 28 after the BTIIC/CFA immunization, when the anti-BTIIC Ab production was actively produced and WT mice had significantly higher titres of serum anti-BTIIC Abs, draining LN cells and bone marrow cells

from WT mice presented significantly higher numbers of anti-BTIIC Ab-secreting plasma cells compared to those from TL1A KO draining LN, according to ELISPOT (Figs. 6D-6F). Collectively, the data from this section suggest that TL1A can directly promote plasma cell survival and function in terms of Ab production, and this effect in turn contributes to the elevated pathogenic Ab production in CIA. Conversely, in the absence of TL1A, the well-being of the plasma cells is compromised, and this is one of the factors leading to decreased levels of pathogenic anti-collagen Ab in TL1A KO mice.

Discussion

In this study, we revealed that TL1A KO mice had ameliorated CIA compared to WT mice. No significant T cell dysfunction including Th17 and Treg differentiation was apparent in the absence of TL1A, and the TL1A KO mice had normal anti-LCMV immune responses. The KO mice presented reduced production of pathogenic anti-collagen Ab. A novel finding in this study is that plasma cells were a direct target of TL1A, that these cells expressed high levels of the full-length isoform of TL1A receptor DR3. TL1A promoted plasma cell's survival and Ab-production.

The results of our current study and several previous studies support the general concept that TL1A can intensify inflammatory response. For example, DR3 KO mice present reduced EAE and antigen-induced arthritis (15). The administration of exogenous TL1A aggravates CIA, while TL1A neutralizing Ab reduces the severity of CIA(5, 23). Transgenic overexpression of TL1A worsens DSS-induced colitis and causes intestinal mucosal inflammation(9, 20, 21, 48). Several mechanistic aspects of these disease models corroborate each other. For example, our data using TL1A KO mice showed that TL1A was not required for constitutive or induced Th1, Th2, Th17 and Treg cell development; studies using deletion of DR3 reached the same conclusion(15). However, there are also discrepancies between the conclusions obtained from DR3 KO mice versus TL1A KO mice, and from TL1A administration/overexpression vs. TL1A/DR3 deletion studies. The discrepancies and possible explanations are discussed as follows.

It seems that excessive TL1A, either from exogenous recombinant protein or endogenous transgenic over-expression often results in enhanced IFN-γ and IL-17 expression, but TL1A KO or DR3 KO has minimal effect on constitutive or inducible Th1 and Th17 cell development (5, 9, 15, 48). A possible explanation for this discrepancy is that such Th cell development is vital to the biological system, and there is sufficient redundancy to compensate for the missing DR3 or TL1A in the KO mice. As a consequence, in the absence of DR3 or TL1A, Th cells could still be developed to near-normal levels. Alternatively, DR3 and TL1A are not utterly essential in Th cell development; the enhanced Th cell development in the presence of non-physiological high doses of exogenous or transgenic TL1A is due to its cross-

reaction with other TNFR superfamily members (12). The results from CIA mice treated with TL1A neutralizing Ab favour the first explanation (23). In this model, there is no excessive exogenous TL1A, and the reduction of the bio-active TL1A occurs at the adult stage and is not complete, less likely triggering a drastic compensation. Such a neutralizing Ab treatment can hampers the development of Th1 and Th17 cells, which are reported essential in CIA pathogenesis, and results in reduced CIA severity (49).

We demonstrated that TL1A KO mice showed no abnormality in anti-viral immune responses against LCMV. However, DR3-KO mice manifest compromised anti-MCMV immunity (24). Although TL1A is a ligand of DR3, there are around 20 other TNF superfamily members that share some degrees of homology with TL1A. In the absence of TL1A, other members of the TNF superfamily might individually or collectively bind to DR3, albeit at a lower affinity, and such binding might trigger some low level DR3 signalling, which could be sufficient to compensate for the missing TL1A. On the other hand, a missing DR3 will totally eliminate the DR3 signalling, resulting more drastic phenotype including compromised anti-virus immune responses. Although we favour this hypothesis, we cannot exclude the possibility that the observed difference in DR3 KO and TL1A KO regarding the anti-virus immune responses is caused by different viruses, i.e., MCMV vs. LCMV.

Another interesting point is the role of TL1A in Treg development. In our TL1A KO and WT mice, no difference was found in constitutive or induced Treg populations. Not surprisingly, there was no aggravation but amelioration of CIA in the TL1A KO mice. In mice with transgenic TL1A expression or mice administered with exogenous recombinant TL1A, the immune/inflammation responses were aggravated but not ameliorated (5, 9, 21, 48). In all the studies using either TL1A or DR3 KO mice models or TL1A neutralizing Abs(3, 15, 23-25), the immune responses were abated. Although the Treg status of the above mentioned studies are not always assessed, at least we could conclude that excessive TL1A does not lead to reduced immune response, a possible functional consequence of Treg upregulation. Conversely, TL1A or DR3 deletion does not lead to exuberant immune responses, which are a possible functional consequence of Treg downregulation.

Our ex vivo data indicated that the percentages of Th1, and Th17 cells in draining LN were comparable between CIA WT and CIA KO mice. However, since there was a drastic reduction of cellularity and absolute T cell number in the draining lymph nodes of KO mice, the absolute numbers of these effector cells were also reduced. Such reduction could likely cause a compromised CIA development in the TL1A KO mice.

Several members of TNF family are involved in regulating the humoral immune responses. They could either affect the B cells directly or indirectly through T cells. A well-studied member is CD40L, which is essential to generation of plasma cells (50). CD40/CD40L signalling initiates GC responses, GC B cell proliferation, isotype switching and differentiation of B cells into plasma cells (51). Since DR3 was reportedly expressed mainly on T cells in the immune system, we assessed the effect of TL1A on Tfh cells. Our *ex vivo* data indicated that the percentages of Tfh cells in draining LN were comparable between WT and KO mice with CIA. The functions of KO Tfh cells, in terms of CD40L expression and IL-21 production, were not compromised, neither. However, since there was a significant reduction of absolute T cell number in the draining LN of KO mice, comparing to that of WT mice, it is conceivable that absolute number of Tfh and GC B cells in the draining LN of KO mice was reduced. Such reduction might contribute to compromised collagen-specific Ab production in CIA TL1A KO mice.

We found that the plasma cells also expressed functional DR3. This finding pin-pointed such plasma cells as a target cell population for TL1A's effect. We demonstrated that TL1A could promote draining LN plasma cell survival in vitro. The direct effect of TL1A on plasma cell survival might be one of the contributing mechanisms for the following observation: 1) TL1A KO results in reduced number of collagen-specific Ab producing plasma cells ex vivo, and reduced collagen-specific Ab titers in vivo; 2) recombinant TL1A enhanced collagen-specific Ab production *in vitro*. However, we noticed that in unimmunized KO mice, their total serum IgG levels and plasma cell population were comparable to those of WT mice. It is possible that the benefit of TL1A to plasma cells is only for a limited time during a humoral response, and perhaps even specific to a restricted stage of the plasma cells.

We demonstrated that reduced pathogenic Ab production is a mechanism contributing to milder CIA in the TL1A-KO mice. However, it is probably not the only mechanism responsible for this phenotype. We have assessed several T cells function in the absence of TL1A, and did not find any anomaly, but such assessment is by no means exhaustive. We did find that there was a significant reduction of inflammatory immune cell infiltration in the CIA paws, and this phenomenon is consistent with the findings with several disease models in that there is always a reduction of inflammatory cells in the diseased organ or tissues when DR3 or TL1A is missing (15, 22). This is certainly an additional mechanism by which TL1A contributes to the pathogenesis of CIA. We tested TL1A KO T cell chemotaxis toward several CIA-related chemokines *in vitro* using Transwell, but no significant defect was detected. More comprehensive investigations in this aspect including assessing local chemokine secretion by T cells, monocyte/macrophages and DC, and the endothelium permeability in the excessive or absence of TL1A are warranted.

Reference

1. Migone, T. S., J. Zhang, X. Luo, L. Zhuang, C. Chen, B. Hu, J. S. Hong, J. W. Perry, S. F. Chen, J. X. H. Zhou, Y. H. Cho, S. Ullrich, P. Kanakaraj, J. Carrell, E. Boyd, H. S. Olsen, G. Hu, L. Pukac, D. Liu, J. Ni, S. Kim, R. Gentz, P. Feng, P. A. Moore, S. M. Ruben, and P. Wei. 2002. TL1A is a TNF-like ligand for DR3 and TR6/DcR3 and functions as a T cell costimulator. *Immunity* 16: 479–492.

2. Bamias, G., M. Mishina, M. Nyce, W. G. Ross, G. Kollias, J. Rivera-Nieves, T. T. Pizarro, and F. Cominelli. 2006. Role of TL1A and its receptor DR3 in two models of chronic murine ileitis. *Proc Natl Acad Sci USA* 103: 8441–8446.

3. Fang, L., B. Adkins, V. Deyev, and E. R. Podack. 2008. Essential role of TNF receptor superfamily 25 (TNFRSF25) in the development of allergic lung inflammation. *J. Exp. Med.* 205: 1037–1048.

4. Takedatsu, H., K. S. Michelsen, B. Wei, C. J. Landers, L. S. Thomas, D. Dhall, J. Braun, and S. R. Targan. 2008. TL1A (TNFSF15) regulates the development of chronic colitis by modulating both T-helper 1 and T-helper 17 activation. *Gastroenterology* 135: 552–567.

5. Zhang, J., X. Wang, H. Fahmi, S. Wojcik, J. Fikes, Y. Yu, J. Wu, and H. Luo. 2009. Role of TL1A in the pathogenesis of rheumatoid arthritis. *The Journal of Immunology* 183: 5350–5357.

6. Prehn, J. L., S. Mehdizadeh, C. J. Landers, X. Luo, S. C. Cha, P. Wei, and S. R. Targan. 2004. Potential role for TL1A, the new TNF-family member and potent costimulator of IFN-gamma, in mucosal inflammation. *Clin Immunol* 112: 66–77.

7. Kim, S., and L. Zhang. 2005. Identification of naturally secreted soluble form of TL1A, a TNF-like cytokine. *J. Immunol. Methods* 298: 1–8.

8. Biener-Ramanujan, E., R. Gonsky, B. Ko, and S. R. Targan. 2010. Functional signaling of membrane-bound TL1A induces IFN-gamma expression. *FEBS letters* 584: 2376–2380.

9. Meylan, F., Y.-J. Song, I. Fuss, S. Villarreal, E. Kahle, I.-J. Malm, K. Acharya, H. L. Ramos, L. Lo, M. M. Mentink-Kane, T. A. Wynn, T.-S. Migone, W. Strober, and R. M. Siegel. 2011. The TNF-family cytokine TL1A drives IL-13-dependent small intestinal inflammation. *Mucosal immunology* 4: 172–185.

10. Wang, E. C., J. Kitson, A. Thern, J. Williamson, S. N. Farrow, and M. J. Owen. 2001. Genomic structure, expression, and chromosome mapping of the mouse homologue for the WSL-1 (DR3, Apo3, TRAMP, LARD, TR3, TNFRSF12) gene. *Immunogenetics* 53: 59–63.

11. Bu, R., C. W. Borysenko, Y. Li, L. Cao, A. Sabokbar, and H. C. Blair. 2003. Expression and function of TNF-family proteins and receptors in human osteoblasts. *Bone* 33: 760–770.

12. Al-Lamki, R. S., J. Wang, A. M. Tolkovsky, J. A. Bradley, J. L. Griffin, S. Thiru, E. C. Y.

Wang, E. Bolton, W. Min, P. Moore, J. S. Pober, and J. R. Bradley. 2008. TL1A both promotes and protects from renal inflammation and injury. 19: 953–960.

13. Craxton, A., G. Shu, J. D. Graves, J. Saklatvala, E. G. Krebs, and E. A. Clark. 1998. p38 MAPK is required for CD40-induced gene expression and proliferation in B lymphocytes. *J Immunol* 161: 3225–3236.

14. Screaton, G. R., X. N. Xu, A. L. Olsen, A. E. Cowper, R. Tan, A. J. McMichael, and J. I. Bell. 1997. LARD: a new lymphoid-specific death domain containing receptor regulated by alternative pre-mRNA splicing. *Proc Natl Acad Sci USA* 94: 4615–4619.

15. Meylan, F., T. S. Davidson, E. Kahle, M. Kinder, K. Acharya, D. Jankovic, V. Bundoc, M. Hodges, E. M. Shevach, A. Keane-Myers, E. C. Y. Wang, and R. M. Siegel. 2008. The TNF-family receptor DR3 is essential for diverse T cell-mediated inflammatory diseases. *Immunity* 29: 79–89.

16. Papadakis, K. A., J. L. Prehn, C. Landers, Q. Han, X. Luo, S. C. Cha, P. Wei, and S. R. Targan. 2004. TL1A synergizes with IL-12 and IL-18 to enhance IFN-gamma production in human T cells and NK cells. *J Immunol* 172: 7002–7007.

17. Bamias, G., C. Martin, M. Marini, S. Hoang, M. Mishina, W. G. Ross, M. A. Sachedina, C. M. Friel, J. Mize, S. J. Bickston, T. T. Pizarro, P. Wei, and F. Cominelli. 2003. Expression, localization, and functional activity of TL1A, a novel Th1-polarizing cytokine in inflammatory bowel disease. *J Immunol* 171: 4868–4874.

18. Bamias, G., S. I. Siakavellas, K. S. Stamatelopoulos, E. Chryssochoou, C. Papamichael, and P. P. Sfikakis. 2008. Circulating levels of TNF-like cytokine 1A (TL1A) and its decoy receptor 3 (DcR3) in rheumatoid arthritis. *Clin Immunol* 129: 249–255.

19. Bamias, G., G. Kaltsa, S. I. Siakavellas, K. Papaxoinis, E. Zampeli, S. Michopoulos, I. Zouboulis-Vafiadis, and S. D. Ladas. 2010. High intestinal and systemic levels of decoy receptor 3 (DcR3) and its ligand TL1A in active ulcerative colitis. *Clin Immunol* 137: 242–249.

20. Taraban, V. Y., T. J. Slebioda, J. E. Willoughby, S. L. Buchan, S. James, B. Sheth, N. R. Smyth, G. J. Thomas, E. C. Y. Wang, and A. Al-Shamkhani. 2011. Sustained TL1A expression modulates effector and regulatory T-cell responses and drives intestinal goblet cell hyperplasia. *Mucosal immunology* 4: 186–196.

21. Shih, D. Q., R. Barrett, X. Zhang, N. Yeager, H. W. Koon, P. Phaosawasdi, Y. Song, B. Ko, M. H. Wong, K. S. Michelsen, G. Martins, C. Pothoulakis, and S. R. Targan. 2011. Constitutive TL1A (TNFSF15) expression on lymphoid or myeloid cells leads to mild intestinal inflammation and fibrosis. *PLoS ONE* 6: e16090.

22. Pappu, B. P., A. Borodovsky, T. S. Zheng, X. Yang, P. Wu, X. Dong, S. Weng, B. Browning, M. L. Scott, L. Ma, L. Su, Q. Tian, P. Schneider, R. A. Flavell, C. Dong, and L. C. Burkly. 2008. TL1A-DR3 interaction regulates Th17 cell function and Th17-mediated

autoimmune disease. *J. Exp. Med.* 205: 1049–1062.

23. Bull, M. J., A. S. Williams, Z. Mecklenburgh, C. J. Calder, J. P. Twohig, C. Elford, B. A. J. Evans, T. F. Rowley, T. J. Slebioda, V. Y. Taraban, A. Al-Shamkhani, and E. C. Y. Wang. 2008. The Death Receptor 3-TNF-like protein 1A pathway drives adverse bone pathology in inflammatory arthritis. *J. Exp. Med.* 205: 2457–2464.

24. Twohig, J. P., M. Marsden, S. M. Cuff, J. R. Ferdinand, A. M. Gallimore, W. V. Perks, A. Al-Shamkhani, I. R. Humphreys, and E. C. Y. Wang. 2012. The death receptor 3/TL1A pathway is essential for efficient development of antiviral CD4+ and CD8+ T-cell immunity. *FASEB J.*

25. Buchan, S. L., V. Y. Taraban, T. J. Slebioda, S. James, A. F. Cunningham, and A. Al-Shamkhani. 2012. Death receptor 3 is essential for generating optimal protective CD4(+) T-cell immunity against Salmonella. *Eur. J. Immunol.* 42: 580–588.

26. Gay, S., R. E. Gay, and W. J. Koopman. 1993. Molecular and cellular mechanisms of joint destruction in rheumatoid arthritis: two cellular mechanisms explain joint destruction? *Ann. Rheum. Dis.* 52 Suppl 1: S39–47.

27. van der Heijden, I. M., B. Wilbrink, I. Tchetverikov, I. A. Schrijver, L. M. Schouls, M. P. Hazenberg, F. C. Breedveld, and P. P. Tak. 2000. Presence of bacterial DNA and bacterial peptidoglycans in joints of patients with rheumatoid arthritis and other arthritides. *Arthritis Rheum* 43: 593–598.

28. Mauri, C., and M. R. Ehrenstein. 2007. Cells of the synovium in rheumatoid arthritis. B cells. *Arthritis Res. Ther.* 9: 205.

29. Cooke, T. D., E. R. Hurd, H. E. Jasin, J. Bienenstock, and M. Ziff. 1975. Identification of immunoglobulins and complement in rheumatoid articular collagenous tissues. *Arthritis Rheum* 18: 541–551.

30. Vetto, A. A., M. Mannik, E. Zatarain-Rios, and M. H. Wener. 1990. Immune deposits in articular cartilage of patients with rheumatoid arthritis have a granular pattern not seen in osteoarthritis. *Rheumatol Int* 10: 13–19.

31. Mollnes, T. E., T. Lea, O. J. Mellbye, J. Pahle, O. Grand, and M. Harboe. 1986. Complement activation in rheumatoid arthritis evaluated by C3dg and the terminal complement complex. *Arthritis Rheum* 29: 715–721.

32. SCRIVO, R., M. DI FRANCO, A. SPADARO, and G. VALESINI. 2007. The Immunology of Rheumatoid Arthritis. *Ann N Y Acad Sci* 1108: 312–322.

33. Manzo, A., and C. Pitzalis. 2007. Lymphoid tissue reactions in rheumatoid arthritis. *Autoimmun Rev* 7: 30–34.

34. Lundy, S. K., S. Sarkar, L. A. Tesmer, and D. A. Fox. 2007. Cells of the synovium in

rheumatoid arthritis. T lymphocytes. *Arthritis Res. Ther.* 9: 202.

35. Stamp, L. K., M. J. James, and L. G. Cleland. 2004. Interleukin-17: the missing link between T-cell accumulation and effector cell actions in rheumatoid arthritis? *Immunol Cell Biol* 82: 1–9.

36. Imamura, F., H. Aono, T. Hasunuma, T. Sumida, H. Tateishi, S. Maruo, and K. Nishioka. 1998. Monoclonal expansion of synoviocytes in rheumatoid arthritis. *Arthritis Rheum* 41: 1979–1986.

37. Liu, P., N. A. Jenkins, and N. G. Copeland. 2003. A highly efficient recombineering-based method for generating conditional knockout mutations. *Genome Res.* 13: 476–484.

38. Nagy, A., J. Rossant, R. Nagy, W. Abramow-Newerly, and J. C. Roder. 1993. Derivation of completely cell culture-derived mice from early-passage embryonic stem cells. *Proc Natl Acad Sci USA* 90: 8424–8428.

39. Luo, H., T. Charpentier, X. Wang, S. Qi, B. Han, T. Wu, R. Terra, A. Lamarre, and J. Wu. 2011. Efnb1 and Efnb2 proteins regulate thymocyte development, peripheral T cell differentiation, and antiviral immune responses and are essential for interleukin-6 (IL-6) signaling. *Journal of Biological Chemistry* 286: 41135–41152.

40. Brand, D. D., K. A. Latham, and E. F. Rosloniec. 2007. Collagen-induced arthritis. *Nat Protoc* 2: 1269–1275.

41. Kojima, F., M. Kapoor, L. Yang, E. L. Fleishaker, M. R. Ward, S. U. Monrad, P. C. Kottangada, C. Q. Pace, J. A. Clark, J. G. Woodward, and L. J. Crofford. Defective Generation of a Humoral Immune Response Is Associated with a Reduced Incidence and Severity of Collagen-Induced Arthritis in Microsomal Prostaglandin E Synthase-1 Null Mice. *jimmunol.org*.

42. Smolen, J. S., D. Aletaha, and K. Redlich. 2012. The pathogenesis of rheumatoid arthritis: new insights from old clinical data? *Nat Rev Rheumatol* 8: 235–243.

43. McInnes, I. B., and G. Schett. 2011. The Pathogenesis of Rheumatoid Arthritis. *N Engl J Med* 365: 2205–2219.

44. Brand, D. D., A. H. Kang, and E. F. Rosloniec. 2003. Immunopathogenesis of Collagen Arthritis. *Springer Seminars in Immunopathology* 25: 3–18.

45. Sheibanie, A. F., T. Khayrullina, F. F. Safadi, and D. Ganea. 2007. Prostaglandin E2 exacerbates collagen-induced arthritis in mice through the inflammatory interleukin-23/interleukin-17 axis. *Arthritis Rheum* 56: 2608–2619.

46. Bouaziz, J.-D., K. Yanaba, G. M. Venturi, Y. Wang, R. M. Tisch, J. C. Poe, and T. F. Tedder. 2007. Therapeutic B cell depletion impairs adaptive and autoreactive CD4+ T cell activation in mice. *Proc Natl Acad Sci USA* 104: 20878–20883.

47. Pelletier, N., M. Casamayor-Pallejà, K. De Luca, P. Mondière, F. Saltel, P. Jurdic, C. Bella, L. Genestier, and T. Defrance. 2006. The endoplasmic reticulum is a key component of the plasma cell death pathway. *J Immunol* 176: 1340–1347.

48. Barrett, R., X. Zhang, H. W. Koon, M. Vu, J.-Y. Chang, N. Yeager, M. A. Nguyen, K. S. Michelsen, D. Berel, C. Pothoulakis, S. R. Targan, and D. Q. Shih. 2012. Constitutive TL1A expression under colitogenic conditions modulates the severity and location of gut mucosal inflammation and induces fibrostenosis. *Am. J. Pathol.* 180: 636–649.

49. McInnes, I. B., and G. Schett. 2007. Cytokines in the pathogenesis of rheumatoid arthritis. *Nat Rev Immunol* 7: 429–442.

50. Elgueta, R., M. J. Benson, V. C. de Vries, A. Wasiuk, Y. Guo, and R. J. Noelle. 2009. Molecular mechanism and function of CD40/CD40L engagement in the immune system. *Immunol Rev* 229: 152–172.

51. King, C., S. G. Tangye, and C. R. Mackay. 2008. T follicular helper (TFH) cells in normal and dysregulated immune responses. *Annu. Rev. Immunol.* 26: 741–766.

Figure legends

Figure 1. Generation of TL1A KO mice

A. Targeting strategy to generate TL1A KO mice. The shaded rectangle on the 5' side of the mouse TL1A WT genomic sequence represents the sequence serving as a probe for genotyping by Southern blotting.

B and C. Genotyping of TL1A mutant mice. Tail DNA was digested with StuI, and analyzed by Southern blotting, with the 5' probe whose location is indicated in A. Arrows indicate 11.7-kb bands representing the WT allele and a 5.4-kb band representing the recombinant allele (B). PCR was used for routine genotyping with ear-lobe tissue DNA. The 335-bp bands representing the WT allele and the 581-bp bands representing the recombinant allele are indicated by arrows (C). HET: heterozygous.

D. Absence of TL1A mRNA expression in TL1A KO T cells. Spleen T cells from WT and TL1A KO mice were stimulated with solid anti-CD3 (2μg/ml) and anti-CD28 (2μg/ml) for 24 h. Cell RNA was extracted and analyzed by RT-qPCR for TL1A expression. The results are expressed as ratios of TL1A versus β-actin signals with means $\pm$ SD indicated.

E. Absence of TL1A protein expression in KO T cells. WT and TL1A KO spleen T cells were stimulated as in (D) and stained with anti-CD4 mAb and anti-TL1A Ab and analyzed by 2-color flow cytometry. The shaded lines represent the isotypic Ab control, and the thick lines represent TL1A staining of $CD4^+$-gated T cells of WT (left panel) and KO (right panel) mice. Experiments in D and E were repeated at least twice and representative data are shown.

Figure 2. TL1A KO mice presented normal lymphocyte subpopulations

Experiments in this figure were repeated more than three times, and representative data are presented (A, B and D).

A. T-cell populations in WT and TL1A KO LN, spleens and thymus. Thymocytes, mesenteric LN cells, splenocytes were analyzed by 2-color flow cytometry for percentages of different T cell subpopulations.

B. B-cell populations in the LN and spleen of WT and KO mice. Mesenteric LN cells and splenocytes were analyzed by 2-color flow cytometry for percentages of $CD19^+/B220^+$ B cells.

C. Normal Th1, Th17 and Treg populations in TL1A KO mice ex vivo. WT or TL1A KO spleen cells were stimulated with PMA (50ng/ml) and ionomycin (1μg/ml) for 4 h in the presence of BD Golgistop, and analyzed by flow cytometry *ex vivo* for Th1, Th17 and Treg cell populations based on intracellular IFN-γ, IL-17 and FoxP3 staining. The bar graphs represent the summary of data from 3-4 experiments, with Mean + SD indicated.

D. Normal differentiation of TL1A-KO CD4 cells in vitro. Naïve TL1A-KO CD4 cells were cultured under conditions favouring Th1, Th2, Th17 and Treg cells, using WT or TL1A KO feeder cells, as indicated. Their intracellular cytokine or FoxP3 expression was quantified by 3-color flow cytometry on day 3 for Th1, Th17 and Treg cells, and on day 5 for Th2 cells after 4-h PMA (50ng/ml) and ionomycin (1μg/ml) stimulation in the presence of BD Golgistop before the assay.

Figure 3. TL1A-KO mice manifested less severe CIA

A. Reduced numbers of immune cells in KO draining lymph node during CIA induction. Mice were immunized with BTIIC/CFA at the tail base on day 0. On day 14 after the immunization, draining lymph nodes (dLNs) were collected and photographed (1^{st} panel), cells from dLN of WT (n=10) and TL1A KO (n=11) mice were isolated, enumerated and analysed by flow cytometry for subpopulations. The numbers of total dLN cells per mouse (2^{nd} panel), CD4 T cells ($CD4^+$) of the dLNs per mouse (3^{rd} panel) and B cells ($B220^+$) of the dLNs per mouse (4^{th} panel) are shown. The horizontal bars indicate the means. Student's *t* test was used to assess the statistical significance of the difference between WT and TL1A KO mice and the *p*-value is indicated.

B. CIA clinical scores of WT and KO mice after BTIIC/CFA immunization. WT (n=8) and TL1A KO (n=9) mice were immunized with BTIIC/CFA on day 0, and scored for their RA symptoms daily starting from day 21 until day 50. Mean ± SEM scores are plotted. Scores for

the WT and TL1A KO mice were evaluated statistically by 2-Way ANOVA. *P*-values are indicated.

C. CIA incidence in WT and TL1A KO mice. The CIA incidence of the WT and TL1A KO groups in (A) is plotted.

D and E. Histology of mouse joints. WT and TL1A KO Mice from (B) were sacrificed on day 50, and all the paws were sectioned and stained with haematoxilin/eosin (H&E) or safranin O (for cartilage staining) as indicated. Representative histology images from each group are shown (D). Asterisks indicate synovial hyperplasia and arrow heads indicate cartilage damage. Naïve: joints from normal unimmunized DBA/1 mice; WT-CIA: joints from WT mice immunized with BTIIC/CFA; KO-CIA: joints from KO mice immunized with BTIIC/CFA. The histology of each paw (one section per paw) was evaluated by blinded raters and scored semi-quantitatively based on lining hyperplasia, bone erosion and cell infiltration. Each parameter was scored on a 0–3 scale, and all four paws of each animal were scored. The overall score for each animal, which is the sum of the three parameters of the four paws, is shown in the plot and the horizontal bars represent the mean scores (E). Student's *t* test was performed to assess the statistical significant of the difference between WT and TL1A KO mice and the *p*-value is indicated.

F. Reduced numbers of infiltrating immune cells in KO paws during CIA induction. On day 19 after BTIIC/CFA immunization, before the onset of CIA symptoms, cells infiltrating the paws of WT and TL1A KO mice were isolated, enumerated and analysed by flow cytometry for subpopulations. The total numbers of infiltrating cells of hematopoietic origin ($CD45.2^+$) per paw is shown in the left panel; percentage of dendritic cells ($CD11c^+$), in the second panel; percentage of neutrophils/monocytes/macrophages ($CD11b^+$), the third panel; percentage of T cells ($Thy1.2^+$), in the fourth panel; and percentage of B cells ($B220^+$), in the last panel. Mouse numbers per group are indicated. Student's *t* test was used to assess the statistical significance of the difference between WT and TL1A KO mice and the *p*-value is indicated.

Figure 4. Reduced collagen-specific Ab production in KO mice with CIA

Sera were obtained from WT (n=7) and TL1A KO (n=7) mice on 14, 21, 28, 35, 42 and 50 days after BCTII/CFA immunization. Arbitrary titres of collagen-specific total IgG (A), IgG_1

(B), IgG_{2a} (C) and IgG_{2b} (D) were determined by ELISA. Serum from a WT mouse exhibiting typical arthritis was arbitrarily given a titre of 1 and used as reference in each assay. For A, B, C, D, mean ± SEM are presented and evaluated statistically by 2-Way ANOVA. *P*-values are indicated.

Figure 5. TL1A T cells presented normal help to B cells

The experiments in this figure were repeated three times and representative data are shown.

A. Flow cytometry analysis of Tfh in draining LN of mice after BTIIC/CFA immunization. WT or TL1A KO mice were immunized with BCTII/CFA and then sacrificed on day 18. $CD4^+$ T cells from dLN were purified and stimulated with solid anti-CD3ε (2μg/ml) and anti-CD28 (2μg/ml) Ab for 30 min. The percentage of $CD4^+PD\text{-}1^+CXCR5^+$ Tfh cells among $CD4^+$ cells were determined by flow cytometry and shown (right column). The gated Tfh were further analyzed for their CD40L and ICOS expressions (left column), and the percentages of $CD40L^+$ and $ICOS^+$ cells among Tfh ($PD\text{-}1^+/CXCR5^+$) cells are indicated.

B. Flow cytometry analysis of germinal centre (GC) B cell populations. $B220^+$ B cells from the draining LN of WT and TL1A KO mice on day 18 after BTIIC/CFA immunization were analysed for GL7 and Fas expression. The percentages of $B220^+GL7^+Fas^+$ GC B cells among $B220^+$ B cells are indicated.

C. DR3 expression on Th and Tfh cells. Naïve $CD4^+$ T cells were cultured on anti-CD3ε (2μg/ml for coating) and anti-CD28 (2μg/ml for coating) Ab-coated wells under Th1, Th17 and Tfh-like cell differentiation conditions. After 3 days, DR3 expression on $CD4^+$ cells was assessed by flow cyotmetry. Shaded area: isotypic controls. Thick lines: DR3 signals.

D. IL-21 production by in vitro differentiated WT and KO Tfh cells. WT or TL1A KO naïve $CD4^+$ T cells were cultured in anti-CD3 and anti-CD28 Ab-coated wells under the Tfh-like cell differentiation condition. They were also cultured under Th0 (without reagents for Th differentiation except anti-CD3ε, anti-IFN-γ and anti-IL-4 Abs), Th1 or Th17 conditions as controls. TL1A at 10 and 50 ng/ml was added to some cultures as indicated. On day 3, the cells were re-stimulated with PMA/ionomycin for 9 hours and IL-21 in the supernatants was measured by ELISA. Samples in ELISA were in duplicate and means ± SD are shown.

Figure 6. The effect of TL1A on plasma cells

The experiments in A, B and C were repeated three times and representative data are shown.

A. DR3 expression in plasma cells. dLN cells from WT mice on day 15 after BTIIC/CFA immunization were gated on $B220^{+}CD138^{-}$ regular B cells (left panel), $B220^{+}CD138^{+}$ plasmablast and $Dump^{-}B220^{-}CD138^{+}$ plasma cells and analyzed for their DR3 expression by three-color or four-color flow cytometry. Shaded areas: isotypic controls. Thick lines: DR3 signals. Dump staining used anti-CD8, anti-CD11b, anti-CD11c, anti-F4/80, anti-IgM, anti-IgD and anti-CD4 mAbs.

B. DR3 isoform expression in CD4 cell and plasma cells. RT-qPCR was used to detect the mRNA of full-length DR3 and all DR3 isoforms (including the full-length and all truncated isoforms) in flow cytometer-sorted $CD4^{+}$ T cells (as controls) and $Dump^{-}B220^{-}CD138^{+}$ plasma cells. The results are expressed as ratios of DR3 (full-length or all isoforms) versus β-actin signals with means $\pm$ SD indicated. Left panel: full-length DR3 isoform expression in CD4 T and plasma cells; middle panel: the expression all DR3 isoforms (full-length plus all truncated isoforms) in CD4 T and plasma cells; right panel: ratios of full-length DR3 versus all isoforms of DR3.

C. Higher plasma cell numbers in and collagen-specific Ab production by WT dLN cells cultured in the presence of TL1A. dLN cells from WT mice 21 days after BTIIC/CFA immunization were cultured in the absence or presence of TL1A (50 ng/ml) for 6 days. The number of $Dump^{-}B220^{-}CD138^{+}$ plasma cells were counted by flow cytometry four times on day 6 and the plasma cell numbers per 1×10^{6} total dLN cells (means ± SD) are shown (left panel). The culture supernatants were harvested on day 6 and collagen-specific IgG levels in the supernatants were determined by ELISA, which was conducted in triplicate samples. Arbitrary titres of anti-collagen IgG Abs (means ± SD) are shown (right panel). Experiments were repeated at least twice and representative data are shown. Student's *t* test was used to assess the statistical significance of the difference and the *p*-value is indicated.

D-F. Reduced collagen-specific IgG-producing cells (CSIGGPC) in the dLN and bone marrow (BM). Twenty-eight days after BTIIC/CFA immunization, CSIGGPC in the dLN and BM were enumerated by ELISPOT. Representative images of spots in wells were showed in D. The spots in 8 replicate wells of each experiment were counted, and the data of three

similar experiments were pooled and summarized bar graphs (E for dLN and F for BM). Mean ± SEM are presented. *$p<0.05$; **$p<0.01$ (Student's *t* test).

Figures

Figure 3.1

Figure 1.

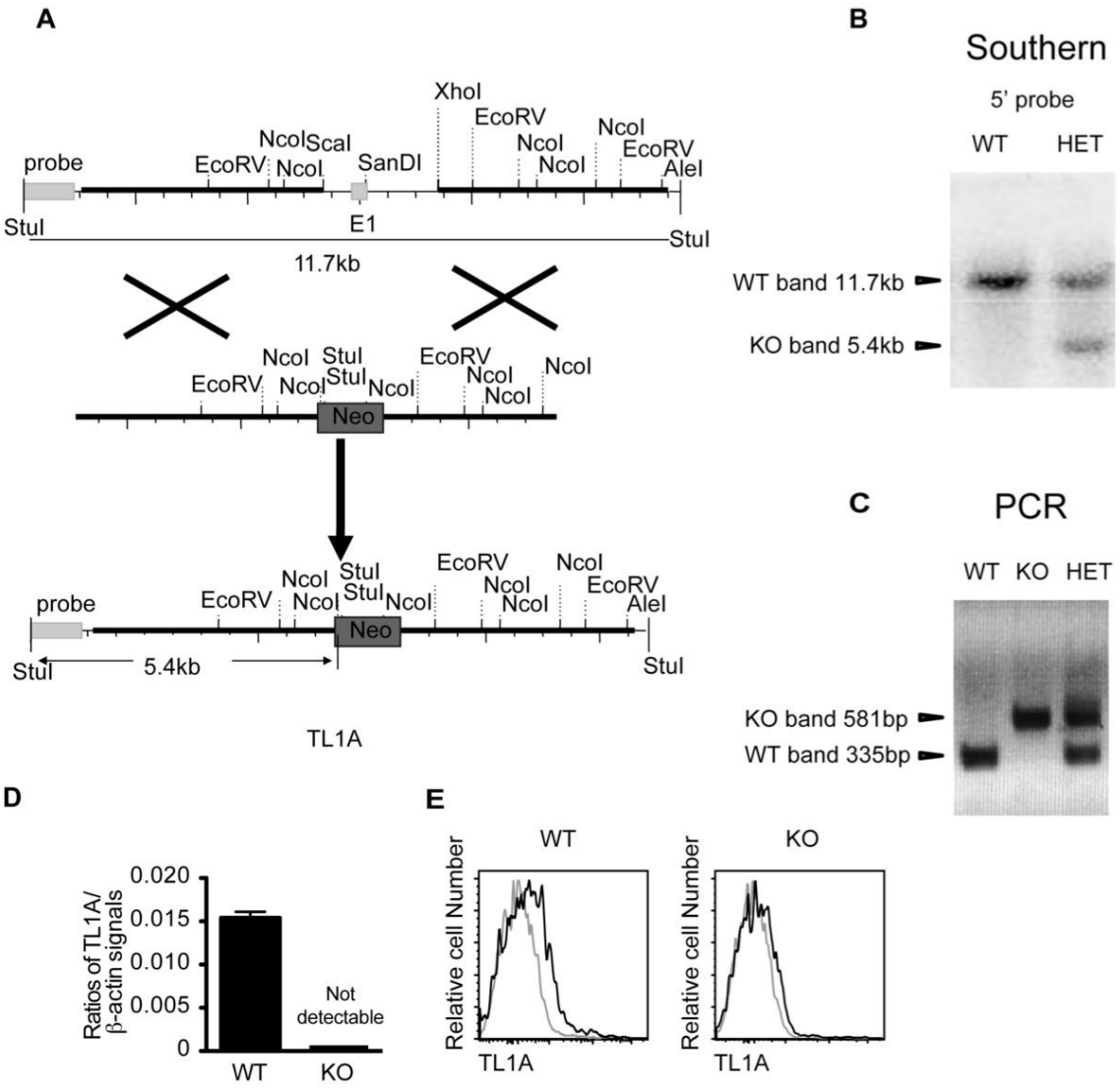

Figure 3.2

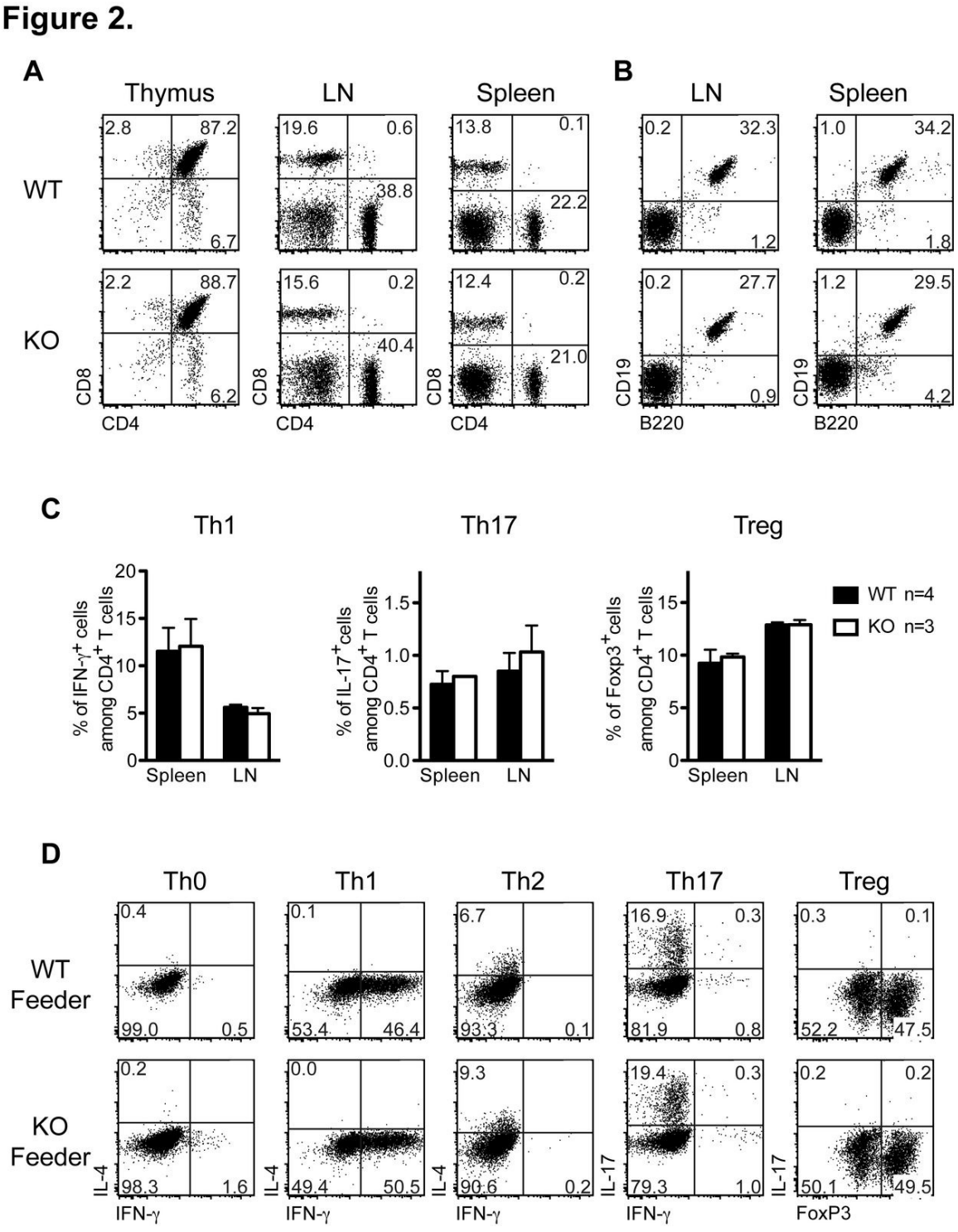
Figure 2.
A
Thymus
LN
Spleen
WT
KO
2.8
87.2
6.7
19.6
0.6
38.8
13.8
0.1
22.2
2.2
88.7
6.2
15.6
0.2
40.4
12.4
0.2
21.0
CD8
CD4
B
LN
Spleen
0.2
32.3
1.2
1.0
34.2
1.8
0.2
27.7
0.9
1.2
29.5
4.2
CD19
B220
C
Th1
Th17
Treg
% of IFN-γ+ cells among CD4+ T cells
% of IL-17+cells among CD4+ T cells
% of Foxp3+cells among CD4+ T cells
Spleen
LN
WT n=4
KO n=3
D
Th0
Th1
Th2
Th17
Treg
WT Feeder
KO Feeder
0.4
99.0
0.5
0.1
53.4
46.4
6.7
93.3
0.1
16.9
81.9
0.3
0.8
0.3
52.2
0.1
47.5
0.2
98.3
1.6
0.0
49.4
50.5
9.3
90.6
0.2
19.4
79.3
0.3
1.0
0.2
50.1
0.2
49.5
IL-4
IL-17
IFN-γ
FoxP3

Figure 3.3

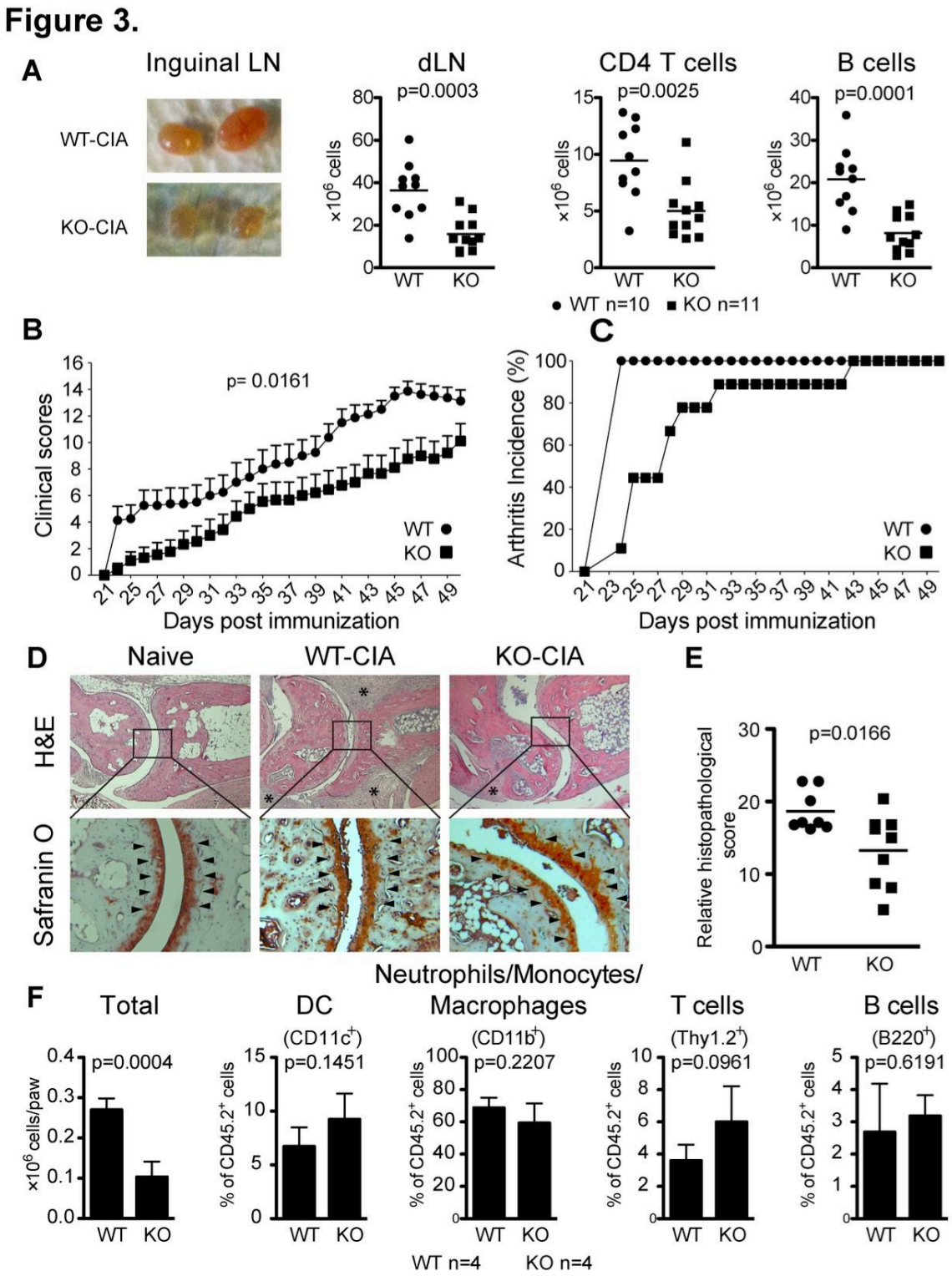
Figure 3.
A
Inguinal LN
dLN
CD4 T cells
B cells
WT-CIA
KO-CIA
p=0.0003
p=0.0025
p=0.0001
×10^6 cells
WT
KO
WT n=10
KO n=11
B
Clinical scores
p= 0.0161
Days post immunization
C
Arthritis Incidence (%)
Days post immunization
D
Naive
WT-CIA
KO-CIA
H&E
Safranin O
E
Relative histopathological score
p=0.0166
F
Neutrophils/Monocytes/
Total
DC
(CD11c+)
Macrophages
(CD11b+)
T cells
(Thy1.2+)
B cells
(B220+)
×10^6 cells/paw
% of CD45.2+ cells
p=0.0004
p=0.1451
p=0.2207
p=0.0961
p=0.6191
WT n=4
KO n=4

Figure 3.4

Figure 4.

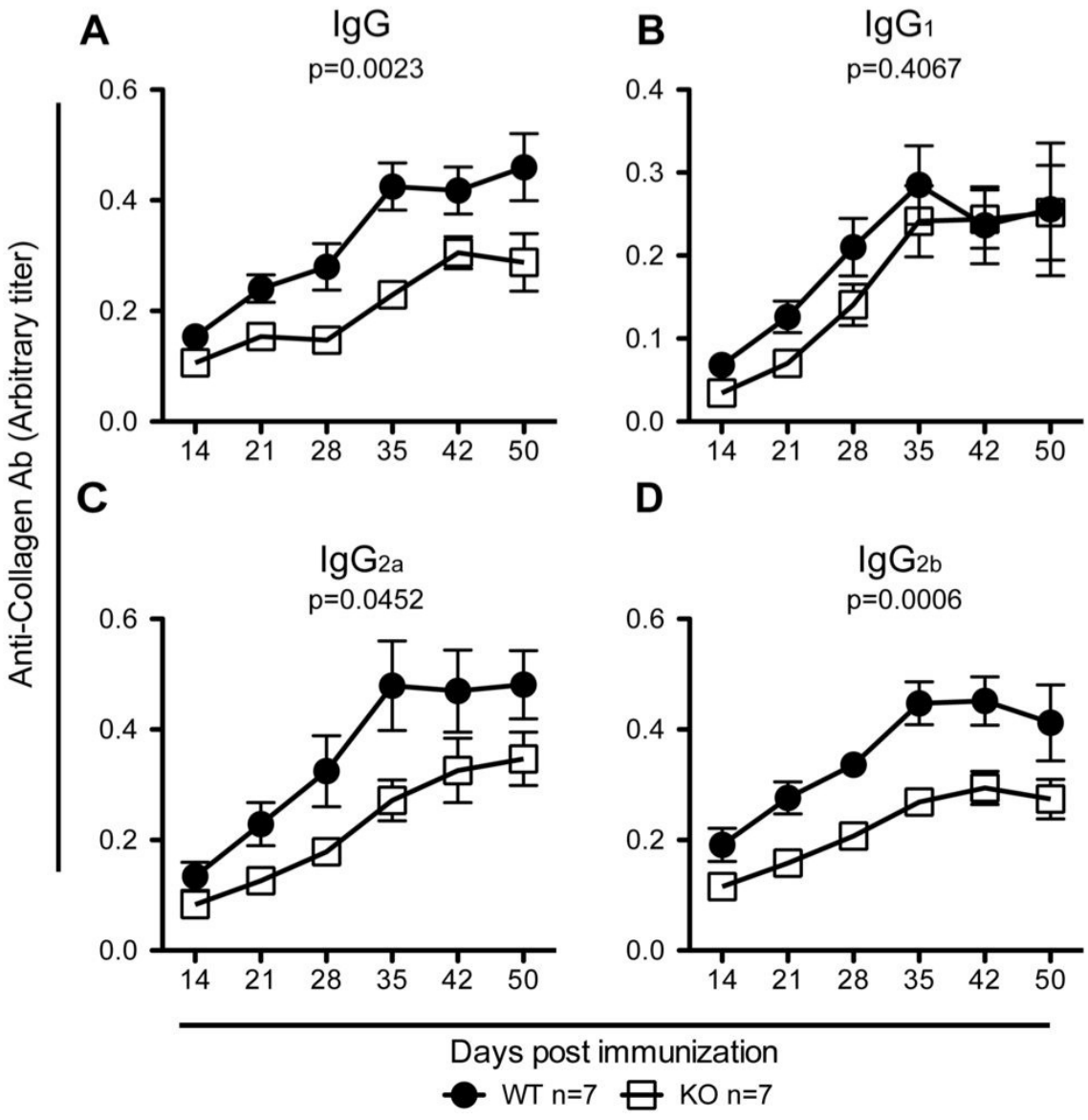

Figure 3.5

Figure 5.

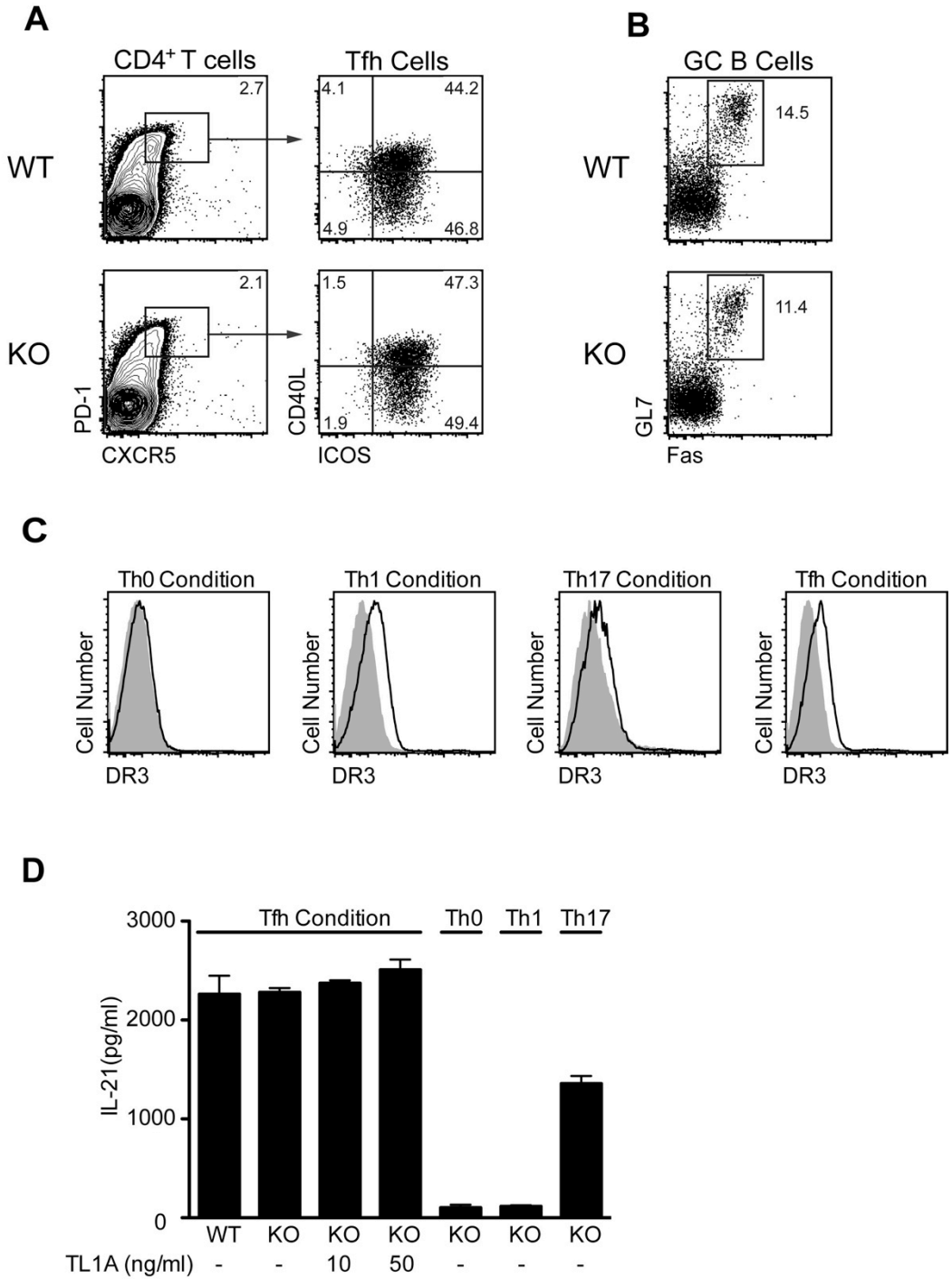

Figure 3.6

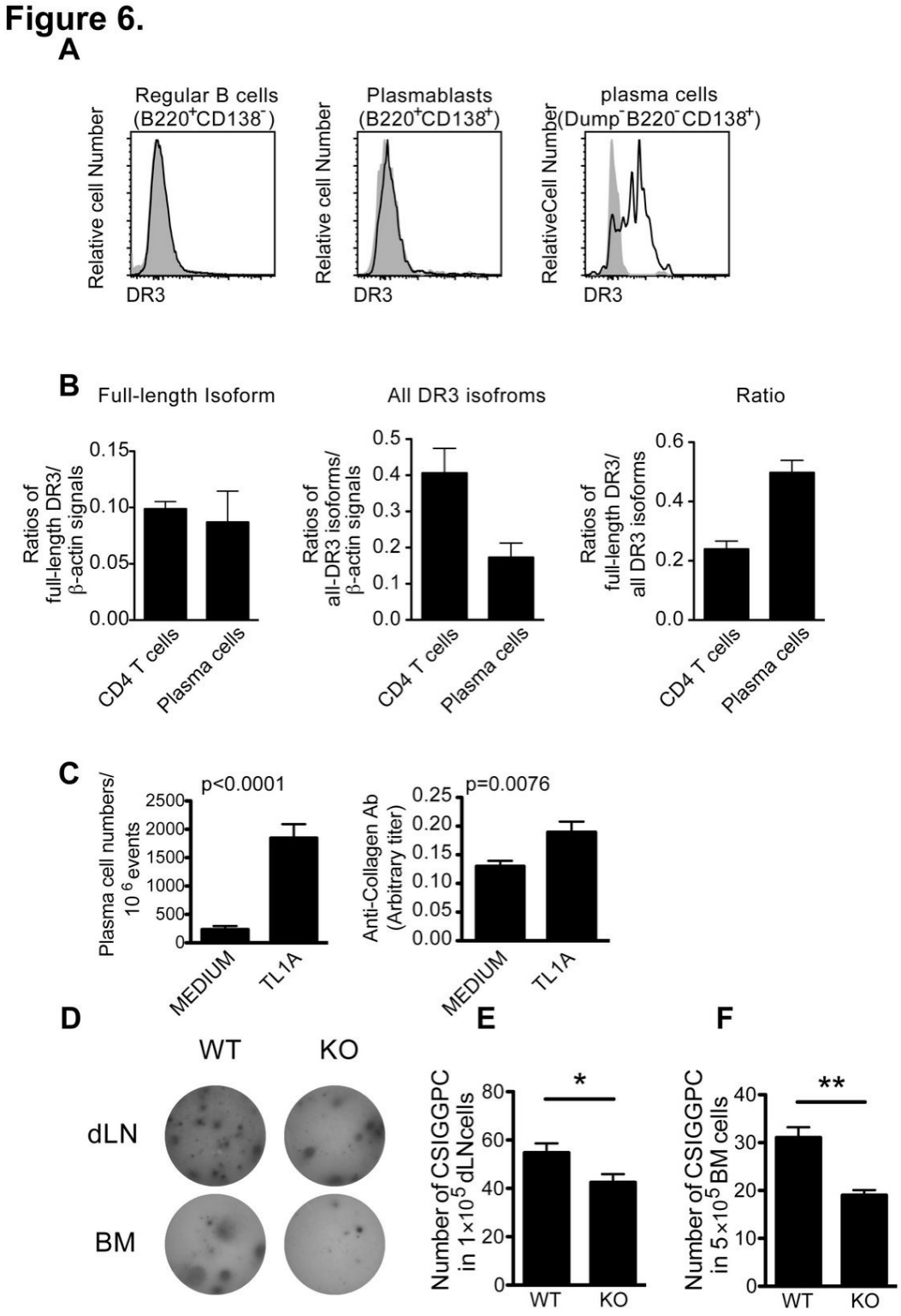
Figure 6.
A
Regular B cells
(B220+CD138-)
Plasmablasts
(B220+CD138+)
plasma cells
(Dump-B220-CD138+)
Relative cell Number
RelativeCell Number
DR3
B
Full-length Isoform
All DR3 isofroms
Ratio
Ratios of full-length DR3/ β-actin signals
Ratios of all-DR3 isoforms/ β-actin signals
Ratios of full-length DR3/ all DR3 isoforms
CD4 T cells
Plasma cells
C
Plasma cell numbers/ 10 6 events
p<0.0001
Anti-Collagen Ab (Arbitrary titer)
p=0.0076
MEDIUM
TL1A
D
WT
KO
dLN
BM
E
Number of CSIGGPC in 1×10^5 dLNcells
*
F
Number of CSIGGPC in 5×10^5 BM cells
**

Supplementary materials

LEGENDS FOR SUPPLEMENTARY FIGURES

Supplementary Figure 1. Normal in vivo anti-LCMV immune responses of TL1A KO mice

Mice were infected by the intravenous route with 2 x 10^6 focus-forming units of LCMV clone 13. The mice were sacrificed 8 days post-infection, and their spleens were harvested for immunological analysis. The absolute numbers of $CD4^+$ cells and $CD8^+$ cells of WT littermate control and TL1A KO mice measured by flow cytometry were reported (A). The absolute numbers of gp33-41 and np396-404 tetramer-positive CD8 T cells per spleen (B) and the percentage of gp33-41 and np396-404 tetramer-positive cells among CD8 cells (C) were measured by flow cytometry. One million splenocytes from these mice were seeded in single wells of 96-well round-bottomed plates and cultured in 5% RPMI-1640 supplemented with 100 units/ml interleukin-2, 10 μg/ml brefeldin A, 10 μM gp33-41 or gp61-80 peptide. After 5 h of incubation at 37 °C, surface and intracellular staining were performed to stained CD4, CD8, TNF-α and IFN-γ. Absolute numbers of TNF-α-producing virus-specific CD4 cells (gp61-80-specific) and CD8 cells (gp33-41-specific) per spleen (D) and their percentages among total CD4 or CD8 cells (E) were measured by flow cytometry. Absolute numbers of IFN-γ-producing virus-specific CD4 cells (gp61-80-specific) and CD8 cells (gp33-41-specific) per spleen (F) and their percentages among total CD4 or CD8 cells (G) were measured by flow cytometry. Mean ± SD of data from three pairs of WT littermate controls and TL1A KO mice are presented. No statistically significant differences between the values of WT and KO mice shown in A-E are detected (paired Student's *t* test).

Supplementary Figure 2. TL1A-KO mice had normal normal germinal centre sizes.

Cryosections of dLNs from WT and TL1A KO mice on day 14 after BTIIC immunization were stained by Peanut agglutinin (PNA)-biotin followed by streptavidin-FITC, and anti-B220-PE. Representative micrographs are shown in A. The cells from dLNs of the immunized WT and KO mice were stained with germinal centre B cell markers and analyzed with flow cytometry. Percentages of GC B cells ($B220^+GL7^+Fas^+$) among the total dLN cells were plotted, as shown in B. The absolute numbers of GC B cells per dLN were shown in C. WT: n=10; KO: n=11.

Supplementary Figure 3. TL1A-KO mice had normal serum IgG and IgG isotype levels

Total serum levels of IgG, IgM, IgA, IgG_1, IgG_{2a}, IgG_{2b} and IgG_3 in TL1A KO (n=5) and WT (n=5) mice were measure by ELISA. The total IgG, IgM and IgA levels were expressed as optical density of ELISA (upper panel). The IgG isotype levels were expressed as the percentage of total IgG levels (lower panel). Means ± SD are shown. No significant difference between TL1A KO and WT mice is found (Student's *t* test) with regard to these parameters.

Supplementary Figure 4. T cells from TL1A-KO mice had normal antigen-specific Th1 and Th17 responses and proliferation

Draining lymph node (dLN) cells from WT and TL1A KO mice on day 14 after the BTIIC immunization were collected and cultured in the presence or absence of BTIIC (25μg/ml). IL-2 (50U/ml) or IL-23 (15ng/ml) was added to cultures for Th1 or Th17 cell expansion, respectively. Cells were cultured for 3 days and treated with PMA/ionomycin in the presence of Golgi-Stop for the last 4 hours of culture. The collagen-specific expansions of Th1 and Th17 cells were examined by intracellular staining of IFN-γ and IL-17. Fold changes of the percentages of IFN-γ- or IL-17-positive CD4 T cells in cultures with BTIIC versus those without BTIIC are shown (A). WT: n=4; KO: n=5.

The same cells were labelled with CFSE and cultured in the presence of IL-2 (50U/ml), with or without BTIIC (25μg/ml). After 3 days, the cells were harvested and analysed by flow cytometry. CD4 cells were gated for CFSE expression as shown in the left panel of B. Fold changes of the percentages of the gated CD4 cells in cultures with BTTIC versus without BTIIC were shown. WT: n=4; KO: n=5.

Figure 3.7

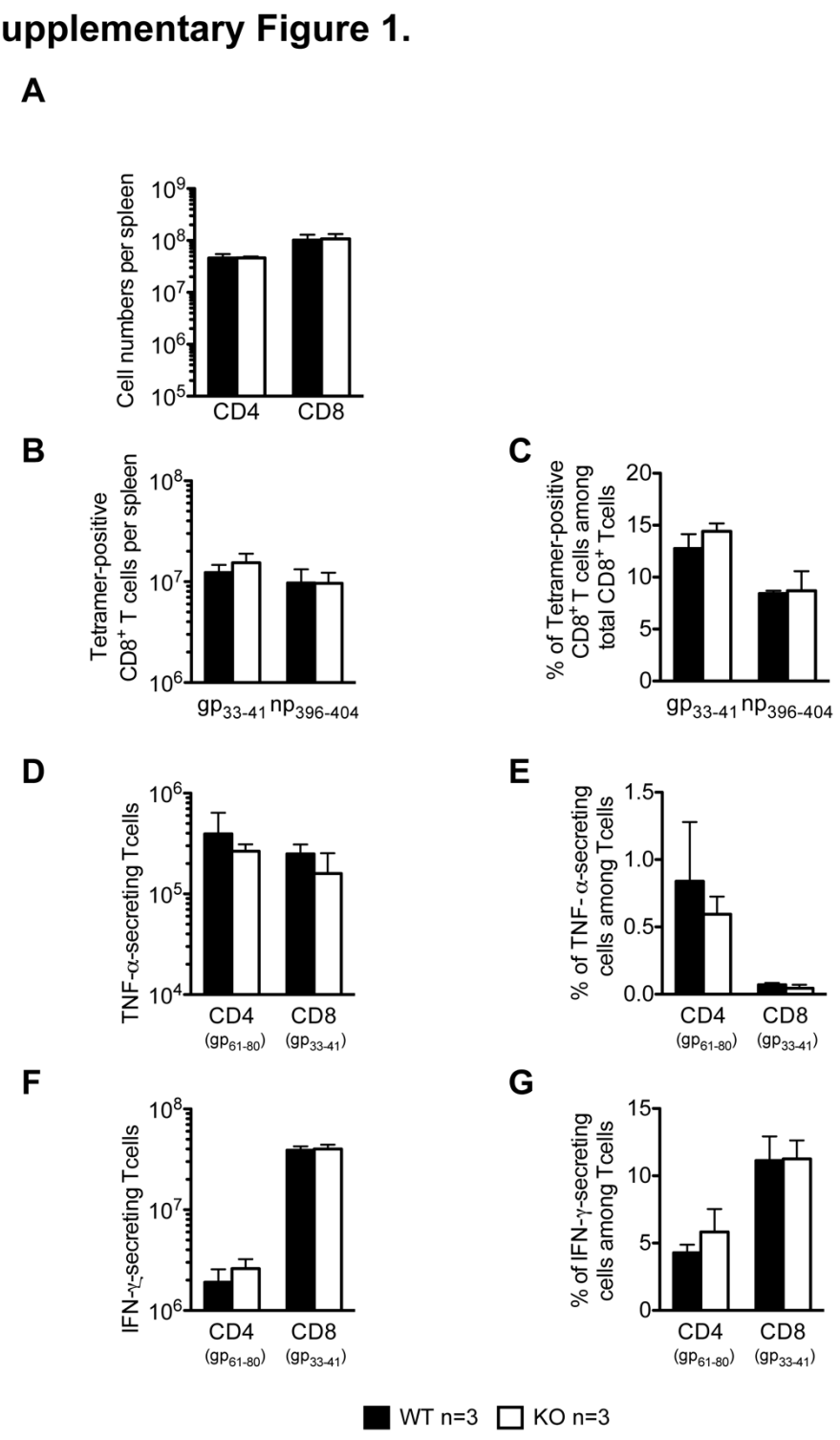
Supplementary Figure 1.
A
Cell numbers per spleen
CD4
CD8
B
Tetramer-positive CD8+ T cells per spleen
gp33-41
np396-404
C
% of Tetramer-positive CD8+ T cells among total CD8+ Tcells
gp33-41
np396-404
D
TNF-α-secreting Tcells
CD4 (gp61-80)
CD8 (gp33-41)
E
% of TNF-α-secreting cells among Tcells
CD4 (gp61-80)
CD8 (gp33-41)
F
IFN-γ-secreting Tcells
CD4 (gp61-80)
CD8 (gp33-41)
G
% of IFN-γ-secreting cells among Tcells
CD4 (gp61-80)
CD8 (gp33-41)
WT n=3
KO n=3

Figure 3.8

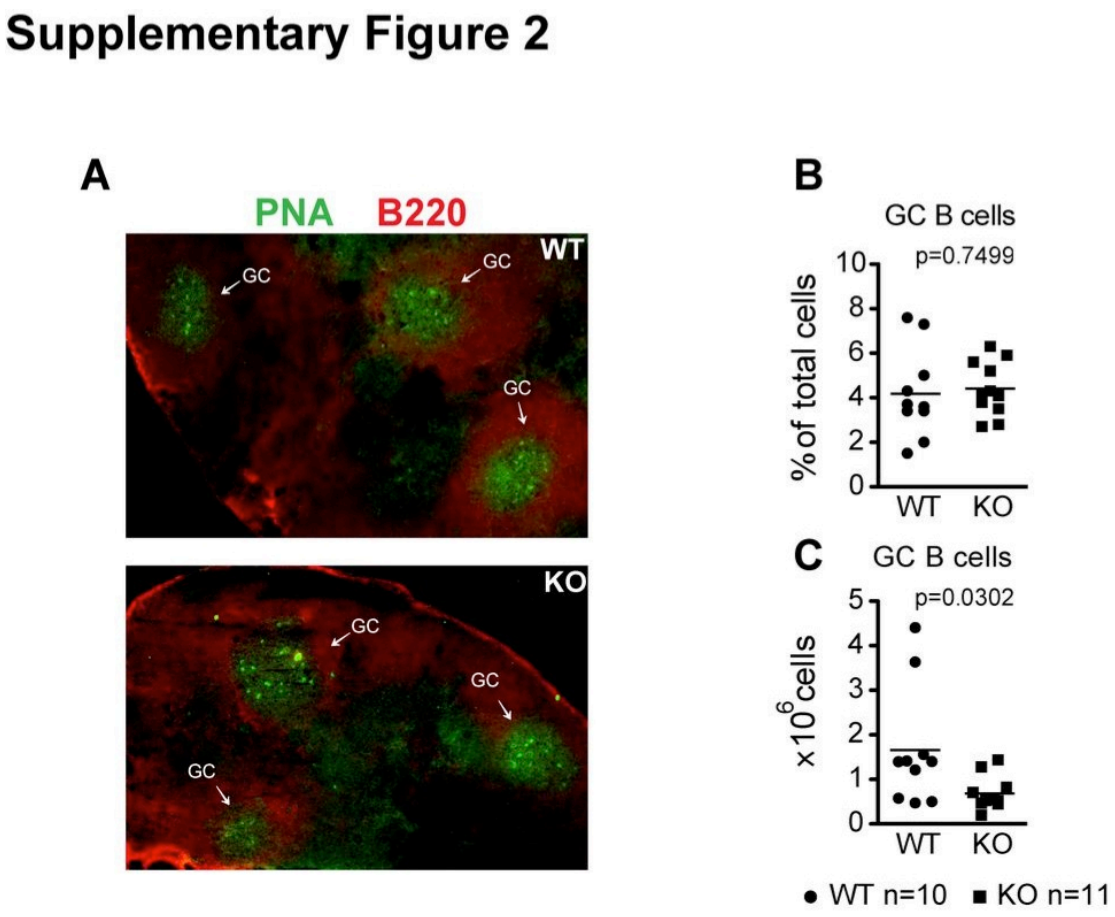
Supplementary Figure 2
A
PNA B220
WT
GC
GC
GC
KO
GC
GC
GC
B
GC B cells
p=0.7499
% of total cells
10
8
6
4
2
0
WT
KO
C
GC B cells
p=0.0302
x10^6 cells
5
4
3
2
1
0
WT
KO
WT n=10
KO n=11

Figure 3.9

Supplementary Figrue 3.

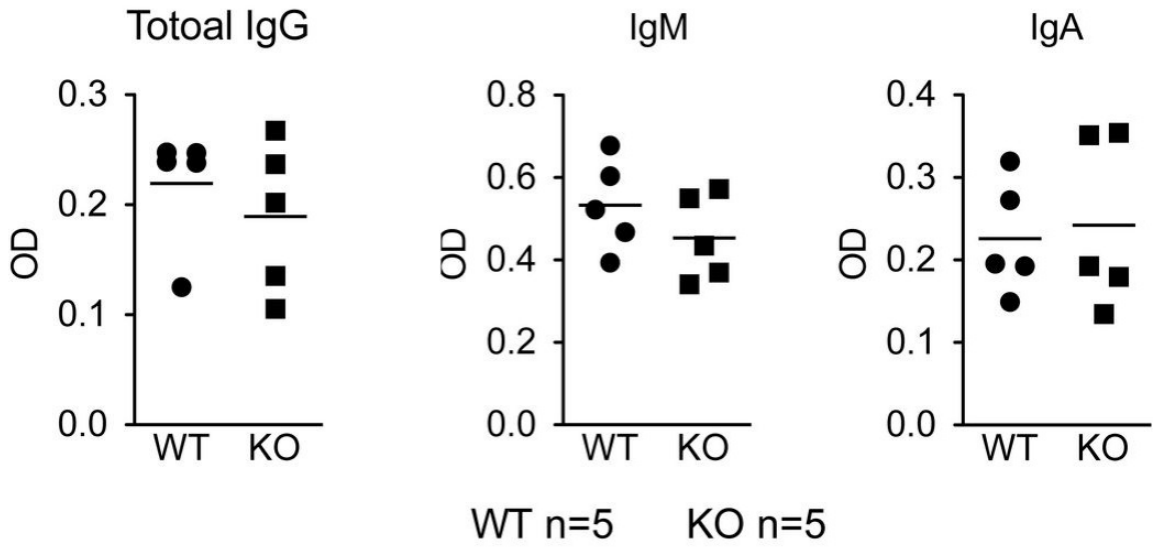

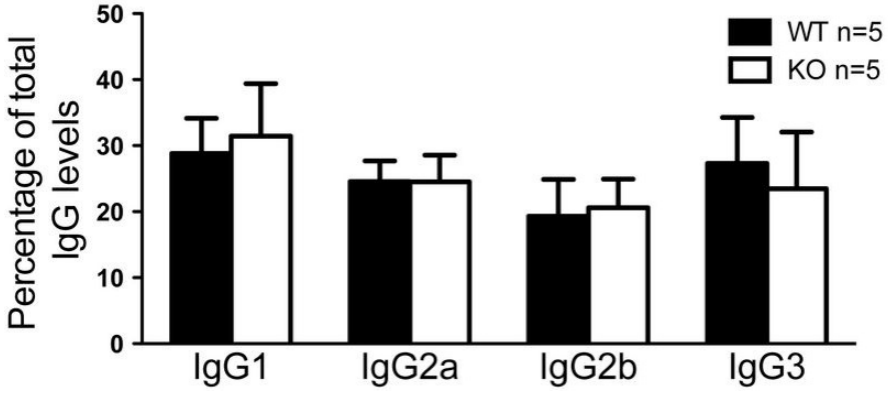

Figure 3.10

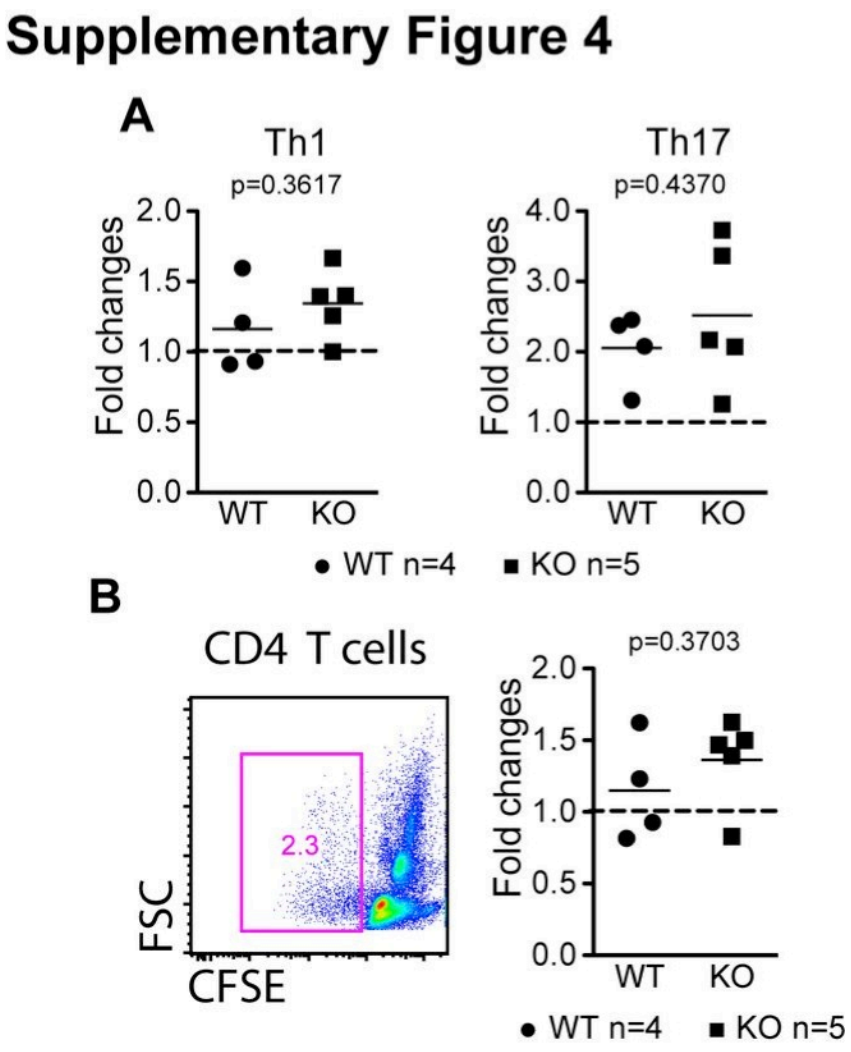
Supplementary Figure 4
A
Th1
p=0.3617
Fold changes
2.0
1.5
1.0
0.5
0.0
WT
KO
Th17
p=0.4370
4.0
3.0
2.0
1.0
0.0
WT
KO
WT n=4
KO n=5
B
CD4 T cells
2.3
FSC
CFSE
p=0.3703
Fold changes
2.0
1.5
1.0
0.5
0.0
WT
KO
WT n=4
KO n=5

CHAPTER 4 ARTICLE-3

As discussed in Section 1.5.4, plasma cells are hypersensitive to proteasome inhibitors due to their strong dependency on the proteasome activity. Proteasome inhibitors have shown effectiveness in protecting the mice from experimental models of SLE and MG by reducing the autoantibodies titers, the consequence of eliminating the plasma cells. Pno1 was reported to be essential for ribosome and proteasome assembly in yeast. We employed *in situ* hybridization (ISH), *in vitro* cell function analysis, Pno1 gene knockout (KO) and transgenic (Tg) over-expression in mice, in order to gain a better knowledge of the function of Pno1 in mammals and test whether it is suitable to be a novel drug target for treating RA.

This work has been published in ***PloS ONE***.

Wang X, Wu T, Hu Y, Marcinkiewicz M, Qi S, et al. (2012) Pno1 Tissue-Specific Expression and Its Functions Related to the Immune Responses and Proteasome Activities. ***PLoS ONE*** 7: e46093.

4.1 Pno1 tissue-specific expression and its functions related to the immune responses and proteasome activities

Xuehai Wang*, Tao Wu*^, Yan Hu*, Martin Marcinkiewicz[#], Shijie Qi*, Hector Valderrama-Carvajal*, Hongyu Luo*, and Jiangping Wu*[+]

*From *Laboratoire d'immunologie and [+]Service de nephrologie, Centre de recherche, Centre hospitalier de l'Université de Montréal (CRCHUM)-Hôpital Notre-Dame, Montreal, Quebec, Canada; ^Institute of Cardiology, First Affiliated Hospital, Zhejiang University Medical College, Hangzhou, China; [#] Cytochem Inc, Montreal, Quebec, Canada*

Address correspondence to: Dr. Jiangping Wu, Laboratory of Immunology, CRCHUM – Hôpital Notre-Dame, Pavillion DeSève, Room Y-5616, 1560 Sherbrooke Street East, Montreal, Quebec H2L 4M1, Canada; Telephone: (514) 890-8000 Extension 25164; Fax: (514) 412-7596.

Current address of H.V: Instituto de Ciencia y Tecnología del Distrito Federal, México. República de Chile # 6, Col. Centro, Del. Cuauhtémoc, Mexico D.F.

Abstract

Pno1 is a protein that plays a role in proteasome and ribosome neogenesis in yeast. So far, its functions in mammalian cells have not been investigated. To understand its function in mammals, we performed *in situ* hybridization analysis of Pno1 expression in different embryonic, postnatal and adult development stages and generated Pno1 gene knockout (KO) and Pno1 transgenic (Tg) mice lineages. The results showed early lethality of homozygous Pno1 KO lineage caused, as demonstrated in parallel by *ex vivo* experiments, by arrest of embryo development before compaction stage. Though, heterozygous (HET) mice with 50% of normal Pno1 mRNA concentration were fertile and showed no obvious anomalies at adulthood. The lymphoid organs of HET mice were normal in size, weight and cellularity, with normal T and B cell subpopulations. TCR-triggered activation and proliferation of HET T cells were normal. Proteasome activities in HET organs were uncompromised. Tg mice with actin promoter-driven Pno1 expression were also fertile, with no apparent anomalies, although they expressed 2-5-fold higher Pno1 mRNA levels. The lymphoid organs of Tg mice were of normal size, weight and cellularity with normal T and B cell sub-populations. TCR-triggered activation and proliferation of Tg T cells were normal. Tg organs and tissues presented normal proteasome activity as did their wild type counterparts. Tagged Pno1 over-expression in L cells and density gradient fractionation established that Pno1 existed in large complexes with sedimentation rates between 20S and 26S, bigger than mature 26S proteasomes. Pno1 in fractions did not coincide with 40S (small) or 60S (large) ribosome subunits. Our study indicates that Pno1 is essential for cellular functions, but only a small percentage of its normal level is sufficient, and excessive amounts are neither harmful nor useful. The nature of the large complexes it associates with remains to be identified, but it is certain that they are not mature proteasomes or ribosomes.

Introduction

Ribosome neogenesis requires more than 200 assembly factors, most of which are not present in mature ribosomes. Many of these factors are needed at certain time points of ribosome maturation; they then dissociate from assembled intermediates and decay in an orderly fashion once their function is performed. Pno1 (partner of Nob1) is such a ribosome neogenesis factor. In yeasts, Pno1 is also called *Dim2, Rrp2* or *Yor145* [1]. It is highly conserved in yeasts up to mammalian species. Mouse *Pno1* mRNA comprises a 746-nt open-reading frame encoding a 248-amino acid peptide. Yeast and mouse Pno1 share 52% identity at their gene coding sequences and 46.7% homology (allowing amino acid substitution) at the protein level. Pno1 contains a K homolog (KH) domain that is capable of binding RNA [2]. Pno1 protein shows dynamic distribution during different phases of yeast growth from nucleolus to cytosol [3]. It is associated with Nob1 [4], which is involved in 90S to 40S pre-ribosome maturation [5] and is an exonuclease [1]. The KH domain of Pno1 is also essential for its binding to Nob1 [6]. Pno1 binds to both 90S and 40S pre-ribosomes [3] via Nob1. During pre-40S ribosome maturation, the kinases Rio2, Nob1 and Pno1 form complexes attached to the front of the late pre-40S ribosome head [7]. Pno1 increases Nob1 RNA affinity, and regulates Nob1's cleavage activity at the 3' end of 18S rRNA [6]. Loss of Pno1 results in accumulation of 35S, 33S and 32S rRNA [3] but with a decrease of 18S rRNA [8].

Pno1 and Nob1 are also critical for proteasome maturation in yeasts [4]. Again, and in this case, Pno1 interacts with Nob1 and both proteins form complexes with the 19S regulatory particle of 26S proteasomes. Mutation of either Pno1 or Nob1 causes defective assembly of 26S proteasomes [4].

The above findings indicate that Pno1 performs important functions in both ribosome and proteasome biogenesis, but whether it undertakes both these functions at the same time or separately is not known.

To date, to the best of our knowledge, all functional and binding studies of Pno1 have been conducted in yeasts. The Pno1 expression pattern in different tissues and organs of mammals is unclear. It is uncertain whether Pno1 is vital and irreplaceable in mammalian cells or if redundancy exists so that a lack of Pno1 will not be fatal to cells and/or animals. It is also not

known whether different Pno1 expression levels impede cellular functions. In this study, we employed in situ hybridization (ISH), gene knockout (KO) and transgenic (Tg) over-expression in mice to address these questions.

Materials and methods

In situ hybridization

Full-length 1526-bp Pno1 cDNA in pSPORT1 (clone H3085H06; accession number NM_025443) from National Institute of Ageing, USA) was employed as a template for sense and anti-sense riboprobe synthesis, using SP6 and T7 RNA polymerase for both ^{35}S-UTP and ^{35}S-CTP incorporation [9].

Tissues from WT mice were frozen in -35°C isopentane, and kept at -80°C until sectioned. ISH, x-ray film and emulsion autoradiography was performed using 10-μm thick cryostat-cut slices, as outlined previously[9].

Generation of Pno1 gene knockout (KO) mice

A polymerase chain reaction (PCR) fragment, amplified on the Pno1 cDNA sequence (clone H3085H06), was used as probe to isolate genomic BAC DNA clone 115L21 from the 129/sv mouse BAC genomic library RPCI-22. Targeting vectors were constructed by recombination and routine cloning methods with a 12.5-kb Pno1 genomic fragment from clone 115L21 (illustrated in Figure 3A). A 3.6-kb SmaI-SaclI genomic fragment containing exons 1 to 5 was replaced by a 1.1-kb Neo cassette from pMC1Neo Poly A (Fig. 3A). The final targeting fragment was excised from its cloning vector backbone by Not I digestion and electroporated into R1 embryonic stem (ES) cells for G418 selection[10]. The targeted ES cell clones were injected into C57BL/6 blastocysts. Chimeric male mice were mated with C57BL/6 females to establish mutated Pno1 allele germline transmission. All mice were housed under specific pathogen-free conditions and used in accordance with a protocol approved by the Institutional Animal Protection Committee of the University of Montreal Hospital Center (NO9055JWs).
Southern blotting with a probe corresponding to 3' sequences outside the targeting region, as illustrated in Figure 3 (black square), screened for and confirmed gene targeting in ES cells and eventually in mouse ear DNA. The targeted allele showed a 8.5-kb BamHI/BamHI fragment, while the wild type (WT) allele had an 18.6-kb BamH1/BamHI fragment (Fig. 3B). PCR was adopted for routine genotyping of the targeted allele(s). The following PCR conditions were applied: 4 min at 95^{o}C, followed by 35 cycles of 30 s at 94^{o}C, 30 s at 58^{o}C, and 60 s at 72^{o}C, with final incubation at 72^{o}C for 10 min. Two forward primers (5'-

CTGCGTGTTCGAATTCGCCAATGA-3', forward primer 1; 5'-ACCACCTGTCAAG GGCAATAGGAA-3', forward primer 2) and 1 reverse primer (5'-TGCTC CCAGT CCAGTC ACTA-3') were included in the PCR, which amplified a 234-bp fragment from the targeted allele and a 548-bp fragment from the WT allele.

Generation of Pno1 Tg mice

1,526-bp mouse full-length Pno1 cDNA was excised from pSPORT1 with Not I/Sal I, blunt-ended, and cloned into blunt-endedBamH I/Xba I sites in vector pAC, between the human β-actin promoter and β-actin polyA signals. The resulting construct was named pAC-Pno1. The 6.4-kb ClaI/ClaI fragment containing the β-actin promoter, Pno1 cDNA and β-actin polyA signals was excised and injected into fertilized C3H x C57BL/6 eggs. Tg mice were genotyped by PCR with tail DNA under the following conditions: 4 min at 95^{o}C, followed by 30 cycles of 30 s at 94^{o}C, 30 s at 58^{o}C, and 30 s at 72^{o}C, with final incubation at 72^{o}C for 10 min. Primers 5'-GTCATGGCAGAAACTTGCAC-3' (forward) and 5'-GAATGCAATTGTTGTTGGTAACTTG-3' (reverse) amplified a 552-bp product.

Reverse transcription and real-time PCR (RT-qPCR)

Pno1 mRNA in cells or tissues from KO, Tg and WT mice was measured by RT-qPCR. Total RNA from cells was extracted with TRIzol® (Invitrogen, Carlsbad, CA, USA) and then reverse-transcribed with Superscript II™ reverse-transcriptase (Invitrogen). The forward and reverse primers were 5'-TGTTCTTGGCTTTCAGGTGGAGGA-3' and 5'-TTCCTATTGCCC TTGACAGGTGGT-3', respectively. A 125-bp product was detected with the following amplification program: 95^{o}C x 15 min, 1 cycle; 94^{o}C x 15 s, 55^{o}C x 30 s, 72^{o}C x 30 s, 40 cycles.

β-actin mRNA levels were measured as internal controls; the forward and reverse primers were 5'-TGGTACCACAGGCATTGTGAT-3' and 5'-TGATGTCACGCACGATTTCCCT-3', respectively, with the same amplification program as for Pno1 mRNA.

qPCR was performed in triplicate, and the results were expressed as the signal ratios of Pno1/β-actin.

qPCR was also employed for embryo genotyping. Embryos were digested at 55^{o}C for 4 h in 2 μl digestion buffer (proteinase K, 0.01% gelatin, 0.005% NP-40, 20 mM Tris (pH 8.35), 40 mM KCl, 0.5 mM $MgCl_2$). Forward primer 5'-GGTTTGCTCGACATTGGGGTGGAAA-3' and reverse primer 5'-AGCGCGAGTATTCACCTAGAACAA-3' detected a 185-bp fragment from the KO allele. Forward primer 5'-GGTCCAAGAACGTTGCCAGGAAAT-3' and reverse primer 5'-AGGGTCTGATTCCTCAATGCTCCA-3' detected a 168-bp fragment from the WT allele. PCR conditions for the reactions were as follows: 50^{o}C x 2 min, 1 cycle; 95^{o}C x 2 min, 1 cycle; 94^{o}C x 10 s, 58^{o}C x 20 s, 72^{o}C x 20, 35 cycles.

Flow cytometry

Single cell suspensions from the thymus, spleen and in certain experiments the draining lymph nodes were prepared and stained for flow cytometry, as described in our previous publications[11,12].

T and B cell proliferation

T cell proliferation was assessed by ^{3}H-thymidine uptake, as detailed elsewhere[13].

Mouse immunization and ELISA

Eight- to 10-wk old WT, HET and Tg mice were immunized at the base of the tail with 100 μg of chick type II collagen (Chondrex, Redmond, WA), which was emulsified in equal volumes of Freund's complete adjuvant (2 mg/ml Mycobacterium tuberculosis, strain H37Ra; Difco, Detroit, MI). On day 21, the mice were sacrificed and sera were collected for collagen-specific Ab assays[14].

Proteasome activities

Lysates from WT, Tg, and heterozygous (HET) mouse thymus and spleen cells were assayed for 3 major protease activities (chymotrypsin-like activity, trypsin-like activity, and caspase-like activity) of proteasomes based on enzymatic digestion of fluorogenic substrates (Suc-LLVY-AMC for chemotrypsin-like activity, Z-LLA-AMC for trypsin-like activity, and Z-LLG-βNA for caspase-like activity). 20 μg of lysate protein were reacted with the substrates (100 nM) in 100 μl buffer containing 100 mM Tris-HCl (pH 8.2) at 37^{o}C for 20 min. The reaction was stopped by adding 4 μl 2M HCl, and fluorescence intensity of the reaction

solution was measured in a BioTek Synergy™ 4 Hybrid Microplate Reader with excitation at 380 nm and emission at 460 nm for AMC-conjugated substrates, and with excitation at 335 nm and emission at 410 nm for Z-LLG-βNA.

Pno1 overexpression in L cells

1,526-bp mouse full-length Pno1 cDNA was inserted downstream of the cytomegalovirus (CMV) promoter and upstream of hemagglutinin (HA) tags in mammalian expression vector pCEP4-HA. The construct, named pCEP4-Pno1-HA, drove HA-tagged Pno1 over-expression in mammalian cells. L cells were transfected by pCEP4-Pno1-HA with Lipofectamine followed by Hygromycin B selection.

Protein fractionation by glycerol density gradients

About 60 million pCEP4-Pno1-HA-transfected L cells were sonicated in 1 ml lysis buffer (25 mM Tris, pH 7.6, 10 μg/ml PMSF, 1 mg/ml LA, 1 mM DTT, 2 mM ATP, and 2 mM $MgCl_2$). The lysates were centrifuged at 12,000*g* for 30 min at 4^{o}C to remove debris. The cleared supernatants (700 ml) were laid on top of a 15-ml 10-40% glycerol density gradient (diluted in lysis buffer) in a 15-ml centrifuge tube and centrifuged at 83,000*g* for 22 h at 4^{o}C in a Beckman SW28 rotor. The gradient was separated into thirty 0.5-ml fractions for further tests.

Immunoblotting

200-ml aliquots from each gradient fraction were mixed with 800 ml cold acetone and stored at -20^{o}C for 60 min to precipitate proteins dissolved in 30 ml RIPA buffer (25 mM Tris, pH 7.6, 150 mM NaCl, 1% NP-40, 1% sodium deoxycholate, 0.1% SDS) supplemented with protease inhibitors (Complete™ Protease Inhibitor Cocktail, Roche Diagnostics, Laval, Quebec, Canada) and centrifuged for 20 min at 12,000*g* at room temperature. Total supernatants were resolved by 12% SDS-PAGE and transferred to nitrocellulose membranes. The proteasome b5 subunit and b-actin were detected by blotting with rabbit anti-human b5 antibody (Ab, Millipore, Billerica, MA, USA), followed by horseradish peroxidase-conjugated goat anti-rabbit IgG (GE Healthcare, Little Chalfont, Bucks, United Kingdom.). The membranes were then stripped and re-probed with horseradish peroxidase-conjugated rabbit anti-b-actin Ab (#4967, Cell Signaling Technology, Danvers, MA). Signals were detected with SuperSignal West Pico Chemiluminescent Substrate (Thermo Scientific, Rockford, IL, USA).

Results

Pno1 expression pattern in WT mice according to in situ hybridization

Based on the exposure time (optimal time: 4 days) necessary to produce X-Ray film autoradiogram, Pno1 mRNA belonged to a class of low abundant mouse mRNAs.

At mid-gestation embryo on day 9 (e9), Pno1 signals in most tissues, including the rudimental brain (MB: midbrain; FB: forebrain; NT: neural tube) and cardiovascular system (H: heart; AA: aortic arch), were relatively high, as illustrated in Figure 1A-I. After this stage and at subsequent gestation ages, density and spatial hybridization patterns underwent substantial change. The large cerebral Pno1-positive area was reduced to the periventricular band region on e11 and e13 (Figs. 1A-II and 1A-III). Pno1 mRNA level in the liver (Li) was moderate to high on e13 (Fig. 1A-III), but dropped significantly on e16 (Fig. 1A-IV). In contrast, Pno1 mRNA signals became perceptible in the kidneys (K) and Th, starting on e16 (Fig. 1A-IVD). Peak of Pno1 expression was observed in developing striated muscles (M) and intermingled adipose tissue on e16 (Fig. 1A-IV). Heart ventricles on e19 transiently displayed Pno1 mRNA levels (Fig. 1A-V) higher than on e9 (panel H in Fig. 1A-I). Around parturition (e19 and post-natal day 1 [p1]), Pno1 mRNA was clearly present in the immune system such as the thymus(Th), the digestive system such as the submaxillary gland (SMax), stomach (St), intestine (Int) and colon (descending) (CD)), peripheral nervous system (dorsal root ganglia (DRG), sympathetic ganglia (SG)), and skin (Sk) (Figs. 1A-V and 1A-IV). However, Pno1 mRNA signals were only slightly above background in the remaining tissues.

The Pno1 expression pattern on p10 remained similar to that on p1 (Fig. 1A-VI). Several particular brain regions, such as the olfactory lobe (OL), olfactory neuroepithelium (ONE) and hippocampus (Hip), manifested high expression levels; signals in the molars (Mol), trigeminal ganglion (TriG), Int and bone marrow (BM) were also elevated; the spleen displayed moderate expression (Fig. 1B).

In adulthood, Pno1 expression was noted in teeth, such as the incisors (Inc) (Fig. 1C-1), vertebrate bone marrow (Vb) (Figs. 1C-II and V) and testes (Ts) (Fig. 1C-IV). Pno1 expression in adult Sk seemed to be less abundant than in p10 Sk (comparative data not included). In lymphoid organs, the Th continued to present high expression levels (Fig. 1C-V),

while expression in the Spl remained moderate or low (Fig. 1C-III). Expression in the Th occurred mainly in the cortex (Fig. 2A). Adult mouse BM cells displayed Pno1 signals both in x-ray film autoradiography (Fig. 2B-I) and emulsion autoradiography (Figs. 2B-II and III). BM in the Vb cavity showed labelled islands containing cells with small diameters (likely hematopoietic cells) in the midst of a meshwork of unlabelled connective tissue cells (Figs. 2B-II and III). The adrenal glands that are composed of amine- and peptide-producing medulla (Me), and steroid hormone-producing cortex (Cx) displayed Pno1 mRNA labelling in both regions, but predominantly in Cx (Figs. 2C-I, II and III).

Generation of Pno1 gene KO mice

To understand Pno1 function, we generated Pno1 gene KO mice. The targeting strategy is depicted in Figure 3A. With the 3' end probe, the WT allele after BamHI digestion gave an 18.6-kb band on Southern blotting, and the KO allele, a 7.7-kb band (Fig. 3B). Germline transmission was confirmed by Southern blotting of tail DNA, and WT and HET mice were thus identified (Fig. 3B, left panel). PCR was undertaken for routine genotyping of ear DNA. WT samples presented a 546-bp band, and HET samples, a 224-bp band (Fig. 3B, right panel).

To ascertain if Pno1 gene deletion affected its expression, we measured Pno1 mRNA levels in different tissues by RT-qPCR. As shown in Fig. 3C, HET samples from the Li, Th and Spl presented lower Pno1 mRNA levels compared to WT samples. Pno1 was previously selected for study because it was inducible after T cell activation (data not reported). We activated T cells with solid phase anti-CD3 and anti-CD28 monoclonal antibodies (mAbs), and quantified Pno1 mRNA levels at different time points (1, 2, 6, 12 and 24 h after the initiation of culture). As expected, WT T cells presented augmented Pno1 mRNA levels between 6 and 24 h after activation. On the other hand, HET T cells only up-regulated Pno1 mRNA to about half of that in WT T cells (Fig. 3D). The data in Figures 3C and 3D confirmed the gene deletion of Pno1 in HET mice. They also indicated that Pno1 expression was gene copy number-dependent, as HET cells only expressed half of Pno1 at the mRNA level compared to WT cells.

Pno1 KO is lethal in embryos

We failed to generate any live Pno1 KO mice. Systemic tracking of fetus genotype in different gestation stages revealed that KO fetuses could only be found at e3.5 but not e6.5 (Table I). Therefore, the embros must have died between e3.5 and e6.5. We then cultured e1.5 embryos from HET male and HET female mating to observe their development *in vitro*. As depicted in Figure 4, up to e2.5, WT, HET and KO development seemed to be comparable. However, after e3.5, KO embryos stopped developing, while WT and HET embryos proceeded normally at this stage and beyond, indicating that Pno1 is vital in embryonic development.

No detectable anomalies in the immune system of Pno1 HET mice

As Pno1 was prominently expressed in the thymus and was up-regulated in T cells upon their activation, we set out to investigate whether a lack of Pno1 causes immune system abnormalities. HET mice, which expressed Pno1 at about 50% the normal Pno1 level, were used for this purpose because no KO mice could be produced. There were no apparent lymphoid organ anomalies in HET mice in terms of size, weight and colour (data not reported). T, B, CD4 and CD8 sub-populations in the Spleen and lymph nodes (LN) of HET mice were comparable to those in WT mice, as were thymocyte sub-populations, such as CD4CD8 double-negative, CD4CD8 double-positive, CD4 single-positive and CD8 single-positive cells (Fig. 5A and B).

Although HET T cells could only express Pno1 at about 50% the normal Pno1 level upon activation by anti-TCR mAb on solid phase, they proliferated as well as WT T cells (Fig. 5C). Activation markers, such as CD25 and CD69, were up-regulated in HET CD4 and CD8 T cells comparably to their WT counterparts (Fig. 5D). Therefore, it seems that 50% of normal Pno1 expression is sufficient to maintain T cell development and function.

We also assessed B cell subpopulations in the spleen and peritoneal cavity of WT and HET mice. In the spleen of WT and HET mice, there was no consistent difference in terms of the percentage of $B220^{+}CD21^{hi}CD23^{lo/-}$ mantel zone B cells (Fig. 6A), or the percentage of $B220^{+}CD21^{int/hi}CD23^{hi}$ follicular B cells (Fig. 6A). For B cells of the WT and HET mouse peritoneal exudates, there was no consistent difference in terms of the percentage of $B220^{+}CD23^{-}CD5^{+}IgM^{hi}$ B1a cells (Fig. 6B), $B220^{+}CD23^{-}CD5^{-}IgM^{hi}$ B1b (Fig. 6B) and $B220^{+}CD23^{+}IgM^{int/hi}$ B2 cells (Fig. 6B). Spleen B cells from WT and HET mice proliferated

comparably upon anti-IgM plus IL-4, anti-CD40 plus IL-4, or anti-CD40 plus LPS stimulation (Fig. 6C). The upregulation of B cell activation markers CD86 and CD80 in WT and HET spleen B cells 24 h after the above-described stimulation showed no apparent difference neither (Fig. 6D). We next examined the percentage of $IgD^{-}IgM^{-}CD138^{+}B220^{lo/-}$ isotype-switched plasmablast/plasma cells in the draining lymph nodes of WT and HET mice 21 days after immununization with chick type II collagen, but not significant difference was found (Fig. 6E). The serum collagen-specific Ab levels in these WT and HET mice 21 days after the chick type II collagen immunization showed no significant difference (Fig. 6F). Therefore, it seems that a 50% reduction of Pno1 level does not affect the B cells functions in vitro and in vivo.

Normal proteasome activity in HET tissues

Because Pno1 is involved in proteasome maturation, according to studies in yeasts, we questioned whether reduced Pno1 expression in HET mice leads to decreased proteasome activity in cells. We tested 3 major proteasome protease activities (i.e., chymotrypsin-like, trypsin-like and caspase-like proteases, but the caspase-like proteases activity is not detectable) in splenocytes and thymocytes of HET mice, and discerned that they were comparable to those of WT mice (Fig. 7A). We also measured the protein level of 1 subunit (β5) of the proteasome complex in the lungs, spleens, thymuses, livers and kidneys of HET mice, and found that it was comparable to that of WT tissues (Fig. 7B). Taken together, these data suggest that a 50% reduction of Pno1 expression does not elicit abnormal proteasome levels or activities.

Generation of Pno1 Tg mice

Since we could not obtain live Pno1 KO mice, and since HET mice manifested no apparent anomalies in general and in immune system and proteasome activities in particular, we wondered whether Pno1 over-expression in mice would reveal some phenotype. We generated Tg mice with β-actin promoter-driven Pno1 expression. The plasmid construct is shown in Figure 8A. Tail DNA was routinely genotyped by PCR, and Tg mice presented a 552-bp band (Fig. 8B). In Tg organs, such as the Lung, liver, kidney, thymus and spleen, Pno1 mRNA expression was universally heightened, although to different degrees (Fig. 8C). We also tested

chymotrypsin-like and Trypsin-like protease activities in the Tg thymus and spleen, and found that they were similar to those of their WT counterparts (Fig. 8D).

Pno1 Tg mice manifest no apparent immune system anomalies

Pno1 Tg mice were fertile and had no gross anomalies. Their immune organs, the thymus, LN and Spleen, were of normal size and cellularity (data not reported). T and B cell populations and CD4 and CD8 T cell populations in the Spleen and LN were comparable to those of WT mice (Fig. 9A). In the Tg Thymus, the different thymic sub-populations (e.g., CD4CD8 double-negative, CD4CD8 double-positive, CD4 single-positive and CD8 single-positive cells) were similar to those in the WT thmus (Fig. 9B). Pno1 over-expression did not compromise T cell proliferation caused by solid phase anti-CD3 mAb stimulation (Fig. 9C). Tg CD4 and CD8 T cells up-regulated their activation markers CD25 and CD69 in comparison to their WT counterparts upon activation (Fig. 9D). Therefore, excessive Pno1 expression does not seem to affect proteasome activity.

We also assessed B cell subpopulations in the spleen and peritoneal cavity of WT and Tg mice. In the spleen of WT and Tg mice, there was no consistent difference in terms of the percentage of $B220^{+}CD21^{hi}CD23^{lo/-}$ mantel zone B cells (Fig. 10A), or the percentage of $B220^{+}CD21^{int/hi}CD23^{hi}$ follicular B cells (Fig. 10A). For B cells of the WT and Tg mouse peritoneal exudates, there was no consistent difference in terms of the percentage of $B220^{+}CD23^{-}CD5^{+}IgM^{hi}$ B1a cells (Fig. 10B), $B220^{+}CD23^{-}CD5^{-}IgM^{hi}$ B1b (Fig. 10B) and $B220^{+}CD23^{+}IgM^{int/hi}$ B2 cells (Fig. 10B). Spleen B cells from WT and Tg mice proliferated comparably upon anti-IgM plus IL-4, anti-CD40 plus IL-4, or anti-CD40 plus LPS stimulation (Fig. 10C). The upregulation of B cell activation markers CD86 and CD80 in WT and Tg spleen B cells 24 h after the above-described stimulation showed no apparent difference neither (Fig. 10D). We next examined the percentage of $IgD^{-}IgM^{-}CD138^{+}B220^{lo/-}$ isotype-switched plasmablast/plasma cells in the draining lymph nodes of WT and Tg mice 21 days after immunization with chick type II collagen, but not significant difference was found (Fig. 10E). The serum collagen-specific Ab levels in these WT and Tg mice 21 days after the chick type II collagen immunization showed no significant difference (Fig. 10F).

The results from this section suggest that a normal endogenous Pno1 expression level is sufficient for the tested T cell functions. Pno1 over-expression does not confer additional advantages.

Pno1 occurs in complexes larger than 26S proteasomes

We wondered whether Pno1 is present in proteasome complexes in mammalian cells. For this purpose, we stably transfected L cells with a Pno1-expressing construct, pCEP-Pno1, in which Pno1 was fused with 3 copies of HA tags at the N-terminus. The transfected cells expressed greatly-enhanced Pno1 mRNA levels (Fig. 11A), but their proteasome activity remained similar to that of empty vector-transfected cells (Fig. 11B). L cell lysates were fractionated with glycerol density gradients, and the chymotrypsin-like proteasome activity of each fraction was quantified. As seen in Figure 11C, there were 2 peaks of enzymatic activity at fractions 13 and 17, corresponding to 20S and 26S proteasomes, respectively. Western blotting showed that the proteasome β5 subunit was present from fractions 13 to 21, with trace amounts found up to fraction 23 (Fig. 11D), confirming that proteasome complexes (20S and 26S) were in these fractions, which contained 2 peaks of proteasome activities (Fig. 11C). Interestingly, Pno1, as detected by anti-HA Ab, made a major appearance, starting from fraction 19 and ending at fraction 25, with trace amounts occurring until fraction 27 (Fig. 11E). Its location did not correspond to that of 20S or 26S proteasomes based on both proteasome activity and β5 location, but obviously resided in fractions larger than 26S.

Is Pno1 then a part of ribosomes? We assessed small and large ribosome subunits in glycerol gradient fractions by anti-S6 and anti-L7 mAb Western blotting (Figs. 11F and 11G, respectively). S6 signals appeared from fraction 17 and ended at fraction 27, consistent with the size of the small 40S ribosome subunit. L7 signals presented from fraction 25 until fraction 27, consistent with the size of large 60S ribosome subunits. Fractions containing the small subunit overlapped with but were not identical to those of Pno1.

The results of this sedimentation study indicate that Pno1 does not co-localize exactly with proteasomes, small or large ribosome subunits, but seems to exist in complexes with sedimentation rates higher than 26S, probably between 30S to 40S, employing a low ribosome sedimentation rate as marker.

Discussion

So far, all known functions of Pno1 are based on findings in yeasts, in which Pno1 is reportedly involved in both ribosome and proteasome biogenesis. In this study, we attempted to understand Pno1 function in mammalian cells, via a combination of ISH, gene KO, Tg and *in vitro* cell transfection techniques.

First of all, according to signal intensity in ISH, Pno1 mRNA belonged to a class of low-abundant species. In biological systems, such low-abundant species normally play regulatory roles so that a small change in their expression can be leveraged and amplified for much larger biological reactions at the molecular level.

The general expression pattern from the fetal stage to adulthood indicates that this gene is highly expressed in organs or tissues containing fast-proliferating cells, such as the e9 fetus, thymus at different ages, skin, bone marrow, intestine and testes. This is compatible with the presumed function of Pno1 in ribosome and proteasome neogenesis, because fast-growing cells need high rates of protein synthesis as well as protein degradation. However, Pno1 was also expressed at high levels in certain tissues with no proliferation or enhanced protein synthesis, such as neuroganglia (DRG, SG and TriG), OL and ONE in the brain, and Me of the Ad. On the other hand, although the adult liver is very active in protein synthesis, its Pno1 expression is very low. These observations raise an intriguing question that Pno1 might have important functions unrelated to either ribosome or proteasome neogenesis.

We observed that a 50% Pno1 reduction in HET cells or 4-5-fold Pno1 increase in Tg cells did not cause any disruption of embryonic development, proteasome activity, T cell development, B cell development, or i*n vitro* T and B cell activation and proliferation. Proteasome is important to plasma cell generation, and the proteasome inhibitors could induce apoptosis in malignant and primary plasma cells both in vitro and in vivo as a result of activation of the terminal unfolded protein response (UPR)[15,16]. However, no anomaly was observed in HET and Tg mice in terms of plasma cell percentage and their antibody production.

We introduced small interfering RNA into HET fibroblasts to further lower Pno1 expression to about 15% of the normal level, but the cells proliferated normally with proteasome

activities comparable to those of their WT counterparts (data not included). However, a complete lack of Pno1 is disastrous: it led to arrest of embryonic development before e3.5, at which time embryo contain about 8-30 cells[17]. There are 2 possible interpretations of this observation: 1) around e2.5, Pno1 is critical for a certain developmental event; or 2) embryonic cells before eight cell stage depend on maternal Pno1 protein or mRNA for their vital functions until its concentration drops below the critical level because of cell division (i.e., less than 1/8 of the normal Pno1 cellular level on e2.5 due to cell division) and the cells then cease to function owing to a lack of Pno1. In support of this hypothesis, it is worth mentioning that maternal ribosomes are exhausted before the blastocyst stage at e3.5 [18,19]. Regardless of what function Pno1 has, it is obviously a vital molecule with no redundancy and is absolutely required for cell function. Cells only need a small fraction of the normal Pno1 level to be functional. Excessive Pno1 does not bring any perceivable benefit, but without it, cells will die.

In yeasts, Pno1 has been implicated in ribosome and proteasome neogenesis. Whether it has similar functions in mammalian cells is not known. With density gradient sedimentation, we were able to identify fractions containing 20S and 26S proteasomes. However, Pno1 did not exactly fall in fractions containing proteasomes, but appeared in fractions containing complexes with sedimentation rates higher than 26S. This at least indicates that Pno1 is not a constitutive part of mature 20S or 26S proteasomes. In cells, the only macromolecules larger than proteasomes are ribosomes. In eukaryotic cells, mature ribosomes are 40S and 60S in size and derive from 90S precursors with some 66S and 43S intermediate products occurring during the maturation process [20,21]. We used S6, a component of the small ribosome subunit, and L7, a component of the large ribosome subunit, as markers to establish fraction profiles of small 40S and large 60S ribosome subunits. The fraction profile of Pno1 did not fit either of them. Pno1-containing fractions appeared earlier than large ribosome-containing fractions. On the other hand, Pno1 overlapped with but appeared about 2 fractions later than small ribosome subunit-containing fractions. Several possibilities exist: 1) If Pno1 is involved in mammalian ribosome neogenesis, it is not a part of mature ribosome particles, but could transiently associate with certain pre-ribosome species and play a critical role in their assembly and maturation. Indeed, it is known that more than 200 molecules transiently

associate with ribosomes during their neogenesis and are critical in their assembly. Pno1 could be one of them and an irreplaceable one at that. 2) As the size of Pno1-containing complexes is larger than 26S but smaller than 60S, the complexes might contain a 26S proteasome and some malformed ribosomes, smaller than 40S, to facilitate their elimination.

Because of early embryo lethality, we could not obtain sufficient KO cells to study the roles of Pno1 in proteasome or ribosome functions. As a consequence, we could not confirm whether a lack of Pno1 compromises mammalian proteasome or ribosome maturation or function. We immunoprecipitated Pno1 and tried to find proteasome subunits or ribosome subunits in precipitates, or *vice versa*, but met with little success (data not reported). This has raised an intriguing possibility that if Pno1 does link with proteasome and/or ribosome precursors, the association is transient and probably of low affinity. Additional studies with inducible gene KO in mice are needed to reveal the possible role of Pno1 in mammalian cells.

Reference

1. Zemp I, Kutay U (2007) Nuclear export and cytoplasmic maturation of ribosomal subunits. FEBS letters 581: 2783–2793. doi:10.1016/j.febslet.2007.05.013.

2. Gibson TJ, Thompson JD, Heringa J (1993) The KH domain occurs in a diverse set of RNA-binding proteins that include the antiterminator NusA and is probably involved in binding to nucleic acid. FEBS letters 324: 361–366.

3. Vanrobays E, Gélugne J-P, Caizergues-Ferrer M, Lafontaine DLJ (2004) Dim2p, a KH-domain protein required for small ribosomal subunit synthesis. RNA 10: 645–656.

4. Tone Y, Toh-E A (2002) Nob1p is required for biogenesis of the 26S proteasome and degraded upon its maturation in Saccharomyces cerevisiae. Genes Dev 16: 3142–3157.

5. Schäfer T, Strauss D, Petfalski E, Tollervey D, Hurt E (2003) The path from nucleolar 90S to cytoplasmic 40S pre-ribosomes. EMBO J 22: 1370–1380.

6. Woolls HA, Lamanna AC, Karbstein K (2011) Roles of Dim2 in ribosome assembly. Journal of Biological Chemistry 286: 2578–2586.

7. Campbell MG, Karbstein K (2011) Protein-protein interactions within late pre-40S ribosomes. PLoS ONE 6: e16194.

8. Senapin S, Clark-Walker GD, Chen XJ, Séraphin B, Daugeron M-C (2003) RRP20, a component of the 90S preribosome, is required for pre-18S rRNA processing in Saccharomyces cerevisiae. Nucleic Acids Res 31: 2524–2533.

9. Marcinkiewicz M (2002) BetaAPP and furin mRNA concentrates in immature senile plaques in the brain of Alzheimer patients. J Neuropathol Exp Neurol 61: 815–829.

10. Nagy A, Rossant J, Nagy R, Abramow-Newerly W, Roder JC (1993) Derivation of completely cell culture-derived mice from early-passage embryonic stem cells. 90: 8424–8428.

11. Luo H, Charpentier T, Wang X, Qi S, Han B, et al. (2011) Efnb1 and Efnb2 proteins regulate thymocyte development, peripheral T cell differentiation, and antiviral immune responses and are essential for interleukin-6 (IL-6) signaling. Journal of Biological Chemistry 286: 41135–41152.

12. Han B, Moore PA, Wu J, Luo H (2007) Overexpression of human decoy receptor 3 in mice results in a systemic lupus erythematosus-like syndrome. Arthritis Rheum 56: 3748–3758.

13. Mao J, Qiao X, Luo H, Wu J (2006) Transgenic drak2 overexpression in mice leads to increased T cell apoptosis and compromised memory T cell development. The Journal of biological chemistry 281: 12587–12595.

14. Zhang J, Wang X, Fahmi H, Wojcik S, Fikes J, et al. (2009) Role of TL1A in the pathogenesis of rheumatoid arthritis. J Immunol 183: 5350–5357.

15. Lee A-H, Iwakoshi NN, Anderson KC, Glimcher LH (2003) Proteasome inhibitors disrupt the unfolded protein response in myeloma cells. Proc Natl Acad Sci USA 100: 9946–9951.

16. Neubert K, Meister S, Moser K, Weisel F, Maseda D, et al. (2008) The proteasome inhibitor bortezomib depletes plasma cells and protects mice with lupus-like disease from nephritis. Nat Med 14: 748–755.

17. Nagy A (2003) Manipulating the Mouse Embryo. CSHL Press. pp.

18. Copp AJ (1995) Death before birth: clues from gene knockouts and mutations. Trends Genet 11: 87–93.

19. Oliver ER (2004) Ribosomal protein L24 defect in Belly spot and tail (Bst), a mouse Minute. Development 131: 3907–3920.

20. Udem SA, Warner JR (1972) Ribosomal RNA synthesis in Saccharomyces cerevisiae. J Mol Biol 65: 227–242.

21. Trapman J, Retèl J, Planta RJ (1975) Ribosomal precursor particles from yeast. Exp Cell Res 90: 95–104.

Figure legends

Figure 1. ISH analysis of Pno1 expression during ontogeny

Abbreviations: AA: arch artery; Ad – adult; BM: bone marrow; Br: brain; Cb: cerebellum; CD: colon, descending; Cx: cerebral cortex; DRG: dorsal root ganglion; FB: forebrain; H: heart; Hip: hippocampus; Inc: incisors, teeth; Int: intestine; K: kidney; Li: liver; Lg: lacrimal gland; Lu: lungs; M: muscles, striated; MB: midbrain; Mol: molars, teeth; NT: neural tube; OL: olfactory lobe; ONE: olfactory neuroepithelium; R: rib; SG: sympathetic ganglion; Sk: skin; SMax: submaxillary gland; SpC: spinal cord; Spl: spleen; St: stomach; Th: thymus. TriG; trigeminal ganglion; Ts: testes; Vb: vertebrae. Bars = 1 cm. (s): sense cRNA used as a probe. The bars = 1 cm. Darkfield x-ray film autoradiography is shown.

A. Pno1 expression from embryonic day 9 (e9) to post-natal day 1 (p1)

Panels I-VI: anti-sense cRNA as probe. Panels I'-VI': sense cRNA as probe.

B. Pno1 expression on p10

Panel I: anti-sense cRNA as probe. Panel I': sense cRNA as probe.

C. Pno1 expression in adulthood

Panels I-V: anti-sense cRNA as probe. Panel V': sense cRNA as probe.

Figure 2. Pno1 expression in adult tissues according to ISH

Ad: adrenal gland; B: bone; Me: medulla; Cx: cortex; SpC: spinal cord; BM: bone marrow; Vb: vertebrae. (s): sense cRNA as probe.

A. Pno1 expression in Th

Panel I: Dark field X-ray film autography with anti-sense cRNA as probe. Panel I': sense cRNA as probe. Bar = 1 mm. Panels II to IV (antisense) and (II' to IV', sense) are brightfield images of emulsion autoradiography in p1, p10 and adult mice.

B. Pno1 expression in the vertebrae region of adult mouse whole-body section

Panel I: Dark field X-ray film autography with anti-sense cRNA as probe. Panels I (anti-sense cRNA as probe) and II (sense cRNA as probe): emulsion autoradiography seen under

brightfield illumination at higher magnification. Fine black grains represent Pno1 mRNA labelling. Bar = 1 mm (in I) and 50 μm (in II). Arrows point to small hematopoietic cells.

C. Pno1 expression in the Ad

Panels I-III: Anti-sense cRNA as probe. Panels I'-III': sense cRNA as probe. Panels I and I' are dark field X-ray film autography. Panels II, III, II' and III' are emulsion autoradiography seen under higher magnification. Bar = 1 mm (in I) and 100 μm (in II).

Figure 3. Generation of Pno1 KO mice

A. Targeting strategy to generate Pno1 KO mice

The black square marked as 3' probe represents the sequence used as probe in Southern blotting for genotyping. A 18.6-kb BamH1 fragment detected by this probe represents the WT allele, and a 7.5-kb BamH1 fragment, the KO allele.

B. Genotyping of Pno1 mutant mice

Tail DNA was digested with BamHI, and analyzed by Southern blotting (left panel), with a 3' probe whose sequence location is indicated in A. A 18.6-kb band representing the WT allele and a 7.5-kb band representing the recombinant allele are indicated by arrows. Ear lobe DNA without digestion was analyzed by PCR for routine genotyping (right panel). A 548-bp band representing the WT allele and a 224-bp band representing the recombinant allele are indicated by arrows.

C. Reduced Pno1 mRNA expression in $Pno1^{+/-}$ tissues

mRNA from the Li, Th and Spl of WT and heterozygous Pno1+/- (HET) mice were analyzed by reverse transcription-real time PCR (RT-qPCR) for Pno1 mRNA levels. The results are expressed as ratios of Pno1 versus β-actin signals with means + SD indicated.

D. Reduced Pno1 mRNA up-regulation in $Pno1^{+/-}$ T cells upon activation

T cells from WT and HET Spl were stimulated with solid phase anti-CD3 mAb and anti-CD28 mAb (0.5 μg/ml and 4 μg/ml respectively for coating) for 1 to 24 h, and their Pno1 mRNA levels were quantified by RT-qPCR. The results are expressed as ratios of Pno1 versus β-actin signals with means + SD indicated.

Figure 4. In vitro development of WT, HET and KO embryos

e1.5 embryos were harvested, and cultured in M16 medium and photographed daily until e4.5. Phase contrast micrographs are shown. At the end of culture on e4.5, the embryos were genotyped with qPCR.

Figure 5. Sub-populations of lymphocytes in lymphoid organs and T cell function of Pno1 HET mice

A. T cell subpopulations in the spleen and LN

CD4 and CD8 T-cell populations in WT and HET spleens, LN and thymuses were analyzed by 2-color flow cytometry. Percentages are indicated.

B. B cell population in lymphoid organs

B cell populations in the spleen and LN were analyzed according to B220 and CD19 expression by 2-color flow cytometry.

C. T cell proliferation

WT and HET spleen T cells were stimulated with solid phase anti-CD3 mAb (0.5 μg/ml for coating). The cells were pulsed with 3H-thymidine 16 h before harvesting. 3H-thymidine uptake by the cells was measured at 24, 48 and 72 h. Samples were tested in triplicate, and means + SD of CPM are shown.

D. C69 and CD25 expression on activated WT and HET T cells

WT and HET T cells were stimulated overnight by solid phase anti-CD3 mAb plus anti-CD28 mAb (0.5 μg/ml and 4 mg/ml respectively for coating). CD69 and CD25 expression on CD4 (left panel) and CD8 (right panel) T cells was measured by 2-color flow cytometry.

All experiments in this figure were repeated at least 3 times and representative data are reported.

Figure 6. B cell development and function in HET mice

A. Normal marginal zone B cell and follicular B cell populations in the spleen of HET mice

Marginal Zone B cell (B220+CD21hiCD23low/-) and follicular B cell (B220+CD21int/hiCD23hi) populations in WT and HET spleens were analyzed by 3-color flow cytometry. Percentages are indicated.

B. B1 B cell and B2 B cell subpopulation in peritoneal exudates of HET mice

Peritoneal exudate B1a (B220+CD23-CD5+IgMhi), B1b (B220+CD23-CD5-IgMhi) and B2 (B220+CD23+IgMint/hi) B cells of WT and HET mice were analyzed by by 4-color flow cytometery. Percentages are indicated.

C. Proliferation of B cells from HET mice

WT and HET spleen B cells were stimulated with different stimuli as indicated (anti-IgM: 5μg/ml; IL-4: 10ng/ml; anti-CD40 mAb: 2mg/ml; LPS: 2mg/ml). The cells were pulsed with 3H-thymidine 6 h before harvesting. 3H-thymidine uptake by the cells was measured at 24 h and 48 after the initiation of the culture. Samples were in triplicate, and means + SD of CPM are shown.

D. B cell activation markers CD80 and CD86 expression on activated WT and HET B cells

WT and HET spleen B cells were stimulated as described in C. CD80 and CD86 expression on B220+ B cells was measured by 3-color flow cytometry 24 h after the initiation of the culture.

E. Plasma cells in the draining lymph nodes of immunized WT and HET mice

WT and HET mice were immunized with chick type II collagen with adjuvants at the tail base and sacrificed 21 days after the immunization. Isotype-switched plasmablast/plasma cells (IgD-IgM-CD138+B220lo/-) from the draining lymph nodes of WT and HET were analyzed by 4-color flow cytometry.

F. Serum collagen-specific antibody production in WT and HET mice

Sera from mice (WT n=7, HET n=4) as described in E were collected on day 21 after the immunization. Chick collagen-specific IgG Abs were measured by ELISA. The data are expressed as arbitrary titres. The titres between WT and HET groups were not statiscially significant ($p=0.8724$, Student's t test).

Experiments A-E were repeated at least 3 times and representative data are shown.

Figure 7. Proteasome activities WT and HET tissues

A. Proteasome activities in spleen and thymus

Lysates from the Sp and Th of WT and HET mice were assayed for chymotrypsin-like and trypsin-like proteasome protease activities. Samples were tested in triplicate, and means + SD are shown.

B. HET and WT organs have similar proteasome levels

Lysate proteins from the lung, spleen, thymus, liver and kidney were analyzed for proteasome content according to proteasome β5 subunit levels based on immunoblotting (upper panel). β-actin levels were used to show even loading of lysate proteins (lower panel).

Figure 8. Generation of Pno1 Tg mice

A. pAC-Pno1 construct for Tg mice generation

The 6.4-kb ClaI/ClaI fragment was microinjected.

B. Genotyping of ear lobe DNA by PCR

The 552-bp band specific to the Pno1 transgene is indicated by an arrow.

C. RT-qPCR of Pno1 mRNA in different organs of Tg mice

Means + SD of Pno1 versus β-actin signal ratios of the lung, kidney and spleen of Tg and WT mice.

D. Proteasome activities in spleen and thymus

Lysates from the Sp and Th of WT and Tg mice were assayed for chymotrypsin-like and trypsin-like proteasome protease activities. Samples were tested in triplicate, and means + SD are shown.

Figure 9. Sub-populations of lymphocytes in lymphoid organs and T cell function of Pno1 Tg mice

A. T cell sub-populations in the spleen and LN

CD4 and CD8 T cell populations in the WT and Tg spleen LN and thymus were analyzed by 2-color flow cytometry. Percentages are indicated.

B. B cell population in lymphoid organs

The B cell population in the spleen and LN was analyzed according to B220 and CD19 expression by 2-color flow cytometry.

C. T cell proliferation

WT and Tg spleen T cells were stimulated with solid phase anti-CD3 mAb (0.5 ìg/ml for coating). The cells were pulsed with 3H-thymidine 16 h before harvesting. 3H-thymidine uptake by cells was measured at 24, 48 and 72 h. The samples were tested in triplicate, and means + SD of CPM are shown.

D. C69 and CD25 expression on activated WT and HET T cells

WT and Tg T cells were stimulated overnight by solid phase anti-CD3 plus anti-CD28 mAbs (0.5 ìg/ml and 4 ìg/ml respectively for coating). CD69 and CD25 expression on CD4 (left panel) and CD8 (right panel) T cells was measured by 2-color flow cytometry.

All experiments in this figure were repeated at least 3 times and representative data are shown.

Figure 10. B cell development and function in HET mice

A. Normal marginal zone B cell and follicular B cell populations in the spleen of Tg mice

Marginal Zone B cell (B220+CD21hiCD23low/-) and follicular B cell (B220+CD21int/hiCD23hi) populations in WT and Tg spleens were analyzed by 3-color flow cytometry. Percentages are indicated.

B. B1 B cell and B2 B cell subpopulation in peritoneal exudates of Tg mice

Peritoneal exudate B1a ($B220^{+}CD23^{-}CD5^{+}IgM^{hi}$), B1b ($B220^{+}CD23^{-}CD5^{-}IgM^{hi}$) and B2 ($B220^{+}CD23^{+}IgM^{int/hi}$) B cells of WT and Tg mice were analyzed by by 4-color flow cytometery. Percentages are indicated.

C. Proliferation of B cells from Tg mice

WT and Tg spleen B cells were stimulated with different stimuli as indicated (anti-IgM: 5ìg/ml; IL-4: 10ng/ml; anti-CD40 mAb: 2ìg/ml; LPS: 2ìg/ml). The cells were pulsed with 3H-thymidine 6 h before harvesting. 3H-thymidine uptake by the cells was measured at 24 h and 48 after the initiation of the culture. Samples were in triplicate, and means + SD of CPM are shown.

D. B cell activation markers CD80 and CD86 expression on activated WT and Tg B cells

WT and Tg spleen B cells were stimulated as described in C. CD80 and CD86 expression on B220+ B cells was measured by 3-color flow cytometry 24 h after the initiation of the culture.

E. Plasma cells in the draining lymph nodes of immunized WT and Tg mice

WT and Tg mice were immunized with chick type II collagen with adjuvants at the tail base and sacrificed 21 days after the immunization. Isotype-switched plasmablast/plasma cells (IgD-IgM-CD138+B220lo/-) from the draining lymph nodes of WT and Tg were analyzed by 4-color flow cytometry.

F. Serum collagen-specific antibody production in WT and Tg mice

Sera from mice (WT n=7, Tg n=4) as described in E were collected on day 21 after the immunization. Chick collagen-specific IgG Abs were measured by ELISA. The data are expressed as arbitrary titres. The titres between WT and Tg groups were not statiscially significant (p=0.1927, Student's t test).

Experiments A-E were repeated at least 3 times and representative data are shown.

Figure 11. Pno1 is associated with macromolecules with a sedimentation rate greater than 26S

A. Pno1 mRNA over-expression in L cells stably transfected with the Pno1-expressing construct pCEP-Pno1-HA

Pno1 mRNA levels were quantified by RT-qPCR. Samples were tested in triplicate and means + SD of Pno1 versus β-actin signal ratios are shown. L cells stably transfected with empty vectors were used as controls.

B. L cells over-expressing Pno1 presented similar proteasome activity as vector-transfected cells

The chymotrypsin-like activity of L cells stably transfected with pCEP-Pno1-HA was quantified, and L cells transfected with empty vectors were used as controls. The assay was conducted in triplicate, and means ± SD are shown.

C. Proteasome activities in glycerol density gradient fractions

Lysates from L cells stably transfected with Pno1-expressing constructs or empty vectors were fractionated with glycerol gradients, and chymotrypsin-like proteasome activity in fractions 1 to 30 was quantified. 20S and 26S fractions are indicated.

D-G. Location of Pno1, β5, S6 and L7 in glycerol density gradients

Proteins in fractions 1 to 27 of the glycerol gradient of L cells overexpressing Pno1 were analyzed by immunoblotting. The b5 proteasome subunit (D), Pno1 (E), S6 subunit of the small ribosome complex (F) and L7 subunit of the large ribosome complex (G) were detected by their respective Abs (Pno1 was detected by anti-HA Ab).

Tables

Table 4.1 Genotypic analysis of embryos from $Pno1^{+/-}$ × $Pno1^{+/-}$ mating

	Genotype			
Stage	+/+	+/-	-/-	Total
e6.5	6	12	0	18
e3.5	8	15	4	27

Figures

Figure 4.1

Figure 1.

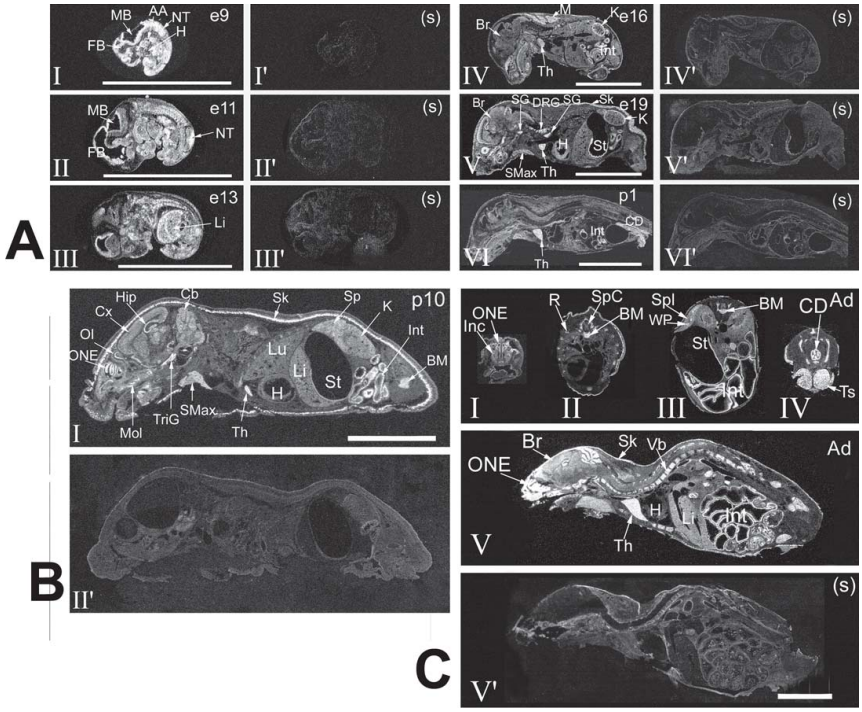

Figure 4.2

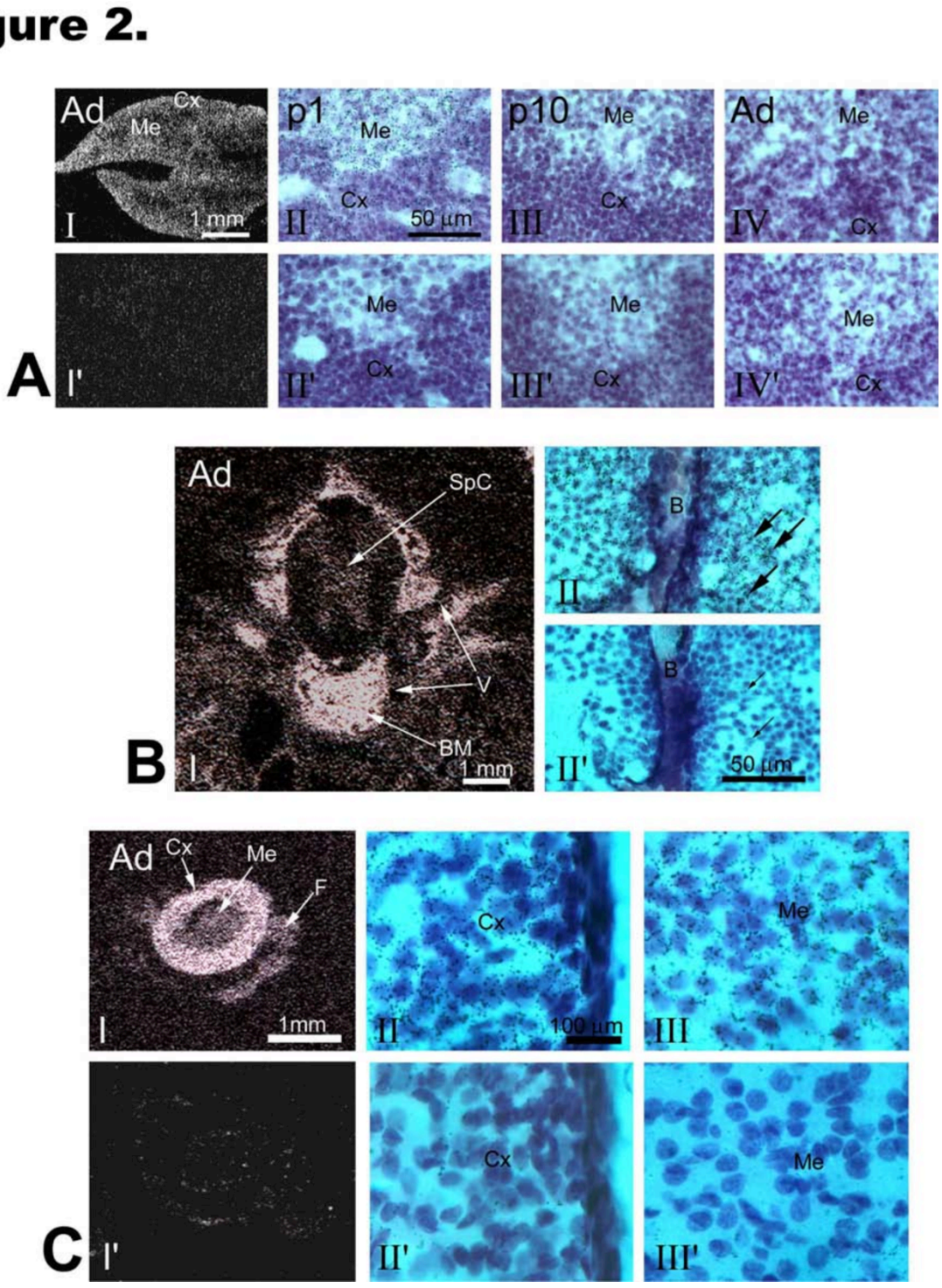
Figure 2.
A
Ad
Cx
Me
I
1 mm
p1
Me
Cx
II
50 µm
p10
Me
Cx
III
Ad
Me
Cx
IV
I'
Me
Cx
II'
Me
Cx
III'
Me
Cx
IV'
B
Ad
SpC
V
BM
I
1 mm
B
II
B
II'
50 µm
C
Ad
Cx
Me
F
I
1mm
Cx
II
100 µm
Me
III
I'
Cx
II'
Me
III'

Figure 4.3

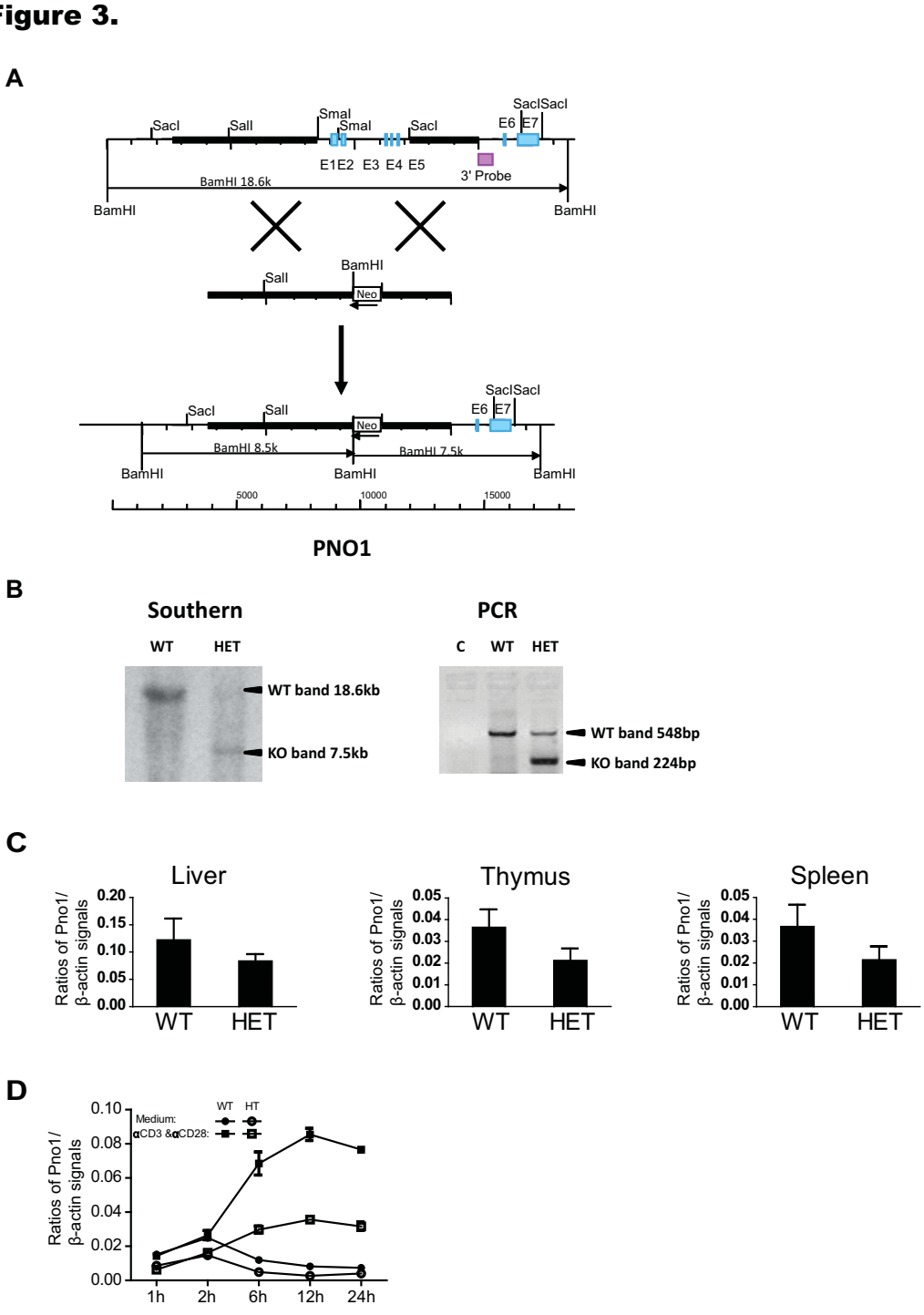
Figure 3.
A
SacI
SalI
SmaI
SmaI
SacI
SacISacI
E6 E7
E1E2 E3 E4 E5
3' Probe
BamHI 18.6k
BamHI
BamHI
SalI
BamHI
Neo
SacI
SalI
SacISacI
E6 E7
Neo
BamHI 8.5k
BamHI 7.5k
BamHI
BamHI
BamHI
5000
10000
15000
PNO1
B
Southern
WT
HET
WT band 18.6kb
KO band 7.5kb
PCR
C
WT
HET
WT band 548bp
KO band 224bp
C
Liver
Thymus
Spleen
Ratios of Pno1/ β-actin signals
0.20
0.15
0.10
0.05
0.00
0.05
0.04
0.03
0.02
0.01
0.00
WT
HET
D
Ratios of Pno1/ β-actin signals
0.10
0.08
0.06
0.04
0.02
0.00
Medium:
αCD3 &αCD28:
WT
HT
1h
2h
6h
12h
24h

Figure 4.4

Figure 4.

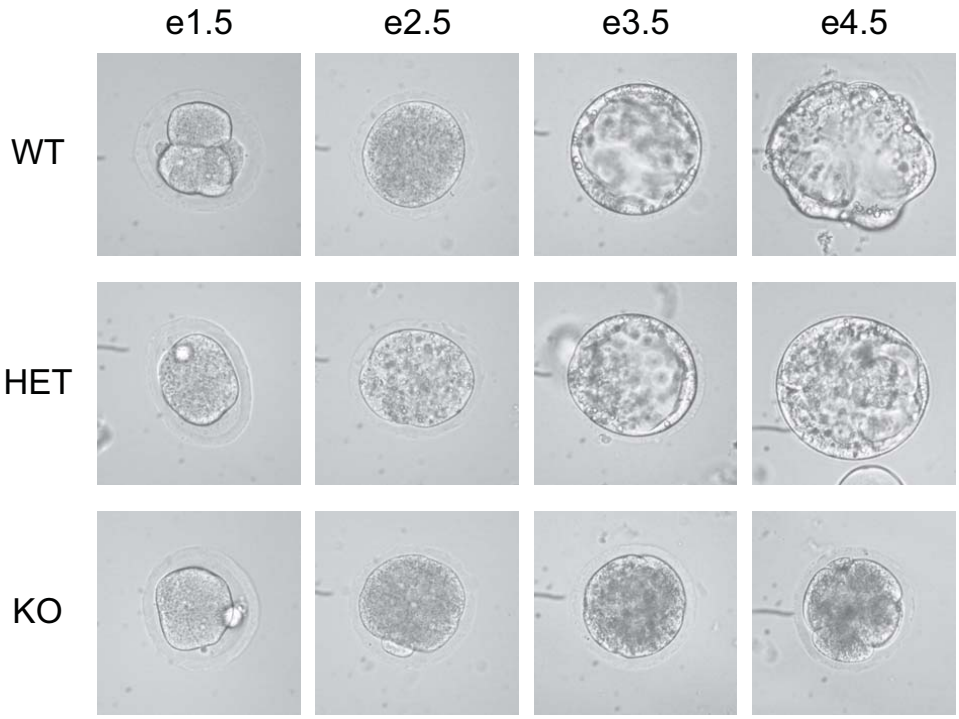

Figure 4.5

Figure 5.

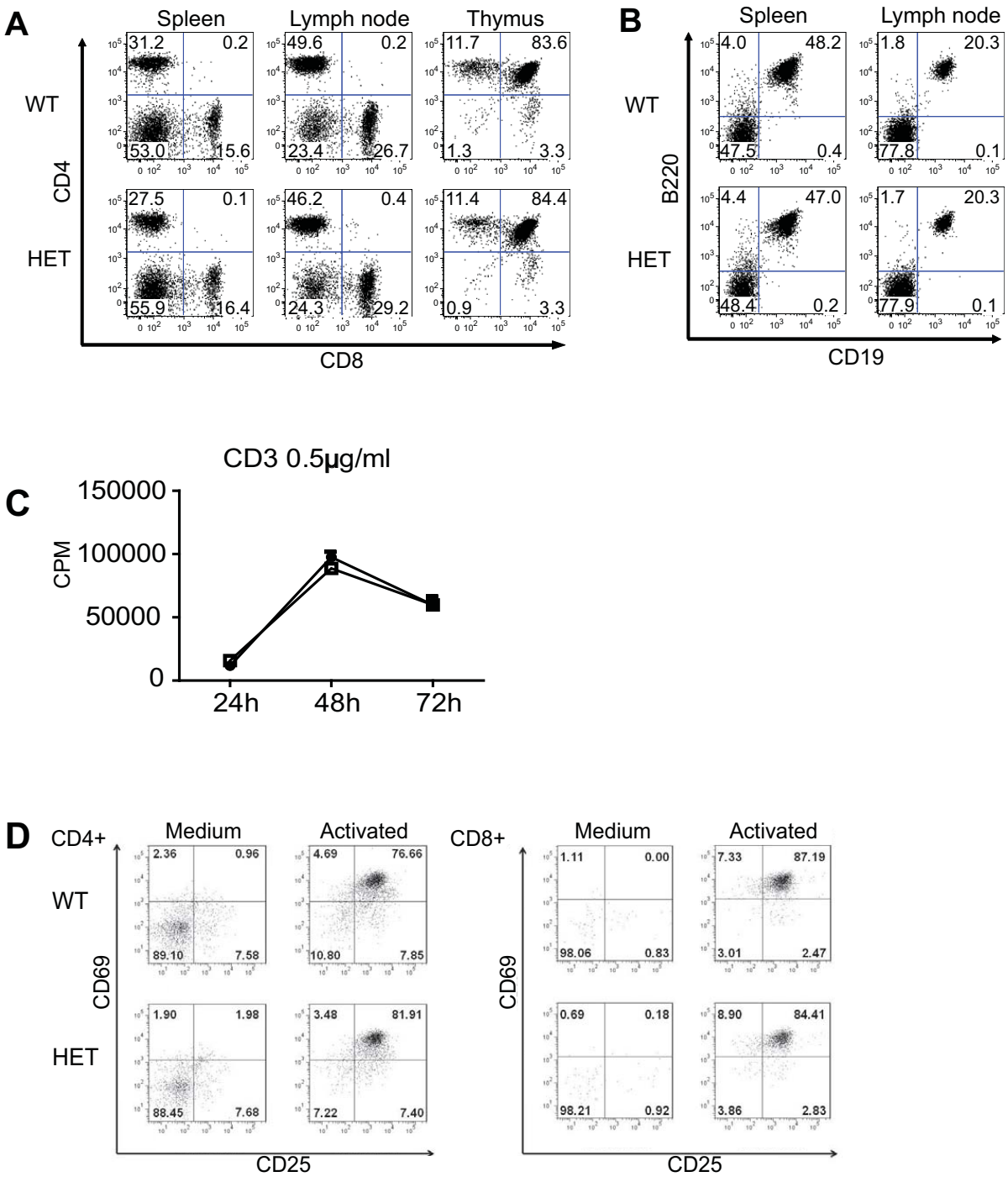

Figure 4.6

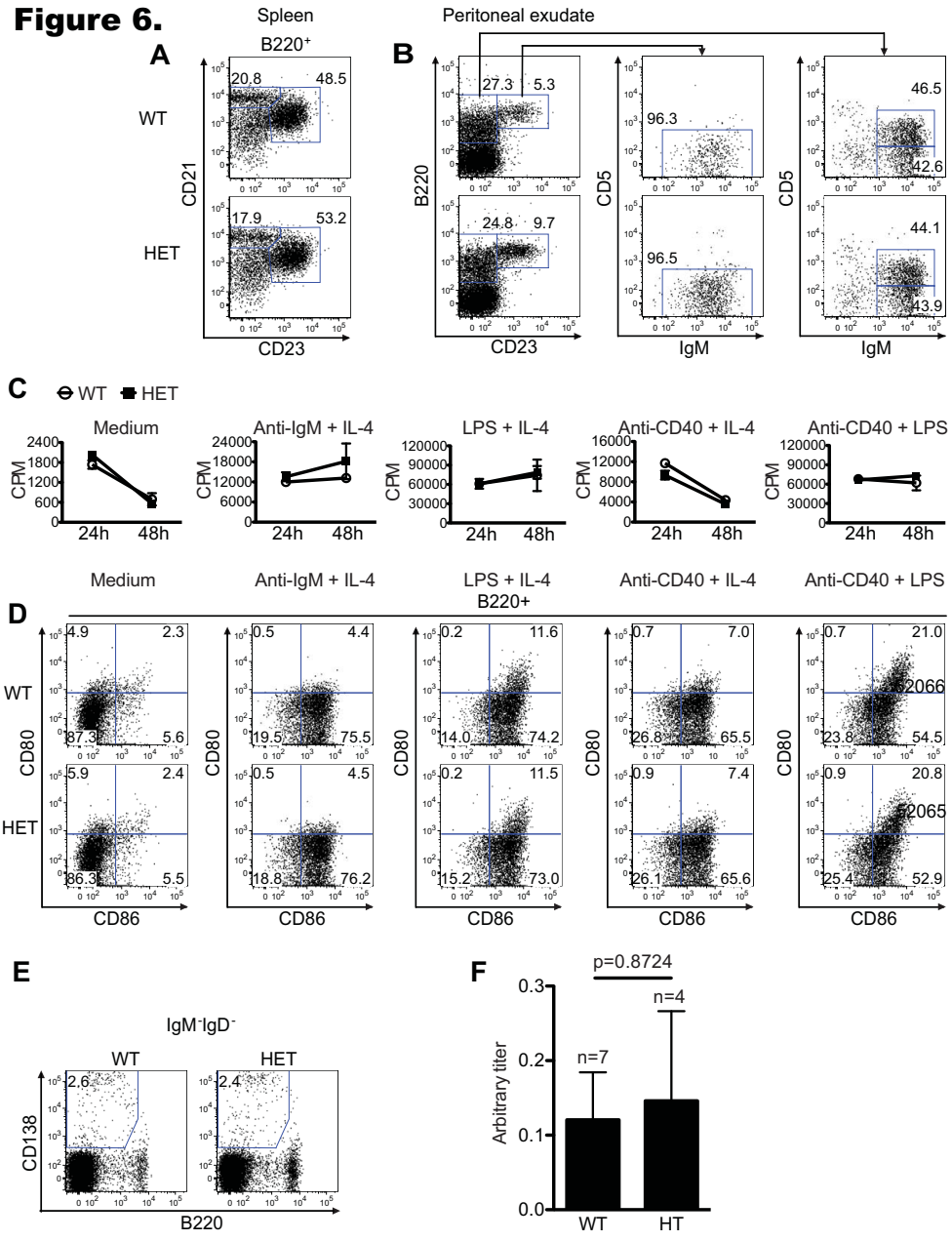
Figure 6.
A
Spleen
B220+
WT
HET
CD21
CD23
20.8
48.5
17.9
53.2
B
Peritoneal exudate
B220
CD23
CD5
IgM
27.3
5.3
96.3
46.5
42.6
24.8
9.7
96.5
44.1
43.9
C
WT
HET
Medium
Anti-IgM + IL-4
LPS + IL-4
Anti-CD40 + IL-4
Anti-CD40 + LPS
CPM
24h
48h
D
B220+
CD80
CD86
4.9
2.3
87.3
5.6
0.5
4.4
19.5
75.5
0.2
11.6
14.0
74.2
0.7
7.0
26.8
65.5
0.7
21.0
2066
23.8
54.5
5.9
2.4
86.3
5.5
0.5
4.5
18.8
76.2
0.2
11.5
15.2
73.0
0.9
7.4
26.1
65.6
0.9
20.8
2065
25.4
52.9
E
IgM-IgD-
CD138
B220
2.6
2.4
F
p=0.8724
n=4
n=7
Arbitrary titer
0.3
0.2
0.1
0.0
WT
HT

Figure 4.7

Figure 7.

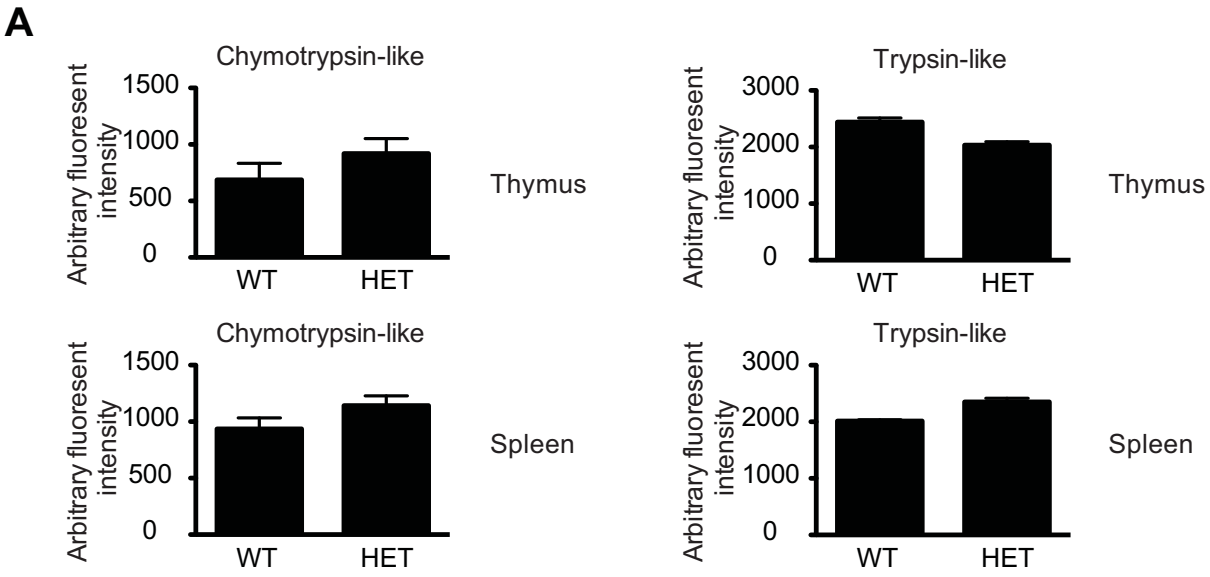

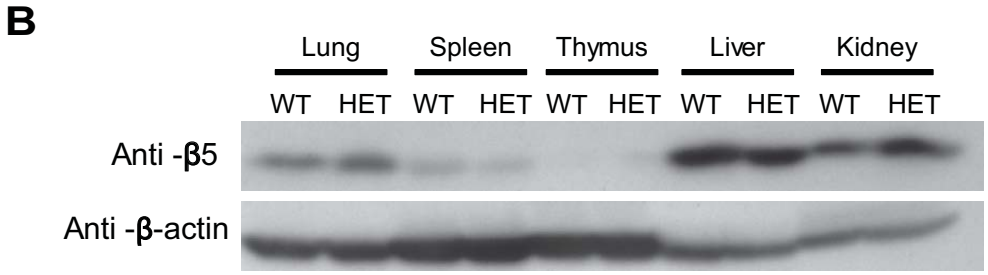

Figure 4.8

Figure 8.

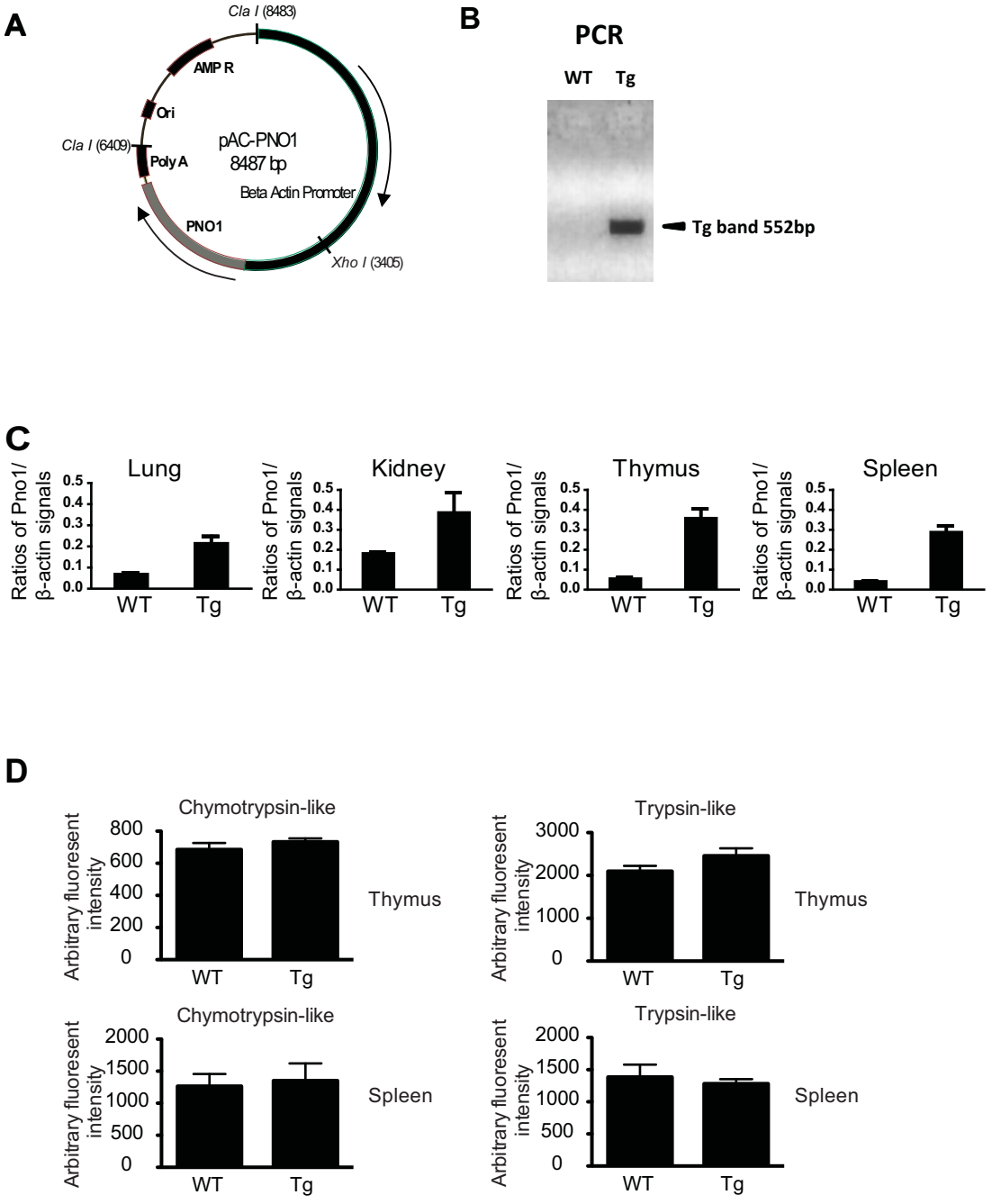

Figure 4.9

Figure 9.

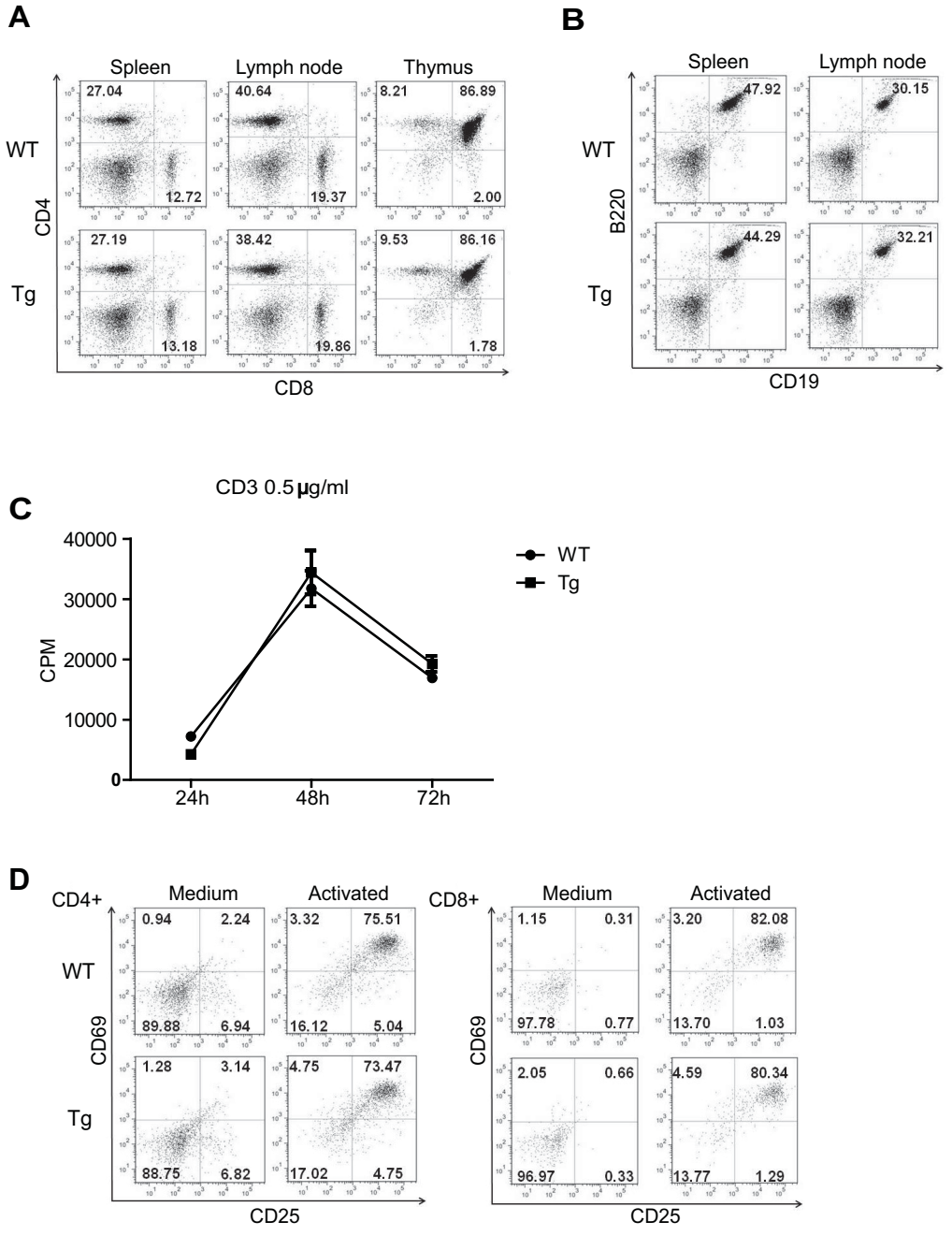

Figure 4.10

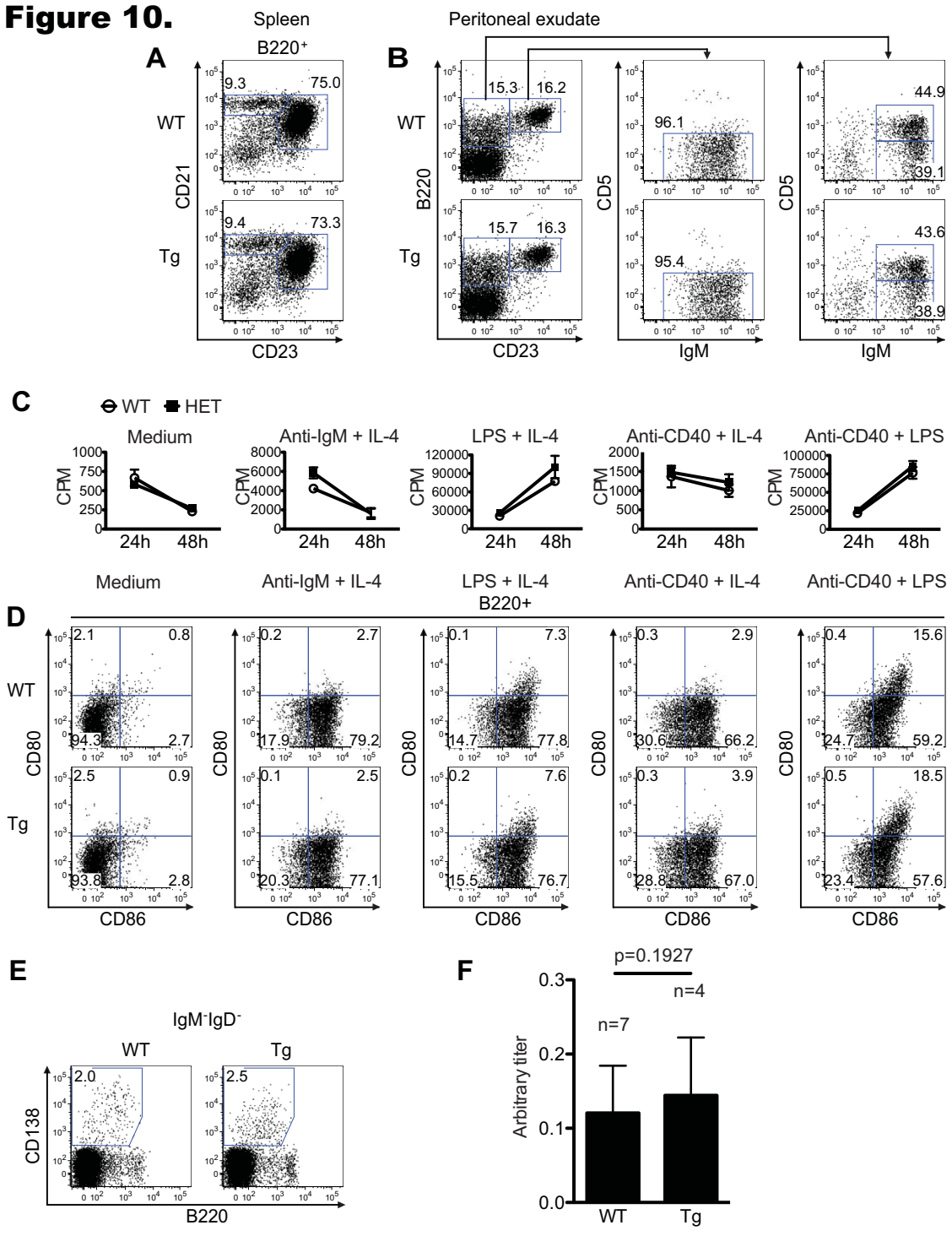
Figure 10.
Spleen
B220+
A
WT
Tg
CD21
CD23
9.3
75.0
9.4
73.3
Peritoneal exudate
B
B220
CD5
IgM
15.3
16.2
96.1
44.9
39.1
15.7
16.3
95.4
43.6
38.9
C
WT
HET
Medium
Anti-IgM + IL-4
LPS + IL-4
Anti-CD40 + IL-4
Anti-CD40 + LPS
CPM
24h
48h
D
CD80
CD86
2.1
0.8
94.3
2.7
2.5
0.9
93.8
2.8
0.2
2.7
17.9
79.2
0.1
2.5
20.3
77.1
0.1
7.3
14.7
77.8
0.2
7.6
15.5
76.7
0.3
2.9
30.6
66.2
0.3
3.9
28.8
67.0
0.4
15.6
24.7
59.2
0.5
18.5
23.4
57.6
E
IgM-IgD-
CD138
2.0
2.5
F
p=0.1927
n=4
n=7
Arbitrary titer
0.3
0.2
0.1
0.0

Figure 4.11

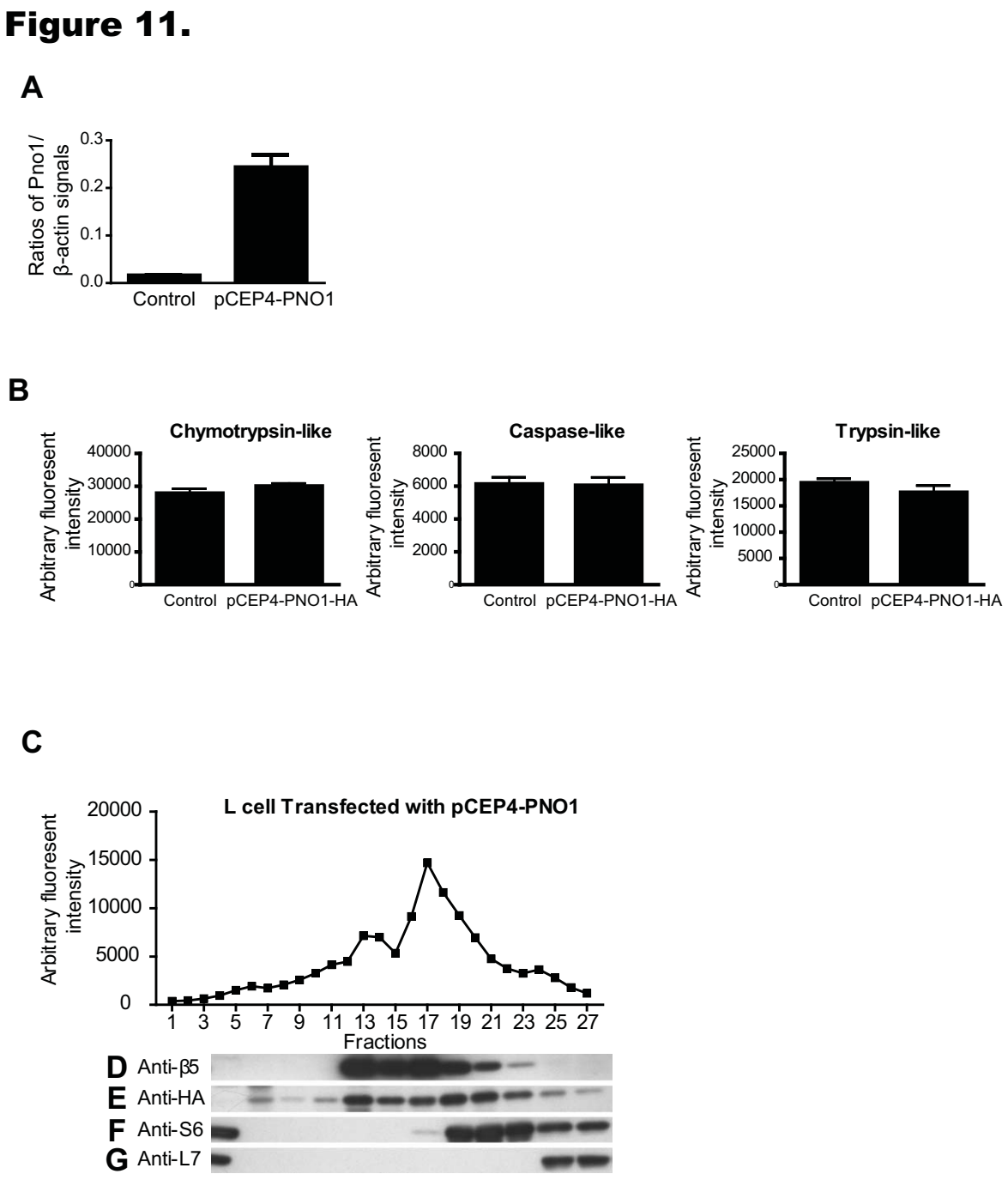
Figure 11.
A
Ratios of Pno1/ β-actin signals
0.3
0.2
0.1
0.0
Control
pCEP4-PNO1
B
Chymotrypsin-like
Caspase-like
Trypsin-like
Arbitrary fluoresent intensity
40000
30000
20000
10000
0
8000
6000
4000
2000
25000
20000
15000
10000
5000
Control
pCEP4-PNO1-HA
C
L cell Transfected with pCEP4-PNO1
Arbitrary fluoresent intensity
20000
15000
10000
5000
0
1 3 5 7 9 11 13 15 17 19 21 23 25 27
Fractions
D Anti-β5
E Anti-HA
F Anti-S6
G Anti-L7

CHAPTER 5 DISCUSSION

5.1 Summary of the Novel Findings in this Thesis

In Chapter 2, we have provided direct evidence that TL1A could aggravate RA by showing that administration of exogenous TL1A significantly increases the disease clinical score, incidence, histopathological score and serum anti-CII antibodies titers in a mouse CIA model. We for the first time discovered elevated levels of TL1A in synovial fluids (SF) from RA patients and in arthritic mouse joint tissues in CIA, and further identified chondrocytes and synovial fibroblasts as the source of TL1A in the RA joints. Furthermore, dendritic cells and monocytes were shown in this study to produce TL1A in the secondary lymphoid organs during CIA. This suggests a systematic role of TL1A such as promoting antibody production, in the RA. Mechanistically, we demonstrated that TL1A specifically increases the TNF-α and IL-17 production *in vitro*.

In Chapter 3, we generated TL1A gene knockout mice and found that the roles of TL1A in the immune system are negligible for mice under a normal condition, but it has important pathological functions in CIA. An absence of endogenous TL1A in mice caused opposite phenotypes to those found in mice with exogenous TL1A administration as shown in our earlier study (Chapter 2). Moreover, TL1A knockout mice have less cell infiltration/accumulation in paws and have smaller sizes and lower cellularity of their draining lymph nodes in CIA. We further explored the role of TL1A in humoral immune responses, and discovered, for the first time, plasma cells as potential targets of TL1A. TL1A might promote the humoral response by prolonging the survival of these cells.

In Chapter 4, we performed whole body *in situ* hybridization to investigate the expression patterns of Pno1 in different developmental stages of mice. We found that, in fetal and adult mice, Pno1 is expressed in tissues with fast-proliferating cells. We further discovered that null-mutation of Pno1 in mice causes embryonic lethality at the pre-implantation stage, while reducing the Pno1 expression by half in heterozygous mice or overexpressing Pno1 in transgenic mice has no effect on the proteasome activities and immune responses.

Heterozygous Pno1 KO mice and Pno1 transgenic mice have similar anti-CII antibody levels in the CIA mouse model.

5.2 Significance of the Major Findings in this Thesis

5.2.1 The implication of TL1A in the RA

Prior to our study, several reports have suggested a potential pathogenic role of TL1A and DR3 in RA. Early genome-wide association studies have identified several RA susceptibility loci in the *dr3* gene (Borysenko et al., 2005; Cornélis et al., 1998; Kayamuro et al., 2009; Shiozawa et al., 1998). Experimental data have been later provided by two studies indicating the presence of TL1A in RA. Cassatella et al. showed that both DR3 and TL1A are deposited in the synovium tissues of RA patients, while Bamias et al. reported that increased levels of TL1A are detected in the sera of RA patients (Bamias et al., 2008; Cassatella et al., 2007). Our studies have confirmed the presence of TL1A in RA and mice CIA joints, and discovered that TL1A directly promotes local inflammation and systematic humoral immune responses in mouse CIA.

5.2.1.1 TL1A promotes the immune cell expansion in RA

Elevated levels of TL1A in the arthritic joints from patients and mice were observed in our studies. We further identified that, in addition to the cells of the hematopoietic origin, non-immune cells as synovial fibroblasts (SFs) and chondrocytes, also produce TL1A upon stimulation (Cassatella et al., 2007; Zhang et al., 2009a). SFs are believed to be a key player in the initiation and perpetuation of RA. In RA, SFs acquire an activation status and produce various pro-inflammatory cytokines thereafter; this activation process may even happen prior to the onset of joint inflammation (Müller-Ladner et al., 2007). The fact that TL1A is produced by activated SF in the joints indicates that TL1A's influences to the joint inflammation could start from a very early stage of CIA. This idea is supported by the findings in Chapter 3. We observed that TL1A KO mice have reduced number of lymphocytes in their paws right before the onset of the disease, and displayed the delayed disease onset as a possible consequence. Positive correlation between the presence of local TL1A and accumulation of inflammatory cells was also well in line with pervious studies showing

reduced number of inflammatory cells in diseased tissues when TL1A/DR3 signaling is disrupted (Fang et al., 2008; Meylan et al., 2008; Pappu et al., 2008). This phenotype of reduced immune cells in the inflammatory sites could be caused by two events: 1) compromised cell migration; and/or 2) poor on-site expansion. We and another group have tried to assess these two possibilities using TL1A deletion or supplying exogenous TL1A, but failed to provide evidence to support the first possibility (Meylan et al., 2008). Based on the known function of TL1A in costimulating T cell proliferation, we speculate that the reduced cell infiltration in CIA paws in the absence of TL1A is probably due to an attenuated expansion of cells after their migrating to the CIA paws in KO mice (Meylan et al., 2011b). Nevertheless, further experiments are needed to provide direct evidence to prove this possibility.

5.2.1.2 TL1A promotes the RA-related pro-inflammatory cytokines production

TL1A is actively involved in IBD by promoting the production of disease-specific pro-inflammatory cytokines (Fang et al., 2008; Pappu et al., 2008; Shih and Targan, 2009). For example, TL1A induces IFN-γ in Th1-mediated Crohn's disease (CD), but IL-4, -5, and -13 in Th2-mediated ulcerative colitis (UC) (Shih et al., 2011b). Our results from Chapter 2 indicate that TNF-α and IL-17, the two most notorious pathogenic cytokines in RA, could be induced by TL1A in T cells (Zhang et al., 2009a). TL1A-induced TNF-α production by T cells has been confirmed by a recent study(Jin et al., 2012). Notably, TNF-α could, in turn, promote the TL1A production by the joint SFs, thus forming a self-feeding vicious circle in RA joints locally. The role of TL1A in Th17 cells is more complicated. Data from *in vivo* and *ex vivo* studies suggest that the presence of either endogenous or exogenous TL1A promotes the expansion of Th17 cells under disease conditions (Kamada et al., 2010; Meylan et al., 2008; Pappu et al., 2008; Takedatsu et al., 2008). In line with these *in vivo* and *ex vivo* data our results in Chapter 2 showed that exogenous TL1A promotes the IL-17 production under *in vitro*, dose dependently. However, two previous studies reported that the exogenous TL1A could inhibit the Th17 generation *in vitro* (Jones et al., 2011; Pappu et al., 2008). Based on *in vivo* data by most of the studies, there is little doubt that TL1A promotes inflammation (Meylan et al., 2011b). Therefore, it is contradictory for TL1A to inhibit Th17 generation in vitro. The observed inhibition in some studies could be due to some artificial factors during

experimentation, such as feeder cells, the strength of TCR stimulation and/or kinetics of Th17 measurement. Furthermore, the opposing roles of exogenous TL1A played during the Th17 differentiation also implies the possibilities of having divergent net results (Jones et al., 2011; Pappu et al., 2008).

5.2.1.3 TL1A and bone erosion in RA

We have shown in Chapters 2 and 3 that TL1A aggravates joint inflammation and tissue destruction in CIA. Consistent with our findings, Bull et al. also showed reduced pathological changes in mice treated with anti-TL1A antagonist antibodies (Bull et al., 2008). In addition, they showed that DR3 KO mice are completely protected from bone destruction in the AIA model and suggested a specific role of TL1A in promoting the osteoclastogenesis (Bull et al., 2008). However, the TL1A KO mice in our study are still susceptible to bone destruction in CIA. Although the average pathological score in the TL1A KO mice is reduced, certain KO mice are still able to reach similar levels of disease severity as their WT counterpart. The reason for this discrepancy is most likely due to the different pathogenic mechanisms of these two animal models. However, different gene KO mice (i.e., DR3 KO versus TL1A KO) used in these two studies could also be a reason. Although DR3 is the known high affinity receptor for TL1A in mice, we cannot totally exclude the possibility that TL1A binds with some unidentified receptors, and vice versa. Therefore, it seems that DR3 KO does not equate to TL1A KO.

5.2.1.4 TL1A promotes the humoral immune responses in RA

Autoantibodies serve as important RA diagnosis factors in clinic for disease stages and severity (Conrad et al., 2010; Hirano, 2002; Stuart et al., 1984). As mentioned in Chapter 1, autoantibodies play essential pathogenic roles in several animal arthritis models. Our studies have discovered, for the first time, a novel function of TL1A in promoting humoral response in the murine CIA model. In accordance with our findings in mice, Bamias et al. showed that TL1A levels are augmented in sera of RA patients, particularly in those RF^+ RA patients (Bamias et al., 2008). Moreover, Sun et al. recently reported that serum levels of TL1A in RF^+ RA patients are positively correlated to those of RFs and ACPAs (Sun et al., 2013). This evidence consolidates the relevance of TL1A's role in pathogenic antibody production in

human RA. In addition, the positive effect of TL1A in humoral response was also demonstrated in an interesting study showing that TL1A, acting as a mucosal adjuvant, escalates the antibody productions in both serum and mucosal secretions (Kayamuro et al., 2009). Our studies indicate that TL1A affects the humoral responses in murine CIA by two different mechanisms.

Firstly, TL1A enhances the general immune responses, as well as the humoral response, at the acute inflammatory stage. At the initial phase of CIA, the components in the adjuvant pose danger signals to those innate immune cells such as DC and macrophages, which then trigger the adaptive immune responses to break self-tolerance against CII (Benson et al., 2010; Billiau and Matthys, 2011; Bouaziz et al., 2007). The interplays between T and B cell are essential for the latter event, since the disruption of such interaction delays or protects the rodents from developing arthritis (Yanaba et al., 2007; 2005). Exogenous human TL1A increases the germinal center reaction in mice (Zhang et al., 2009a). In contrast, endogenous TL1A exhibits a limited effect on CII-specific T cell response and GC formation, but simply amplifies the general immune response in the dLN during the acute inflammation stage. The effects of TL1A on the general immune response are most likely starting with its costimulatory effect on the T cells; the expanded T cells then provide more help for the activation, proliferation and recruitment of B cells, as well as the other immune cells (Bai et al., 2008; Cantor and Haskins, 2007; Martin-Fontecha et al., 2003; McHeyzer-Williams et al., 2011). Consequently, there are more anti-CII antibody-producing cells from the WT dLN after immunization than those from TL1A KO dLN, due to a significant increase of total dLN cells.

Secondly, TL1A promotes the survival of plasma cells (PC). Previous studies concerning the functions of TL1A mainly focused on its co-stimulating role in T cells (Meylan et al., 2011b). Recent studies have extended the TL1A's target cells to NKT cells, macrophages and tubular epithelial cells (TEC) (Al-Lamki et al., 2008; 2012; Fang et al., 2008; Kang et al., 2005; McLaren et al., 2010). Whether TL1A could affect plasma cells was never in the scope of previous studies, except one publication mentioning briefly that DR3 together with CD95 is expressed on the *in vitro*-generated human PC (Meylan et al., 2011b; Pelletier et al., 2006). We discovered that murine PCs express full-length DR3, and more importantly, the PCs

survive better in the presence of TL1A. Indeed, several other TNF family members such as BAFF (B cell-activation factor; TNFSF13B) and APRIL (a proliferation-induced ligand; TNFSF13) were reported to be involved in the survival of plasma cells (Cassese et al., 2003; O'Connor et al., 2004; Ou et al., 2012; Peperzak et al., 2013). BAFF binds to BAFF-R, and shares two other receptors, BCMA (B cell maturation Ag) and TACI (transmembrane activator and calcium modulator ligand interactor) with APRIL. BCMA is expressed not only on the plasma cells, but also on GC B and memory B cells. BAFF-R and TACI have even broader expression spectrums, which extend to all B cells (Darce et al., 2007). Therefore, in addition to helping PCs to survive better, BAFF and APRIL also affect the proliferation, differentiation, isotype-switching and survival of B cells (Batten et al., 2000; Moore et al., 1999; Schneider et al., 1999; Thompson et al., 2000; Tsuji et al., 2011; Yu et al., 2000). Our findings indicate that, at least in the murine B cell lineage, full-length DR3 is only expressed on the PC but not any other upstream B cells. Furthermore, it is known that secondary lymphoid organs such as the spleen and dLN can only support the survival of a finite number of plasma cells. The excessive plasma cells either undergo apoptosis or migrate to the bone marrow (BM). The resident cells there are a mixture of PCs derived from germinal centers and extra follicular reactions (Sze et al., 2000). PCs that successfully migrate to BM receive survival signals and become so-called long-lived PCs (LLPCs), while those stay in the secondary lymphoid organs become short-lived PCs (SLPCs), and will eventually die within a period from a few days to a couple weeks due to a lack of environmental survival signals (Oracki et al., 2010). We have assessed the DR3 expression on the PCs from the BM, LN and spleen, and found that only a subset of PCs express DR3, no matter from where these PCs are isolated. Therefore, the expression of DR3 on PCs seems not to depend on whether or not they are LLPCs. In supporting of this notion, we have noticed that the benefits of TL1A for the survival of PCs during CIA occur in both dLN and BM. More detailed studies are needed to determine the nature of this specific subset of PC that express DR3 and their potential roles compared to those DR3-negative PCs. It is worth mentioning that two murine hybridoma cells (OKT4 and 4610 used in our study) express DR3 according to flow cytometry, but DR3 expressed on these two cell lines is a short isoform of DR3 ($mDR3_{iIII}$) lacking the fourth CRD, according to PCR analysis. The functions of this truncated form of DR3 remain unclear. Collectively, this differential expression of DR3, either a full-length or truncated form, on the

B cell lineage implies a special regulatory role of different DR3 isoforms in the homeostasis of humoral responses during infection or autoimmune responses.

5.2.1.5 TL1A and Treg cells

Another interesting point is the role of TL1A in Treg development and function. In our TL1A KO and WT mice, no difference is found in constitutive or induced Treg populations. Not surprisingly, there is no aggravation but amelioration of CIA in the TL1A KO mice. Also, in mice with transgenic TL1A overexpression or mice administered with exogenous recombinant TL1A, the immune/inflammation responses are aggravated but not ameliorated (Barrett et al., 2012; Meylan et al., 2011a; Shih et al., 2011a; Zhang et al., 2009a). In all the studies using either TL1A or DR3 KO mice models, or using TL1A-neutralizing Abs, the immune responses are always abated. Although the Treg status of the above-mentioned studies is not always assessed, at least we could conclude that excessive TL1A does not lead to reduced immune responses, a possible functional consequence of Treg upregulation (Buchan et al., 2012; Bull et al., 2008; Fang et al., 2008; Meylan et al., 2008; Twohig et al., 2012). Conversely, TL1A or DR3 deletion does not lead to exuberant immune responses, which are a possible functional consequence of Treg downregulation. Schreiber and colleagues reported that an agonist mAb against DR3 specifically induces Treg population and is protective against allergic lung inflammation (Schreiber et al., 2010). To some extent, the work by other two groups also provided evidence in supporting such Treg upregulation effect of TL1A, showing that transgenic overexpression of TL1A expands the nTreg *in vivo*. However, they also showed, in the same study, that TL1A attenuates suppressive function of nTreg and inhibits the differentiation of iTreg *in vitro* (Meylan et al., 2011a; Taraban et al., 2011). More importantly, the excessive TL1A in these transgenic mice upregulates the number of T effector cells as well as Treg cells, and the overall phenotype of the Tg mice is small intestinal inflammation (Meylan et al., 2011a). How do we reconcile these findings? A previous study found that in addition to the full-length DR3, murine Treg cells also express a short-form of DR3 ($mDR3_{iIII}$) which lacks the forth CRD domain in its extracellular region (Pappu et al., 2008). Thus, one possible explanation of these discrepancies could be that the agonist mAb against DR3 by Schreiber et al. specifically binds to $mDR3_{iIII}$, but not full-length DR3, and

confers great proliferation ability only to those Treg cells. The same group later showed that a format of recombinant TL1A (aa68-252) with an Ig tag has similar effects with regard to Treg induction (Khan et al., 2013). The fact that they chose this special format of TL1A over the commercial one (aa76-252) implies that $TL1A_{68-252}$-Ig possibly has certain unique features comparing to the regular full-length TL1A, given that a short form of TL1A (20aa shorter than regular TL1A) displays total different biological activity (Zhai et al., 1999). It is likely that $TL1A_{68-252}$-Ig could bind specifically to $mDR3_{iIII}$ and selectively expand the Treg cells. Whatever the mechanisms could be, the Treg-enhancing and protective effect of this particular mAb clone and this particular format of $TL1A_{68-252}$-Ig produced by Schreiber et al. are of therapeutic interest. However from the scientific point of view, it will certainly be necessary to: 1) confirm the physical interaction between $TL1A_{68-252}$-Ig and $mDR3_{iIII}$; 2) confirm such Treg expansion effect using other clones of anti-DR3 Ab or other formats of recombinant TL1A, to rule out the possibility of the agonist mAb or TL1A-Ig used in the studies binding to other unrelated TNFR superfamily members; and 3) prove that such an effect applies to immune/inflammation models other than allergic lung inflammation.

5.2.2 Unidentified ligand(s) and receptor(s) of TL1A/DR3 pair

It is known that TL1A in human has a soluble receptor called DcR3, which also binds to FasL and Light (Shi et al., 2003). Mice do not have a human DcR3 orthologue. As many TNF family ligands share one or more receptors, it will not be surprising that TL1A has additional receptor(s) other than DR3 and DcR3, and vice versa (Aggarwal, 2003). In fact, there are many hints in studies conducted by us and other groups, suggesting the existences of additional binding partners of TL1A or DR3. We demonstrated in the supplementary data of Chapter 3, that TL1A KO mice had no abnormality in anti-viral immune responses against *Lymphocytic choriomenigitis* (LCMV). However, a previous study showed DR3-KO mice manifest compromised anti-MCMV immunity (Twohig et al., 2012). The observed difference between these two studies could have several explanations, and one of the possible scenarios could simply be that an unknown DR3 ligand (s) has compensated the missing TL1A. Similarly, both DR3 and TL1A KO mice were shown to develop EAE with reduced disease

severity comparing to the WT mice. However, deficiency in TL1A only reduces the disease clinical scores by 30%, while null-mutation of DR3 almost completely inhibits development of the disease (Meylan et al., 2008; Pappu et al., 2008). It seems that the missing of TL1A only partially disrupts the TL1A/DR3 pathway, and something else is compensating its function in its absence. Indeed, such functional compensation has been identified between several known ligands from TNF family members, such as LIGHT and LT, both of which could bind to herpesvirus entry mediator (HVEM) and trigger costimulating signals (Cai et al., 2008). On the other hand, Al-Lamki et al. reported that TL1A is able to upregulate TNFR2 in renal tubular endothelial cells (TEC) without the presence of DR3 and suggested the existence of an unidentified receptor of TL1A on TEC (Al-Lamki et al., 2008). According to the characteristics of other members of TNF and TNFR superfamilies, it is not unusual that several ligands/receptors share one or more receptors/ligands. Interactions of these alternative ligand/receptor pairs are likely to trigger signal events that might be similar, irrelevant or even opposite to those induced by the orthologue combinations. Therefore, it will be interesting to explore the additional ligand(s) for DR3 and additional receptor(s) for TL1A, and identify their respective functions.

5.2.3 Exogenous TL1A vs endogenous TL1A

The results from Chapter 2 and several recent studies suggest that excessive TL1A aggravates the autoimmune diseases, even under conditions without disease induction (Meylan et al., 2011a; Taraban et al., 2011; Zhang et al., 2009a). On the other hand, null-mutation of TL1A or DR3 has negligible effect on mice under normal circumstances. Furthermore, no anomaly is observed in the *in vitro* differentiation of TL1A or DR3 KO T cells (Meylan et al., 2008; Pappu et al., 2008). In addition to the possible reasons discussed in Chapter 3, another explanation would simply be that endogenous TL1A is barely expressed in cells or tissues of WT animal under a normal circumstance. As multiple studies have shown that although many types of cells are found to produce TL1A upon stimulation, very little TL1A is produced in the resting state by these cells (Cassatella et al., 2007; Meylan et al., 2008; Prehn et al., 2007; Zhang et al., 2009a). Therefore, those resting WT cells or unmanipulated WT mice without diseases might not express or express very low level of TL1A. Thus, no effect of “endogenous

TL1A" would be observed under such a condition. It is conceivable that the difference between WT and DR3/TL1A KO mice only appears in the disease models, in which the TL1A is upregulated in inflammatory tissues in WT mice but not in KO mice (Bamias et al., 2006; Kamada et al., 2010; Meylan et al., 2008; Pappu et al., 2008; Zhang et al., 2009a).

5.2.4 Implication of Pno1 in RA

Pno1 was brought to our attention because of its potential role in the assembly of proteasomes, which play an essential role in antigen presentation and humoral responses (Cenci et al., 2006; Lecker et al., 2006). Previous studies provided multiple evidence showing that inhibiting the proteasome activities decreases the number of plasma cells and antibody titers, and ameliorates the symptoms in mice with experimental autoimmune diseases (Gomez et al., 2011; Neubert et al., 2008; Perry et al., 2009). In Chapter 4, we sought to understand the function of Pno1 in the mammals by using mouse models with Pno1 gene manipulated,, and test whether Pno1 could affect humoral immune responses in mouse CIA. We have demonstrated that mammalian Pno1 has a similar distribution profile in terms of sedimentation rates as that of yeasts and the rates overlap with those of both 20S and 26S proteasome (Tone and Toh-E, 2002). However, Pno1 seems only to participate in the assembling process of these proteasomes. It leaves the proteasome once the assembling process is finished. Due to the embryonic lethality of Pno1 KO mice at a very early gestation stage, we are not able to explore the consequences of Pno1 deletion *in vivo* or in primary cell cultures. On the other hand, 50% reduction or overexpression of Pno1 in the heterozygouos KO mice or in Tg mice, respectively, does not compromise the amount and functions of proteasomes, nor the functions of T and B cell and humoral immune responses of these mice in CIA. According to the disastrous consequence of gene knockout of Pno1 in mice, and the minimal effect of Pno1 knockdown in heterozygous KO mice on the immune system and humoral responses, it seems that the therapeutic dose window of Pno1 inhibition is pretty narrow. Therefore, we suspect that Pno1 might not be a good target for treating RA. Collectively, although we have failed to provide evidence in Chapter 4 to support the idea of using Pno1 as a therapeutic target for RA, it will still be of great interests to explore the mechanisms by which Pno1 participates in proteasome neogenesis, using an inducible gene knockout approach.

5.3 Conclusions and Future Perspectives

TL1A is discovered as a T cell costimulator and later found to be involved in several autoimmune diseases. Our studies revealed that TL1A participates in the pathogenesis of RA, by aggravating the local inflammation in the synovium, and by promoting the systemic humoral immune responses. Our findings also suggest that TL1A is a good therapeutic target for RA

Consistent with findings in the yeast, Pno1 plays critical roles in maintaining certain basic cellular functions, most likely in proteasome or (and) ribosome neogenesis. However, Pno1 might not be a good therapeutic target for RA.

Following are some interesting questions to be explored in future studies:

1. To identify the putative additional receptors for TL1A and ligands for DR3.

2. To study the roles of DR3 in plasma cells, and find out survival signaling pathway triggered by TL1A.

3. To study the roles of the short isoforms of DR3.

4. Using conditional or inducible Pno1 gene KO mice to investigate the role of Pno1 in proteasome and ribosome neogenesis.

5. To investigate whether Pno1 mediates the destruction of dysfunctional ribosomes by proteasome.

REFERENCES

Aaltonen, K.J., Virkki, L.M., Malmivaara, A., Konttinen, Y.T., Nordström, D.C., and Blom, M. (2012). Systematic Review and Meta-Analysis of the Efficacy and Safety of Existing TNF Blocking Agents in Treatment of Rheumatoid Arthritis. PLoS ONE *7*, e30275.

Aggarwal, B.B. (2003). Signalling pathways of the TNF superfamily: a double-edged sword. Nat Rev Immunol *3*, 745–756.

Aggarwal, R., Liao, K., Nair, R., Ringold, S., and Costenbader, K.H. (2009). Anti-citrullinated peptide antibody assays and their role in the diagnosis of rheumatoid arthritis. Arthritis Rheum *61*, 1472–1483.

Ahn, J.K., Oh, J.-M., Lee, J., Bae, E.-K., Ahn, K.-S., Cha, H.-S., and Koh, E.-M. (2010). Increased extracellular survivin in the synovial fluid of rheumatoid arthritis patients: fibroblast-like synoviocytes as a potential source of extracellular survivin. Inflammation *33*, 381–388.

Al-Lamki, R.S., Lu, W., Finlay, S., Twohig, J.P., Wang, E.C.Y., Tolkovsky, A.M., and Bradley, J.R. (2012). DR3 signaling protects against cisplatin nephrotoxicity mediated by tumor necrosis factor. Am. J. Pathol. *180*, 1454–1464.

Al-Lamki, R.S., Wang, J., Thiru, S., Pritchard, N.R., Bradley, J.A., Pober, J.S., and Bradley, J.R. (2003). Expression of silencer of death domains and death-receptor-3 in normal human kidney and in rejecting renal transplants. Am. J. Pathol. *163*, 401–411.

Al-Lamki, R.S., Wang, J., Tolkovsky, A.M., Bradley, J.A., Griffin, J.L., Thiru, S., Wang, E.C.Y., Bolton, E., Min, W., Moore, P., et al. (2008). TL1A both promotes and protects from renal inflammation and injury. J. Am. Soc. Nephrol. *19*, 953–960.

Alamanos, Y., Voulgari, P.V., and Drosos, A.A. (2006). Incidence and Prevalence of Rheumatoid Arthritis, Based on the 1987 American College of Rheumatology Criteria: A Systematic Review. Seminars in Arthritis and Rheumatism *36*, 182–188.

Aletaha, D., Neogi, T., Silman, A.J., Funovits, J., Felson, D.T., Bingham, C.O., Birnbaum, N.S., Burmester, G.-R., Bykerk, V.P., Cohen, M.D., et al. (2010). 2010 Rheumatoid arthritis classification criteria: an American College of Rheumatology/European League Against Rheumatism collaborative initiative. Arthritis Rheum *62*, 2569–2581.

Allen, J.B., Bansal, G.P., Feldman, G.M., Hand, A.O., Wahl, L.M., and Wahl, S.M. (1991). Suppression of bacterial cell wall-induced polyarthritis by recombinant gamma interferon. Cytokine *3*, 98–106.

American College of Rheumatology Subcommittee on Rheumatoid Arthritis Guidelines (2002). Guidelines for the management of rheumatoid arthritis: 2002 Update. Arthritis Rheum *46*, 328–346.

Amirahmadi, S.F., Whittingham, S., Crombie, D.E., Nandakumar, K.S., Holmdahl, R., Mackay, I.R., van Damme, M.-P., and Rowley, M.J. (2005). Arthritogenic anti-type II collagen antibodies are pathogenic for cartilage-derived chondrocytes independent of inflammatory cells. Arthritis Rheum *52*, 1897–1906.

Andersson, A.K., Feldmann, M., and Brennan, F.M. (2008). Neutralizing IL-21 and IL-15 Inhibits Pro-inflammatory Cytokine Production in Rheumatoid Arthritis. Scand. J. Immunol. *68*, 103–111.

Angeli, V., Ginhoux, F., Llodrà, J., Quemeneur, L., Frenette, P.S., Skobe, M., Jessberger, R., Merad, M., and Randolph, G.J. (2006). B cell-driven lymphangiogenesis in inflamed lymph nodes enhances dendritic cell mobilization. Immunity *24*, 203–215.

Arnett, F.C., Edworthy, S.M., Bloch, D.A., Mcshane, D.J., Fries, J.F., Cooper, N.S., Healey, L.A., Kaplan, S.R., Liang, M.H., Luthra, H.S., et al. (1988). The american rheumatism association 1987 revised criteria for the classification of rheumatoid arthritis. Arthritis Rheum *31*, 315–324.

Ash, Z., and Emery, P. (2012). The role of tocilizumab in the management of rheumatoid arthritis. Expert Opin. Biol. Ther. *12*, 1277–1289.

Bacchetta, R., Passerini, L., Gambineri, E., Dai, M., Allan, S.E., Perroni, L., Dagna-Bricarelli, F., Sartirana, C., Matthes-Martin, S., Lawitschka, A., et al. (2006). Defective regulatory and effector T cell functions in patients with FOXP3 mutations. J Clin Invest *116*, 1713–1722.

Baeten, D., Peene, I., Union, A., Meheus, L., Sebbag, M., Serre, G., Veys, E.M., and De Keyser, F. (2001). Specific presence of intracellular citrullinated proteins in rheumatoid arthritis synovium: Relevance to antifilaggrin autoantibodies. Arthritis Rheum *44*, 2255–2262.

Bai, Y., Liu, R., Huang, D., La Cava, A., Tang, Y.-Y., Iwakura, Y., Campagnolo, D.I., Vollmer, T.L., Ransohoff, R.M., and Shi, F.-D. (2008). CCL2 recruitment of IL-6-producing CD11b+ monocytes to the draining lymph nodes during the initiation of Th17-dependent B cell-mediated autoimmunity. Eur. J. Immunol. *38*, 1877–1888.

Baker, S.J., and Reddy, E.P. (1998). Modulation of life and death by the TNF receptor superfamily. Oncogene *17*, 3261–3270.

Bamias, G., Kaltsa, G., Siakavellas, S.I., Papaxoinis, K., Zampeli, E., Michopoulos, S., Zouboulis-Vafiadis, I., and Ladas, S.D. (2010). High intestinal and systemic levels of decoy receptor 3 (DcR3) and its ligand TL1A in active ulcerative colitis. Clin Immunol *137*, 242–249.

Bamias, G., Martin, C., Marini, M., Hoang, S., Mishina, M., Ross, W.G., Sachedina, M.A., Friel, C.M., Mize, J., Bickston, S.J., et al. (2003). Expression, localization, and functional activity of TL1A, a novel Th1-polarizing cytokine in inflammatory bowel disease. J Immunol *171*, 4868–4874.

Bamias, G., Mishina, M., Nyce, M., Ross, W.G., Kollias, G., Rivera-Nieves, J., Pizarro, T.T., and Cominelli, F. (2006). Role of TL1A and its receptor DR3 in two models of chronic murine ileitis. Proc Natl Acad Sci USA *103*, 8441–8446.

Bamias, G., Siakavellas, S.I., Stamatelopoulos, K.S., Chryssochoou, E., Papamichael, C., and Sfikakis, P.P. (2008). Circulating levels of TNF-like cytokine 1A (TL1A) and its decoy receptor 3 (DcR3) in rheumatoid arthritis. Clin Immunol *129*, 249–255.

Bang, H., Mollenhauer, J., Schulmeister, A., Nager, C., van Eden, W., Wand-Württenberger, A., Kaufmann, S.H., and Brune, K. (1994). Isolation and characterization of a cartilage-specific membrane antigen (CH65): comparison with cytokeratins and heat-shock proteins. Immunology *81*, 322–329.

Barrett, R., Zhang, X., Koon, H.W., Vu, M., Chang, J.-Y., Yeager, N., Nguyen, M.A., Michelsen, K.S., Berel, D., Pothoulakis, C., et al. (2012). Constitutive TL1A expression under colitogenic conditions modulates the severity and location of gut mucosal inflammation and induces fibrostenosis. Am. J. Pathol. *180*, 636–649.

Barton, A., Jury, F., Eyre, S., Bowes, J., Hinks, A., Ward, D., and Worthington, J. (2004). Haplotype analysis in simplex families and novel analytic approaches in a case-control cohort reveal no evidence of association of the CTLA-4 gene with rheumatoid arthritis. Arthritis Rheum *50*, 748–752.

Batten, M., Groom, J., Cachero, T.G., Qian, F., Schneider, P., Tschopp, J., Browning, J.L., and MacKay, F. (2000). BAFF mediates survival of peripheral immature B lymphocytes. J. Exp. Med. *192*, 1453–1466.

Beard, H.K., Ryvar, R., Skingle, J., and Greenbury, C.L. (1980). Anti-collagen antibodies in sera from rheumatoid arthritis patients. Journal of Clinical Pathology *33*, 1077–1081.

Begovich, A.B., Carlton, V.E.H., Honigberg, L.A., Schrodi, S.J., Chokkalingam, A.P., Alexander, H.C., Ardlie, K.G., Huang, Q., Smith, A.M., Spoerke, J.M., et al. (2004). A missense single-nucleotide polymorphism in a gene encoding a protein tyrosine phosphatase (PTPN22) is associated with rheumatoid arthritis. Am. J. Hum. Genet. *75*, 330–337.

Benoist, C., and Mathis, D. (2000). A revival of the B cell paradigm for rheumatoid arthritis pathogenesis? Arthritis Res. *2*, 90–94.

Benson, R.A., Patakas, A., Conigliaro, P., Rush, C.M., Garside, P., McInnes, I.B., and Brewer, J.M. (2010). Identifying the cells breaching self-tolerance in autoimmunity. The Journal of Immunology *184*, 6378–6385.

Berner, B., Akça, D., Jung, T., Muller, G.A., and Reuss-Borst, M.A. (2000). Analysis of Th1 and Th2 cytokines expressing CD4+ and CD8+ T cells in rheumatoid arthritis by flow cytometry. The Journal of Rheumatology *27*, 1128–1135.

Bettelli, E., Korn, T., Oukka, M., and Kuchroo, V.K. (2008). Induction and effector functions

of T(H)17 cells. Nature *453*, 1051–1057.

Biener-Ramanujan, E., Gonsky, R., Ko, B., and Targan, S.R. (2010). Functional signaling of membrane-bound TL1A induces IFN-gamma expression. FEBS Letters *584*, 2376–2380.

Billiau, A., and Matthys, P. (2011). Collagen-induced arthritis and related animal models: how much of their pathogenesis is auto-immune, how much is auto-inflammatory? Cytokine Growth Factor Rev. *22*, 339–344.

Bläss, S., Engel, J.M., and Burmester, G.R. (1999). The immunologic homunculus in rheumatoid arthritis. Arthritis Rheum *42*, 2499–2506.

Bläss, S., Specker, C., Lakomek, H.J., Schneider, E.M., and Schwochau, M. (1995). Novel 68 kDa autoantigen detected by rheumatoid arthritis specific antibodies. Ann. Rheum. Dis. *54*, 355–360.

Bläss, S., Union, A., and Raymackers, J. (2001). The stress protein BiP is overexpressed and is a major B and T cell target in rheumatoid arthritis - Bläß - 2001 - Arthritis & Rheumatism - Wiley Online Library. Arthritis & ….

Bodman-Smith, M.D., Corrigall, V.M., Kemeny, D.M., and Panayi, G.S. (2003). BiP, a putative autoantigen in rheumatoid arthritis, stimulates IL-10-producing CD8-positive T cells from normal individuals. Rheumatology (Oxford) *42*, 637–644.

Bodmer, J.L., Burns, K., Schneider, P., Hofmann, K., Steiner, V., Thome, M., Bornand, T., Hahne, M., Schröter, M., Becker, K., et al. (1997). TRAMP, a novel apoptosis-mediating receptor with sequence homology to tumor necrosis factor receptor 1 and Fas(Apo-1/CD95). Immunity *6*, 79–88.

Bodmer, J.-L., Schneider, P., and Tschopp, J. (2002). The molecular architecture of the TNF superfamily. Trends Biochem. Sci. *27*, 19–26.

Borsellino, G., Kleinewietfeld, M., Di Mitri, D., Sternjak, A., Diamantini, A., Giometto, R., Höpner, S., Centonze, D., Bernardi, G., Dell'Acqua, M.L., et al. (2007). Expression of ectonucleotidase CD39 by Foxp3+ Treg cells: hydrolysis of extracellular ATP and immune suppression. Blood *110*, 1225–1232.

Bortnick, A., Chernova, I., Quinn, W.J., Mugnier, M., Cancro, M.P., and Allman, D. (2012). Long-lived bone marrow plasma cells are induced early in response to T cell-independent or T cell-dependent antigens. The Journal of Immunology *188*, 5389–5396.

Borysenko, C.W., Furey, W.F., and Blair, H.C. (2005). Comparative modeling of TNFRSF25 (DR3) predicts receptor destabilization by a mutation linked to rheumatoid arthritis. Ageing Research Reviews *328*, 794–799.

Bouaziz, J.-D., Yanaba, K., Venturi, G.M., Wang, Y., Tisch, R.M., Poe, J.C., and Tedder, T.F. (2007). Therapeutic B cell depletion impairs adaptive and autoreactive CD4+ T cell activation

in mice. Proc Natl Acad Sci USA *104*, 20878–20883.

Brahn, E., Peacock, D.J., Banquerigo, M.L., and Liu, D.Y. (1992). Effects of tumor necrosis factor alpha (TNF-alpha) on collagen arthritis. Lymphokine Cytokine Res. *11*, 253–256.

Brand, D.D., Kang, A.H., and Rosloniec, E.F. (2003). Immunopathogenesis of Collagen Arthritis. Springer Seminars in Immunopathology *25*, 3–18.

Brand, D.D., Latham, K.A., and Rosloniec, E.F. (2007). Collagen-induced arthritis. Nat Protoc *2*, 1269–1275.

Breedveld, F.C., Weisman, M.H., Kavanaugh, A.F., Cohen, S.B., Pavelka, K., Vollenhoven, R.V., Sharp, J., Perez, J.L., Spencer-Green, G.T., PREMIER Investigators (2005). The PREMIER study: A multicenter, randomized, double-blind clinical trial of combination therapy with adalimumab plus methotrexate versus methotrexate alone or adalimumab alone in patients with early, aggressive rheumatoid arthritis who had not had previous methotrexate treatment. Arthritis Rheum *54*, 26–37.

Breitfeld, D., Ohl, L., Kremmer, E., Ellwart, J., Sallusto, F., Lipp, M., and Förster, R. (2000). Follicular B helper T cells express CXC chemokine receptor 5, localize to B cell follicles, and support immunoglobulin production. J. Exp. Med. *192*, 1545–1552.

Brentano, F., Kyburz, D., and Gay, S. (2009). Toll-Like Receptors and Rheumatoid Arthritis. In Toll-Like Receptors, (Totowa, NJ: Humana Press), pp. 329–343.

Britsemmer, K., Ursum, J., Gerritsen, M., van Tuyl, L.H., van Tuyl, L., and van Schaardenburg, D. (2011). Validation of the 2010 ACR/EULAR classification criteria for rheumatoid arthritis: slight improvement over the 1987 ACR criteria. Ann. Rheum. Dis. *70*, 1468–1470.

Brühl, H., Cihak, J., Plachý, J., Kunz-Schughart, L., Niedermeier, M., Denzel, A., Rodriguez Gomez, M., Talke, Y., Luckow, B., Stangassinger, M., et al. (2007). Targeting of Gr-1+,CCR2+ monocytes in collagen-induced arthritis. Arthritis Rheum *56*, 2975–2985.

Buchan, S.L., Taraban, V.Y., Slebioda, T.J., James, S., Cunningham, A.F., and Al-Shamkhani, A. (2012). Death receptor 3 is essential for generating optimal protective CD4(+) T-cell immunity against Salmonella. Eur. J. Immunol. *42*, 580–588.

Bucht, A., LARSSON, P., WEISBROT, L., THORNE, C., PISA, P., SMEDEGÅRD, G., KEYSTONE, E.C., and GRÖNBERG, A. (1996). Expression of interferon-gamma (IFN-gamma), IL-10, IL-12 and transforming growth factor-beta (TGF-beta) mRNA in synovial fluid cells from patients in the early and late phases of rheumatoid arthritis (RA). Clinical and Experimental Immunology *103*, 357–367.

Bull, M.J., Williams, A.S., Mecklenburgh, Z., Calder, C.J., Twohig, J.P., Elford, C., Evans, B.A.J., Rowley, T.F., Slebioda, T.J., Taraban, V.Y., et al. (2008). The Death Receptor 3-TNF-like protein 1A pathway drives adverse bone pathology in inflammatory arthritis. J. Exp. Med.

205, 2457–2464.

Burbelo, P.D., Browne, S.K., Sampaio, E.P., Giaccone, G., Zaman, R., Kristosturyan, E., Rajan, A., Ding, L., Ching, K.H., Berman, A., et al. Anti-cytokine autoantibodies are associated with opportunistic infection in patients with thymic neoplasia.

Bush, K.A., Farmer, K.M., Walker, J.S., and Kirkham, B.W. (2002). Reduction of joint inflammation and bone erosion in rat adjuvant arthritis by treatment with interleukin-17 receptor IgG1 Fc fusion protein. Arthritis Rheum *46*, 802–805.

Cai, G., Anumanthan, A., Brown, J.A., Greenfield, E.A., Zhu, B., and Freeman, G.J. (2008). CD160 inhibits activation of human CD4+ T cells through interaction with herpesvirus entry mediator. Nat Immunol *9*, 176–185.

Campbell, M.G., and Karbstein, K. (2011). Protein-protein interactions within late pre-40S ribosomes. PLoS ONE *6*, e16194.

Cantagrel, A., Navaux, F.D.R., Loubet-Lescouli, P., Nourhashemi, F., Enault, G.V., Abbal, M., Constantin, A., Laroche, M., and Bernard Mazi res (1999). Interleukin-1?, interleukin-1 receptor antagonist, interleukin-4, and interleukin-10 gene polymorphisms: Relationship to occurrence and severity of rheumatoid arthritis. Arthritis Rheum *42*, 1093–1100.

Cantor, J., and Haskins, K. (2007). Recruitment and activation of macrophages by pathogenic CD4 T cells in type 1 diabetes: evidence for involvement of CCR8 and CCL1. J Immunol *179*, 5760–5767.

Cao, D., Malmström, V., Baecher-Allan, C., Hafler, D., Klareskog, L., and Trollmo, C. (2003). Isolation and functional characterization of regulatory CD25brightCD4+ T cells from the target organ of patients with rheumatoid arthritis. Eur. J. Immunol. *33*, 215–223.

Carson, D.A., Chen, P.P., Fox, R.I., Kipps, T.J., Jirik, F., Goldfien, R.D., Silverman, G., Radoux, V., and Fong, S. (1987). Rheumatoid factor and immune networks. Annu. Rev. Immunol. *5*, 109–126.

Cassatella, M.A., Pereira-da-Silva, G., da Silva, G.P., Tinazzi, I., Facchetti, F., Scapini, P., Calzetti, F., Tamassia, N., Wei, P., Nardelli, B., et al. (2007). Soluble TNF-like cytokine (TL1A) production by immune complexes stimulated monocytes in rheumatoid arthritis. J Immunol *178*, 7325–7333.

Cassese, G., Arce, S., Hauser, A.E., Lehnert, K., Moewes, B., Mostarac, M., Muehlinghaus, G., Szyska, M., Radbruch, A., and Manz, R.A. (2003). Plasma cell survival is mediated by synergistic effects of cytokines and adhesion-dependent signals. J Immunol *171*, 1684–1690.

Catrina, A.I., Trollmo, C., af Klint, E., Engstrom, M., Lampa, J., Hermansson, Y., Klareskog, L., and Ulfgren, A.K. (2005). Evidence that anti-tumor necrosis factor therapy with both etanercept and infliximab induces apoptosis in macrophages, but not lymphocytes, in rheumatoid arthritis joints: extended report. Arthritis Rheum *52*, 61–72.

Caulfield, J.P., Hein, A., Dynesius-Trentham, R., and Trentham, D.E. (1982). Morphologic demonstration of two stages in the development of type II collagen-induced arthritis. Lab. Invest. *46*, 321–343.

Cenci, S., Mezghrani, A., Cascio, P., Bianchi, G., Cerruti, F., Fra, A., Lelouard, H., Masciarelli, S., Mattioli, L., Oliva, L., et al. (2006). Progressively impaired proteasomal capacity during terminal plasma cell differentiation. Embo J *25*, 1104–1113.

Ceponis, A., Konttinen, Y.T., Imai, S., Tamulaitiene, M., Li, T.F., Xu, J.W., Hietanen, J., Santavirta, S., and Fassbender, H.G. (1998). Synovial lining, endothelial and inflammatory mononuclear cell proliferation in synovial membranes in psoriatic and reactive arthritis: a comparative quantitative morphometric study. Br. J. Rheumatol. *37*, 170–178.

Chabaud, M., Fossiez, F., Taupin, J.L., and Miossec, P. (1998). Enhancing effect of IL-17 on IL-1-induced IL-6 and leukemia inhibitory factor production by rheumatoid arthritis synoviocytes and its regulation by Th2 cytokines. J Immunol *161*, 409–414.

Chabaud, M., Lubberts, E., Joosten, L., van den Berg, W., and Miossec, P. (2001). IL-17 derived from juxta-articular bone and synovium contributes to joint degradation in rheumatoid arthritis. Arthritis Res. *3*, 168–177.

Chaudhry, A., Samstein, R.M., Treuting, P., Liang, Y., Pils, M.C., Heinrich, J.-M., Jack, R.S., Wunderlich, F.T., Brüning, J.C., Müller, W., et al. (2011). Interleukin-10 signaling in regulatory T cells is required for suppression of Th17 cell-mediated inflammation. Immunity *34*, 566–578.

Chavele, K.-M., and Ehrenstein, M.R. (2011). Regulatory T-cells in systemic lupus erythematosus and rheumatoid arthritis. FEBS Letters *585*, 3603–3610.

Chen, Y.-F., Jobanputra, P., Barton, P., Jowett, S., Bryan, S., Clark, W., Fry-Smith, A., and Burls, A. (2006). A systematic review of the effectiveness of adalimumab, etanercept and infliximab for the treatment of rheumatoid arthritis in adults and an economic evaluation of their cost-effectiveness. Health Technol Assess *10*, iii–iv–xi–xiii–1–229.

Chew, L.-J., Pan, H., Yu, J., Tian, S., Huang, W.-Q., Zhang, J.Y., Pang, S., and Li, L.-Y. (2002). A novel secreted splice variant of vascular endothelial cell growth inhibitor. Faseb J *16*, 742–744.

Chinnaiyan, A.M., O'Rourke, K., Yu, G.L., Lyons, R.H., Garg, M., Duan, D.R., Xing, L., Gentz, R., Ni, J., and Dixit, V.M. (1996). Signal transduction by DR3, a death domain-containing receptor related to TNFR-1 and CD95. Science *274*, 990–992.

Clavel, C., Nogueira, L., Laurent, L., Iobagiu, C., Vincent, C., Sebbag, M., and Serre, G. (2008). Induction of macrophage secretion of tumor necrosis factor α through Fcγ receptor IIa engagement by rheumatoid arthritis–specific autoantibodies to citrullinated proteins complexed with fibrinogen. Arthritis Rheum *58*, 678–688.

Cohavy, O., Shih, D.Q., Doherty, T.M., Ware, C.F., and Targan, S.R. (2011). CD161 DEFINES EFFECTOR T CELLS THAT EXPRESS LIGHT AND RESPOND TO TL1A-DR3 SIGNALING. Eur J Microbiol Immunol (Bp) *1*, 70–79.

Committee of the American Rheumatism Association (2008). 1958 revision of diagnostic criteria for rheumatoid arthritis. Arthritis Rheum *58*, S15–S19.

Conrad, K., Roggenbuck, D., Reinhold, D., and Dörner, T. (2010). Profiling of rheumatoid arthritis associated autoantibodies. Autoimmun Rev *9*, 431–435.

Constantinescu, C.S., Farooqi, N., O'Brien, K., and Gran, B. (2011). Experimental autoimmune encephalomyelitis (EAE) as a model for multiple sclerosis (MS). Br. J. Pharmacol. *164*, 1079–1106.

Cook, A.D., Rowley, M.J., Mackay, I.R., Gough, A., and Emery, P. (1996). Antibodies to type II collagen in early rheumatoid arthritis. Correlation with disease progression. Arthritis Rheum *39*, 1720–1727.

Cornélis, F., Fauré, S., Martinez, M., Prud'homme, J.-F., Fritz, P., Dib, C., Alves, H., Barrera, P., de Vries, N., Balsa, A., et al. (1998). New susceptibility locus for rheumatoid arthritis suggested by a genome-wide linkage study. Proc Natl Acad Sci USA *95*, 10746–10750.

Costenbader, K.H., Chang, S.-C., Vivo, I.D., Plenge, R., and Karlson, E.W. (2008). Genetic polymorphisms in PTPN22, PADI-4, and CTLA-4 and risk for rheumatoid arthritis in two longitudinal cohort studies: evidence of gene-environment interactions with heavy cigarette smoking. Arthritis Res. Ther. *10*, R52.

Coulie, P., and Van Snick, J. (1983). Rheumatoid factors and secondary immune responses in the mouse II. Incidence, kinetics and induction mechanisms. Eur. J. Immunol. *13*, 895–899.

Courtenay, J.S., Dallman, M.J., Dayan, A.D., Martin, A., and Mosedale, B. (1980). Immunisation against heterologous type II collagen induces arthritis in mice. Nature *283*, 666–668.

Criswell, L.A., Mu, H., Such, C.L., and King, M.-C. (1998). Inheritance of the shared epitope and long-term outcomes of rheumatoid arthritis among community-based Caucasian females. Genet. Epidemiol. *15*, 61–72.

Crotty, S. (2011). Follicular helper CD4 T cells (TFH). Annu. Rev. Immunol. *29*, 621–663.

Cutolo, M., Capellino, S., Montagna, P., Villaggio, B., Sulli, A., Seriolo, B., and Straub, R.H. (2003). New roles for estrogens in rheumatoid arthritis. Clin Exp Rheumatol *21*, 687–690.

Cutolo, M., and Straub, R.H. (2006). Stress as a Risk Factor in the Pathogenesis of Rheumatoid Arthritis. Neuroimmunomodulation *13*, 277–282.

Daha, N.A., Kurreeman, F.A.S., Marques, R.B., Stoeken-Rijsbergen, G., Verduijn, W.,

Huizinga, T.W.J., and Toes, R.E.M. (2009). Confirmation of STAT4, IL2/IL21, and CTLA4polymorphisms in rheumatoid arthritis. Arthritis Rheum *60*, 1255–1260.

Darce, J.R., Arendt, B.K., Wu, X., and Jelinek, D.F. (2007). Regulated expression of BAFF-binding receptors during human B cell differentiation. J Immunol *179*, 7276–7286.

Dong, H., Strome, S.E., Matteson, E.L., Moder, K.G., Flies, D.B., Zhu, G., Tamura, H., Driscoll, C.L.W., and Chen, L. (2003). Costimulating aberrant T cell responses by B7-H1 autoantibodies in rheumatoid arthritis. J Clin Invest *111*, 363–370.

Doodes, P.D., Cao, Y., Hamel, K.M., Wang, Y., Rodeghero, R.L., Mikecz, K., Glant, T.T., Iwakura, Y., and Finnegan, A. (2010). IFN-γ Regulates the Requirement for Il-17 in Proteoglycan-Induced Arthritis. The Journal of Immunology *184*, 1552–1559.

Doran, M.F., Crowson, C.S., O'Fallon, W.M., and Gabriel, S.E. (2004). The effect of oral contraceptives and estrogen replacement therapy on the risk of rheumatoid arthritis: a population based study. The Journal of Rheumatology *31*, 207–213.

Doran, M.F., Pond, G.R., Crowson, C.S., O'Fallon, W.M., and Gabriel, S.E. (2002). Trends in incidence and mortality in rheumatoid arthritis in Rochester, Minnesota, over a forty-year period. Arthritis Rheum *46*, 625–631.

Egan, P.J., van Nieuwenhuijze, A., Campbell, I.K., and Wicks, I.P. (2008). Promotion of the local differentiation of murine Th17 cells by synovial macrophages during acute inflammatory arthritis. Arthritis Rheum *58*, 3720–3729.

Ehinger, M., Vestberg, M., and Johansson, Å. (2001). Influence of CD4 or CD8 deficiency on collagen-induced arthritis - Ehinger - 2001 - Immunology - Wiley Online Library. ….

Ehrenstein, M.R., Evans, J.G., Singh, A., Moore, S., Warnes, G., Isenberg, D.A., and Mauri, C. (2004). Compromised function of regulatory T cells in rheumatoid arthritis and reversal by anti-TNFalpha therapy. J. Exp. Med. *200*, 277–285.

Endo, K., Kinouchi, Y., Kakuta, Y., Ueki, N., Takahashi, S., and Shimosegawa, T. (2010). Involvement of NF-kappa B pathway in TL1A gene expression induced by lipopolysaccharide. Cytokine *49*, 215–220.

Eskdale, J., McNicholl, J., Wordsworth, P., Jonas, B., Huizinga, T., Field, M., and Gallagher, G. (1998). Interleukin-10 microsatellite polymorphisms and IL-10 locus alleles in rheumatoid arthritis susceptibility. Lancet *352*, 1282–1283.

Evans, J.G., Chavez-Rueda, K.A., Eddaoudi, A., Meyer-Bahlburg, A., Rawlings, D.J., Ehrenstein, M.R., and Mauri, C. (2007). Novel suppressive function of transitional 2 B cells in experimental arthritis. J Immunol *178*, 7868–7878.

Fang, L., Adkins, B., Deyev, V., and Podack, E.R. (2008). Essential role of TNF receptor superfamily 25 (TNFRSF25) in the development of allergic lung inflammation. J. Exp. Med.

205, 1037–1048.

Fatica, A., Oeffinger, M., Dlakić, M., and Tollervey, D. (2003). Nob1p is required for cleavage of the 3' end of 18S rRNA. Mol Cell Biol *23*, 1798–1807.

Finckh, A., Liang, M.H., van Herckenrode, C.M., and de Pablo, P. (2006). Long-term impact of early treatment on radiographic progression in rheumatoid arthritis: A meta-analysis. Arthritis Rheum *55*, 864–872.

Finnegan, A., Grusby, M.J., Kaplan, C.D., O'Neill, S.K., Eibel, H., Koreny, T., Czipri, M., Mikecz, K., and Zhang, J. (2002). IL-4 and IL-12 regulate proteoglycan-induced arthritis through Stat-dependent mechanisms. J Immunol *169*, 3345–3352.

Finnegan, A., Kaplan, C.D., Cao, Y., Eibel, H., Glant, T.T., and Zhang, J. (2003). Collagen-induced arthritis is exacerbated in IL-10-deficient mice. *5*, R18–R24.

Firestein, G.S. (2003). Evolving concepts of rheumatoid arthritis. Nature *423*, 356–361.

Firestein, G.S., Budd, R., Gabriel, S.E., O'Dell, J.R., and McInnes, I.B. (2012). Kelley's Textbook of Rheumatology (Elsevier Health Sciences).

Flores-Borja, F., Jury, E.C., Mauri, C., and Ehrenstein, M.R. (2008). Defects in CTLA-4 are associated with abnormal regulatory T cell function in rheumatoid arthritis. Proceedings of the National Academy of Sciences *105*, 19396–19401.

Fossiez, F., Djossou, O., Chomarat, P., Flores-Romo, L., Ait-Yahia, S., Maat, C., Pin, J.J., Garrone, P., Garcia, E., Saeland, S., et al. (1996). T cell interleukin-17 induces stromal cells to produce proinflammatory and hematopoietic cytokines. J. Exp. Med. *183*, 2593–2603.

FRANKLIN, E.C., HOLMAN, H.R., MULLER-EBERHARD, H.J., and KUNKEL, H.G. (1957). An unusual protein component of high molecular weight in the serum of certain patients with rheumatoid arthritis. J. Exp. Med. *105*, 425–438.

Franz, J.K., Pap, T., Hummel, K.M., Nawrath, M., Aicher, W.K., Shigeyama, Y., Müller-Ladner, U., Gay, R.E., and Gay, S. (2000). Expression of sentrin, a novel antiapoptotic molecule, at sites of synovial invasion in rheumatoid arthritis. Arthritis Rheum *43*, 599–607.

Frey, O., Mitera, T., Kelchtermans, H., Schurgers, E., Kamradt, T., and Matthys, P. (2011). Ameliorated course of glucose-6-phosphate isomerase (G6PI)-induced arthritis in IFN-γ receptor knockout mice exposes an arthritis-promoting role of IFN-γ. J. Autoimmun. *36*, 161–169.

Frey, O., Petrow, P.K., Gajda, M., Siegmund, K., Huehn, J., Scheffold, A., Hamann, A., Radbruch, A., and Bräuer, R. (2005). The role of regulatory T cells in antigen-induced arthritis: aggravation of arthritis after depletion and amelioration after transfer of CD4+CD25+ T cells. Arthritis Res. Ther. *7*, R291–R301.

Fujii, K., Tsuji, M., Kitamura, A., and Murota, K. (1992). The diagnostic significance of anti-Type II collagen antibody assay in rheumatoid arthritis. International Orthopaedics *16*.

Fujikawa, Y., Sabokbar, A., Neale, S., and Athanasou, N.A. (1996). Human osteoclast formation and bone resorption by monocytes and synovial macrophages in rheumatoid arthritis. Ann. Rheum. Dis. *55*, 816–822.

Gabriel, S.E., Crowson, C.S., and O'Fallon, M. (1999). The epidemiology of rheumatoid arthritis in Rochester, Minnesota, 1955-1985. Arthritis Rheum *42*, 415–420.

Gaffen, S.L. (2008). An overview of IL-17 function and signaling. Cytokine *43*, 402–407.

Gallastegui, N., and Groll, M. (2010). The 26S proteasome: assembly and function of a destructive machine. Trends Biochem. Sci. *35*, 634–642.

Gass, J.N., Gifford, N.M., and Brewer, J.W. (2002). Activation of an unfolded protein response during differentiation of antibody-secreting B cells. The Journal of Biological Chemistry *277*, 49047–49054.

Gass, J.N., Gunn, K.E., Sriburi, R., and Brewer, J.W. (2004). Stressed-out B cells? Plasma-cell differentiation and the unfolded protein response. Trends in Immunology *25*, 17–24.

Geboes, L., Dumoutier, L., Kelchtermans, H., Schurgers, E., Mitera, T., Renauld, J.-C., and Matthys, P. (2009). Proinflammatory role of the Th17 cytokine interleukin-22 in collagen-induced arthritis in C57BL/6 mice. Arthritis Rheum *60*, 390–395.

Gibbons, L.J., and Hyrich, K.L. (2009). Biologic therapy for rheumatoid arthritis: clinical efficacy and predictors of response. BioDrugs *23*, 111–124.

Gibson, T.J., Thompson, J.D., and Heringa, J. (1993). The KH domain occurs in a diverse set of RNA-binding proteins that include the antiterminator NusA and is probably involved in binding to nucleic acid. FEBS Letters *324*, 361–366.

Gomez, A.M., Vrolix, K., Martínez-Martínez, P., Molenaar, P.C., Phernambucq, M., van der Esch, E., Duimel, H., Verheyen, F., Voll, R.E., Manz, R.A., et al. (2011). Proteasome inhibition with bortezomib depletes plasma cells and autoantibodies in experimental autoimmune myasthenia gravis. The Journal of Immunology *186*, 2503–2513.

Gondek, D.C., Lu, L.-F., Quezada, S.A., Sakaguchi, S., and Noelle, R.J. (2005). Cutting edge: contact-mediated suppression by CD4+CD25+ regulatory cells involves a granzyme B-dependent, perforin-independent mechanism. J Immunol *174*, 1783–1786.

Gowen, M., Wood, D.D., Ihrie, E.J., McGuire, M.K.B., and Russell, R.G.G. (1983). An interleukin 1 like factor stimulates bone resorption in vitro. Nature *306*, 378–380.

Gravallese, E.M., Manning, C., Tsay, A., Naito, A., Pan, C., Amento, E., and Goldring, S.R. (2000). Synovial tissue in rheumatoid arthritis is a source of osteoclast differentiation factor.

Arthritis Rheum *43*, 250–258.

Gravallese, E.M., Pettit, A.R., Lee, R., Madore, R., Manning, C., Tsay, A., Gaspar, J., Goldring, M.B., Goldring, S.R., and Oettgen, P. (2003). Angiopoietin-1 is expressed in the synovium of patients with rheumatoid arthritis and is induced by tumour necrosis factor alpha. Ann. Rheum. Dis. *62*, 100–107.

Gregersen, P.K., Silver, J., and Winchester, R.J. (1987). The shared epitope hypothesis. an approach to understanding the molecular genetics of susceptibility to rheumatoid arthritis. Arthritis Rheum *30*, 1205–1213.

Groll, M., Ditzel, L., Löwe, J., Stock, D., Bochtler, M., Bartunik, H.D., and Huber, R. (1997). Structure of 20S proteasome from yeast at 2.4 A resolution. Nature *386*, 463–471.

Groll, M., Bochtler, M., Brandstetter, H., Clausen, T., and Huber, R. (2005). Molecular machines for protein degradation. Chembiochem *6*, 222–256.

Hakala, B.E., White, C., and Recklies, A.D. (1993). Human cartilage gp-39, a major secretory product of articular chondrocytes and synovial cells, is a mammalian member of a chitinase protein family. The Journal of Biological Chemistry *268*, 25803–25810.

Hammoudeh, M., Alarfaj, A., Chen, D.-Y., Djoudi, H., Youseif, E., and Zhu, J. (2013). Safety of tumor necrosis factor inhibitors use for rheumatoid arthritis and ankylosing spondylitis in Africa, the Middle East, and Asia: focus on severe infections and tuberculosis. Clin Rheumatol *32*, 293–300.

Hansen, M.B., Svenson, M., and Abell, K. (1994). Sex- and age-dependency of IgG auto-antibodies against IL-1α in healthy humans - HANSEN - 2008 - European Journal of Clinical Investigation - Wiley Online Library. European Journal of ….

Harding, H.P., Novoa, I., Zhang, Y., Zeng, H., Wek, R., Schapira, M., and Ron, D. (2000). Regulated translation initiation controls stress-induced gene expression in mammalian cells. Mol. Cell *6*, 1099–1108.

Harding, H.P., Zhang, Y., and Ron, D. (1999). Protein translation and folding are coupled by an endoplasmic-reticulum-resident kinase. Nature *397*, 271–274.

Harre, U., Georgess, D., Bang, H., Bozec, A., Axmann, R., Ossipova, E., Jakobsson, P.-J., Baum, W., Nimmerjahn, F., Szarka, E., et al. (2012). Induction of osteoclastogenesis and bone loss by human autoantibodies against citrullinated vimentin. J Clin Invest *122*, 1791–1802.

Hart, J.E., Laden, F., Puett, R.C., Costenbader, K.H., and Karlson, E.W. (2009). Exposure to traffic pollution and increased risk of rheumatoid arthritis. Environ. Health Perspect. *117*, 1065–1069.

Hartung, E.F. (1943). The Treatment of Rheumatoid Arthritis Including Gold Salts Therapy. Bull N Y Acad Med *19*, 693–703.

Hassfeld, W., Steiner, G., Hartmuth, K., Kolarz, G., Scherak, O., Graninger, W., Thumb, N., and Smolen, J.S. (1989). Demonstration of a new antinuclear antibody (anti-RA33) that is highly specific for rheumatoid arthritis. Arthritis Rheum *32*, 1515–1520.

Hassfeld, W., Steiner, G., Studnicka-Benke, A., Skriner, K., Graninger, W., Fischer, I., and Smolen, J.S. (1995). Autoimmune response to the spliceosome. An immunologic link between rheumatoid arthritis, mixed connective tissue disease, and systemic lupus erythematosus. Arthritis Rheum *38*, 777–785.

Hata, H., Sakaguchi, N., Yoshitomi, H., Iwakura, Y., Sekikawa, K., Azuma, Y., Kanai, C., Moriizumi, E., Nomura, T., Nakamura, T., et al. (2004). Distinct contribution of IL-6, TNF-alpha, IL-1, and IL-10 to T cell-mediated spontaneous autoimmune arthritis in mice. J Clin Invest *114*, 582–588.

Heo, Y.-J., Joo, Y.-B., Oh, H.-J., Park, M.-K., Heo, Y.-M., Cho, M.-L., Kwok, S.-K., Ju, J.H., Park, K.S., Cho, S.G., et al. (2010). IL-10 suppresses Th17 cells and promotes regulatory T cells in the CD4+ T cell population of rheumatoid arthritis patients. Immunol. Lett. *127*, 150–156.

Hill, J.A., Bell, D.A., Brintnell, W., Yue, D., Wehrli, B., Jevnikar, A.M., Lee, D.M., Hueber, W., Robinson, W.H., and Cairns, E. (2008). Arthritis induced by posttranslationally modified (citrullinated) fibrinogen in DR4-IE transgenic mice. J. Exp. Med. *205*, 967–979.

Hirano, T. (2002). Revival of the autoantibody model in rheumatoid arthritis. Nat Immunol *3*, 342–344.

HOLMDAHL, R., Jansson, L., Larsson, A., and Jonsson, R. (1990). Arthritis in DBA/1 mice induced with passively transferred type II collagen immune serum. Immunohistopathology and serum levels of anti-type II collagen auto-antibodies. Scand. J. Immunol. *31*, 147–157.

Hom, J.T., Cole, H., Estridge, T., and Gliszczynski, V.L. (1992). Interleukin-1 enhances the development of type II collagen-induced arthritis only in susceptible and not in resistant mice. Clinical Immunology and Immunopathology *62*, 56–65.

Horsfall, A.C., Butler, D.M., Marinova, L., Warden, P.J., Williams, R.O., Maini, R.N., and Feldmann, M. (1997). Suppression of collagen-induced arthritis by continuous administration of IL-4. J Immunol *159*, 5687–5696.

Hou, W.-S., Li, W., Keyszer, G., Weber, E., Levy, R., Klein, M.J., Gravallese, E.M., Goldring, S.R., and Br mme, D. (2002). Comparison of cathepsins K and S expression within the rheumatoid and osteoarthritic synovium. Arthritis Rheum *46*, 663–674.

Hou, W.-S., Li, Z., Gordon, R.E., Chan, K., Klein, M.J., Levy, R., Keysser, M., Keyszer, G., and Brömme, D. (2001). Cathepsin K Is a Critical Protease in Synovial Fibroblast-Mediated Collagen Degradation. Am. J. Pathol. *159*, 2167–2177.

Hu, Y.-L., Metz, D.P., Chung, J., Siu, G., and Zhang, M. (2009). B7RP-1 blockade

ameliorates autoimmunity through regulation of follicular helper T cells. J Immunol *182*, 1421–1428.

Huang, Q., Ma, Y., Adebayo, A., and Pope, R.M. (2007). Increased macrophage activation mediated through toll-like receptors in rheumatoid arthritis - Huang - 2007 - Arthritis & Rheumatism - Wiley Online Library. Arthritis Rheum *56*, 2192–2201.

Hueber, A.J., Asquith, D.L., Miller, A.M., Reilly, J., Kerr, S., Leipe, J., Melendez, A.J., and McInnes, I.B. (2010). Mast cells express IL-17A in rheumatoid arthritis synovium. The Journal of Immunology *184*, 3336–3340.

Huizinga, T.W.J. (2003). Genetics in rheumatoid arthritis. Best Practice & Research Clinical Rheumatology *17*, 703–716.

Hussein, M.R., Fathi, N.A., El-Din, A.M.E., Hassan, H.I., Abdullah, F., Al-Hakeem, E., and Backer, E.A. (2008). Alterations of the CD4(+), CD8 (+) T cell subsets, interleukins-1beta, IL-10, IL-17, tumor necrosis factor-alpha and soluble intercellular adhesion molecule-1 in rheumatoid arthritis and osteoarthritis: preliminary observations. Pathol. Oncol. Res. *14*, 321–328.

Ikeuchi, H., Kuroiwa, T., Hiramatsu, N., Kaneko, Y., Hiromura, K., Ueki, K., and Nojima, Y. (2005). Expression of interleukin-22 in rheumatoid arthritis: potential role as a proinflammatory cytokine. Arthritis Rheum *52*, 1037–1046.

Imanaka, T., Shichikawa, K., Inoue, K., Shimaoka, Y., Takenaka, Y., and Wakitani, S. (1997). Increase in age at onset of rheumatoid arthritis in Japan over a 30 year period. Ann. Rheum. Dis. *56*, 313–316.

Irmler, I.M., Gajda, M., and Bräuer, R. (2007). Exacerbation of antigen-induced arthritis in IFN-gamma-deficient mice as a result of unrestricted IL-17 response. J Immunol *179*, 6228–6236.

Ishikawa, H., Smiley, J.D., and Ziff, M. (1975). Electron microscopic demonstration of immunoglobulin deposition in rheumatoid cartilage. Arthritis Rheum *18*, 563–576.

Iwakoshi, N.N., Lee, A.-H., Vallabhajosyula, P., Otipoby, K.L., Rajewsky, K., and Glimcher, L.H. (2003). Plasma cell differentiation and the unfolded protein response intersect at the transcription factor XBP-1. Nat Immunol *4*, 321–329.

Jacobsson, L.T.H., Hanson, R.L., Knowler, W.C., Pillemer, S., Pettitt, D.J., Mccance, D.R., and Bennett, P.H. (1994). Decreasing incidence and prevalence of rheumatoid arthritis in pima indians over a twenty-five—year period. Arthritis Rheum *37*, 1158–1165.

Jin, S., Chin, J., Seeber, S., Niewoehner, J., Weiser, B., Beaucamp, N., Woods, J., Murphy, C., Fanning, A., Shanahan, F., et al. (2012). TL1A/TNFSF15 directly induces proinflammatory cytokines, including TNFα, from CD3+CD161+ T cells to exacerbate gut inflammation. Mucosal Immunology.

JOHANSEN, J.S., HVOLRIS, J., HANSEN, M., BACKER, V., LORENZEN, I., and PRICE, P.A. (1996). Serum YKL-40 levels in healthy children and adults. Comparison with serum and synovial fluid levels of YKL-40 in patients with osteoarthritis or trauma of the knee joint. Br. J. Rheumatol. *35*, 553–559.

John, S., and Worthington, J. (2001). Genetic epidemiology. Approaches to the genetic analysis of rheumatoid arthritis. Arthritis Res. *3*, 216–220.

Jones, G.W., Stumhofer, J.S., Foster, T., Twohig, J.P., Hertzog, P., Topley, N., Williams, A.S., Hunter, C.A., Jenkins, B.J., Wang, E.C.Y., et al. (2011). Naive and activated T cells display differential responsiveness to TL1A that affects Th17 generation, maintenance, and proliferation. Faseb J *25*, 409–419.

Jongbloed, S.L., Lebre, M.C., Fraser, A.R., Gracie, J.A., Sturrock, R.D., Tak, P.P., and McInnes, I.B. (2006). Enumeration and phenotypical analysis of distinct dendritic cell subsets in psoriatic arthritis and rheumatoid arthritis. Arthritis Res. Ther. *8*, R15.

Joosten, L.A., Lubberts, E., Helsen, M.M., Saxne, T., Coenen-de Roo, C.J., Heinegård, D., and van den Berg, W.B. (1999). Protection against cartilage and bone destruction by systemic interleukin-4 treatment in established murine type II collagen-induced arthritis. Arthritis Res. *1*, 81–91.

Jovanovic, D.V., Di Battista, J.A., Martel-Pelletier, J., Jolicoeur, F.C., He, Y., Zhang, M., Mineau, F., and Pelletier, J.P. (1998). IL-17 stimulates the production and expression of proinflammatory cytokines, IL-beta and TNF-alpha, by human macrophages. J Immunol *160*, 3513–3521.

Kadowaki, K.M., Matsuno, H., Tsuji, H., and Tunru, I. (1994). CD4+ T cells from collagen-induced arthritic mice are essential to transfer arthritis into severe combined immunodeficient mice. Clinical and Experimental Immunology *97*, 212–218.

Kaipiainen-Seppanen, O., Aho, K., Isomaki, H., and Laakso, M. (1996). Incidence of rheumatoid arthritis in Finland during 1980-1990. Ann. Rheum. Dis. *55*, 608–611.

Kaipiainen-Seppanen, O., and Kautiainen, H. (2006). Declining trend in the incidence of rheumatoid factor-positive rheumatoid arthritis in Finland 1980-2000. The Journal of Rheumatology.

Kallies, A., Hasbold, J., Fairfax, K., Pridans, C., Emslie, D., McKenzie, B.S., Lew, A.M., Corcoran, L.M., Hodgkin, P.D., Tarlinton, D.M., et al. (2007). Initiation of Plasma-Cell Differentiation Is Independent of the Transcription Factor Blimp-1. Immunity *26*, 555–566.

Kamada, N., Hisamatsu, T., Honda, H., Kobayashi, T., Chinen, H., Takayama, T., Kitazume, M.T., Okamoto, S., Koganei, K., Sugita, A., et al. (2010). TL1A produced by lamina propria macrophages induces Th1 and Th17 immune responses in cooperation with IL-23 in patients with Crohn's disease. Inflamm. Bowel Dis. *16*, 568–575.

Kang, Y.M. (2002). CD8 T Cells Are Required for the Formation of Ectopic Germinal Centers in Rheumatoid Synovitis. Journal of Experimental Medicine *195*, 1325–1336.

Kang, Y.-J., Kim, W.-J., Bae, H.-U., Kim, D.-I., Park, Y.B., Park, J.-E., Kwon, B.S., and Lee, W.-H. (2005). Involvement of TL1A and DR3 in induction of pro-inflammatory cytokines and matrix metalloproteinase-9 in atherogenesis. Cytokine *29*, 229–235.

Karlson, E.W., Mandl, L.A., Aweh, G.N., and Grodstein, F. (2003). Coffee consumption and risk of rheumatoid arthritis. Arthritis Rheum *48*, 3055–3060.

Kassahn, D., Kolb, C., Solomon, S., Bochtler, P., and Illges, H. (2002). Few human autoimmune sera detect GPI. Nat Immunol *3*, 411–2–authorreply412–3.

Katsikis, P.D., Chu, C.Q., Brennan, F.M., Maini, R.N., and Feldmann, M. (1994). Immunoregulatory role of interleukin 10 in rheumatoid arthritis. J. Exp. Med. *179*, 1517–1527.

Kawakami, A., Eguchi, K., Matsuoka, N., Tsuboi, M., Urayama, S., Kawabe, Y., Aoyagi, T., Maeda, K., and Nagataki, S. (1997). Inhibitory effects of interleukin-10 on synovial cells of rheumatoid arthritis. Immunology *91*, 252–259.

Kayamuro, H., Yoshioka, Y., Abe, Y., Katayama, K., Yoshida, T., Yamashita, K., Yoshikawa, T., Hiroi, T., Itoh, N., Kawai, Y., et al. (2009). TNF superfamily member, TL1A, is a potential mucosal vaccine adjuvant. Biochem Biophys Res Commun *384*, 296–300.

Kelchtermans, H., Geboes, L., Mitera, T., Huskens, D., Leclercq, G., and Matthys, P. (2009). Activated CD4+CD25+ regulatory T cells inhibit osteoclastogenesis and collagen-induced arthritis. Ann. Rheum. Dis. *68*, 744–750.

Kelchtermans, H., De Klerck, B., Mitera, T., Van Balen, M., Bullens, D., Billiau, A., Leclercq, G., and Matthys, P. (2005). Defective CD4+CD25+ regulatory T cell functioning in collagen-induced arthritis: an important factor in pathogenesis, counter-regulated by endogenous IFN-gamma. Arthritis Res. Ther. *7*, R402–R415.

Keystone, E.C., Kavanaugh, A.F., Sharp, J.T., Tannenbaum, H., Hua, Y., Teoh, L.S., Fischkoff, S.A., and Chartash, E.K. (2004). Radiographic, clinical, and functional outcomes of treatment with adalimumab (a human anti-tumor necrosis factor monoclonal antibody) in patients with active rheumatoid arthritis receiving concomitant methotrexate therapy: a randomized, placebo-controlled, 52-week trial. Arthritis Rheum *50*, 1400–1411.

Khan, S.Q., Tsai, M.S., Schreiber, T.H., Wolf, D., Deyev, V.V., and Podack, E.R. (2013). Cloning, Expression, and Functional Characterization of TL1A-Ig. The Journal of Immunology *190*, 1540–1550.

Khan, S., Greenberg, J.D., and Bhardwaj, N. (2009). Dendritic cells as targets for therapy in rheumatoid arthritis. Nat Rev Rheumatol *5*, 566–571.

Kim, C.H., Rott, L.S., Clark-Lewis, I., Campbell, D.J., Wu, L., and Butcher, E.C. (2001a).

Subspecialization of CXCR5+ T cells: B helper activity is focused in a germinal center-localized subset of CXCR5+ T cells. J. Exp. Med. *193*, 1373–1381.

Kim, K.-W., Cho, M.-L., Lee, S.-H., Oh, H.-J., Kang, C.-M., Ju, J.H., Min, S.-Y., Cho, Y.-G., Park, S.-H., and Kim, H.-Y. (2007). Human rheumatoid synovial fibroblasts promote osteoclastogenic activity by activating RANKL via TLR-2 and TLR-4 activation. Immunol. Lett. *110*, 54–64.

Kim, S.H., Kim, S., Evans, C.H., Ghivizzani, S.C., Oligino, T., and Robbins, P.D. (2001b). Effective treatment of established murine collagen-induced arthritis by systemic administration of dendritic cells genetically modified to express IL-4. J Immunol *166*, 3499–3505.

Kim, S., and Zhang, L. (2005). Identification of naturally secreted soluble form of TL1A, a TNF-like cytokine. J. Immunol. Methods *298*, 1–8.

Kim, W.-J., Kang, Y.-J., Suk, K., Park, J.-E., Kwon, B.S., and Lee, W.-H. (2008). Comparative analysis of the expression patterns of various TNFSF/TNFRSF in atherosclerotic plaques. Immunol. Invest. *37*, 359–373.

Kindt, T.J., Goldsby, R.A., Osborne, B.A., and Kuby, J. (2007). Kuby immunology (W. H. Freeman).

Kinloch, A., Lundberg, K., Wait, R., Wegner, N., Lim, N.H., Zendman, A.J.W., Saxne, T., Malmström, V., and Venables, P.J. (2008). Synovial fluid is a site of citrullination of autoantigens in inflammatory arthritis. Arthritis Rheum *58*, 2287–2295.

Kinne, R.W., Bräuer, R., Stuhlmüller, B., Palombo-Kinne, E., and Burmester, G.R. (2000). Macrophages in rheumatoid arthritis. Arthritis Res. *2*, 189–202.

Kitson, J., Raven, T., Jiang, Y.P., Goeddel, D.V., Giles, K.M., Pun, K.T., Grinham, C.J., Brown, R., and Farrow, S.N. (1996). A death-domain-containing receptor that mediates apoptosis. Nature *384*, 372–375.

Klareskog, L., van der Heijde, D., de Jager, J.P., Gough, A., Kalden, J., Malaise, M., Martín Mola, E., Pavelka, K., Sany, J., Settas, L., et al. (2004). Therapeutic effect of the combination of etanercept and methotrexate compared with each treatment alone in patients with rheumatoid arthritis: double-blind randomised controlled trial. Lancet *363*, 675–681.

Kleinau, S., Martinsson, P., and Heyman, B. (2000). Induction and suppression of collagen-induced arthritis is dependent on distinct fcgamma receptors. J. Exp. Med. *191*, 1611–1616.

Koch, A.E. (2003). Angiogenesis as a target in rheumatoid arthritis. Ann. Rheum. Dis. *62 Suppl 2*, ii60–ii67.

Konisti, S., Kiriakidis, S., and Paleolog, E.M. (2012). Hypoxia—a key regulator of angiogenesis and inflammation in rheumatoid arthritis. Nat Rev Rheumatol *8*, 153–162.

Kontoyiannis, D., Pasparakis, M., Pizarro, T.T., Cominelli, F., and Kollias, G. (1999). Impaired on/off regulation of TNF biosynthesis in mice lacking TNF AU-rich elements: implications for joint and gut-associated immunopathologies. Immunity *10*, 387–398.

Korganow, A.S., Ji, H., Mangialaio, S., Duchatelle, V., Pelanda, R., Martin, T., Degott, C., Kikutani, H., Rajewsky, K., Pasquali, J.L., et al. (1999). From systemic T cell self-reactivity to organ-specific autoimmune disease via immunoglobulins. Immunity *10*, 451–461.

Kostova, Z., and Wolf, D.H. (2003). For whom the bell tolls: protein quality control of the endoplasmic reticulum and the ubiquitin-proteasome connection. Embo J *22*, 2309–2317.

Kotake, S., Udagawa, N., Takahashi, N., Matsuzaki, K., Itoh, K., Ishiyama, S., Saito, S., Inoue, K., Kamatani, N., Gillespie, M.T., et al. (1999). IL-17 in synovial fluids from patients with rheumatoid arthritis is a potent stimulator of osteoclastogenesis. J Clin Invest *103*, 1345–1352.

Kouskoff, V., Korganow, A.-S., Duchatelle, V., Degott, C., Benoist, C., and Mathis, D. (1996). Organ-Specific Disease Provoked by Systemic Autoimmunity. Cell *87*, 811–822.

Kuhn, K.A., Kulik, L., Tomooka, B., Braschler, K.J., Arend, W.P., Robinson, W.H., and Holers, V.M. (2006). Antibodies against citrullinated proteins enhance tissue injury in experimental autoimmune arthritis. J Clin Invest *116*, 961–973.

Kurz, P.A., Reem, R.E., Kurz, D.E., and Weleber, R.G. (2011). A Unique Case of Autoimmune Retinopathy Associated with Anti-Alpha-Enolase Antibodies. Case Reports in Ophthalmological Medicine *2011*, 1–3.

Kusaba, M., Honda, J., Fukuda, T., and Oizumi, K. (1998). Analysis of type 1 and type 2 T cells in synovial fluid and peripheral blood of patients with rheumatoid arthritis. The Journal of Rheumatology *25*, 1466–1471.

Kwok, S.-K., Cho, M.-L., Park, M.-K., Oh, H.-J., Park, J.-S., Her, Y.-M., Lee, S.-Y., Youn, J., Ju, J.H., Park, K.S., et al. (2012). Interleukin-21 promotes osteoclastogenesis in humans with rheumatoid arthritis and in mice with collagen-induced arthritis. Arthritis Rheum *64*, 740–751.

Lamanna, A.C., and Karbstein, K. (2009). Nob1 binds the single-stranded cleavage site D at the 3'-end of 18S rRNA with its PIN domain. Proceedings of the National Academy of Sciences *106*, 14259–14264.

Lawson, C.A., Brown, A.K., Bejarano, V., Douglas, S.H., Burgoyne, C.H., Greenstein, A.S., Boylston, A.W., Emery, P., Ponchel, F., and Isaacs, J.D. (2006). Early rheumatoid arthritis is associated with a deficit in the CD4+CD25high regulatory T cell population in peripheral blood. Rheumatology (Oxford) *45*, 1210–1217.

Leavenworth, J.W., Tang, X., Kim, H.-J., Wang, X., and Cantor, H. (2013). Amelioration of arthritis through mobilization of peptide-specific CD8+ regulatory T cells. J Clin Invest *123*, 1382–1389.

Lecker, S.H., Goldberg, A.L., and Mitch, W.E. (2006). Protein degradation by the ubiquitin-proteasome pathway in normal and disease states. J. Am. Soc. Nephrol. *17*, 1807–1819.

Lee, A.-H., Iwakoshi, N.N., Anderson, K.C., and Glimcher, L.H. (2003). Proteasome inhibitors disrupt the unfolded protein response in myeloma cells. Proc Natl Acad Sci USA *100*, 9946–9951.

Lee, S.-Y., Kwok, S.-K., Son, H.-J., Ryu, J.-G., Kim, E.-K., Oh, H.-J., Cho, M.-L., Ju, J., Park, S.-H., and Kim, H.-Y. (2013). IL-17-mediated Bcl-2 expression regulates survival of fibroblast-like synoviocytes in rheumatoid arthritis through STAT3 activation. Arthritis Res. Ther. *15*, R31.

Lefèvre, S., Knedla, A., Tennie, C., Kampmann, A., Wunrau, C., Dinser, R., Korb, A., Schnäker, E.-M., Tarner, I.H., Robbins, P.D., et al. (2009). Synovial fibroblasts spread rheumatoid arthritis to unaffected joints. Nat Med *15*, 1414–1420.

Leipe, J., Schramm, M.A., Grunke, M., Baeuerle, M., Dechant, C., Nigg, A.P., Witt, M.N., Vielhauer, V., Reindl, C.S., Schulze-Koops, H., et al. (2011). Interleukin 22 serum levels are associated with radiographic progression in rheumatoid arthritis. Ann. Rheum. Dis. *70*, 1453–1457.

Li, J., Hsu, H.-C., Yang, P., Wu, Q., Li, H., Edgington, L.E., Bogyo, M., Kimberly, R.P., and Mountz, J.D. (2012a). Treatment of arthritis by macrophage depletion and immunomodulation: Testing an apoptosis-mediated therapy in a humanized death receptor mouse model. Arthritis Rheum *64*, 1098–1109.

Li, X., Zhang, C., Zhang, J., Zhang, Y., Wu, Z., Yang, L., Xiang, Z., Qi, Z., Zhang, X., and Xiao, X. (2012b). Polymorphisms in the CTLA-4 gene and rheumatoid arthritis susceptibility: a meta-analysis. Journal of Clinical Immunology *32*, 530–539.

Liang, B., Workman, C., Lee, J., Chew, C., Dale, B.M., Colonna, L., Flores, M., Li, N., Schweighoffer, E., Greenberg, S., et al. (2008). Regulatory T cells inhibit dendritic cells by lymphocyte activation gene-3 engagement of MHC class II. J Immunol *180*, 5916–5926.

Lim, H.W., Hillsamer, P., and Kim, C.H. (2004). Regulatory T cells can migrate to follicles upon T cell activation and suppress GC-Th cells and GC-Th cell-driven B cell responses. J Clin Invest *114*, 1640–1649.

Lin, J.P., Hirsch, R., Jacobsson, L.T., Scott, W.W., Ma, L.D., Pillemer, S.R., Knowler, W.C., Kastner, D.L., and Bale, S.J. (1999). Genealogy construction in a historically isolated population: application to genetic studies of rheumatoid arthritis in the Pima Indian. Genet. Med. *1*, 187–193.

Lin, K.-I., Lin, Y., and Calame, K. Repression of c-myc Is Necessary but Not Sufficient for Terminal Differentiation of B Lymphocytes In Vitro.

Linterman, M.A., Rigby, R.J., Wong, R.K., Yu, D., Brink, R., Cannons, J.L., Schwartzberg,

P.L., Cook, M.C., Walters, G.D., and Vinuesa, C.G. (2009). Follicular helper T cells are required for systemic autoimmunity. J. Exp. Med. *206*, 561–576.

Lioté, F., CHAMPY, R., MOENNER, M., BOVAL-BOIZARD, B., and BADET, J. (2003). Elevated angiogenin levels in synovial fluid from patients with inflammatory arthritis and secretion of angiogenin by cultured synovial fibroblasts. Clinical and Experimental Immunology *132*, 163–168.

Lipsky, P.E., van der Heijde, D.M., St Clair, E.W., Furst, D.E., Breedveld, F.C., Kalden, J.R., Smolen, J.S., Weisman, M., Emery, P., Feldmann, M., et al. (2000). Infliximab and methotrexate in the treatment of rheumatoid arthritis. Anti-Tumor Necrosis Factor Trial in Rheumatoid Arthritis with Concomitant Therapy Study Group. N Engl J Med *343*, 1594–1602.

Liu, R., Wu, Q., Su, D., Che, N., Chen, H., Geng, L., Chen, J., Chen, W., Li, X., and Sun, L. (2012). A regulatory effect of IL-21 on T follicular helper-like cell and B cell in rheumatoid arthritis. Arthritis Res. Ther. *14*, R255.

Lubberts, E., Joosten, L.A., Chabaud, M., van den Bersselaar, L., Oppers, B., Coenen-de Roo, C.J., Richards, C.D., Miossec, P., and van den Berg, W.B. (2000a). IL-4 gene therapy for collagen arthritis suppresses synovial IL-17 and osteoprotegerin ligand and prevents bone erosion. J Clin Invest *105*, 1697–1710.

Lubberts, E., Joosten, L.A., Helsen, M.M., and van den Berg, W.B. (1998). Regulatory role of interleukin 10 in joint inflammation and cartilage destruction in murine streptococcal cell wall (SCW) arthritis. More therapeutic benefit with IL-4/IL-10 combination therapy than with IL-10 treatment alone. Cytokine *10*, 361–369.

Lubberts, E., Joosten, L.A.B., Van De Loo, F.A.J., Van Den Bersselaar, L.A.M., and van den Berg, W.B. (2000b). Reduction of interleukin‐17–induced inhibition of chondrocyte proteoglycan synthesis in intact murine articular cartilage by interleukin‐4. Arthritis Rheum *43*, 1300–1306.

Lubberts, E., Koenders, M.I., Oppers-Walgreen, B., Van Den Bersselaar, L., Coenen-de Roo, C.J.J., Joosten, L.A.B., and van den Berg, W.B. (2004). Treatment with a neutralizing anti-murine interleukin-17 antibody after the onset of collagen-induced arthritis reduces joint inflammation, cartilage destruction, and bone erosion. Arthritis Rheum *50*, 650–659.

Lubberts, E., Van Den Bersselaar, L., Oppers-Walgreen, B., Schwarzenberger, P., Coenen-de Roo, C.J.J., Kolls, J.K., Joosten, L.A.B., and van den Berg, W.B. (2003). IL-17 promotes bone erosion in murine collagen-induced arthritis through loss of the receptor activator of NF-kappa B ligand/osteoprotegerin balance. J Immunol *170*, 2655–2662.

Lundberg, K., Nijenhuis, S., Vossenaar, E.R., Palmblad, K., van Venrooij, W.J., Klareskog, L., Zendman, A., and Harris, H. (2005). Citrullinated proteins have increased immunogenicity and arthritogenicity and their presence in arthritic joints correlates with disease severity.

Arthritis Res. Ther. *7*, R458.

Lundström, E., Källberg, H., Alfredsson, L., Klareskog, L., and Padyukov, L. (2009). Gene–environment interaction between the DRB1 shared epitope and smoking in the risk of anti–citrullinated protein antibody–positive rheumatoid arthritis: all alleles are important. Arthritis Rheum *60*, 1597–1603.

M J Welch, S.F.J.V.D.C. (1983). Increased frequency of rheumatoid factor precursor B lymphocytes after immunization of normal adults with tetanus toxoid. Clinical and Experimental Immunology *51*, 299.

Ma, J., Zhu, C., Ma, B., Tian, J., Baidoo, S.E., Mao, C., Wu, W., Chen, J., Tong, J., Yang, M., et al. (2012). Increased frequency of circulating follicular helper T cells in patients with rheumatoid arthritis. Clinical and Developmental Immunology *2012*, 827480.

Maccioni, M., Zeder-Lutz, G., Huang, H., Ebel, C., Gerber, P., Hergueux, J., Marchal, P., Duchatelle, V., Degott, C., van Regenmortel, M., et al. (2002). Arthritogenic Monoclonal Antibodies from K/BxN Mice. The Journal of ….

MacLennan, I.C.M., Toellner, K.-M., Cunningham, A.F., Serre, K., Sze, D.M.-Y., Zúñiga, E., Cook, M.C., and Vinuesa, C.G. (2003). Extrafollicular antibody responses. Immunol Rev *194*, 8–18.

Malemud, C.J. (2007). Growth hormone, VEGF and FGF: Involvement in rheumatoid arthritis. Clinica Chimica Acta *375*, 10–19.

Manoury-Schwartz, B., Chiocchia, G., Bessis, N., Abehsira-Amar, O., Batteux, F., Muller, S., Huang, S., Boissier, M.C., and Fournier, C. (1997). High susceptibility to collagen-induced arthritis in mice lacking IFN-gamma receptors. J Immunol *158*, 5501–5506.

Marrelli, A., Cipriani, P., Liakouli, V., Carubbi, F., Perricone, C., Perricone, R., and Giacomelli, R. (2011). Angiogenesis in rheumatoid arthritis: a disease specific process or a common response to chronic inflammation? Autoimmun Rev *10*, 595–598.

Marsters, S.A., Sheridan, J.P., Donahue, C.J., Pitti, R.M., Gray, C.L., Goddard, A.D., Bauer, K.D., and Ashkenazi, A. (1996). Apo-3, a new member of the tumor necrosis factor receptor family, contains a death domain and activates apoptosis and NF-κB. Immunity *6*, 1669–1676.

Martin-Fontecha, A., Sebastiani, S., Hopken, U.E., Uguccioni, M., Lipp, M., Lanzavecchia, A., and Sallusto, F. (2003). Regulation of Dendritic Cell Migration to the Draining Lymph Node: Impact on T Lymphocyte Traffic and Priming. J. Exp. Med. *198*, 615–621.

Martins, G., and Calame, K. (2008). Regulation and functions of Blimp-1 in T and B lymphocytes. Annu. Rev. Immunol. *26*, 133–169.

Maruotti, N., Crivellato, E., Cantatore, F.P., Vacca, A., and Ribatti, D. (2006). Mast cells in rheumatoid arthritis. Clin Rheumatol *26*, 1–4.

Mathsson, L., Lampa, J., Mullazehi, M., and Rönnelid, J. (2006). Immune complexes from rheumatoid arthritis synovial fluid induce FcgammaRIIa dependent and rheumatoid factor correlated production of tumour necrosis factor-alpha by peripheral blood mononuclear cells. Arthritis Res. Ther. *8*, R64.

Matsumoto, I., Staub, A., Benoist, C., and Mathis, D. (1999). Arthritis provoked by linked T and B cell recognition of a glycolytic enzyme. Science *286*, 1732–1735.

Matsumoto, I., Lee, D.M., Goldbach-Mansky, R., Sumida, T., Hitchon, C.A., Schur, P.H., Anderson, R.J., Coblyn, J.S., Weinblatt, M.E., Brenner, M., et al. (2003). Low prevalence of antibodies to glucose-6-phosphate isomerase in patients with rheumatoid arthritis and a spectrum of other chronic autoimmune disorders. Arthritis Rheum *48*, 944–954.

Matsumoto, I., Maccioni, M., Lee, D.M., Maurice, M., Simmons, B., Brenner, M., Mathis, D., and Benoist, C. (2002). How antibodies to a ubiquitous cytoplasmic enzyme may provoke joint-specific autoimmune disease. Nat Immunol *3*, 360–365.

Matthys, P., Vermeire, K., and Billiau, A. (2001). Mac-1(+) myelopoiesis induced by CFA: a clue to the paradoxical effects of IFN-gamma in autoimmune disease models. Trends in Immunology *22*, 367–371.

Matthys, P., Vermeire, K., Mitera, T., Heremans, H., Huang, S., Schols, D., De Wolf-Peeters, C., and Billiau, A. (1999). Enhanced autoimmune arthritis in IFN-gamma receptor-deficient mice is conditioned by mycobacteria in Freund's adjuvant and by increased expansion of Mac-1+ myeloid cells. J Immunol *163*, 3503–3510.

Mauri, C., Gray, D., Mushtaq, N., and Londei, M. (2003). Prevention of arthritis by interleukin 10-producing B cells. J. Exp. Med. *197*, 489–501.

McGettrick, H.M., Smith, E., Filer, A., Kissane, S., Salmon, M., Buckley, C.D., Rainger, G.E., and Nash, G.B. (2009). Fibroblasts from different sites may promote or inhibit recruitment of flowing lymphocytes by endothelial cells. Eur. J. Immunol. *39*, 113–125.

McHeyzer-Williams, M., Okitsu, S., Wang, N., and McHeyzer-Williams, L. (2011). Molecular programming of B cell memory. Nat Rev Immunol.

McInnes, I.B. (2003). Leukotrienes, mast cells, and T cells. Arthritis Res. Ther.

McInnes, I.B., and Schett, G. (2007). Cytokines in the pathogenesis of rheumatoid arthritis. Nat Rev Immunol *7*, 429–442.

McLaren, J.E., Calder, C.J., McSharry, B.P., Sexton, K., Salter, R.C., Singh, N.N., Wilkinson, G.W.G., Wang, E.C.Y., and Ramji, D.P. (2010). The TNF-like protein 1A-death receptor 3 pathway promotes macrophage foam cell formation in vitro. The Journal of Immunology *184*, 5827–5834.

Meinecke, I., Pap, G., Mendoza, H., Drange, S., Ender, S., Strietholt, S., Gay, R.E., Seyfert,

C., Ink, B., Gay, S., et al. (2009). Small ubiquitin-like modifier 1 [corrected] mediates the resistance of prosthesis-loosening fibroblast-like synoviocytes against Fas-induced apoptosis. Arthritis Rheum *60*, 2065–2070.

Meister, S., Schubert, U., Neubert, K., Herrmann, K., Burger, R., Gramatzki, M., Hahn, S., Schreiber, S., Wilhelm, S., Herrmann, M., et al. (2007). Extensive immunoglobulin production sensitizes myeloma cells for proteasome inhibition. Cancer Res. *67*, 1783–1792.

Meron, M.K., Amital, H., Shepshelovich, D., Barzilai, O., Ram, M., Anaya, J.-M., Gerli, R., Nicola, B., and Shoenfeld, Y. (2010). Infectious aspects and the etiopathogenesis of rheumatoid arthritis. Clin Rev Allergy Immunol *38*, 287–291.

Meylan, F., Song, Y.-J., Fuss, I., Villarreal, S., Kahle, E., Malm, I.-J., Acharya, K., Ramos, H.L., Lo, L., Mentink-Kane, M.M., et al. (2011a). The TNF-family cytokine TL1A drives IL-13-dependent small intestinal inflammation. Mucosal Immunology *4*, 172–185.

Meylan, F., Davidson, T.S., Kahle, E., Kinder, M., Acharya, K., Jankovic, D., Bundoc, V., Hodges, M., Shevach, E.M., Keane-Myers, A., et al. (2008). The TNF-family receptor DR3 is essential for diverse T cell-mediated inflammatory diseases. Immunity *29*, 79–89.

Meylan, F., Richard, A.C., and Siegel, R.M. (2011b). TL1A and DR3, a TNF family ligand-receptor pair that promotes lymphocyte costimulation, mucosal hyperplasia, and autoimmune inflammation. Immunol Rev *244*, 188–196.

Ménard, H.A., and el-Amine, M. (1996). The calpain-calpastatin system in rheumatoid arthritis. Immunol. Today *17*, 545–547.

Migone, T.S., Zhang, J., Luo, X., Zhuang, L., Chen, C., Hu, B., Hong, J.S., Perry, J.W., Chen, S.F., Zhou, J.X.H., et al. (2002). TL1A is a TNF-like ligand for DR3 and TR6/DcR3 and functions as a T cell costimulator. Immunity *16*, 479–492.

Mikuls, T.R., Cerhan, J.R., Criswell, L.A., Merlino, L., Mudano, A.S., Burma, M., Folsom, A.R., and Saag, K.G. (2002). Coffee, tea, and caffeine consumption and risk of rheumatoid arthritis: results from the Iowa Women's Health Study. Arthritis Rheum *46*, 83–91.

Mimori, T., Suganuma, K., Tanami, Y., Nojima, T., Matsumura, M., Fujii, T., Yoshizawa, T., Suzuki, K., and Akizuki, M. (1995). Autoantibodies to calpastatin (an endogenous inhibitor for calcium-dependent neutral protease, calpain) in systemic rheumatic diseases. Proc Natl Acad Sci USA *92*, 7267–7271.

Miossec, P., Chomarat, P., Dechanet, J., Moreau, J.F., Roux, J.P., Delmas, P., and Banchereau, J. (1994). Interleukin-4 inhibits bone resorption through an effect on osteoclasts and proinflammatory cytokines in an ex vivo model of bone resorption in rheumatoid arthritis. Arthritis Rheum *37*, 1715–1722.

Misharin, A.V., Haines, G.K.I., and Perlman, H.R. (2012). Non Classical Monocytes Are Required for Initiation Phase While Macrophages Are Necessary for the Resolution Phase in

the K/BxN Murine of Inflammatory Arthritis. Arthritis Rheum *64*, S149–S149.

Miyata, M., Ohira, H., Sasajima, T., Suzuki, S., Ito, M., Sato, Y., and Kasukawa, R. (2000). Significance of low mRNA levels of interleukin-4 and -10 in mononuclear cells of the synovial fluid of patients with rheumatoid arthritis. Clin Rheumatol *19*, 365–370.

Mizoguchi, A., and Bhan, A.K. (2006). A Case for Regulatory B Cells. The Journal of Immunology.

Moore, P.A., Belvedere, O., Orr, A., Pieri, K., LaFleur, D.W., Feng, P., Soppet, D., Charters, M., Gentz, R., Parmelee, D., et al. (1999). BLyS: member of the tumor necrosis factor family and B lymphocyte stimulator. Science *285*, 260–263.

Morgan, M.E., Flierman, R., van Duivenvoorde, L.M., Witteveen, H.J., van Ewijk, W., van Laar, J.M., de Vries, R.R.P., and Toes, R.E.M. (2005). Effective treatment of collagen-induced arthritis by adoptive transfer of CD25+ regulatory T cells. Arthritis Rheum *52*, 2212–2221.

Morgan, M.E., Sutmuller, R.P.M., Witteveen, H.J., van Duivenvoorde, L.M., Zanelli, E., Melief, C.J.M., Snijders, A., Offringa, R., de Vries, R.R.P., and Toes, R.E.M. (2003). CD25+ cell depletion hastens the onset of severe disease in collagen-induced arthritis. Arthritis Rheum *48*, 1452–1460.

Morita, Y., Yamamura, M., Kawashima, M., Harada, S., Tsuji, K., Shibuya, K., Maruyama, K., and Makino, H. (1998). Flow cytometric single-cell analysis of cytokine production by CD4+ T cells in synovial tissue and peripheral blood from patients with rheumatoid arthritis. Arthritis Rheum *41*, 1669–1676.

Möttönen, M., Heikkinen, J., Mustonen, L., Isomäki, P., Luukkainen, R., and Lassila, O. (2005). CD4+ CD25+ T cells with the phenotypic and functional characteristics of regulatory T cells are enriched in the synovial fluid of patients with rheumatoid arthritis. Clinical and Experimental Immunology *140*, 360–367.

Mulherin, D., Fitzgerald, O., and Bresnihan, B. (1996). Synovial tissue macrophage populations and articular damage in rheumatoid arthritis. Arthritis Rheum *39*, 115–124.

Mullazehi, M., Mathsson, L., Lampa, J., and Rönnelid, J. (2006). Surface-bound anti-type II collagen-containing immune complexes induce production of tumor necrosis factor alpha, interleukin-1beta, and interleukin-8 from peripheral blood monocytes via Fc gamma receptor IIA: a potential pathophysiologic mechanism for humoral anti-type II collagen immunity in arthritis. Arthritis Rheum *54*, 1759–1771.

Mullazehi, M., Mathsson, L., Lampa, J., and Rönnelid, J. (2007). High anti-collagen type-II antibody levels and induction of proinflammatory cytokines by anti-collagen antibody-containing immune complexes in vitro characterise a distinct rheumatoid arthritis phenotype associated with acute inflammation at the time of disease onset. Ann. Rheum. Dis. *66*, 537–541.

Mullazehi, M., Wick, M.C., Klareskog, L., van Vollenhoven, R., and Ronnelid, J. (2012). Anti-type II collagen antibodies are associated with early radiographic destruction in rheumatoid arthritis. Arthritis Res. Ther. *14*, R100.

Murata, S., Yashiroda, H., and Tanaka, K. (2009). Molecular mechanisms of proteasome assembly. Nat. Rev. Mol. Cell Biol. *10*, 104–115.

Mück, C., Herndler-Brandstetter, D., Micutkova, L., Grubeck-Loebenstein, B., and Jansen-Dürr, P. (2010). Two functionally distinct isoforms of TL1A (TNFSF15) generated by differential ectodomain shedding. J. Gerontol. a Biol. Sci. Med. Sci. *65*, 1165–1180.

Müller-Ladner, U., Ospelt, C., Gay, S., Distler, O., and Pap, T. (2007). Cells of the synovium in rheumatoid arthritis. Synovial fibroblasts. Arthritis Res. Ther. *9*, 223.

Myasoedova, E., Davis, J.M., Crowson, C.S., and Gabriel, S.E. (2010). Epidemiology of rheumatoid arthritis: rheumatoid arthritis and mortality. Curr Rheumatol Rep *12*, 379–385.

Myers, L.K., Tang, B., Stuart, J.M., and Kang, A.H. (2002). The role of IL-4 in regulation of murine collagen-induced arthritis. Clin Immunol *102*, 185–191.

Nakae, S., Nambu, A., Sudo, K., and Iwakura, Y. (2003a). Suppression of immune induction of collagen-induced arthritis in IL-17-deficient mice. J Immunol *171*, 6173–6177.

Nakae, S., Saijo, S., Horai, R., Sudo, K., Mori, S., and Iwakura, Y. (2003b). IL-17 production from activated T cells is required for the spontaneous development of destructive arthritis in mice deficient in IL-1 receptor antagonist. Proc Natl Acad Sci USA *100*, 5986–5990.

Nandakumar, K.S., Andrén, M., Martinsson, P., Bajtner, E., Hellström, S., Holmdahl, R., and Kleinau, S. (2003a). Induction of arthritis by single monoclonal IgG anti-collagen type II antibodies and enhancement of arthritis in mice lacking inhibitory FcgammaRIIB. Eur. J. Immunol. *33*, 2269–2277.

Nandakumar, K.S., Svensson, L., and Holmdahl, R. (2003b). Collagen type II-specific monoclonal antibody-induced arthritis in mice: description of the disease and the influence of age, sex, and genes. Am. J. Pathol. *163*, 1827–1837.

Nardella, F.A., Dayer, J.-M., Roelke, M., Krane, S.M., and Mannik, M. (1983). Self-associating IgG rheumatoid factors stimulate monocytes to release prostaglandins and mononuclear cell factor that stimulates collagenase and prostaglandin production by synovial cells. Rheumatol Int *3*, 183–186.

Nell, V.P.K., Machold, K.P., Stamm, T.A., Eberl, G., Heinzl, H., Uffmann, M., Smolen, J.S., and Steiner, G. (2005). Autoantibody profiling as early diagnostic and prognostic tool for rheumatoid arthritis. Ann. Rheum. Dis. *64*, 1731–1736.

Neubert, K., Meister, S., Moser, K., Weisel, F., Maseda, D., Amann, K., Wiethe, C., Winkler, T.H., Kalden, J.R., Manz, R.A., et al. (2008). The proteasome inhibitor bortezomib depletes

plasma cells and protects mice with lupus-like disease from nephritis. Nat Med *14*, 748–755.

Neumann, E., Lefèvre, S., Zimmermann, B., Gay, S., and Müller-Ladner, U. (2010). Rheumatoid arthritis progression mediated by activated synovial fibroblasts. Trends Mol Med *16*, 458–468.

Németh, T., and Mócsai, A. (2012). The role of neutrophils in autoimmune diseases. Immunol. Lett. *143*, 9–19.

Nie, H., Zheng, Y., Li, R., Guo, T.B., He, D., Fang, L., Liu, X., Xiao, L., Chen, X., Wan, B., et al. (2013). Phosphorylation of FOXP3 controls regulatory T cell function and is inhibited by TNF-α in rheumatoid arthritis. Nat Med *19*, 322–328.

Nigrovic, P.A., and Lee, D.M. (2005). Mast cells in inflammatory arthritis. *7*, 1.

Niu, X., He, D., Zhang, X., Yue, T., Li, N., Zhang, J.Z., Dong, C., and Chen, G. (2010). IL-21 regulates Th17 cells in rheumatoid arthritis. Hum. Immunol. *71*, 334–341.

NONOMURA, Y., MIZOGUCHI, F., SUZUKI, A., NANKI, T., KATO, H., Miyasaka, N., and KOHSAKA, H. (2009). Hypoxia-induced Abrogation of Contact-dependent Inhibition of Rheumatoid Arthritis Synovial Fibroblast Proliferation. The Journal of Rheumatology *36*, 698–705.

Notley, C.A., McCann, F.E., Inglis, J.J., and Williams, R.O. (2010). ANTI-CD3 therapy expands the numbers of CD4+ and CD8+ Treg cells and induces sustained amelioration of collagen-induced arthritis. Arthritis Rheum *62*, 171–178.

O'Connor, B.P., Raman, V.S., Erickson, L.D., Cook, W.J., Weaver, L.K., Ahonen, C., Lin, L.-L., Mantchev, G.T., Bram, R.J., and Noelle, R.J. (2004). BCMA is essential for the survival of long-lived bone marrow plasma cells. J. Exp. Med. *199*, 91–98.

O'Neill, S.K., Cao, Y., Hamel, K.M., Doodes, P.D., Hutas, G., and Finnegan, A. (2007). Expression of CD80/86 on B cells is essential for autoreactive T cell activation and the development of arthritis. J Immunol *179*, 5109–5116.

O'Neill, S.K., Shlomchik, M.J., Glant, T.T., Cao, Y., Doodes, P.D., and Finnegan, A. (2005). Antigen-specific B cells are required as APCs and autoantibody-producing cells for induction of severe autoimmune arthritis. J Immunol *174*, 3781–3788.

O, K.-S., and K, A. (2000). Incidence of chronic inflammatory joint diseases in Finland in 1995. The Journal of Rheumatology *27*, 94–100.

O, K.-S., K, A., H, I., and M, L. (1996). Shift in the incidence of rheumatoid arthritis toward elderly patients in Finland during 1975-1990. Clin Exp Rheumatol *14*, 537–542.

Obeng, E.A., Carlson, L.M., Gutman, D.M., Harrington, W.J., Lee, K.P., and Boise, L.H. (2006). Proteasome inhibitors induce a terminal unfolded protein response in multiple

myeloma cells. Blood *107*, 4907–4916.

Ohata, J., Miura, T., Johnson, T.A., Hori, S., Ziegler, S.F., and Kohsaka, H. (2007). Enhanced efficacy of regulatory T cell transfer against increasing resistance, by elevated Foxp3 expression induced in arthritic murine hosts. Arthritis Rheum *56*, 2947–2956.

Ohmura, K., Nguyen, L.T., Locksley, R.M., Mathis, D., and Benoist, C. (2005). Interleukin-4 can be a key positive regulator of inflammatory arthritis. Arthritis Rheum *52*, 1866–1875.

Oracki, S.A., Walker, J.A., Hibbs, M.L., Corcoran, L.M., and Tarlinton, D.M. (2010). Plasma cell development and survival. Immunol Rev *237*, 140–159.

Orozco, G., Eyre, S., Hinks, A., Ke, X., Wellcome Trust Case Control consortium YEAR Consortium, Wilson, A.G., Bax, D.E., Morgan, A.W., Emery, P., Steer, S., et al. (2010). Association of CD40 with rheumatoid arthritis confirmed in a large UK case-control study. Ann. Rheum. Dis. *69*, 813–816.

Ou, X., Xu, S., and Lam, K.-P. (2012). Deficiency in TNFRSF13B (TACI) expands T-follicular helper and germinal center B cells via increased ICOS-ligand expression but impairs plasma cell survival. Proc Natl Acad Sci USA *109*, 15401–15406.

Padyukov, L., Silva, C., Stolt, P., Alfredsson, L., Klareskog, L., for the Epidemiological Investigation of Rheumatoid Arthritis Study Group (2004). A gene-environment interaction between smoking and shared epitope genes in HLA-DR provides a high risk of seropositive rheumatoid arthritis. Arthritis Rheum *50*, 3085–3092.

Pandiyan, P., Zheng, L., Ishihara, S., Reed, J., and Lenardo, M.J. (2007). CD4+CD25+Foxp3+ regulatory T cells induce cytokine deprivation-mediated apoptosis of effector CD4+ T cells. Nat Immunol *8*, 1353–1362.

Papadakis, K.A., Zhu, D., Prehn, J.L., Landers, C., Avanesyan, A., Lafkas, G., and Targan, S.R. (2005). Dominant role for TL1A/DR3 pathway in IL-12 plus IL-18-induced IFN-gamma production by peripheral blood and mucosal CCR9+ T lymphocytes. J Immunol *174*, 4985–4990.

Papadopoulos, N.G., Alamanos, Y., Voulgari, P.V., Epagelis, E.K., Tsifetaki, N., and Drosos, A.A. (2005). Does cigarette smoking influence disease expression, activity and severity in early rheumatoid arthritis patients? Clin Exp Rheumatol *23*, 861.

Pappu, B.P., Borodovsky, A., Zheng, T.S., Yang, X., Wu, P., Dong, X., Weng, S., Browning, B., Scott, M.L., Ma, L., et al. (2008). TL1A-DR3 interaction regulates Th17 cell function and Th17-mediated autoimmune disease. J. Exp. Med. *205*, 1049–1062.

Pasare, C., and Medzhitov, R. (2003). Toll pathway-dependent blockade of CD4+CD25+ T cell-mediated suppression by dendritic cells. Science *299*, 1033–1036.

Paulissen, S.M.J., van Hamburg, J.P., Davelaar, N., Asmawidjaja, P.S., Hazes, J.M.W., and

Lubberts, E. (2013). Synovial Fibroblasts Directly Induce Th17 Pathogenicity via the Cyclooxygenase/Prostaglandin E2 Pathway, Independent of IL-23. The Journal of Immunology.

Peichl, P., Ceska, M., Broell, H., Effenberger, F., and Lindley, I.J. (1992). Human neutrophil activating peptide/interleukin 8 acts as an autoantigen in rheumatoid arthritis. Ann. Rheum. Dis. *51*, 19–22.

Pelletier, N., Casamayor-Pallejà, M., De Luca, K., Mondière, P., Saltel, F., Jurdic, P., Bella, C., Genestier, L., and Defrance, T. (2006). The endoplasmic reticulum is a key component of the plasma cell death pathway. J Immunol *176*, 1340–1347.

Peperzak, V., Vikstrom, I., Walker, J., Glaser, S.P., LePage, M., Coquery, C.M., Erickson, L.D., Fairfax, K., Mackay, F., Strasser, A., et al. (2013). Mcl-1 is essential for the survival of plasma cells. Nat Immunol *14*, 290–297.

Perlman, H., and Pope, R.M. (2010). The synovial lining micromass system: toward rheumatoid arthritis in a dish? Arthritis Rheum *62*, 643–646.

Perry, D.K., Burns, J.M., Pollinger, H.S., Amiot, B.P., Gloor, J.M., Gores, G.J., and Stegall, M.D. (2009). Proteasome inhibition causes apoptosis of normal human plasma cells preventing alloantibody production. Am. J. Transplant. *9*, 201–209.

Pertschy, B., Schneider, C., Gnädig, M., Schäfer, T., Tollervey, D., and Hurt, E. (2009). RNA helicase Prp43 and its co-factor Pfa1 promote 20 to 18 S rRNA processing catalyzed by the endonuclease Nob1. The Journal of Biological Chemistry *284*, 35079–35091.

Pikwer, M., Giwercman, A., Bergström, U., Nilsson, J.-Å., Jacobsson, L.T.H., and Turesson, C. (2013). Association between testosterone levels and risk of future rheumatoid arthritis in men: a population-based case-control study. Ann. Rheum. Dis.

Pistoia, V. (1997). Production of cytokines by human B cells in health and disease. Immunol. Today *18*, 343–350.

Plant, D., Bowes, J., Potter, C., Hyrich, K.L., Morgan, A.W., Wilson, A.G., Isaacs, J.D., Wellcome Trust Case Control Consortium, British Society for Rheumatology Biologics Register, and Barton, A. (2011). Genome-wide association study of genetic predictors of anti-tumor necrosis factor treatment efficacy in rheumatoid arthritis identifies associations with polymorphisms at seven loci. Arthritis Rheum *63*, 645–653.

Plenge, R.M., Cotsapas, C., Davies, L., Price, A.L., de Bakker, P.I.W., Maller, J., Pe'er, I., Burtt, N.P., Blumenstiel, B., DeFelice, M., et al. (2007). Two independent alleles at 6q23 associated with risk of rheumatoid arthritis. Nat. Genet. *39*, 1477–1482.

Prehn, J.L., Mehdizadeh, S., Landers, C.J., Luo, X., Cha, S.C., Wei, P., and Targan, S.R. (2004). Potential role for TL1A, the new TNF-family member and potent costimulator of IFN-gamma, in mucosal inflammation. Clin Immunol *112*, 66–77.

Prehn, J.L., Thomas, L.S., Landers, C.J., Yu, Q.T., Michelsen, K.S., and Targan, S.R. (2007). The T cell costimulator TL1A is induced by FcgammaR signaling in human monocytes and dendritic cells. J Immunol *178*, 4033–4038.

Presta, M., Andrés, G., Leali, D., Dell'Era, P., and Ronca, R. (2009). Inflammatory cells and chemokines sustain FGF2-induced angiogenesis. Eur. Cytokine Netw. *20*, 39–50.

Radner, H., Neogi, T., Smolen, J.S., and Aletaha, D. Performance of the 2010 ACR/EULAR classification criteria for rheumatoid arthritis: a systematic literature review. Ard.Bmj.com.

Raposo, B.R., Rodrigues-Santos, P., Carvalheiro, H., Água-Doce, A.M., Carvalho, L., Pereira da Silva, J.A., Graça, L., and Souto-Carneiro, M.M. (2010). Monoclonal anti-CD8 therapy induces disease amelioration in the K/BxN mouse model of spontaneous chronic polyarthritis. Arthritis Rheum *62*, 2953–2962.

Raza, K., Mullazehi, M., Salmon, M., Buckley, C.D., and Ronnelid, J. (2007). Anti-collagen type II antibodies in patients with very early synovitis. Ann. Rheum. Dis. *67*, 1354–1355.

Remmers, E.F., Plenge, R.M., Lee, A.T., Graham, R.R., Hom, G., Behrens, T.W., de Bakker, P.I.W., Le, J.M., Lee, H.-S., Batliwalla, F., et al. (2007). STAT4 and the risk of rheumatoid arthritis and systemic lupus erythematosus. N Engl J Med *357*, 977–986.

Rico, M.C., Rough, J.J., Del Carpio-Cano, F.E., Kunapuli, S.P., and Cadena, DeLa, R.A. (2010). The axis of thrombospondin-1, transforming growth factor beta and connective tissue growth factor: an emerging therapeutic target in rheumatoid arthritis. Curr Vasc Pharmacol *8*, 338–343.

Rivera-Nieves, J., Bamias, G., Vidrich, A., Marini, M., Pizarro, T.T., McDuffie, M.J., Moskaluk, C.A., Cohn, S.M., and Cominelli, F. (2003). Emergence of perianal fistulizing disease in the SAMP1/YitFc mouse, a spontaneous model of chronic ileitis. Gastroenterology *124*, 972–982.

Rogers, K. (2010). Bone and Muscle: Structure, Force, and Motion.

Ropes, M.W., Bennett, G.A., Cobb, S., Jacox, R., and Jessar, R.A. (1957). Proposed diagnostic criteria for rheumatoid arthritis: report of a study conducted by a committee of the American Rheumatism Association. Ann. Rheum. Dis. *16*, 118.

Rosengren, S., Corr, M., and Boyle, D.L. (2010). Platelet-derived growth factor and transforming growth factor beta synergistically potentiate inflammatory mediator synthesis by fibroblast-like synoviocytes. Arthritis Res. Ther. *12*, R65.

Rönnelid, J., Lysholm, J., Engström-Laurent, A., Klareskog, L., and Heyman, B. (1994). Local anti—type ii collagen antibody production in rheumatoid arthritis synovial fluid. Arthritis Rheum *37*, 1023–1029.

S, B., HS, L., SB, M., and WM, O. (1988). Serum IgG anti-native type II collagen antibodies

in rheumatoid arthritis: association with HLA DR4 and lack of clinical correlation. Clin Exp Rheumatol *6*, 373–380.

Saag, K.G., Teng, G.G., Patkar, N.M., Anuntiyo, J., Finney, C., Curtis, J.R., Paulus, H.E., Mudano, A., Pisu, M., Elkins-Melton, M., et al. (2008). American College of Rheumatology 2008 recommendations for the use of nonbiologic and biologic disease-modifying antirheumatic drugs in rheumatoid arthritis. Arthritis Rheum *59*, 762–784.

Sakata, M., Tsuruha, J.I., Masuko-Hongo, K., Nakamura, H., Matsui, T., Sudo, A., Nishioka, K., and Kato, T. (2001). Autoantibodies to osteopontin in patients with osteoarthritis and rheumatoid arthritis. The Journal of Rheumatology *28*, 1492–1495.

Sarkar, S., Cooney, L.A., White, P., Dunlop, D.B., Endres, J., Jorns, J.M., Wasco, M.J., and Fox, D.A. (2009). Regulation of pathogenic IL-17 responses in collagen-induced arthritis: roles of endogenous interferon-gamma and IL-4. Arthritis Res. Ther. *11*, R158.

Sarris, M., Andersen, K.G., Randow, F., Mayr, L., and Betz, A.G. (2008). Neuropilin-1 expression on regulatory T cells enhances their interactions with dendritic cells during antigen recognition. Immunity *28*, 402–413.

Saruta, M., Michelsen, K.S., Thomas, L.S., Yu, Q.T., Landers, C.J., and Targan, S.R. (2009). TLR8-mediated activation of human monocytes inhibits TL1A expression. Eur. J. Immunol. *39*, 2195–2202.

Saulot, V., Vittecoq, O., Charlionet, R., Fardellone, P., Lange, C., Marvin, L., Machour, N., Le Lo t, X., Gilbert, D.L., and Tron, F.O. (2002). Presence of autoantibodies to the glycolytic enzyme ?-enolase in sera from patients with early rheumatoid arthritis. Arthritis Rheum *46*, 1196–1201.

Schaerli, P., Willimann, K., Lang, A.B., Lipp, M., Loetscher, P., and Moser, B. (2000). CXC chemokine receptor 5 expression defines follicular homing T cells with B cell helper function. J. Exp. Med. *192*, 1553–1562.

Schaller, M., Burton, D.R., and Ditzel, H.J. (2001). Autoantibodies to GPI in rheumatoid arthritis: linkage between an animal model and human disease - Nature Immunology. Nat Immunol *2*, 746–753.

Schedel, J., Gay, R.E., Kuenzler, P., Seemayer, C., Simmen, B., Michel, B.A., and Gay, S. (2002). FLICE-inhibitory protein expression in synovial fibroblasts and at sites of cartilage and bone erosion in rheumatoid arthritis. Arthritis Rheum *46*, 1512–1518.

Schellekens, G.A., Visser, H., de Jong, B.A., van den Hoogen, F.H., Hazes, J.M., Breedveld, F.C., and van Venrooij, W.J. (2000). The diagnostic properties of rheumatoid arthritis antibodies recognizing a cyclic citrullinated peptide. Arthritis Rheum *43*, 155–163.

Schneider, P., MacKay, F., Steiner, V., Hofmann, K., Bodmer, J.L., Holler, N., Ambrose, C., Lawton, P., Bixler, S., Acha-Orbea, H., et al. (1999). BAFF, a novel ligand of the tumor

necrosis factor family, stimulates B cell growth. J. Exp. Med. *189*, 1747–1756.

Schreiber, T.H., Wolf, D., Tsai, M.S., Chirinos, J., Deyev, V.V., Gonzalez, L., Malek, T.R., Levy, R.B., and Podack, E.R. (2010). Therapeutic Treg expansion in mice by TNFRSF25 prevents allergic lung inflammation. J Clin Invest *120*, 3629–3640.

Schubert, D., Schmidt, M., and Zaiss, D. (2002). Autoantibodies to GPI and creatine kinase in RA. Nature.

Schuerwegh, A.J.M., Ioan-Facsinay, A., Dorjee, A.L., Roos, J., Bajema, I.M., van der Voort, E.I.H., Huizinga, T.W.J., and Toes, R.E.M. (2010). Evidence for a functional role of IgE anticitrullinated protein antibodies in rheumatoid arthritis. Proceedings of the National Academy of Sciences *107*, 2586–2591.

Scott, D.L. (2012). Biologics-based therapy for the treatment of rheumatoid arthritis. Clin. Pharmacol. Ther. *91*, 30–43.

Scott, D.L., Wolfe, F., and Huizinga, T.W.J. (2010). Rheumatoid arthritis. Lancet *376*, 1094–1108.

Screaton, G.R., Xu, X.N., Olsen, A.L., Cowper, A.E., Tan, R., McMichael, A.J., and Bell, J.I. (1997). LARD: a new lymphoid-specific death domain containing receptor regulated by alternative pre-mRNA splicing. Proc Natl Acad Sci USA *94*, 4615–4619.

Senapin, S., Clark-Walker, G.D., Chen, X.J., Séraphin, B., and Daugeron, M.-C. (2003). RRP20, a component of the 90S preribosome, is required for pre-18S rRNA processing in Saccharomyces cerevisiae. Nucleic Acids Res. *31*, 2524–2533.

Shaffer, A.L., Shapiro-Shelef, M., Iwakoshi, N.N., Lee, A.-H., Qian, S.-B., Zhao, H., Yu, X., Yang, L., Tan, B.K., Rosenwald, A., et al. (2004). XBP1, downstream of Blimp-1, expands the secretory apparatus and other organelles, and increases protein synthesis in plasma cell differentiation. Immunity *21*, 81–93.

Shahrara, S., Pickens, S.R., Dorfleutner, A., and Pope, R.M. (2009). IL-17 induces monocyte migration in rheumatoid arthritis. The Journal of Immunology *182*, 3884–3891.

Shahrara, S., Pickens, S.R., Mandelin, A.M., Karpus, W.J., Huang, Q., Kolls, J.K., and Pope, R.M. (2010). IL-17-mediated monocyte migration occurs partially through CC chemokine ligand 2/monocyte chemoattractant protein-1 induction. The Journal of Immunology *184*, 4479–4487.

Shalev, I., Liu, H., Koscik, C., Bartczak, A., Javadi, M., Wong, K.M., Maknojia, A., He, W., Liu, M.F., Diao, J., et al. (2008). Targeted deletion of fgl2 leads to impaired regulatory T cell activity and development of autoimmune glomerulonephritis. J Immunol *180*, 249–260.

Shalom-Barak, T., Quach, J., and Lotz, M. (1998). Interleukin-17-induced gene expression in articular chondrocytes is associated with activation of mitogen-activated protein kinases and

NF-kappaB. The Journal of Biological Chemistry *273*, 27467–27473.

Shelef, M.A., Bennin, D.A., Mosher, D.F., and Huttenlocher, A. (2012). Citrullination of fibronectin modulates synovial fibroblast behavior. Arthritis Res. Ther. *14*, R240.

Shevach, E.M. (2009). Mechanisms of foxp3+ T regulatory cell-mediated suppression. Immunity *30*, 636–645.

Shi, G., Wu, Y., Zhang, J., and Wu, J. (2003). Death decoy receptor TR6/DcR3 inhibits T cell chemotaxis in vitro and in vivo. J Immunol *171*, 3407–3414.

Shichikawa, K., Inoue, K., Hirota, S., Maeda, A., Ota, H., Kimura, M., Ushiyama, T., and Tsujimoto, M. (1999). Changes in the incidence and prevalence of rheumatoid arthritis in Kamitonda, Wakayama, Japan, 1965-1996. Ann. Rheum. Dis. *58*, 751–756.

Shih, D.Q., and Targan, S.R. (2009). Insights into IBD Pathogenesis. *11*, 473–480.

Shih, D.Q., Barrett, R., Zhang, X., Yeager, N., Koon, H.W., Phaosawasdi, P., Song, Y., Ko, B., Wong, M.H., Michelsen, K.S., et al. (2011a). Constitutive TL1A (TNFSF15) expression on lymphoid or myeloid cells leads to mild intestinal inflammation and fibrosis. PLoS ONE *6*, e16090.

Shih, D.Q., Kwan, L.Y., Chavez, V., Cohavy, O., Gonsky, R., Chang, E.Y., Chang, C., Elson, C.O., and Targan, S.R. (2009). Microbial induction of inflammatory bowel disease associated gene TL1A (TNFSF15) in antigen presenting cells. Eur J Immunol *39*, 3239–3250.

Shih, D.Q., Michelsen, K.S., Barrett, R.J., Biener-Ramanujan, E., Gonsky, R., Zhang, X., and Targan, S.R. (2011b). Insights into TL1A and IBD pathogenesis. Adv Exp Med Biol *691*, 279–288.

Shiozawa, S., Hayashi, S., Tsukamoto, Y., Goko, H., Kawasaki, H., Wada, T., Shimizu, K., Yasuda, N., Kamatani, N., Takasugi, K., et al. (1998). Identification of the gene loci that predispose to rheumatoid arthritis. Int. Immunol. *10*, 1891–1895.

Silman, A., Kay, A., and Brennan, P. (1992). Timing of pregnancy in relation to the onset of rheumatoid arthritis. Arthritis Rheum *35*, 152–155.

Simpson, N., Gatenby, P.A., Wilson, A., Malik, S., Fulcher, D.A., Tangye, S.G., Manku, H., Vyse, T.J., Roncador, G., Huttley, G.A., et al. (2010). Expansion of circulating T cells resembling follicular helper T cells is a fixed phenotype that identifies a subset of severe systemic lupus erythematosus. Arthritis Rheum *62*, 234–244.

Singh, J.A., Furst, D.E., Bharat, A., Curtis, J.R., Kavanaugh, A.F., Kremer, J.M., Moreland, L.W., O'dell, J., Winthrop, K.L., Beukelman, T., et al. (2012). 2012 Update of the 2008 American College of Rheumatology recommendations for the use of disease-modifying antirheumatic drugs and biologic agents in the treatment of rheumatoid arthritis. Arthritis Care Res *64*, 625–639.

Singh, J.A., Pando, J.A., Tomaszewski, J., and Schumacher, H.R. (2004). Quantitative analysis of immunohistologic features of very early rheumatoid synovitis in disease modifying antirheumatic drug- and corticosteroid-naïve patients. The Journal of Rheumatology *31*, 1281–1285.

Singh, J.A., Wells, G.A., Christensen, R., Tanjong Ghogomu, E., Maxwell, L., Macdonald, J.K., Filippini, G., Skoetz, N., Francis, D., Lopes, L.C., et al. (2011). Adverse effects of biologics: a network meta-analysis and Cochrane overview. Cochrane Database Syst Rev CD008794.

Skapenko, A., Leipe, J., and Lipsky, P.E. (2005). The role of the T cell in autoimmune inflammation. Arthritis Research and ….

Smith, K.G., Hewitson, T.D., Nossal, G.J., and Tarlinton, D.M. (1996). The phenotype and fate of the antibody-forming cells of the splenic foci. Eur. J. Immunol. *26*, 444–448.

Sokolove, J., Zhao, X., Chandra, P.E., and Robinson, W.H. (2011). Immune complexes containing citrullinated fibrinogen costimulate macrophages via Toll-like receptor 4 and Fcγ receptor. Arthritis Rheum *63*, 53–62.

Spector, T.D., Perry, L.A., Tubb, G., Silman, A.J., and Huskisson, E.C. (1988). Low free testosterone levels in rheumatoid arthritis. Ann. Rheum. Dis. *47*, 65–68.

Spolski, R., and Leonard, W.J. (2008). Interleukin-21: Basic Biology and Implications for Cancer and Autoimmunity*. Annu. Rev. Immunol. *26*, 57–79.

Steinert, P.M., Parry, D.A., Idler, W.W., Johnson, L.D., Steven, A.C., and Roop, D.R. (1985). Amino acid sequences of mouse and human epidermal type II keratins of Mr 67,000 provide a systematic basis for the structural and functional diversity of the end domains of keratin intermediate filament subunits. Journal of Biological ….

Strand, V., Kimberly, R., and Isaacs, J.D. (2007). Biologic therapies in rheumatology: lessons learned, future directions. Nat Rev Drug Discov *6*, 75–92.

Stuart, J.M., and Dixon, F.J. (1983). Serum transfer of collagen-induced arthritis in mice. J. Exp. Med. *158*, 378–392.

Stuart, J.M., Cremer, M.A., Townes, A.S., and Kang, A.H. (1982). Type II collagen-induced arthritis in rats. Passive transfer with serum and evidence that IgG anticollagen antibodies can cause arthritis. J. Exp. Med. *155*, 1–16.

Stuart, J.M., Townes, A.S., and Kang, A.H. (1984). Collagen autoimmune arthritis. Annu. Rev. Immunol. *2*, 199–218.

Su, W.B., Chang, Y.-H., Lin, W.-W., and Hsieh, S.-L. (2006). Differential regulation of interleukin-8 gene transcription by death receptor 3 (DR3) and type I TNF receptor (TNFRI). Exp. Cell Res. *312*, 266–277.

Sun, X., Zhao, J., Liu, R., Jia, R., Sun, L., Li, X., and Li, Z. (2013). Elevated serum and synovial fluid TNF-like ligand 1A (TL1A) is associated with autoantibody production in patients with rheumatoid arthritis. Scand. J. Rheumatol. *42*, 97–101.

Suzuki, A., Yamada, R., Chang, X., Tokuhiro, S., Sawada, T., Suzuki, M., Nagasaki, M., Nakayama-Hamada, M., Kawaida, R., Ono, M., et al. (2003). Functional haplotypes of PADI4, encoding citrullinating enzyme peptidylarginine deiminase 4, are associated with rheumatoid arthritis. Nat. Genet. *34*, 395–402.

Symmons, D.P., Bankhead, C.R., Harrison, B.J., Brennan, P., Silman, A.J., Barrett, E.M., and Scott, D.G. (1997). Blood transfusion, smoking, and obesity as risk factors for the development of rheumatoid arthritis. Results from a primary care‐based incident case‐control study in Norfolk, England. Arthritis Rheum *40*, 1955–1961.

Szabo, S.J., Kim, S.T., Costa, G.L., Zhang, X., Fathman, C.G., and Glimcher, L.H. (2000). A novel transcription factor, T-bet, directs Th1 lineage commitment. Cell *100*, 655–669.

Sze, D.M., Toellner, K.M., García de Vinuesa, C., Taylor, D.R., and MacLennan, I.C. (2000). Intrinsic constraint on plasmablast growth and extrinsic limits of plasma cell survival. J. Exp. Med. *192*, 813–821.

Tabushi, Y., Nakanishi, T., Takeuchi, T., Nakajima, M., Ueda, K., Kotani, T., Makino, S., Shimizu, A., Hanafusa, T., and Takubo, T. Detection of citrullinated proteins in synovial fluids derived from patients with rheumatoid arthritis by proteomics-based analysis. Acb.Sagepub.com.

Tada, Y., Ho, A., Koh, D.R., and Mak, T.W. (1996). Collagen-induced arthritis in CD4- or CD8-deficient mice: CD8+ T cells play a role in initiation and regulate recovery phase of collagen-induced arthritis. J Immunol *156*, 4520–4526.

Tak, P.P., Smeets, T.J., Daha, M.R., Kluin, P.M., Meijers, K.A., Brand, R., Meinders, A.E., and Breedveld, F.C. (1997). Analysis of the synovial cell infiltrate in early rheumatoid synovial tissue in relation to local disease activity. Arthritis Rheum *40*, 217–225.

Takagi, T., and Jasin, H.E. (1992). Interactions between anticollagen antibodies and chondrocytes. Arthritis Rheum *35*, 224–230.

Takahashi, M., Miura, Y., Hayashi, S., Tateishi, K., Fukuda, K., and Kurosaka, M. (2011). DcR3-TL1A signalling inhibits cytokine-induced proliferation of rheumatoid synovial fibroblasts. Int J Mol Med *28*, 423–427.

Takedatsu, H., Michelsen, K.S., Wei, B., Landers, C.J., Thomas, L.S., Dhall, D., Braun, J., and Targan, S.R. (2008). TL1A (TNFSF15) regulates the development of chronic colitis by modulating both T-helper 1 and T-helper 17 activation. Gastroenterology *135*, 552–567.

Takemura, S., Klimiuk, P.A., Braun, A., Goronzy, J.J., and Weyand, C.M. (2001). T cell activation in rheumatoid synovium is B cell dependent. J Immunol *167*, 4710–4718.

Tan, K.B., Harrop, J., Reddy, M., Young, P., Terrett, J., Emery, J., Moore, G., and Truneh, A. (1997). Characterization of a novel TNF-like ligand and recently described TNF ligand and TNF receptor superfamily genes and their constitutive and inducible expression in hematopoietic and non-hematopoietic cells. Gene *204*, 35–46.

Tan, L.C., Mowat, A.G., Fazou, C., Rostron, T., Roskell, H., Dunbar, P.R., Tournay, C., Romagné, F., Peyrat, M.A., Houssaint, E., et al. (2000). Specificity of T cells in synovial fluid: high frequencies of CD8(+) T cells that are specific for certain viral epitopes. Arthritis Res. *2*, 154–164.

Tanaka, D., Kagari, T., and Shimozato, T. (2006). Essential role of neutrophils in anti-type II collagen antibody and lipopolysaccharide-induced arthritis. Immunology.

Taneja, V., Taneja, N., Paisansinsup, T., Behrens, M., Griffiths, M., Luthra, H., and David, C.S. (2002). CD4 and CD8 T cells in susceptibility/protection to collagen-induced arthritis in HLA-DQ8-transgenic mice: implications for rheumatoid arthritis. J Immunol *168*, 5867–5875.

Taraban, V.Y., Slebioda, T.J., Willoughby, J.E., Buchan, S.L., James, S., Sheth, B., Smyth, N.R., Thomas, G.J., Wang, E.C.Y., and Al-Shamkhani, A. (2011). Sustained TL1A expression modulates effector and regulatory T-cell responses and drives intestinal goblet cell hyperplasia. Mucosal Immunology *4*, 186–196.

Taylor, A., Verhagen, J., Blaser, K., Akdis, M., and Akdis, C.A. (2006). Mechanisms of immune suppression by interleukin-10 and transforming growth factor-beta: the role of T regulatory cells. Immunology *117*, 433–442.

Terato, K., Hasty, K.A., Reife, R.A., Cremer, M.A., Kang, A.H., and Stuart, J.M. (1992). Induction of arthritis with monoclonal antibodies to collagen. The Journal of ….

Thompson, J.S., Schneider, P., Kalled, S.L., Wang, L., Lefevre, E.A., Cachero, T.G., MacKay, F., Bixler, S.A., Zafari, M., Liu, Z.Y., et al. (2000). BAFF binds to the tumor necrosis factor receptor-like molecule B cell maturation antigen and is important for maintaining the peripheral B cell population. J. Exp. Med. *192*, 129–135.

Tobón, G.J., Youinou, P., and Saraux, A. (2010). The environment, geo-epidemiology, and autoimmune disease: Rheumatoid arthritis. J. Autoimmun. *35*, 10–14.

Todd, D.J., McHeyzer-Williams, L.J., Kowal, C., Lee, A.-H., Volpe, B.T., Diamond, B., McHeyzer-Williams, M.G., and Glimcher, L.H. (2009). XBP1 governs late events in plasma cell differentiation and is not required for antigen-specific memory B cell development. J. Exp. Med. *206*, 2151–2159.

Tone, Y., Tanahashi, N., Tanaka, K., Fujimuro, M., Yokosawa, H., and Toh-e, A. (2000). Nob1p, a new essential protein, associates with the 26S proteasome of growing saccharomyces cerevisiae cells. Gene *243*, 37–45.

Tone, Y., and Toh-E, A. (2002). Nob1p is required for biogenesis of the 26S proteasome and

degraded upon its maturation in Saccharomyces cerevisiae. Genes Dev *16*, 3142–3157.

Trentham, D.E., Townes, A.S., and Kang, A.H. (1977). Autoimmunity to type II collagen an experimental model of arthritis. J. Exp. Med. *146*, 857–868.

Trentham, D.E., Townes, A.S., Kang, A.H., and David, J.R. (1978). Humoral and cellular sensitivity to collagen in type II collagen-induced arthritis in rats. J Clin Invest *61*, 89–96.

Tschochner, H., and Hurt, E. (2003). Pre-ribosomes on the road from the nucleolus to the cytoplasm. Trends Cell Biol. *13*, 255–263.

Tsuji, S., Cortesao, C., Bram, R.J., Platt, J.L., and Cascalho, M. (2011). TACI deficiency impairs sustained Blimp-1 expression in B cells decreasing long-lived plasma cells in the bone marrow. Blood *118*, 5832–5839.

Twohig, J.P., Marsden, M., Cuff, S.M., Ferdinand, J.R., Gallimore, A.M., Perks, W.V., Al-Shamkhani, A., Humphreys, I.R., and Wang, E.C.Y. (2012). The death receptor 3/TL1A pathway is essential for efficient development of antiviral CD4+ and CD8+ T-cell immunity. Faseb J.

Uo, M., Hisamatsu, T., Miyoshi, J., Kaito, D., Yoneno, K., Kitazume, M.T., Mori, M., Sugita, A., Koganei, K., Matsuoka, K., et al. (2012). Mucosal CXCR4+ IgG plasma cells contribute to the pathogenesis of human ulcerative colitis through FcγR-mediated CD14 macrophage activation. Gut.

Upchurch, K.S., and Kay, J. (2012). Evolution of treatment for rheumatoid arthritis. Rheumatology (Oxford) *51*, vi28–vi36.

Valencia, X., Stephens, G., Goldbach-Mansky, R., Wilson, M., Shevach, E.M., and Lipsky, P.E. (2006). TNF downmodulates the function of human CD4+CD25hi T-regulatory cells. Blood *108*, 253–261.

van Amelsfort, J.M.R., Jacobs, K.M.G., Bijlsma, J.W.J., Lafeber, F.P.J.G., and Taams, L.S. (2004). CD4(+)CD25(+) regulatory T cells in rheumatoid arthritis: differences in the presence, phenotype, and function between peripheral blood and synovial fluid. Arthritis Rheum *50*, 2775–2785.

van Anken, E., Romijn, E.P., Maggioni, C., Mezghrani, A., Sitia, R., Braakman, I., and Heck, A.J.R. (2003). Sequential Waves of Functionally Related Proteins Are Expressed When B Cells Prepare for Antibody Secretion. Immunity *18*, 243–253.

van den Berg, W.B., and Miossec, P. (2009). IL-17 as a future therapeutic target for rheumatoid arthritis. Nat Rev Rheumatol *5*, 549–553.

van der Helm-van Mil, A.H.M., Verpoort, K.N., le Cessie, S., Huizinga, T.W.J., de Vries, R.R.P., and Toes, R.E.M. (2007). The HLA-DRB1 shared epitope alleles differ in the interaction with smoking and predisposition to antibodies to cyclic citrullinated peptide.

Arthritis Rheum *56*, 425–432.

van der Helm-van Mil, A.H.M., Wesoly, J.Z., and Huizinga, T.W.J. (2005). Understanding the genetic contribution to rheumatoid arthritis. Curr Opin Rheumatol *17*, 299–304.

Van der Linden, M., and Knevel, R. (2011). Classification of rheumatoid arthritis: Comparison of the 1987 American College of Rheumatology criteria and the 2010 American College of Rheumatology/European League Against Rheumatism criteria - van der Linden - 2010 - Arthritis & Rheumatism - Wiley Online Library. … & Rheumatism.

van Hamburg, J.P., Asmawidjaja, P.S., Davelaar, N., Mus, A.M.C., Colin, E.M., Hazes, J.M.W., Dolhain, R.J.E.M., and Lubberts, E. (2010). Th17 cells, but not Th1 cells, from patients with early rheumatoid arthritis are potent inducers of matrix metalloproteinases and proinflammatory cytokines upon synovial fibroblast interaction, including autocrine interleukin-17A production - van Hamburg - 2010 - Arthritis & Rheumatism - Wiley Online Library. Arthritis Rheum *63*, 73–83.

van Roon, J.A., van Roy, J.L., Gmelig-Meyling, F.H., Lafeber, F.P., and Bijlsma, J.W. (1996). Prevention and reversal of cartilage degradation in rheumatoid arthritis by interleukin-10 and interleukin-4. Arthritis Rheum *39*, 829–835.

Vanrobays, E., Gélugne, J.-P., Caizergues-Ferrer, M., and Lafontaine, D.L.J. (2004). Dim2p, a KH-domain protein required for small ribosomal subunit synthesis. Rna *10*, 645–656.

Vanrobays, E., Leplus, A., Osheim, Y.N., Beyer, A.L., Wacheul, L., and Lafontaine, D.L.J. (2008). TOR regulates the subcellular distribution of DIM2, a KH domain protein required for cotranscriptional ribosome assembly and pre-40S ribosome export. Rna *14*, 2061–2073.

Vermeire, K., Heremans, H., Vandeputte, M., Huang, S., Billiau, A., and Matthys, P. (1997). Accelerated collagen-induced arthritis in IFN-gamma receptor-deficient mice. J Immunol *158*, 5507–5513.

Verpoort, K.N., Papendrecht-van der Voort, E.A.M., van der Helm-van Mil, A.H.M., Jol-van der Zijde, C.M., van Tol, M.J.D., Drijfhout, J.W., Breedveld, F.C., de Vries, R.R.P., Huizinga, T.W.J., and Toes, R.E.M. (2007). Association of smoking with the constitution of the anti-cyclic citrullinated peptide response in the absence of HLA-DRB1 shared epitope alleles. Arthritis Rheum *56*, 2913–2918.

Villarino, A.V., and Hunter, C.A. (2004). Biology of recently discovered cytokines: discerning the pro- and anti-inflammatory properties of interleukin-27. Arthritis Res. Ther. *6*, 225–233.

Vinuesa, C.G., Cook, M.C., Angelucci, C., Athanasopoulos, V., Rui, L., Hill, K.M., Yu, D., Domaschenz, H., Whittle, B., Lambe, T., et al. (2005). A RING-type ubiquitin ligase family member required to repress follicular helper T cells and autoimmunity. Nature *435*, 452–458.

Vossenaar, E.R., Radstake, T.R.D., van der Heijden, A., van Mansum, M.A.M., Dieteren, C., de Rooij, D.-J., Barrera, P., Zendman, A.J.W., and van Venrooij, W.J. (2004). Expression and

activity of citrullinating peptidylarginine deiminase enzymes in monocytes and macrophages. Ann. Rheum. Dis. *63*, 373–381.

Vossenaar, E.R., Zendman, A.J.W., van Venrooij, W.J., and Pruijn, G.J.M. (2003). PAD, a growing family of citrullinating enzymes: genes, features and involvement in disease. Bioessays *25*, 1106–1118.

Vukmanovic-Stejic, M., Vyas, B., Gorak-Stolinska, P., Noble, A., and Kemeny, D.M. Human Tc1 and Tc2/Tc0 CD8 T-cell clones display distinct cell surface and functional phenotypes. Bloodjournal.Hematologylibrary.org.

Waaler, E. (1940). ON THE OCCURRENCE OF A FACTOR IN HUMAN SERUM ACTIVATING THE SPECIFIC AGGLUTINATION OF SHEEP BLOOD CORPUSCLES. Acta Pathologica Microbiologica Scandinavica *17*, 172–188.

Wagner, U.G., Kurtin, P.J., Wahner, A., Brackertz, M., Berry, D.J., Goronzy, J.J., and Weyand, C.M. (1998). The role of CD8+ CD40L+ T cells in the formation of germinal centers in rheumatoid synovitis. J Immunol *161*, 6390–6397.

Wahl, S.M., Allen, J.B., Ohura, K., Chenoweth, D.E., and Hand, A.R. (1991). IFN-gamma inhibits inflammatory cell recruitment and the evolution of bacterial cell wall-induced arthritis. J Immunol *146*, 95–100.

Wakasa-Morimoto, C., Toyosaki-Maeda, T., Matsutani, T., Yoshida, R., Nakamura-Kikuoka, S., Maeda-Tanimura, M., Yoshitomi, H., Hirota, K., Hashimoto, M., Masaki, H., et al. (2008). Arthritis and pneumonitis produced by the same T cell clones from mice with spontaneous autoimmune arthritis. Int. Immunol. *20*, 1331–1342.

Walter, P., and Ron, D. (2011). The unfolded protein response: from stress pathway to homeostatic regulation. Science *334*, 1081–1086.

Wang, E.C., Kitson, J., Thern, A., Williamson, J., Farrow, S.N., and Owen, M.J. (2001). Genomic structure, expression, and chromosome mapping of the mouse homologue for the WSL-1 (DR3, Apo3, TRAMP, LARD, TR3, TNFRSF12) gene. Immunogenetics *53*, 59–63.

Wang, J., Shan, Y., Jiang, Z., Feng, J., Li, C., Ma, L., and Jiang, Y. (2013). High frequencies of activated B cells and follicular helper T cells are correlated with disease activity in patients with new onset rheumatoid arthritis. Clinical and Experimental Immunology.

Wasserman, A.M. (2011). Diagnosis and management of rheumatoid arthritis. American Family Physician *84*, 1245.

Weaver, C.T., Harrington, L.E., Mangan, P.R., Gavrieli, M., and Murphy, K.M. (2006). Th17: an effector CD4 T cell lineage with regulatory T cell ties. Immunity *24*, 677–688.

Weinblatt, M.E., Kremer, J.M., Bankhurst, A.D., Bulpitt, K.J., Fleischmann, R.M., Fox, R.I., Jackson, C.G., Lange, M., and Burge, D.J. (1999). A Trial of Etanercept, a Recombinant

Tumor Necrosis Factor Receptor:Fc Fusion Protein, in Patients with Rheumatoid Arthritis Receiving Methotrexate. N Engl J Med *340*, 253–259.

Wen, L., Zhuang, L., Luo, X., and Wei, P. (2003). TL1A-induced NF-kappaB activation and c-IAP2 production prevent DR3-mediated apoptosis in TF-1 cells. The Journal of Biological Chemistry *278*, 39251–39258.

Wiest, D.L., Burkhardt, J.K., Hester, S., Hortsch, M., Meyer, D.I., and Argon, Y. (1990). Membrane biogenesis during B cell differentiation: most endoplasmic reticulum proteins are expressed coordinately. J. Cell Biol. *110*, 1501–1511.

Wildin, R.S., Ramsdell, F., Peake, J., Faravelli, F., Casanova, J.L., Buist, N., Levy-Lahad, E., Mazzella, M., Goulet, O., Perroni, L., et al. (2001). X-linked neonatal diabetes mellitus, enteropathy and endocrinopathy syndrome is the human equivalent of mouse scurfy. Nat. Genet. *27*, 18–20.

Wing, K., Onishi, Y., Prieto-Martin, P., Yamaguchi, T., Miyara, M., Fehervari, Z., Nomura, T., and Sakaguchi, S. (2008). CTLA-4 control over Foxp3+ regulatory T cell function. Science *322*, 271–275.

Wipke, B.T., and Allen, P.M. (2001). Essential role of neutrophils in the initiation and progression of a murine model of rheumatoid arthritis. J Immunol *167*, 1601–1608.

Wipke, B.T., Wang, Z., Kim, J., McCarthy, T.J., and Allen, P.M. (2002). Dynamic visualization of a joint-specific autoimmune response through positron emission tomography. Nat Immunol *3*, 366–372.

Wood, K.J., and Sawitzki, B. (2006). Interferon gamma: a crucial role in the function of induced regulatory T cells in vivo. Trends in Immunology *27*, 183–187.

Woolls, H.A., Lamanna, A.C., and Karbstein, K. (2011). Roles of Dim2 in ribosome assembly. Journal of Biological Chemistry *286*, 2578–2586.

Yahya, A., Bengtsson, C., Larsson, P., Too, C.L., Mustafa, A.N., Abdullah, N.A., Muhamad, N.A., Klareskog, L., Murad, S., and Alfredsson, L. (2013). Silica exposure is associated with an increased risk of developing ACPA-positive rheumatoid arthritis in an Asian population: evidence from the Malaysian MyEIRA case–control study. Mod Rheumatol 1–5.

Yanaba, K., Hamaguchi, Y., Venturi, G.M., Steeber, D.A., St Clair, E.W., and Tedder, T.F. (2007). B cell depletion delays collagen-induced arthritis in mice: arthritis induction requires synergy between humoral and cell-mediated immunity. J Immunol *179*, 1369–1380.

Yoo, S.-A., Yoon, H.-J., Kim, H.-S., Chae, C.-B., De Falco, S., Cho, C.-S., and Kim, W.-U. (2009). Role of placenta growth factor and its receptor flt-1 in rheumatoid inflammation: A link between angiogenesis and inflammation. Arthritis Rheum *60*, 345–354.

Yoo, S.-A., You, S., Yoon, H.-J., Kim, D.-H., Kim, H.-S., Lee, K., Ahn, J.H., Hwang, D., Lee,

A.S., Kim, K.-J., et al. (2012). A novel pathogenic role of the ER chaperone GRP78/BiP in rheumatoid arthritis. J. Exp. Med. *209*, 871–886.

Yoshida, M., Tsuji, M., Kurosaka, D., Kurosaka, D., Yasuda, J., Ito, Y., Nishizawa, T., and Yamada, A. (2006). Autoimmunity to citrullinated type II collagen in rheumatoid arthritis. Mod Rheumatol *16*, 276–281.

Yu, G., Boone, T., Delaney, J., Hawkins, N., Kelley, M., Ramakrishnan, M., McCabe, S., Qiu, W.-R., Kornuc, M., Xia, X.-Z., et al. (2000). APRIL and TALL-1 and receptors BCMA and TACI: system for regulating humoral

immunity. Nat Immunol *1*, 252–256.

Yudoh, K., Matsuno, H., Nakazawa, F., Yonezawa, T., and Kimura, T. (2000). Reduced expression of the regulatory CD4+ T cell subset is related to Th1/Th2 balance and disease severity in rheumatoid arthritis. Arthritis Rheum *43*, 617–627.

Zeng, Q.Y., Chen, R., Darmawan, J., Xiao, Z.Y., Chen, S.B., Wigley, R., Chen, S.L., and Zhang, N.Z. (2008). Rheumatic diseases in China. Arthritis Res. Ther. *10*, R17.

Zhai, Y., Ni, J., Jiang, G.W., Lu, J., Xing, L., Lincoln, C., Carter, K.C., Janat, F., Kozak, D., Xu, S., et al. (1999). VEGI, a novel cytokine of the tumor necrosis factor family, is an angiogenesis inhibitor that suppresses the growth of colon carcinomas in vivo. Faseb J *13*, 181–189.

Zhang, J., Wang, X., Fahmi, H., Wojcik, S., Fikes, J., Yu, Y., Wu, J., and Luo, H. (2009a). Role of TL1A in the pathogenesis of rheumatoid arthritis. The Journal of Immunology *183*, 5350–5357.

Zhang, Q., Wu, J., Cao, Q., Xiao, L., and Wang, L. (2009b). A critical role of Cyr61 in interleukin-17–dependent proliferation of fibroblast-like synoviocytes in rheumatoid arthritis - Zhang - 2009 - Arthritis & Rheumatism - Wiley Online Library. Arthritis & ….

Ziolkowska, M., Koc, A., Luszczykiewicz, G., Ksiezopolska-Pietrzak, K., Klimczak, E., Chwalinska-Sadowska, H., and Maslinski, W. (2000). High levels of IL-17 in rheumatoid arthritis patients: IL-15 triggers in vitro IL-17 production via cyclosporin A-sensitive mechanism. J Immunol *164*, 2832–2838.

Zvaifler, N.J., Steinman, R.M., Kaplan, G., Lau, L.L., and Rivelis, M. (1985). Identification of immunostimulatory dendritic cells in the synovial effusions of patients with rheumatoid arthritis. J Clin Invest *76*, 789–800.

APPENDIX

Appendix-1 Article: Investigation of tissue-specific expression and functions of MLF1-IP during development and in the immune system

Xuehai Wang*, Martin Marcinkiewicz[#], Yaned Gatain[+], Maxime Bouchard[+], Jianning Mao*, Michel Tremblay[+], Noriko Uetani[+], Silva Hanissian^, Shijie Qi*, Jiangping Wu*[$] and Hongyu Luo*

*From *Laboratoire d'immunologie and $Service de nephrologie, Centre de recherche, Centre hospitalier de l'Université de Montréal (CRCHUM) – Hôpital Notre-Dame, Montreal, Quebec, Canada; #Cytochem Inc., Montreal, Quebec, Canada; +Rosalind and Morris Goodman Cancer Research Centre (GCRC), McGill University, Montreal, Quebec, Canada; ^Department of Neurosurgery, University of Tennessee, Memphis, TN, USA*

Address correspondence to: Dr. Hongyu Luo, Laboratory of Immunology, CRCHUM – Hôpital Notre-Dame, Pavillion Mailloux, Room M-5213, 1560 Sherbrooke Street East, Montreal, Quebec H2L 4M1, Canada; Telephone: (514) 890-8000 Extension 25319; Fax: (514) 412-7596.

This work has been published *in **PloS ONE***.

Wang X, Marcinkiewicz M, Gatain Y, Bouchard M, Mao J, Tremblay M, Uetani N, Hanissian S, Qi S, Wu J, Luo H. (2013) Investigation of Tissue-Specific Expression and Functions of MLF1-IP during Development and in the Immune System. ***PLoS ONE*** 8:e63783

ABSTRACT

Myeloid leukemia factor 1-interacting protein (MLF1-IP) has been found to exert functions in mitosis, although studies have been conducted only in cell lines up to now. To understand its roles during ontogeny and immunity, we analyzed its mRNA expression pattern by *in situ* hybridization and generated MLF1-IP gene knockout (KO) mice. MLF1-IP was expressed at elevated levels in most rudimentary tissues during the mid-gestation stage, between embryonic day 9.5 (e9.5) and e15.5. It declined afterwards in these tissues, but was very high in the testes and ovaries in adulthood. At post-natal day 10 (p10), the retina and cerebellum still expressed moderate MLF1-IP levels, although these tissues do not contain fast-proliferating cells at this stage. MLF1-IP expression in lymphoid organs, such as the thymus, lymph nodes, spleen and bone marrow, was high between e15.5 and p10, and decreased in adulthood. MLF1-IP KO embryos failed to develop beyond e6.5. On the other hand, MLF1-IP$^{+/-}$ mice were alive and fertile, with no obvious anomalies. Lymphoid organ size, weight, cellularity and cell sub-populations in MLF1-IP$^{+/-}$ mice were in the normal range. The functions of MLF1-IP$^{+/-}$ T cells and naïve CD4 cells, in terms of TCR-stimulated proliferation and Th1, Th17 and Treg cell differentiation *in vitro,* were comparable to those of wild type T cells. Our study demonstrates that MLF1-IP performs unique functions during mouse embryonic development, particularly around e6.5, when there was degeneration of epiblasts. However, the cells could proliferate dozens of rounds without MLF1-IP. MLF1-IP expression at about 50% of its normal level is sufficient to sustain mice life and the development of their immune system without apparent abnormalities. Our results also raise an intriguing question that MLF1-IP might have additional functions unrelated to cell proliferation.

INTRODUCTION

Myeloid leukemia factor 1-interacting protein (MLF1-IP) has several other designations: Kaposi's sarcoma-associated herpes virus latent nuclear antigen-interacting protein 1 (KLIP1); centromere protein of 50 kDa (CENP50); centromere protein U (CENPU); interphase centromere complex protein 24; polo-box-interacting protein 1 (PBIP1).

Although MLF1-IP cDNA was identified by the human genome project, its initial functional attributes were reported by 2 groups. Yeast 2-hybrid screening by Pan et al. discerned that the protein interacts with the latent nuclear antigen of Kaposi's sarcoma-associated herpes virus [1], while Hanissian et al. reported that it interacts with myeloid leukemia factor 1 [2]. More earnest functional characterization ensued in subsequent years. Minoshima et al. discovered, again by yeast 2-hybrid screening, that MLF1-IP is a constitutive component of centromeres and named it CENP50[3]. It interacts with a Rho GTPase-activating protein, MgcRacGAP. MLF1-IP-deficient cells are viable but undergo delayed mitosis and severe mitotic defects, such as chromosome misalignment and premature sister chromatid separation, demonstrating, for the first time, that it is located in centromeres and plays a role in mitosis. Employing multiple tandem affinity purification, Foltz et al. identified MLF1-IP in CENP-A nucleosome-associated complexes in centromeres[4]. Yeast 2-hybrid screening by Kang et al. determined that MLF1-IP is associated with polo-like kinase 1 (Plk1), and its T78 is a substrate of this kinase[5]. MLF1-IP T78 phosphorylation creates self-tethering sites for interaction with Plk1, and such interaction is crucial for Plk1 recruitment to interphase and mitotic kinetochores. Lack of MLF1-IP T78 phosphorylation induces a chromosome congression defect and compromises the spindle checkpoint. Later in mitosis, Plk1 also evokes MLF1-IP degradation in a T78 phosphorylation-dependent manner. Recently, the same group established that MLF1-IP interacts directly with CENP-Q, and these interactions are necessary for the centromere localization of both CENP-Q and MLF1-IP to form ternary complexes with Plk1[6]. Hua et al. determined that MLF1-IP also interacts with Hec1, a kinetochore core component[7]. It not only binds directly to microtubules but also shows cooperative microtubule binding with Hec1. MLF1-IP knockdown results in impaired kinetochore-microtubule attachment.

All the above-described MLF1-IP functions are based on *in vitro* experiments in cell lines. It is not known whether MLF1-IP has functions other than that in mitosis. Also, no *in vivo* study has explored whether MLF1-IP is essential in mouse development. In our investigation, we conducted *in situ* hybridization (ISH) analysis to assess the tissue-specific expression of MLF1-IP during ontogeny with a view to identifying its functions. We also generated MLF1-IP gene null mutation in mice to evaluate the importance of this gene *in vivo* and *in vitro*.

MATERIALS AND METHODS

ISH

Full-length 1.25-kb MLF1-IP cDNA in pENBR/SD/D-TOPO was isolated with NotI/SalI and sub-cloned into NotI/SalI sites of pSPORT6[2]. The resulting plasmid was named pSPORT6-MLF1-IP and was employed as a template for sense and anti-sense riboprobe synthesis, using SP6 and T7 RNA polymerase for both ^{35}S-UTP and ^{35}S-CTP incorporation[8].

Tissues were frozen in -35°C isopentane and kept at -80°C until sectioned. We studied 10-μm thick cryostat-cut slices by ISH and x-ray film autoradiography, as outlined previously[8].

In situ hybridization in embryos was performed as described using digoxigenin-labeled RNA probes[9]. Hybridization was carried out with probes for *Lim1* and *Otx2*[10,11].

Hematoxylin and eosin staining was performed using standard procedures.

Generation of MLF1-IP gene knockout (KO) mice

A polymerase chain reaction (PCR) fragment, amplified on the MLF1-IP cDNA sequence in pSPORT6-MLF1-IP, served as probe to isolate genomic BAC DNA clone 325N12 from the 129/sv mouse BAC genomic library RPCI-22. The targeting vector was constructed by recombination and routine cloning methods, with a 10.6-kb MLF1-IP genomic fragment from clone 325N12, as illustrated in Fig. 1A[12]. A 2.39-kb BamHI/HpaI genomic fragment containing exon 1 was replaced by a 1.1-kb Neo cassette from pMC1Neo Poly A. The final targeting fragment was excised from its cloning vector backbone by NotI digestion and electroporated into R1 embryonic stem (ES) cells for G418 selection[13].

Southern blotting with a probe corresponding to the 5' sequence outside the targeting region, as illustrated in Figure 1A (red square), screened for and confirmed gene-targeting in ES cells and eventually in mouse tail DNA. The targeted allele showed a 6.8-kb NcoI band, and the wild type (WT) allele, a 10-kb NcoI band (Fig. 1A). PCR was adopted for routine genotyping of the targeted allele(s). The following PCR conditions were applied: 4 min at 95^{o}C, followed

by 35 cycles of 30 s at 94°C, 30 s at 58°C, and 30 s at 72°C, with final incubation at 72°C for 10 min. KO forward primer 5'-GCC AAG TCC AAC GTC TTG AT-3' and reverse primer 5'-CTC TTG CAA AAC CAC ACT GC-3' detected a 202-bp fragment from the targeted allele. WT forward primer 5'-TTA CTG CGG TAT TCT GTG CTG GGA-3' and reverse primer 5' ATC TAC TTG CAT CTG CCT CCG AGT-3' detected a 588-bp fragment from the WT allele.

The targeted ES cell clones were injected into C57BL/6 blastocysts. Chimeric male mice were mated with C57BL/6 females to establish mutated MLF1-IP allele germline transmission. All mice were housed under specific pathogen-free conditions and the project including the generation of the KO mice was approved by the Institutional Animal Protection Committee of the CRCHUM (NO9055JWs).

Real time reverse transcription-quantitative PCR (RT-qPCR)

MLF1-IP mRNA in cells or tissues from KO, heterozygous (HET) and WT mice was measured by RT-qPCR. Total RNA was extracted with TRIzol® (Invitrogen, Carlsbad, CA, USA) and then reverse-transcribed with Superscript II™ reverse-transcriptase (Invitrogen). The forward and reverse primers were 5'-GCA AGG AGA AGT TTG AGA TAC TCG GG-3' and 5'-CCA GCT TTC TGT TTC CTG GAA TAT GTG C-3', respectively. A 91-bp product was detected with the following amplification program: 95°C x 15 min, 1 cycle; 94°C x 15 s, 55°C x 30 s, 72°C x 30 s, 35 cycles.

Oct-4 and Nanog mRNA in ES cells was quantified by RT-qPCR. For Oct-4, a forward primier 5'- CCT ACA GCA GAT CAC TCA CAT C -3' and a reverse primer 5'- GCC GGT TAC AGA ACC ATA CTC -3' were employed; for Nanog, a forward primier 5'- TGC AAG AAC TCT CCT CCA TTC -3' and a reverse primer 5'- CGC TTG CAC TTC ATC CTT TG -3' were used.

β-actin mRNA levels were measured as internal controls; the forward and reverse primers were 5'-TGG TAC CAC AGG CAT TGT GAT-3' and 5'-TGA TGT CAC GCA CGA TTT CCC T-3', respectively, with the same amplification program as for MLF1-IP mRNA.

RT-qPCR was performed in triplicate, and the results were expressed as the signal ratios of MLF1-IP/β-actin.

RT-qPCR was also undertaken for embryo genotyping. Embryos were digested at 55^{o}C for 4 h in 2 μl digestion buffer (proteinase K, 0.01% gelatin, 0.005% NP-40, 20 mM Tris (pH 8.35), 40 mM KCl, 0.5 mM $MgCl_2$). Forward primer 5'-GCC TGG AAT GTT TCC ACC CAA TGT-3' and reverse primer 5'-CTG CGT GTT CGA ATT CGC CAA TGA-3' detected a 144-bp fragment from the KO allele, while forward primer 5'-TTA CTG CGG TAT TCT GTG CTG GGA-3' and reverse primer 5' CTT CCA AGG CGC ACC TTT CCA AAT-3' detected a 193-bp fragment from the WT allele. PCR conditions were as follows: 50^{o}C x 2 min, 1 cycle; 95^{o}C x 2 min, 1 cycle; 94^{o}C x 10 s, 58^{o}C x 20 s, 72^{o}C x 20 s, 35 cycles.

ES cell culture and small interfering RNA (siRNA) transfection

ES cells were maintained in DMEM supplemented with 15% fetal bovine serum, 1×MEM non-essential amino acids, 2mM L-glutamine (WISENT, St. Bruno, Quebec, Canada), 100μM 2-mercaptoethanol (Sigma, St. Louis, MO, USA) and 1000U/ml leukemia inhibitory factor (Chemicon, Billerica, MA, USA). siRNAs to MLF1-IP and negative control siRNAs were synthesized by Integrated DNA Technologies (Coralville, IA, USA). The sequences of the MLF1-IP-specific siRNA and control siRNA are listed in Table 1. ES cells were transfected with a mix of 2 pairs of siRNAs (each pair at a final concentration of 30 nM), with FuGENE HD X-tremeGENE siRNA Transfection Reagent (Roche Applied Science, Mannheim, Germany). The transfected ES cells were further cultured for 48h. The MLF1-IP mRNA knockdown and mRNA expression of Oct-4 and Nanog were measured by RT-qPCR.

Flow cytometry

Single cell suspensions from the thymus, lymph node and spleen were prepared and stained for flow cytometry[14].

T-*cell proliferation*

T-cell proliferation was assessed by ^{3}H-thymidine uptake[15].

Naïve T-cell differentiation into Th1, Th17 and Treg cells

The method has been described in a previous publication[16].

RESULTS

MLF1-IP expression during ontogeny according to ISH

So far, detailed tissue-specific expression of MLF1-IP during ontogeny has not been investigated. Our study provides ISH evidence of spatially- and temporally-restricted MLF1-IP expression patterns in mice from mid-gestation through adulthood. Based on exposure time necessary for autoradiograms (optimal time: 10 days for x-ray films), MLF1-IP mRNA belonged to a class of very low abundant mouse mRNAs. A summary appears in Table 2, and details are given in Figures 1-3. Generally speaking, rudiments of multiple tissues (the brain, liver, optic vesicle and thymus) displayed relatively high MLF-IP mRNA levels, which peaked in the mid-gestation stage. At mid-gestation, on embryonic day 9.5 (e9.5), rudiments of multiple tissues, except for the mesenchymal region, displayed relatively high MLF1-IP mRNA levels (Fig. 1A-II); expression was particularly high in the central nervous system (CNS) structures, such as the mesencephalon, telencephalon, nasal tip and spinal cord (Fig. 1A-II). On day e12.5, MLF1-IP-positive areas in the CNS were limited to a small region in the brain and optic vesicle (Fig. 1B-II). By day e15.5, ventricular wall, ventricular zone and cerebellum displayed MLF1-IP mRNA labelling (Fig. 1C-II). A number of tissues displayed changing levels of MLF1-IP expression through several stages. In the liver, a moderate level of MLF1-IP expression was evident on day e12.5, and it progressively diminished through e15.5, post-natal day 1 (p1), p10 to decline at adulthood (Figs. 1 and 2), showing a pattern reminiscent to that of erythropoiesis genes: such genes have peak expression at prenatal stages, before their function is fully taken by a bone marrow cells. In this respect, MLF1-IP was observed in postnatal p10 and adult mice bone marrow within vertebrae and long bone cavities (Fig. 2B and C), suggesting its possible involvement in the erythropoiesis. Transient expression in the kidney nephrogenic zone was observed from e15.5 to p1. There was no evident MLF1-IP expression in the adult kidney (Fig. 2C-I and II). Long-lasting expression is observed in the intestine, from e15.5 until adulthood. The skin manifested peak MLF1-IP expression on p10. From p1 until adulthood, MLF1-IP was expressed in the retina and cerebellum (Figs. 2A-II, B-II and C-II). MLF1-IP expression peaked in the submaxillary gland between e15.5 and p1 (Figs. 2A-II and 2B-II), but its expression in this gland was not evident in adults (Fig. 2C-II). In the immune system, the thymus and spleen presented moderate to

high MLF1-IP expression from e15.5 to p10; it declined to a detectable level in adulthood (Figs. 1 and 2), and was mainly concentrated in the thymic cortex (Fig. 3A), spleen white pulp (Fig. 3B) and lymph node follicles (Fig. 3C). In the reproductive system, MLF1-IP expression was already moderately high in the testes on p10; it became relatively high in adult testes (Fig. 3D). Moderate to high MLF1-IP expression was found in growing follicles and corpus luteum of the ovaries (Figs. 3D and 3E).

Generation of MLF1-IP gene KO mice

We generated MLF1-IP KO mice to assess the role of MLF1-IP in live animals. The targeting strategy is depicted in Figure 4A. With the 5' end probe, the WT allele after NcoI digestion presented a 10-kb band on Southern blotting, and the KO allele, a 6.8-kb band (Fig. 4A). Germline transmission was confirmed by Southern blotting of tail DNA, and WT and HET mice were thus identified (Fig. 4B, left panel). PCR was undertaken for routine genotyping of ear DNA. The WT allele presented a 588-bp band, and the KO allele, a 202-bp band (Fig. 4B, right panel).

To ascertain if MLF1-IP gene deletion affected its expression, we measured MLF1-IP mRNA levels of WT, HET and KO embryos (Fig. 4C). E7.5 HET embryos only expressed MLF1-IP mRNA at a 50% level of WT embryos, while KO embryos at that time totally lacked the mRNA.

MLF1-IP was previously selected for study because it was inducible after T-cell activation (data not reported). We activated T cells with solid-phase anti-CD3 and anti-CD28 monoclonal antibodies (mAbs), and quantified MLF1-IP mRNA at different time points (0, 24, 48 and 72 h after the initiation of culture). As shown in Fig. 4D, resting HET T cells (0 h, and cells cultured in medium for 24 h) expressed about 50% less MLF1-ip mRNA than their WT counterparts. After T cell activation, the MLF1-IP mRNA levels of both HET and WT T cells were upregulated with respect to their unstimulated controls, but the levels in HET T cells were about 50% that of the WT T cells.

The data in Figure 4C confirmed the gene deletion of MLF1-IP in KO embryos. Figure 4C and 4D also indicated that MLF1-IP expression was gene copy number-dependent, as HET cells expressed only one-half the level of MFL1-IP mRNA compared to WT cells.

MLF1-IP KO is lethal in embryos

We failed to generate any live MLF1-IP KO mice, nor could we obtain any KO embryos between e9 and birth. Systemic tracking of embryo genotype in different gestation stages revealed that intact KO embryos could only be found before and at e7.5 (Table 3) from MLF1-IP$^{+/-}$ x MLF1-IP$^{+/-}$ mating, and the frequency of KO embryo occurrence on e3.5, e6.5 and e7.5 was basically in agreement with Mendelian ratios. E3.5 KO embryos had no anomalies upon visual inspection (data not shown), while e6.5 KO embryos were moderately smaller than their WT counterparts (Fig. 5A). On e7.5, all KO embryos were much smaller size than their WT counterparts (Table 3 and Fig. 5A). We then cultured e3.5 embryos from HET male and female mating to observe their outgrowth *in vitro*. As depicted in Figure 5B, WT, HET and KO embryos manifested no discernible difference upon visual inspection 1 day after culture (e4.5), and their outgrowth seemed to be comparable until e6.5. All these data suggested major developmental blockage between e6.5 and e7.5 in the absence of MLF1-IP.

To better understand embryonic lethality around E6.5, we performed Hematoxylin and eosin staining which revealed a degeneration of the epiblast and its detachment from the surrounding visceral endoderm in e6.5 KO embryos (Fig. 5C, top row), while HET embryos , showed no such anomaly. *In situ* hybridization with an *Otx2* probe that marks both the epiblast and visceral endoderm revealed a hypocellular and disorganized epiblast tissue in KO but not HET embryos at e6.5 (Fig. 5C, middle row). *In situ* hybridization for *Lim1* that marks primarily the visceral endoderm revealed a somewhat thicker but otherwise normal visceral endoderm in e6.5 KO embryos, as compared to that in HET embryos (Fig. 5C, lower row).

These data indicate that MLF1-IP is vital in embryonic development, particularly for epiblast development around e6.5.

As shown in Figure 4C, MLF1-IP mRNA levels in heterozygous embryos was about a half of that in WT ones, but HET embryos develop normally. We failed to generate ES cells from KO embryos, but HET ES cells were generated. We wondered whether by further knocking down the MLF1-IP expression levels in the HET ES cells, we might reveal some anomaly in these cells in terms of their pluripotency. We transfected HET ES cells with MLF1-IP siRNA, and the mRNA knockdown was confirmed by RT-qPCR (Fig. 5D). The siRNA-or control siRNA-transfected ES cells were cultured for 2 days, and their expression of Oct-4 and Nanog, two pluripotent markers was assessed by RT-qPCR[17]. As shown in Figure 5E, no apparent differences in Oct-4 and Nanog expression between the MLF1-IP and control siRNA-transfected HET ES cells were observed. Thus, probably the remaining MLF1-IP is sufficient to maintain the pluripotency of ES cells.

No detectable anomalies in cell sub-populations in lymphoid organs and bone marrow of MLF1-IP HET mice

As MLF1-IP was prominently expressed in the thymus between e15.5 and p10, and was up-regulated in adult T cells upon their activation, we set out to investigate whether reduced MLF1-IP expression causes immune system abnormalities. HET mice were used for this purpose because no KO mice could be produced. HET mice were viable and fertile with not visible abnormalities on either gross or anatomical visual inspection. No lymphoid organ anomalies were apparent in HET mice in terms of size, weight and cellularity (data not reported).

T, B, CD4 and CD8 sub-populations in the spleen and lymph nodes of HET mice were comparable to those in WT controls (Fig. 6A), as were thymocyte sub-populations, such as CD4CD8 double-negative, CD4CD8 double-positive, CD4 single-positive and CD8 single-positive cells (Fig. 6B).

We also assessed the $Lin^{-}c\text{-}Kit^{+}Sca\text{-}1^{+}$ stem cell population in bone marrow, but no significant difference between HET and WT mice was evident (Fig. 6C). Furthermore, populations of $B220^{+}CD43^{+}CD19^{+}AA4.1^{+}$ pro-B cells, $B220^{+}CD43^{-}CD19^{+}AA4.1^{+}$ pre-B cells, $Mac\text{-}1^{+}Gr\text{-}1^{+}$

bone marrow myeloid cells, and $CD71^{+}Ter119^{+}$ erythroid precursors were comparable in the bone marrow of HET and WT mice (Fig. 6D).

Assessment of HET and WT T-cell functions

Although HET T cells only expressed MLF1-IP mRNA at about 50% the WT level upon activation by anti-CD3 and CD28 mAbs on solid phase, they proliferated as well as WT T cells (Fig. 7A). Activation markers, such as CD25 and CD69, were up-regulated in HET CD4 and CD8 T cells comparably to their WT counterparts (Fig. 7B). Furthermore, HET-naïve CD4 T cells could differentiate into Th1, Th17 and Treg cells as efficiently as WT T cells (Fig. 7C). Therefore, it appears that 50% of normal MLF1-IP expression is sufficient to maintain T-cell proliferation and function.

DISCUSSION

MLF1-IP came to our attention about 10 years ago when we screened genes whose expression was up-regulated during T-cell activation, but little was known about its functions at that time. Several years later, its functions in mitosis were reported by several groups (3-6). Our ISH analysis of its temporal and spatial expression during ontogeny in mice by and large concurs with its reported function in mitosis in that regions in organs containing fast-proliferating cells at any given ontogeny stage expressed high MLF1-IP mRNA levels. However, such was not always the case. For example, on p10, moderately high MLF1-IP mRNA expression was still obvious in the retina and cerebellum, although these regions do not have fast growing cells at that stage. This raises an intriguing question: does MLF1-IP have additional functions besides those in mitosis.

Our study, for the first time, examines whether MLF1-IP is irreplaceable or its function can be compensated by other molecules. With complete MLF1-IP deletion, this question was clearly answered in the KO mouse model. At least until close to e6.5, MLF1-IP KO embryos were comparable to WT controls in regard to size and morphology. Multiple rounds of proliferation were carried out from inception to the time point near e6.5, starting from a fertilized egg to an embryo of about 0.5 mm in length containing several hundred thousand cells. Obviously, proliferation could go on without MLF1-IP, and was not absolutely needed for mitosis. On the other hand, it is obvious that without MLF1-IP, embryonic development cannot go beyond e6.5, indicating that certain vital developmental events around this time absolutely require MLF1-IP. We attempted to generate KO ES cells from e3.5 blastocysts. From 100 blastocysts, 50-60 ES cell lines were obtained, but all of them were either WT or HET. Taken together, these findings suggest that MLF1-IP is essential in optimizing the embryonic developmental program: cells might develop without MLF1-IP, but once the condition is stringent, such as during ES cell derivation *in vitro* or near e6.5 *in vivo*, cells without MLF1-IP will fail to develop further. It seems different types of cells in the early development require different levels of MLF1-IP expression; the epiblast is more sensitive to the lack of MLF1-IP at e6.5. We conclude that MLF1-IP is crucially required during embryonic development. However, the fact that a fertilized egg can grow into several hundred thousand cells without MLF1-IP raises

questions as to whether such irreplaceability is simply due to its roles in the proliferation program, or due to its vital roles in other particular cellular processes such as epiblast development around e6.5.

Another useful piece of information from our study is that 50% of normal MLF1-IP expression is sufficient during ontogeny and immunity. HET mice were alive and fertile, with no visible anomalies. Their lymphoid organs and cells all developed normally, and no defective T cell function was observed *in vitro* based on our assays. Thus, normal MLF1-IP expression level has ample buffering latitude for its functions.

In summary, our study, for the first time, demonstrated the irreplaceability of MLF1-IP during mouse embryonic development. It also raised an intriguing possibility that the molecule might have functions unrelated to proliferation, based on its expression pattern in the CNS and successful progression of embryonic development until e6.5.

REFERENCES

1. Pan H-Y, Zhang Y-J, Wang X-P, Deng J-H, Zhou F-C, et al. (2003) Identification of a novel cellular transcriptional repressor interacting with the latent nuclear antigen of Kaposi's sarcoma-associated herpesvirus. J Virol 77: 9758–9768.

2. Hanissian SH, Akbar U, Teng B, Janjetovic Z, Hoffmann A, et al. (2004) Oncogene - cDNA cloning and characterization of a novel gene encoding the MLF1-interacting protein MLF1IP. Oncogene 23: 3700–3707.

3. Minoshima Y, Hori T, Okada M, Kimura H, Haraguchi T, et al. (2005) The constitutive centromere component CENP-50 is required for recovery from spindle damage. Mol Cell Biol 25: 10315–10328.

4. Foltz DR, Jansen LET, Black BE, Bailey AO, Yates JR, et al. (2006) The human CENP-A centromeric nucleosome-associated complex. Nat Cell Biol 8: 458–469.

5. Kang YH, Park J-E, Yu L-R, Soung N-K, Yun S-M, et al. (2006) Self-regulated Plk1 recruitment to kinetochores by the Plk1-PBIP1 interaction is critical for proper chromosome segregation. Mol Cell 24: 409–422.

6. Kang YH, Park CH, Kim T-S, Soung N-K, Bang JK, et al. (2011) Mammalian polo-like kinase 1-dependent regulation of the PBIP1-CENP-Q complex at kinetochores. Journal of Biological Chemistry 286: 19744–19757.

7. Hua S, Wang Z, Jiang K, Huang Y, Ward T, et al. (2011) CENP-U cooperates with Hec1 to orchestrate kinetochore-microtubule attachment. Journal of Biological Chemistry 286: 1627–1638.

8. Marcinkiewicz M (2002) BetaAPP and furin mRNA concentrates in immature senile plaques in the brain of Alzheimer patients. J Neuropathol Exp Neurol 61: 815–829.

9. Henrique D, Adam J, Myat A, Chitnis A, Lewis J, et al. (1995) Expression of a Delta

homologue in prospective neurons in the chick. Nature 375: 787–790.

10. Narlis M, Grote D, Gaitan Y, Boualia SK, Bouchard M (2007) Pax2 and pax8 regulate branching morphogenesis and nephron differentiation in the developing kidney. J Am Soc Nephrol 18: 1121–1129. 11. Simeone A, Acampora D, Mallamaci A, Stornaiuolo A, D'Apice MR, et al. (1993) A vertebrate gene related to orthodenticle contains a homeodomain of the bicoid class and demarcates anterior neuroectoderm in the gastrulating mouse embryo. EMBO J 12: 2735–2747.

12. Liu P, Jenkins NA, Copeland NG (2003) A highly efficient recombineering-based method for generating conditional knockout mutations. Genome Res 13: 476–484.

13. Nagy A, Rossant J, Nagy R, Abramow-Newerly W, Roder JC (1993) Derivation of completely cell culture-derived mice from early-passage embryonic stem cells. Proc Natl Acad Sci USA 90: 8424–8428.

14. Luo H, Charpentier T, Wang X, Qi S, Han B, et al. (2011) Efnb1 and Efnb2 proteins regulate thymocyte development, peripheral T cell differentiation, and antiviral immune responses and are essential for interleukin-6 (IL-6) signaling. Journal of Biological Chemistry 286: 41135–41152.

15. Han B, Moore PA, Wu J, Luo H (2007) Overexpression of human decoy receptor 3 in mice results in a systemic lupus erythematosus-like syndrome. Arthritis Rheum 56: 3748–3758.

16. Zhang J, Wang X, Fahmi H, Wojcik S, Fikes J, et al. (2009) Role of TL1A in the pathogenesis of rheumatoid arthritis. J Immunol 183: 5350–5357.

17. Loh Y-H, Wu Q, Chew J-L, Vega VB, Zhang W, et al. (2006) The Oct4 and Nanog transcription network regulates pluripotency in mouse embryonic stem cells. Nat Genet 38: 431–440.

FIGURE LEGENDS

Figure 1. ISH analysis of MLF1-IP expression in mid-gestation embryos e9.5, e12.5 and e15.5
Sagittal sections of the embryos are shown as follows: (I) crystal violet staining under bright-field illumination, and (II) antisense and (III) sense (control) hybridization x-ray film under dark-field illumination. Column A: an e9.5 embryo with hybridization signal seen over a rudimental brain and spinal cord and with less signal within mesenchymal centers. Column B: an e12.5 embryo with hot spots of MLF1-IP hybridization in the brain, optic vesicle and liver. Column C: an e15.5 embryo showing further differentiation of MLF1-IP expression distribution. Strong hybridization signal is observed in the brain ventricular zone rich in neuroblasts and ventricle wall, submaxillary gland and thymus. Lung parenchyma, liver, kidney marginal zone and growing intestine showed moderate-level MLF1-IP mRNA labelling. Original magnifications: (A) 6.5X; (B) 4.5X and (C) 2.6X.

Abbreviations used in Figures 2-4: Adr – adrenal gland; Al – alveolar bone; AR – aortic root; BM – bone marrow; Br – brain; C – calvaria bone; Cb – cerebellum; CL – corpus luteum; Cx – cortex; DA – dorsal aorta; F – follicles; Fe – femur, bone and bone marrow; H – heart; Int – intestine; K – kidney; LF – lymph follicle; Li – liver; LInt – Large intestine; LN – lymph node; Lu – lung; M – muscles, striated; Me – mesencephalon; Med – medulla; *Mes* – mesenchyme; NT – nasal tip; Ov – ovary; OV – optic vesicle; R – retina; Ri – ribs; SfT – seminiferous tubules; Sk – skin; SMax – submaxillary gland; SpC – spinal cord; St – stomach; T – telencephalon; Tes – testes; Th – thymus; V – ventricular wall; Ve – vertebrae; VZ – ventricular zone; WP – white pulp; (as) – antisense; (s) – sense.

Figure 2. ISH analysis of MLF1-IP mRNAS expression in p1, p10 and adult mice
Sagittal sections of p1, p10 and adult mice were stained with crystal violet (I), antisense probes (II) and sense probes (control) (III) as described in Figure 1. Column A: sections of a newborn (p1) mouse with MLF1-IP mRNA labelling seen in the retina, cerebellum, submaxillary gland, thymus, liver, intestine and kidney marginal zone. Column B: sections of a p10 mouse displaying various levels of MLF1-IP expression in different organs, including bone marrow within vertebrae and testis. Non-specific hybridization is noted in dorsal aorta

(*), aortic root (**) and alveolar bone (***) according to sense probe hybridization. Column C: sections of an adult mouse showing low-level MLF1-IP mRNA in the cerebellum, thymus, spleen and bone marrow. There is no detectable hybridization in the liver and kidney. Non-specific hybridization is seen in the femoral, skull alveolar bones (*), ribs (**) and in the content of the large intestine (***). Original magnifications: (A) 1.5X; (B) 1.3X and (C) 1.0X.

Figure 3. ISH analysis of MLF1-IP expression in individual adult tissues

X-ray autoradiography was under dark-field illumination. The left column shows antisense hybridization, and the right column, sense (control) hybridisation. A and A': thymus, showing ISH signal mostly in the cortex and less in the medulla. B and B': spleen, very low-level ISH signal in the white pulp. C and C': Lymph node, low-level ISH labelling in the lymphatic follicles; D and D': testis, high-level MLF1-IP expression in seminiferous tubules. E and E': MLF1-IP mRNA detectable in the follicles and corpus luteum. Original magnification: 10X.

Figure 4. Generation of MLF1-IP KO mice

A. Targeting strategy for generating MLF1-IP KO mice

The red square on the 5' side of the mouse MLF1-IP WT genome represents the sequence used as a probe in Southern blotting for genotyping.

B. Genotyping of MLF1-IP mutant mice

Tail DNA was digested with NcoI, and analyzed by Southern blotting (left panel), with a 5' probe whose location is indicated in A (red square). A 10-kb band representing the WT allele and a 6.8-kb band representing the recombinant allele are indicated by arrows. Ear lobe DNA sample was analyzed by PCR for routine genotyping (right panel). A 588-bp band representing the WT allele and a 202-bp band representing the recombinant allele are indicated by arrows.

C. MLF1-IP mRNA expression in MLF1-IP WT, HET and KO embryos

mRNA levels from e7.5 WT, HET and KO embryos were analyzed by RT-qPCR. The results are expressed as ratios of MLF1-IP versus β-actin signals with means $\pm$ SD indicated.

D. MLF1-IP mRNA expression in WT and HET T cells upon activation

T cells from WT and HET spleens were stimulated by solid-phase anti-CD3 mAb and anti-CD28 mAb (0.5 μg/ml and 4 μg/ml respectively for coating) for 0, 24, 48 or 72 h, and their MLF1-IP mRNA levels were quantified by RT-qPCR. The results are expressed as ratios of MLF1-IP versus β-actin signals with means ± SD indicated.

Figure 5. Development of WT, HET and KO embryos until e7.5

A. Gross morphology of WT and KO mouse embryos

E6.5 and e7.5 embryos dissected from decidua were photographed, and then genotyped by RT-qPCR. (Scale bar: 100 μm.)

B. Normal outgrowth of HET and KO embryos from e4.5 to e6.5 in vitro

E3.5 embryos were harvested with M2 medium, cultured in M16 medium and photographed daily on e4.5, e5.5 and e6.5. Phase-contrast micrographs are shown. At the end of culture on e6.5, the embryos were genotyped by RT-qPCR. (Scale bar: 100 μm.)

C. Histology and differentiation marker expression at of foetuses e6.5

Top row: Hematoxylin and eosin staining of e6.5 embryos

Middle row: *Oxt2* in situ hybridization.

Bottom row: *Lim1* in situ hybridization.

VE: visceral endoderm; Epi: epiblast; *: detachment of the epiblast from the surrounding visceral endoderm. (Scale bar: 100 μm.)

D. Knockdown of MLF1-IP mRNA expression in HET ES cells by siRNA according to RT-qPCR.

HET ES cells were transfected with MLF1-IP siRNA or control siRNA as indicated, and after 2 days, their MLF1-IP mRNA expression was assessed by RT-qPCR.

E. Oct-4 and Nanog mRNA expression in HET ES cells with MLF1-IP knockdown

Oct-4 (left panel) and Nanog (right panel) expression levels of the cells from Fig. 5D were assessed by RT-qPCR.

Figure 6. Sub-populations of lymphocytes in lymphoid organs of MLF1-IP HET mice

Cells of hematopoietic origin in lymphoid organs and bone marrow were analyzed by flow cytometry. The percentages of key sub-populations are indicated. The experiments were repeated at least 3 times, and representative histograms provided.

A. T- and B -cell sub-populations in the spleen and lymph nodes

CD4 and CD8 T-cell sub-populations in WT and HET spleens, lymph nodes and thymus were analyzed by 2-color flow cytometry. The B-cell population in the spleen and lymph nodes was analyzed according to B220 and CD19 expression by 2-color flow cytometry. Percentages are indicated.

B. Thymocyte sub-populations

Thymocytes from WT and HET mice were stained with CD4 or CD8 for 2-color flow cytometry, or with lineage markers (CD3ε, CD8β, TCRβ, CD11b, CD45R, B220, Ly6C, Ly6G, Ter-119), CD25 and CD44 for 3-color flow cytometry. Lineage$^-$ cells were gated and analyzed for their CD25 and CD44 expression.

C. Lineage-negative bone marrow cell sub-populations

WT and HET bone marrow cells were stained with lineage markers, c-Kit and Sca-1for 3-color flow cytometry. Lineage- cells were gated, and analyzed for their c-Kit$^+$Sca-1$^+$ stem cell population.

D. Pre-B, pro-B, pre-pro-B cell sub-populations and myeloid cell in bone marrow

WT and HET bone marrow cells were stained with B220, CD43, CD19 and AA4.1 and analyzed by 4-color flow cytometry for $B220^{+}CD43^{+}CD19^{-}AA4.1^{+}$ pre-pro-B cell (region II in column 2) $B220^{+}CD43^{+}CD19^{+}AA4.1^{+}$ pro-B cell (region I in column 2) and $B220^{+}CD43^{-}CD19^{+}AA4.1^{+}$ pre-B cell (region III in column 3) populations. Bone marrow cells were also stained with Mac-1 and Gr-1 (column 4) for analysis of mature $Mac\text{-}1^{+}Gr\text{-}1^{+}$ neutrophils, or stained with Ter-119 and CD71 for analysis of $CD71^{+}Ter119^{+}$ erythroid precursor cells.

Figure 7. $MLF1\text{-}IP^{+/-}$ T-cell functions in vitro

All experiments in this figure were repeated at least twice and representative data are presented.

A. T-cell proliferation

WT and HET spleen T cells were stimulated with solid-phase anti-CD3 mAb plus anti-CD28 mAb (0.5 μg/ml and 4 μg/ml respectively for coating) and pulsed with ^{3}H-thymidine for 16 h before harvesting. ^{3}H-thymidine uptake was measured at 24, 48 and 72 h after the initiation of culture. Samples were tested in triplicate, and cpm means $\pm$ SD were reported.

B. C69 and CD25 expression on activated WT and HET T cells

WT and HET T cells were stimulated overnight by solid-phase anti-CD3 mAb plus anti-CD28 mAb (0.5 μg/ml and 4 μg/ml respectively for coating). CD69 and CD25 expression on CD4 (left panel) and CD8 (right panel) T cells was measured by 2-color flow cytometry.

C. Naïve CD4 cell differentiation in vitro

WT and HET Naïve CD4 cells were cultured under conditions favouring Th1 (second column), Th17 (third column), or Treg (last column) cell differentiation for 3 days. Cells without differentiation cytokines (TH0, first column) were included for comparison. Their intracellular cytokine expression was determined by flow cytometry. Experiments were repeated twice, and representative data reported.

TABLES

Table 0.1 *Sequences of siRNA specific to MLF1-IP and control siRNA*

		Sets of siRNA sequences	
Gene		**Sense sequences**	**Antisense sequences**
Control		5'-rCrGrU rUrArA rUrCrG rCrGrU rArUrA rArUrA rCrGrC rGrUA T-3'	5'-rArUrA rCrGrC rGrUrA rUrUrA rUrArC rGrCrG rArUrU rArArC rGrArC-3'
MLF1-IP	Duplex 1:	5'-rGrGrA rArUrA rArArG rArUrU rArGrU rCrArG rArArU rArUrG T-3'	5'-rArCrA rUrArU rUrCrU rGrArC rUrArA rUrCrU rUrUrA rUrUrC rCrUrC-3'
	Duplex 2:	5'-rArGrA rGrUrA rGrArA rUrCrU rGrArA rArGrU rUrGrU rAAT C-3'	5'-rGrArU rUrArC rArArC rUrUrU rCrArG rArUrU rCrUrA rCrUrC rUrUrU-3'

Table 0.2 *Summary of MLF1-IP mRNA expression in various tissues and organs during mouse ontogeny according to ISH*

	Embryonic stage					
Tissue	**e9.5**	**e12.5**	**e15.5**	**p1**	**p10**	**Adult**
Brain and spinal cord	+++	++++	- / +++	-/+	-/+	-/±
Cerebellum	-	-	-	+	++	±
Eyes	+	++	ne	+++	++	ne
Olfactory neuroepithelium			+	ne	ne	ne
Liver	+	+++	++	+	+	±
Kidneys	-	+	++	+++	ne	ne
Submaxillary gland	-	-	++	++	+	±
Vertebrae	-	-	-	+	++	-
Calvaria	-	-	-	+	++	-
Thymus	-	-	+++	++	++	±
Spleen			ne	+++	ne	±
Lymph nodes					ne	±
Ovaries					ne	+++
Testes					++	+++++

Arbitrary scale: absence of labelling (-);weak (+) to high (+++++) concentrations; ne: not examined.

Table 0.3 *Genotyping of embryos from MLF1-IP$^{+/-}$ × MLF1-IP$^{+/-}$ mating*

	Genotype			
Stage	**+/+**	**+/-**	**-/-**	**Total**
e3.5	3	18	9	30
e6.5	12	18	8[a]	41
e7.5	8	16	9[b]	33

[a]*KO embryos were moderately smaller than WT ones.*

[b]*KO embryos drastically shrank to smaller sizes.*

FIGURES

Figure 0.1

Figure 1.

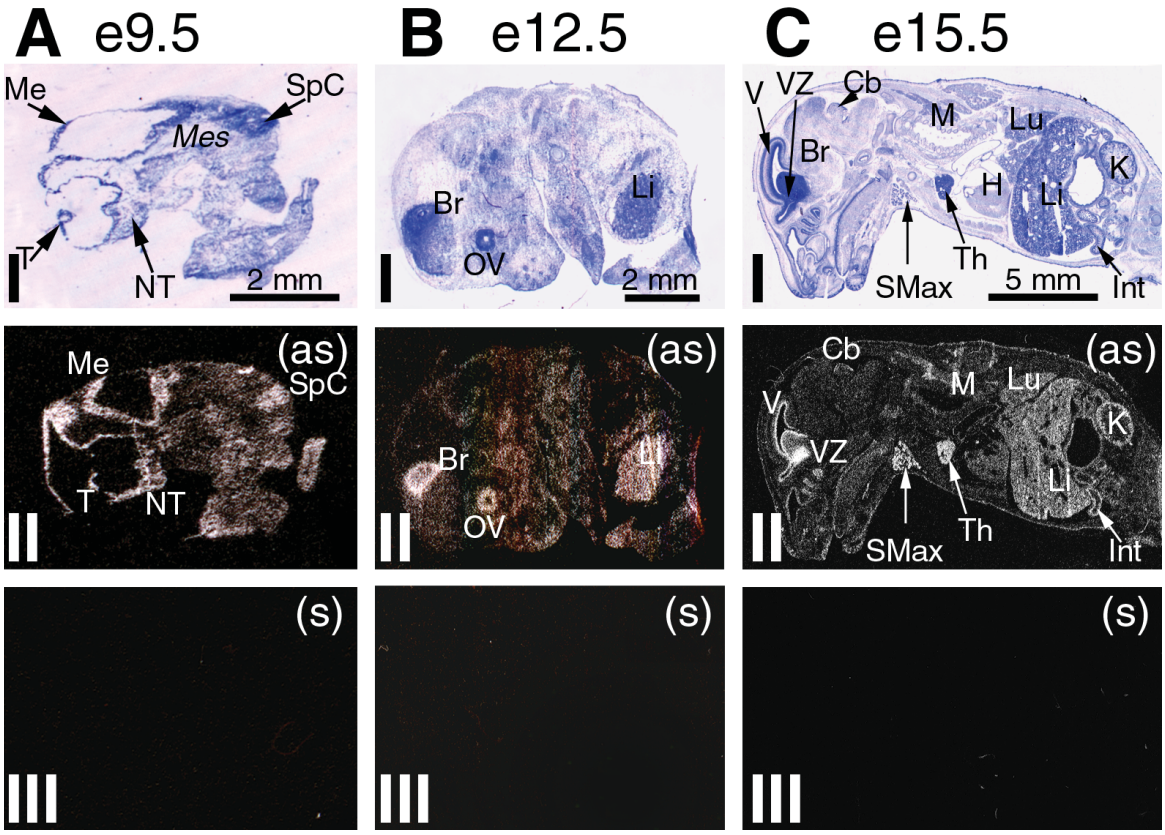

Figure 0.2

Figure 2.

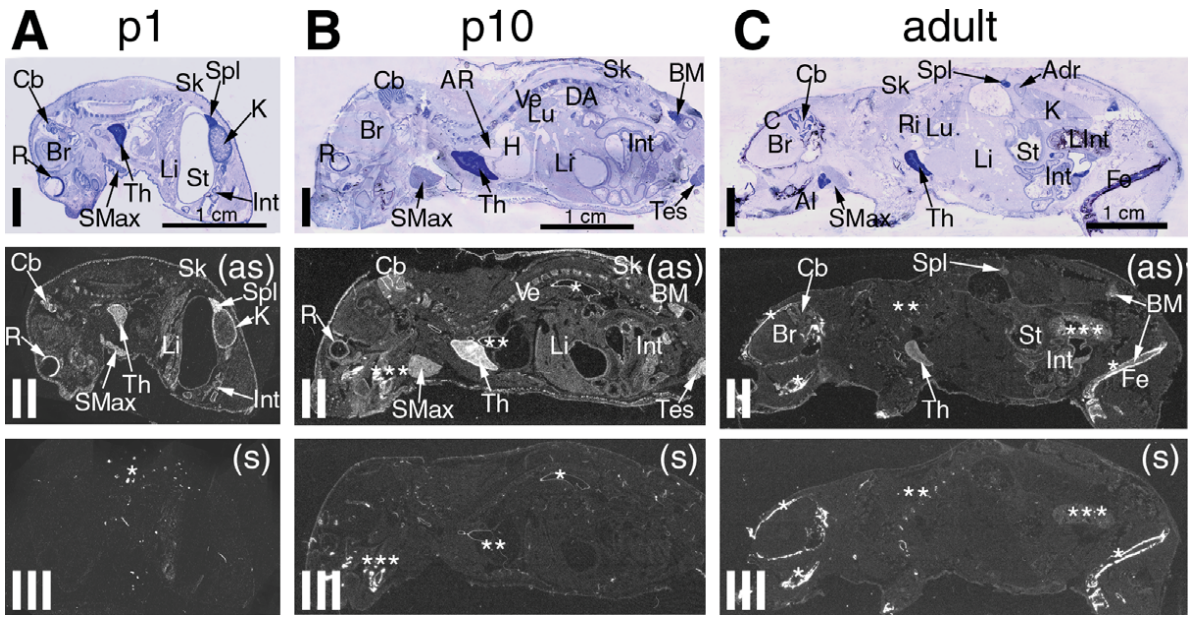

Figure 0.3

Figure 3.

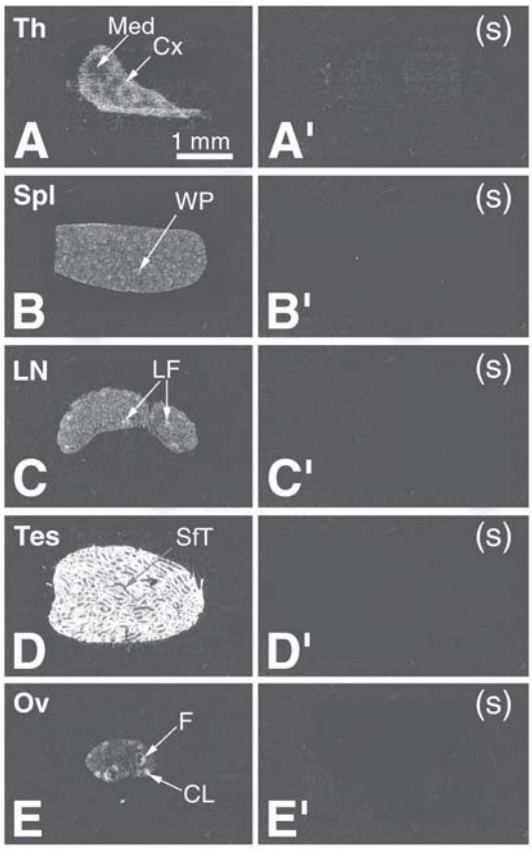

Figure 0.4

Figure 4.

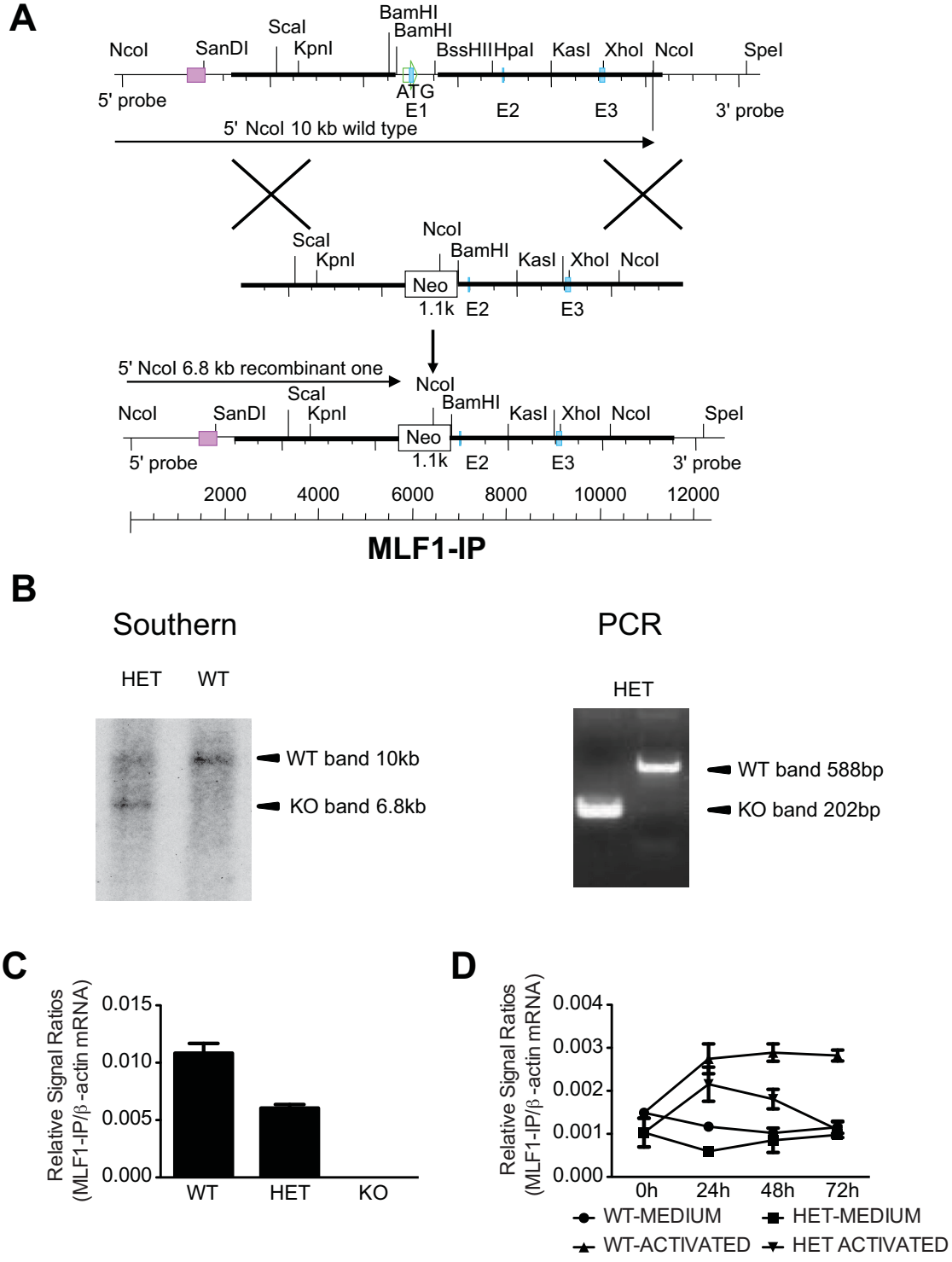

Figure 0.5

Figure 5.

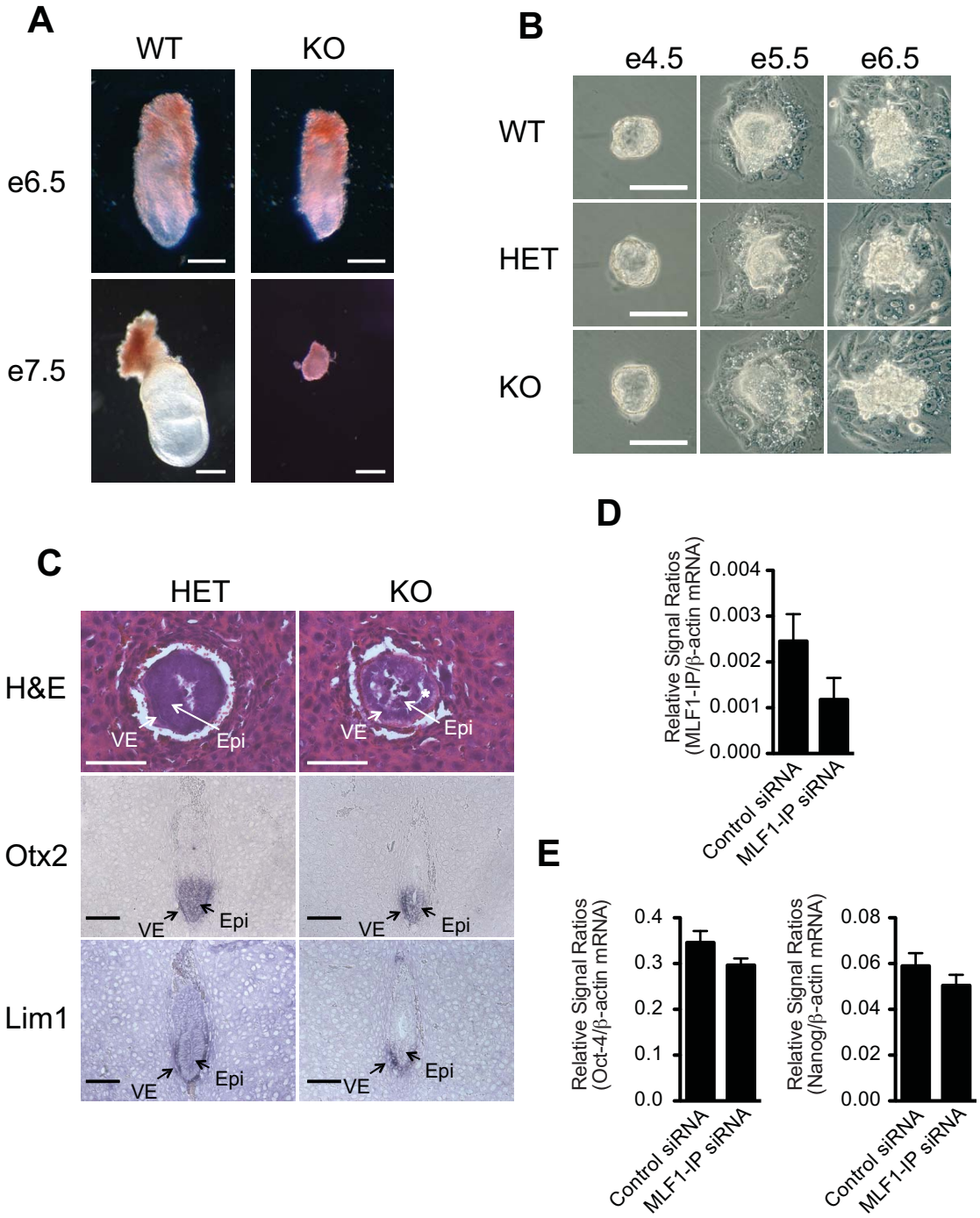

Figure 0.6

Figure 6.

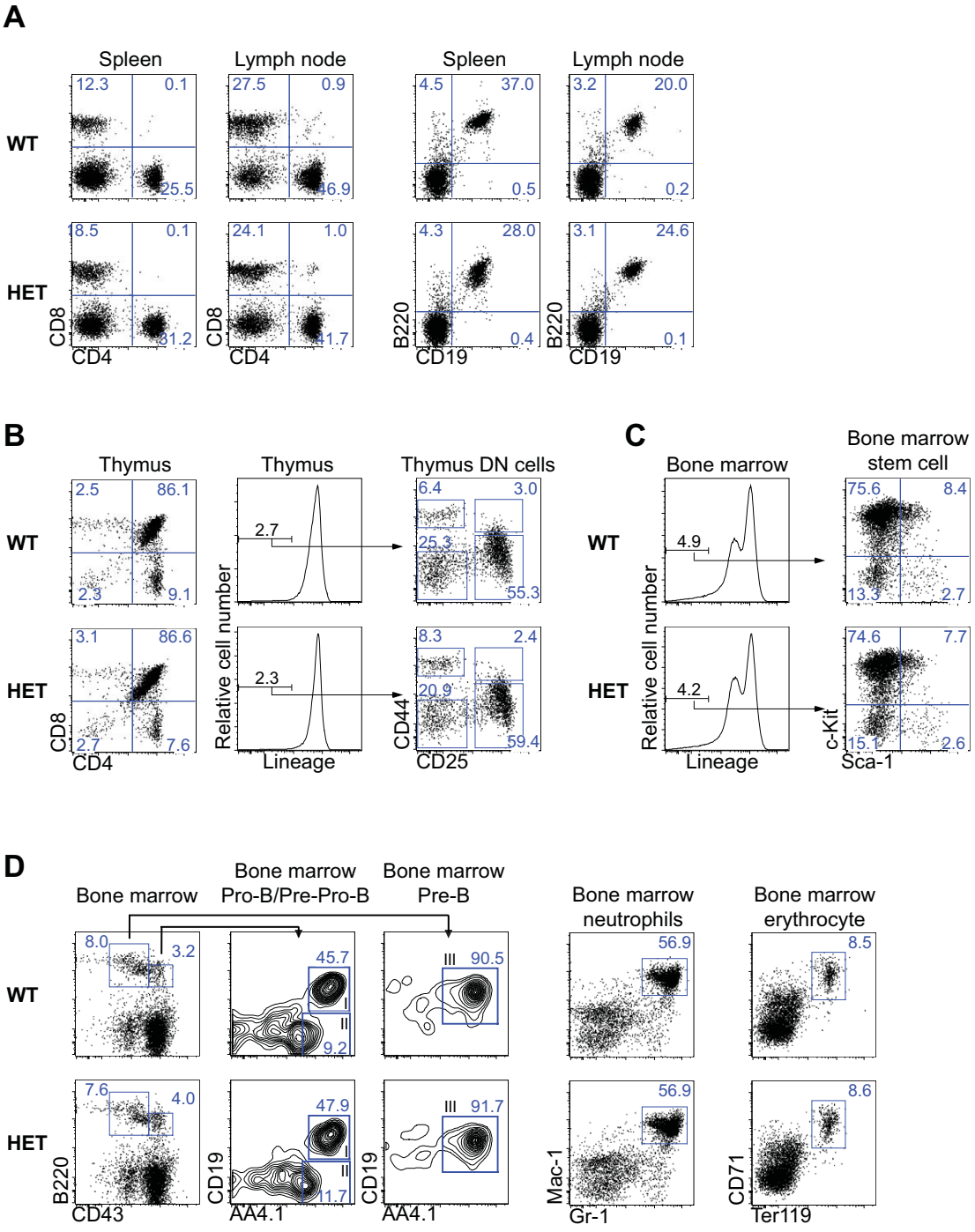

Figure 0.7

Figure 7.

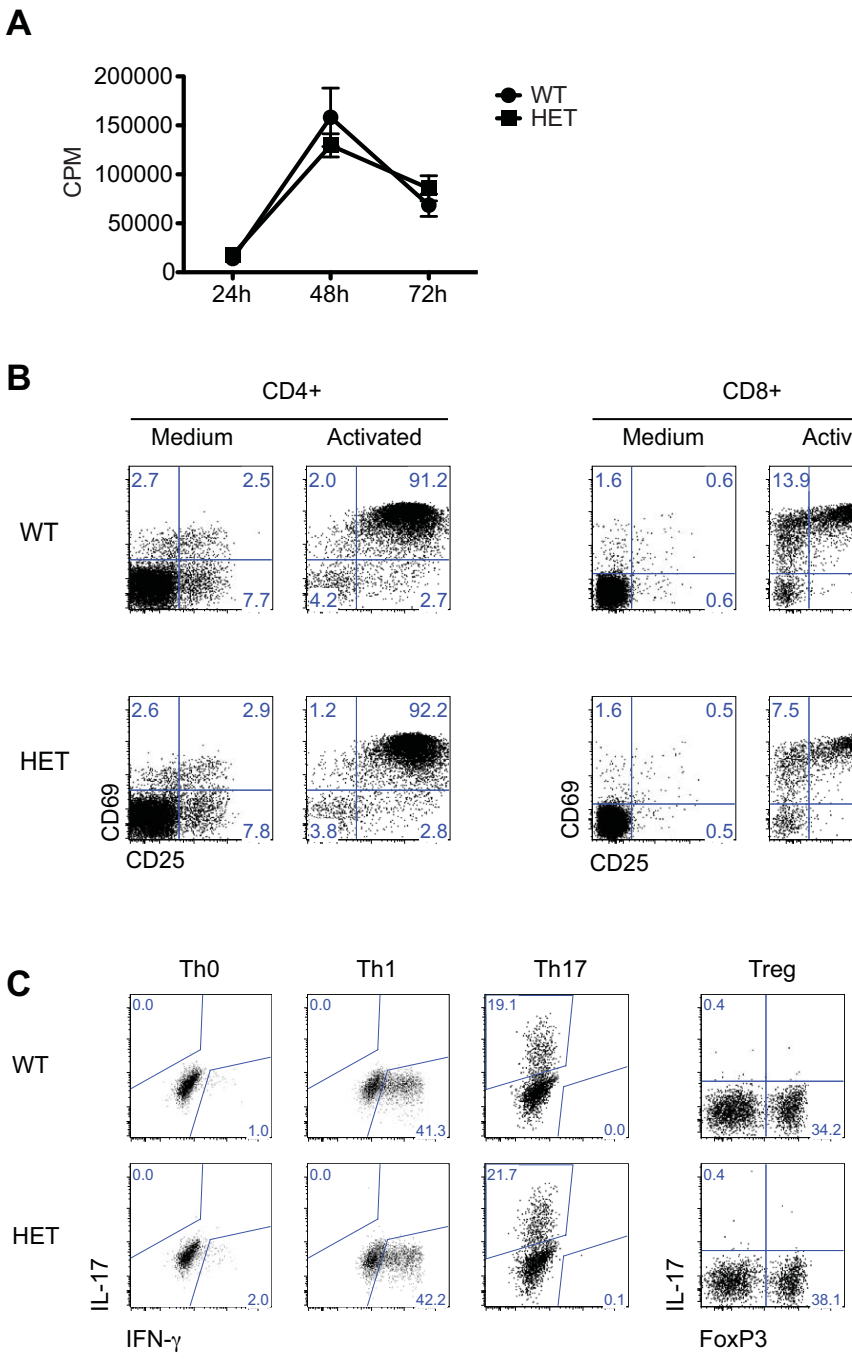

Appendix-2 Article: To investigate the necessity of STRA6 upregulation in T cells during T cell immune responses

Rafik Terra*[1], Xuehai Wang*[1], Yan Hu*[1], Tania Charpentier[#], Alain Lamarre[#], Ming Zhong^, Hui Sun^, Jianning Mao*, Shijie Qi*, Hongyu Luo* and Jiangping Wu*[+]

*From *Laboratoire d'immunologie and [+]Service de néphrologie, Centre de recherche, Centre hospitalier de l'Université de Montréal (CRCHUM) – Hôpital Notre-Dame, Montréal, Québec, Canada; [#]Institut national de la recherche scientifique (INRS) – Institut Armand-Frappier, Laval, Québec, Canada; ^Department of Physiology, Jules Stein Eye Institute, David Geffen School of Medicine, University of California, Los Angeles, California, USA*

Address correspondence to: Dr. Jiangping Wu, Laboratory of Immunology, CRCHUM – Hôpital Notre-Dame, Pavillon DeSève, Room Y-5616, 1560 Sherbrooke Street East, Montreal, Quebec, Canada H2L 4M1; Telephone: (514) 890-8000 Extension 25164; Fax: (514) 412-7596.

[1]These authors contributed equally to the work described in this article.

This work has been submitted to ***PloS ONE***.

Terra R, **Wang X (first co-author)**, Hu Y, Charpentier T, Lamarre A, Zhong M, Sun H, Mao J, Qi S, Luo H, Wu J. (2013) To investigate the necessity of STRA6 upregulation in T cells during T cell immune responses. ***PLoS ONE*** (submitted)

ABSTRACT

In our unbiased survey of genes modulated during the early stage of T-cell activation, we discovered that STRA6 (stimulated by retinoic acid gene 6) was up-regulated within 3 h of TCR stimulation. STRA6 is the high-affinity receptor for plasma retinol-binding protein (RBP) and mediates cellular vitamin A uptake. We generated STRA6 knockout (KO) mice to assess whether such up-regulation was critical for T-cell activation, differentiation and function. Unlike human STRA6 mutation, which causes severe defects in multiple organs, STRA6 KO mice under vitamin A sufficient conditions were fertile without apparent anomalies upon visual inspection. The size, cellularity and lymphocyte subpopulations of STRA6 KO thymus and spleen were comparable to those of their wild type (WT) controls. KO and WT T cells were similar in terms of TCR-stimulated proliferation *in vitro* and homeostatic expansion *in vivo*. Naive KO CD4 cells differentiated *in vitro* into Th1, Th2, Th17 as well as regulatory T cells in an analogous manner as their WT counterparts. *In vivo* experiments revealed that anti-viral immune responses to lymphocytic choriomeningitis virus in KO mice were comparable to those of WT controls. We also demonstrated that STRA6 KO and WT mice had similar glucose tolerance. Total vitamin A levels are dramatically lower in the eyes of KO mice as compared to those of WT mice, but the levels in other organs were not significantly affected after STRA6 deletion under vitamin A sufficient conditions, indicating that the eye is the mouse organ most sensitive to the loss of STRA6.

Our results demonstrate that under vitamin A sufficient conditions, the elimination of STRA6 altogether in T cells does no affect the T-cell immune responses so-far tested; 2) STRA6-independent vitamin A uptake compensated the lack of STRA6 in lymphoid organs under vitamin A sufficient conditions in mice; and 3) STRA6 is critical for vitamin A uptake in the eyes even in vitamin A sufficiency. W also found no evidence that STRA6 can trigger STAT5 signaling in lymphoid organs.

INTRODUCTION

During T-cell immune responses, naive T cells are activated by stimuli through TCR in the company of co-stimulation signals, and undergo multiple rounds of proliferation before entering the differentiation phase, after which they become effector T cells. The expression of many molecules is modulated during activation and differentiation stages, with some of them playing pivotal regulatory roles, while others exert support and house-keeping functions to cope with increased metabolic demands. We undertook unbiased exploration with DNA microarray analysis of molecules up- or down-regulated in T cells within the first 16 h after stimulation by anti-CD3 with a view to identifying those that are critical in the early T-cell activation stage. A group of molecules with the highest levels of altered expression in activated T cells was chosen, with resting T cells as reference, and verified by Northern blotting analysis. STRA6 (stimulated by retinoic acid gene 6) is among those that have been validated. We generated STRA6 gene knockout (KO) mice to assess the significance of its up-regulation in T-cell activation and, consequently, T-cell immune responses.

At the outset of our investigation in 2004, no function was ascribed to STRA6, a 74-kDa protein with multiple transmembrane domains that was first identified in retinoic acid-stimulated P19 embryonic carcinoma cells upon retinoic acid stimulation [1]. In 2007, Kawaguchi et al. used an unbiased technique to identify STRA6 as a specific cell-surface receptor for plasma retinol binding protein (RBP) and showed that STRA6 mediates cellular vitamin A uptake from holo-RBP (RBP/vitamin A complex) in bovine retinal pigment epithelium cells [2]. STRA6-mediated vitamin A uptake from holo-RBP is coupled to intracellular proteins as confirmed by several independent studies [1-5], and its mechanism in coupling to specific intracellular proteins has been elucidated [4]. Pasutto et al. [6] observed that mutations in STRA6 correlated with many eye, heart, diaphragm and lung malformations as well as mental retardation in Matthew-Wood syndrome in humans, corroborating its reported roles in vitamin A uptake by cells as vitamin A is vital in organogenesis. Recent reports indicate that single nucleotide polymorphisms or mutations in STRA6 gene are correlated with the congenital eye malformations microphthalmia, anophthalmia and coloboma [7,8] as well as Matthew-Wood syndrome [9]. Genetic null mutation of STRA6 in

mice results in significant retinoid reduction in the retinal pigment epithelium and neurosensory retina, diminished visual responses and eye morphology, although the last-mentioned defect is not as serious as in patients with STRA6 mutations [10].

There is a report suggesting that STRA6 is not only a vitamin A transporter but can also function as a cytokine receptor. Upon binding with holo-RBP, STRA6 is phosphorylated at tyrosine residue 643, which, in turn, recruits and triggers JAK2 and STAT5 activation [11].

The ascribed roles of STRA6 in vitamin A transport and the STAT5 signalling pathway are certainly relevant to T-cell activation and function. Retinoids are known to modulate Th1 (T helper 1), Th2, Th17 and reglulatory T (T_{reg}) cell development and function [12-17]. At the molecular level, it has been demonstrated that retinoic acid opens up the FoxP3 promoter tertiary structure for activated FoxP3 transcription [18]. RARα can interact with STAT5a and b [19], which are critical molecules in the signaling pathway of a key T activation cytokine IL-2 [20].

Vitamin A is absorbed from dietary nutrients. There are several possible modes of vitamin A transport to cells in different organs. Vitamin A in the diet can be transported to liver cells and other cell types in the form of chylomicron-bound retinyl ester [21,22]. The liver is the primary storage site for vitamin A in the form of all-trans-retinyl ester, which can be reverted to vitamin A [22]. As alluded to above, vitamin A associates with RBP in blood, and such complexes can deliver vitamin A to cells via the RBP receptor STRA6 [2]. Transthyretin can associate with vitamin A-bound RBP, and such coupling serve to prevent renal filtration of the holo-RBP [23], Recently, Alapatt et al. [24] discovered a second RBP receptor, a STRA6 homologue called RBPR2. RBPR2 is expressed in the liver, intestines, fatty tissues, and spleen. Like STRA6, RBPR2 is fully capable of binding to RBP and transporting vitamin A into cells. As vitamin A is hydrophobic, it should also be able to diffuse through cell membranes without any specific receptors.

The relative contribution of STRA6 to vitamin A cellular import in lymphoid organs has not been evaluated and is a secondary goal of our study.

In this study, we demonstrated that STRA6 KO mice were vital and fertile, manifesting no apparent anomalies in their lymphoid organs and T cell-dependent immune responses under vitamin A sufficient conditions. Intracellular vitamin A concentrations in lymphoid organs, such as the thymus and spleen of the KO mice were comparable to those of WT controls, although the vitamin A content in cells from KO eyes was significantly lower that that from the WT eyes. The implications of these data are discussed.

MATERIALS AND METHODS

RT-qPCR

STRA6 mRNA in cells and tissues from KO, heterozygous and WT mice was measured by RT-qPCR. Total RNA was extracted with TRIzol® (Invitrogen, Carlsbad, CA, USA) and then reverse-transcribed with Superscript II™ reverse-transcriptase (Invitrogen). The forward and reverse primers were 5'-AGG CAT CTG AGA ATG GAA GCC AGA-3' and 5'-AGC AGA ACC AGG AAC GAC AGT GAA-3', respectively. A 184-bp product was detected with the following amplification program: 95°C x 15 min, 1 cycle; 94°C x 15 s, 55°C x 30 s, 72°C x 30 s, 35 cycles. β-actin mRNA levels were measured as internal controls; the forward and reverse primers were 5'-TGGTACCACAGGCATTGTGAT-3' and 5'-TGATGTCACGCACGATTTCC CT-3', respectively, with the same amplification program as for STRA6 mRNA. The data were expressed as ratios of STRA6 and β-actin signals.

Generation of STRA6 KO mice

A PCR fragment amplified with the STRA6 cDNA sequence served as a probe to isolate genomic BAC DNA clone 7O8 from the RPCI-22 129/sv mouse BAC genomic library. The targeting vector was constructed by recombination [25] and routine cloning methods using an 11-kb STRA6 genomic fragment from clone 7O8 as the starting meterial. A 2.7-kb MunI-XbaI genomic fragment containing exon 2 was replaced by a 1.1-kb Neo cassette from pMC1Neo-Poly A flanked by 2 diagnostic restriction sites, XbaI and ScaI, as illustrated in Figure 2A. The final targeting fragment was excised from its cloning vector backbone by Not I digestion and electroporated into R1 embryonic stem (ES) cells for G418 selection [26]. The targeted ES cell clones were injected into C57BL/6 blastocysts. Chimeric male mice were mated with C57BL/6 females to establish mutated STRA6 allele germline transmission.

Southern blotting with probes corresponding to the 5' and 3' sequences outside the targeting region, as illustrated in Figure 2A (red squares), were used to screen for gene-targeted ES cells and eventually to confirm gene deletion in mouse tail DNA. With the 5' probe, the targeted allele should present a 7.8-kb XbaI band, and the WT allele, a 5.2-kb XbaI band.

With the 3' probe, the targeted allele should present a 6.9-kb ScaI band, and the WT allele, a 4.3-kb ScaI band (Fig. 2A).

PCR was adopted for routine genotyping of the targeted allele(s). The following PCR conditions were applied: 4 min at 94 °C, followed by 35 cycles of 30 s at 94 °C, 30 s at 60 °C, and 30 s at 72 °C, with final incubation at 72 °C for 10 min. The KO forward primer 5'- GCG TCA CCT TAA TAT GCG AAG TG-3' and reverse primer 5'-CAA GAA GTC CGT GGC TGA GTC TA-3' detected a 400-bp fragment from the targeted allele. The WT forward primer 5'-TCT CCC AGG TCT GGT TTG AG-3' and reverse primer 5'-TTA GGG CAA CAC CCT ACT GG-3' detected a 197-bp fragment from the WT allele.

The KO mice were backcrossed to the C57BL/6 background for 8 generations and then used for experimentation. All mice were housed under specific pathogen-free conditions and fed with mouse chow (Teklad Global 2018, Teklan Diets, Madison, WI) containing 15 IU/g Vitamin A. The mice had access to water and chow *ad libitum*. The studies were approved by the Institutional Animal Protection Committees of the CRCHUM and INRS-IAF.

Flow cytometry

Single cell suspensions from the thymus, spleen and lymph nodes were prepared and stained immediately or after culture with antibodies (Abs) against CD4, CD8, CD25, CD19, B220, CD69 and STRA6. In some experiments, intracellular proteins, such as FoxP3, IFN-γ, IL-4, IL-17, and TNF-α, were detected after the cells were pre-stained with Abs against cell surface antigens fixed with BD Cytofix/Cytoperm™ solution (BD Biosciences, San Diego, CA) and then stained with monoclonal Abs (mAb) against intracellular antigens. The Abs deployed for flow cytometry are listed in Table I. Flow cytometry analysis of the stained cells are described in our previous publications [27-30].

Flow cytometry was also employed to assess lymphocytic choriomeningitis virus (LCMV)-specific T cells. Synthetic peptides gp_{33-41}: KAVYNFATC (LCMV-GP, H-2D^b); $np_{396-404}$: FQPQNGQFI (LCMV-NP, H-2D^b); $gp_{276-286}$: SGVENPGGYCL (LCMV-GP, H-2D^b); and

gp_{61-80}: GLNGPDIYKGVYQFKSVEFD (LCMV-GP, I-A^b) were purchased from Sigma-Genosys (Oakville, Ontario, Canada). PE-gp_{33-41}, PE-$np_{396-404}$ and PE-$gp_{276-286}$ H-$2D^b$ tetrameric complexes were synthesized in-house and used at 1/100 dilution as previously described [26]. These MHC-tetramers were used to detect LCMV-specific $CD8^+$ T cells on day 8 post LCMV infection. Briefly, splenocytes were first stained with PE-gp_{33-41}, PE-$np_{396-404}$ or PE-$gp_{276-286}$ tetramers for 30 minutes at 37°C, followed by staining with FITC-rat anti-mouse CD8α and APC-rat anti-mouse CD62L mAbs at 4°C for another 20 minutes. 7-AAD was used for exclusion of dead cells. After washing, cells were fixed in 0.5% paraformaldehyde and samples were analyzed by flow cytometry. One million splenocytes from LCMV-infected mice were seeded in single wells of 96-well round-bottomed plates. They were maintained in 5% RPMI-1640 supplemented with 100 units/ml interleukin-2, 10 μg/ml brefeldin A, 10 μM gp_{33-41} or gp_{61-80} peptide. After 5 h of incubation at 37°C, the cells were stained with PE-conjugated rat anti-mouse CD8α or CD4 mAbs and 7-AAD. They were then fixed, permeabilized and stained with APC-labeled rat anti-mouse TNF-α and FITC-labeled rat anti-mouse IFN-γ mAbs. IFN-γ and TNF-α-secreting T cells were counted by flow cytometry [31].

T-cell proliferation in vitro and in vivo after being transferred to sub-lethally-irradiated mice

Spleen cells were loaded with carboxyfluorescein succinimidyl ester (CFSE; 5μM for 5 mins), and then cultured in the presence of soluble hamster against mouse CD3 mAb (clone 2C11; 0.5 μg/ml) [27,28,32,33]. After 3 days, CFSE fluorescence of the CD4 and CD8 subpopulations was analyzed by flow cytometry for TCR-stimulated proliferation. T-cell homeostatic expansion was evaluated by i.v. injection of 5 x 10^6 CFSE-loaded spleen cells into C57BL/6 recipients 5 h after sub-lethal irradiation (650 Rad). On day 5, the CFSE fluorescence of CD4 and CD8 cells from the spleen and LN was studied by flow cytometry.

In vitro Th1, Th2, *Th17 and T_{reg} cell polarization*

In vitro Th and T_{reg} cell differentiation was conducted as follows [27,34]. Naïve CD4 T cells ($CD4^+CD62L^+CD44^{low}$) were isolated from KO or WT mouse spleens with MagCellect Mouse Naïve $CD4^+$ T cell Isolation kits (R & D Systems). T cell-depleted WT spleen cells were

irradiated at 3000 Rad and used as feeder cells. The naïve CD4 cells (0.1×10^6/ well) were mixed with the feeder cells (0.5×10^6/well) and cultured in 96-well plates in the presence of soluble anti-CD3ε mAb (clone 145-2C11, 2 μg/ml; BD Biosciences). Cultures were supplemented with recombinant mouse IL-12 (10 ng/ml; R & D Systems) and anti-IL-4 mAb (10 μg/ml; R & D Systems) for the Th1 condition; recombinant mouse IL-4 (20 ng/ml; R & D Systems), and anti-IL-12 mAb (10 μg/ml; BD Biosciences) and anti-IFN-γ mAb (10 μg/ml; R & D Systems) for the Th2 condition; recombinant mouse IL-6 (20 ng/ml; R & D Systems), recombinant human TGF-β1 (5 ng/ml; R & D Systems) and anti-IL-4 and anti-IFN-γ mAbs (10 μg/ml for each; R & D Systems) for the Th17 condition; recombinant human TGF-β1 (5 ng/ml; R & D Systems), and anti-IL-4 and anti-IFN-γ mAb (10 μg/ml; R & D Systems) for the T_{reg} condition.

LCMV infection

LCMV clone 13 was obtained from Dr. R.M. Zinkernagel (University of Zurich, Zurich, Switzerland). Viral stock was propagated *in vitro,* and viral titers were quantified by focus-forming assay [31]. Mice were infected by the i.v. route with 2 x 10^6 focus-forming units of LCMV clone 13. They were sacrificed 8 days post-infection, and their spleens were harvested for primary immune response analysis.

Glucose tolerance tests

The KO and WT mice were fasted for 16 h and injected i.v. with D-glucose (2 mg/g body weight) in PBS. Blood samples from the tail vein were taken at 5, 15, 30, 60, and 90 min after the injection for glucose measurements with a glucose meter (Bayer, Toronto, Ontario).

Measurement of serum and intracellular vitamin A and retinyl ester concentrations by high-pressure liquid chromatography (HPLC)

Serum and tissue samples, collected in a dark, cold room, were stored at -80^{o}C until their analysis. Retinoids were extracted by homogenizing tissues in a butanol-acetonitrile mixture (1:1) with a tissue/solvent ratio of 200 mg/700 μl, in Eppendorf tubes on ice by 5 30-s pulses with 1-min intervals. K_2HPO_4 solution (6.89M) was added to the tubes in proportion to the

homogenized mixture (20 μl for 900 μl homogenized mixture). For retinoid extraction from sera, 200-μl butanol-acetonitrile mixture (1:1) was added to 200-μl serum, and the mixture was vortexed for 1 min; 20 μl K_2HPO_4 solution (6.89M) was then added to the mixture before 30-s vortexing. The tissue and serum samples thus prepared were centrifuged for 20 min at 14,000*g* at 4°C. Cleared supernatants were passed through Spin-X filters (0.45μm pore size; Costar, Batavia, Illinois, USA) at 14,000*g* for 10 min at 4°C. For retinyl ester measurement, the samples prepared as aforementioned before the step of filtration were vacuum-dried and re-dissolved in 100% methanol, followed by centrifugation at 14,000 g for 10 min. The supernatants were then analyzed by HPLC.

Vitamin A in extracts was quantified by HPLC in an ÄKTA Purifier (Model UPC10; GE Healthcare, Baie d'Urfé, Quebec, Canada) and reverse-phase column (μ-RPC C2/C18 ST 4.6/100; GE Healthcare). Samples (100 μl) were eluted with a linear gradient from 100% eluent A (acetontrile:water = 65:35) to 100% eluent B (acetontrile:water = 90:10) in 5-column volumes at a flow rate of 1 ml/min. Both eluates contained 10 mM ammonium acetate. Vitamin A was detected at 313 nm wave-length. Its characteristic retention volume was identified with pure Vitamin A from Sigma (Oakville, ON, Canada) as a standard. Areas under the curves were computed by UNICORN5.11 software (GE Healthcare). The sensitivity of the assay was 250 ng.

Retinyl ester in extracts was quantified by HPLC in an Eclipse XDB-C18 reverse-phase column (4.6 X150 mm, 5 μm, Agilent, Santa Clara, CA). Samples (200 μl) were eluted with a linear gradient from 100% methanol to 100% ethyl acetate in 5 column volumes at a flow rate of 1 ml/min. Retinyl ester was detected at 324 nm wavelength. Its characteristic retention volume was identified with retinyl palmitate (Sigma) as standard. Areas under the curves were computed by Agilent LC software. Sensitivity of the assay was 1.5 ng.

RESULTS

STRA6 expression in different organs and activated T cells

STRA6 mRNA expression was assessed by RT-qPCR. Among the organs and tissues examined, the thymus had the highest expression level, followed by the heart and kidneys (Fig. 1A). STRA6 expression in the spleen was moderate. The skeleton muscles and liver had barely detectable STRA6 mRNA. The STRA6 mRNA expression levels in the lung, liver, spleen and kidney assessed by our RT/qPCR was consistent with Northern results reported previously by Bouillet [1]. High STRA6 expression in the thymus suggested that it might have some critical functions in T-cell development and T-cell function. As depicted in Figure 1B, STRA6 expression in resting spleen T cells (0 h) was modest, consistent with values of the whole spleen. The expression was augmented with in 3 h after T-cell activation by TCR cross-linking, and reached a peak at 48 h. This result corroborates our initial DNA microarray data, through which STRA6 was found upregulated during T-cell activation.

Generation of STRA6 KO mice

To evaluate the roles of STRA6 in the immune system in general and T cell-mediated immune responses in particular, we produced STRA6 KO mice. The targeting strategy is illustrated in Figure 2A. Germline transmission was confirmed by Southern blotting of tail DNA (Fig. 2B). With the 5' end probe, the WT allele after XbaI digestion presented a 7.8-kb band, and the KO allele, a 5.2-kb band (Fig. 2B, upper panel). With the 3' end probe, the WT allele after ScaI digestion presented a 6.9-kb band, and the KO allele, a 4.3-kb band (Fig. 2B, lower panel). WT (mice 3, 4, and 5) and heterozygous mice (mice 1, 2 and 6) were thus identified. Mouse 1 was backcrossed to the C57BL/6 background for 8 generations, and then used in the experiments described hereafter.

To ascertain whether STRA6 gene deletion results in its lack of expression, we measured STRA6 mRNA in spleen cells by RT-qPCR. STRA6 mRNA was detectable in WT but not in KO spleen cells (Fig. 2C). The lack of STRA6 expression in KO cells at the protein level was confirmed by flow cytometry, as STRA6 was detectable in WT but not KO thymocyte surface (Fig. 2D).

Normal lymphoid organs and lymphocyte subpopulations in STRA6 KO mice

STRA6 KO mice were viable and fertile with no apparent anomalies upon visual inspection. Weight and cellularity of the KO thymus and spleen were comparable to those of WT mice (Fig. 3A). T-cell ($CD4^+$ plus $CD8^+$ versus non T-cell ($CD4^-CD8^-$) subpopulations, and CD4 versus CD8 T-cell subpopulations in the spleen and LN of WT and KO mice showed no consistent differences (Fig. 3B). The percentages of B cells

($CD19^+B220^+$) in the spleen and lymph nodes in WT and KO mice were also similar (Fig. 3C). In KO thymi, the percentages of CD4 single-positive and CD8 single-positive, CD4CD8 double-positive cells and $CD4^+/FoxP3^+$ T_{reg} cells were comparable to those in WT thymi (Fig. 3D). The comparable percentages of T_{reg} cells in the thymi of WT and KO mice were confirmed by the measurement of $FoxP3^+$ cells among $CD4^+CD25^+$ thymocytes (Fig. 3E).

In the periphery, the percentages of $FoxP3^+$ T_{reg} cells among CD4 cells in the spleen (Fig. 3F) and lymph nodes (Fig. 3G) from WT and KO mice were also similar.

These results show that STRA6 KO mice have normal lymphoid organ and T-cell development.

Normal activation, proliferation and differentiation of STRA6 KO T cells

KO and WT T cells were stimulated by solid-phase anti-CD3 mAb for 16 h. The activation markers CD25 and CD69 in CD4 and CD8 T cells were quantified by flow cytometry. KO and WT T cells showed similar up-regulation of these markers (Fig. 4A). To assess T-cell proliferation, KO and WT T cells in total spleen cells were loaded with CFSE and stimulated by soluble anti-CD3 mAb. After 3 days, their proliferation was assessed by flow cytometry. CD4 and CD8 KO T cells proliferated like their WT counterparts, as shown in Figure 4B. To measure T-cell homeostatic expansion, spleen T cells were loaded with CFSE and then injected into sub-lethally-irradiated syngeneic recipients. The proliferation of these transferred KO CD4 and CD8 cells in recipient spleens and LN during the 5 days after the injection was measured based on their CFSE content according to flow cytometry. As shown in Figure 4C, the cells from WT and KO mice proliferated similarly in vivo. Therefore, KO T-cell proliferation, whether caused by TCR stimulation in vitro or homeostatic expansion in vivo, was not defective.

When KO and WT naïve CD4 cells were cultured under Th1, Th2, Th17 and T_{reg} conditions, they achieved comparable Th1, Th2, Th17 and T_{reg} cell percentages (Fig. 5), indicating normal differentiation of naïve KO CD4 cells into these subpopulations.

The effect of STRA6 deletion in anti-LCMV immune responses in vivo

The function of STRA6 KO T cells *in vivo* was evaluated in the LCMV infection model. As illustrated in Figure 6A, the number of total splenocytes, and CD4 and CD8 cells on day 8 post-infection (8 dpi) presented no significant differences in WT and KO mice (Fig. 6A). The absolute numbers (Fig. 6B) and relative percentages (Fig. 6C) of LCMV-specific tetramer-positive ($gp33^+$, $np396^+$ and $gp276^+$) CD8 cells in virus-infected mice were all increased in

comparison to uninfected control C57BL/6 mice (data not shown), but there were no significant differences between KO and WT mice with regard to these parameters. The absolute numbers and relative percentages of LCMV-specific TNF-α-producing CD4 (gp61) and CD8 cells (gp33) (Figs. 6D and 6E), and LCMV-specific IFN-γ-producing CD4 and CD8 cells (Figs. 6F and 6G) in KO mice were comparable to those in WT controls. These results indicate that the STRA6 deletion had no discernable effect on anti-LCMV immune responses.

Normal glucose tolerance in STRA6 KO mice

One report suggests that STRA6 stimulation by RBP induces the expression of SOCS3, which inhibits insulin signaling [12]. We assessed the glucose tolerance of KO mice, and found that, KO and WT mice showed no significant difference in glucose tolerance (Fig. 7), suggesting that in the absence of STRA6, the insulin signaling of the KO mice on a normal diet is not enhanced.

Organ retinyl ester and retinol levels in STRA6 KO mice

As vitamin A has been reported to play an important role in immune regulation [12-17], a lack of immunological phenotype so-far tested in the KO mice prompted us to examine vitamin A contents of lymphoid organs as well as several other organs including the eyes. Vitamin A is stored in organs predominantly in the form of retinyl ester, which is a lipid and can reach high concentrations. A minor stored form is retinol bound to CRBP, and the retinol content in the cells is limited by the availability of CRBP. Retinyl esters and retinol and can be quickly converted to each other inside the cells. We thus measured the contents of both retinyl esters and retinol in these organs.

As shown in Figure 8A, the WT and KO spleen and thymus had no significant difference in their retinyl ester contents, nor did the brains and kidneys. The retinyl ester contents in WT eyes were much higher than that of other organs, and the contents in the KO eyes were significantly lower compared to those of the WT counterparts. WT or KO blood had no detectable retinyl ester (data not shown). Retinyl ester is known to be high in the blood only right after a meal enriched in vitamin A.

The retinol levels in these WT and KO organs were of the same pattern as retinyl ester, although at much lower levels (Fig. 8B; note the scale difference). The KO spleen, thymus, kidney and brain had no significant difference in retinol contents compared to their WT counterparts. Unlike retinyl ester, the retinol was detectable in the sera, but was of similar levels in WT and KO sera. The eyes contained the highest levels of retinol. KO eyes presented significantly lower levels of retinol than the WT counterparts.

These data indicate that under a vitamin A sufficient condition, lymphoid organs still take up vitamin A without STRA6 in mice. This explains the lack of immunological phenotype in the KO mice. However, even under such a vitamin A sufficient condition, the eyes still heavily depend on SRAT6 for vitamin A uptake, as they are the organ with the highest vitamin A demand.

DISCUSSION

STRA6 is a receptor of holo-RBP (i.e., vitamin A-bound RBP) for cellular vitamin A uptake. STRA6 is up-regulated after T-cell activation. In this study, we generated STRA6 KO mice to assess whether such up-regulation was essential for T cell-mediated immune responses and STRA6's role in vitamin A uptake. Under a vitamin A sufficient condition, STRA6 KO mice developed normally and were fertile. Their T cells presented no signs of abnormality in terms of development, activation marker up-regulation, proliferation, and Th and T_{reg} cell differentiation. KO mice also had normal anti-LCMV immune responses. There was no significant difference in intracellular vitamin A content, in the forms of both retinyl ester and retinol, in lymphoid organs from WT and KO mice. However, even under the vitamin A sufficient condition, the KO eyes contained significantly lower amounts of retinyl ester and retinol, indicating a critical role of vitamin A uptake in this organ.

A caveat of whole organ retinoid analysis is that contribution of retinoid in the blood can affect the total retinoid levels. This is especially true if the organ is rich in blood, which contains RBP-bound vitamin A. Despite this caveat, whole organ retinoid analysis can be used as an approximation of cellular retinoid uptake. This is especially true as several of the organs we tested (i.e., the thymus, brain and eyes) are not blood rich. Moreover, sera had no detectable retinyl ester (data not shown); so the retinyl ester levels of the organs tested will not be upward influenced by the blood retinyl ester levels. The reduced vitamin A contents in the eyes of STRA6 KO mice is not unexpected, as the eyes have the highest concentrations of vitamin A among all the organs (Fig. 8) due to its heavy reliance on vitamin A for vision, and probably need all the capacities of vitamin A transport including the pathway of RBP/STRA6 to achieve this high vitamin A content, even in vitamin A sufficiency. Consistent to our findings, RBP KO mice have normal vitamin A levels in most of their organs, but a reduced one in the eyes [35].

Vitamin A and its metabolites – retinoic acids – are clearly required in immune responses [13-18, 36]. It is reported that in hepatocytes, holo-RBP triggers STRA6, leading to the activation of JAK2/STAT5 signaling pathway, which is also essential in the activation and function of

immune cells. STRA6 is up-regulated within 24 h of T-cell activation (Fig. 1B). Is such up-regulation, or more fundamentally, the existence of STRA6, essential for T cell-mediated immune responses? We demonstrated that in STRA6 KO mice, a lack of STRA6 did not affect T-cell activation/proliferation/differentiation *in vitro* and anti-viral immune responses *in vivo* under a vitamin A sufficient condition. These observations suggest following possible and not necessarily mutually exclusive explanations: 1) STRA6 up-regulation/existence only becomes important for T-cell functions during vitamin A deficiency, when all capacities of vitamin A import to immune cells are required; 2) STRA6 homologue RBPR2 can compensate for STRA6 function in the immune cells, as this homologue is expressed in the spleen; also, retinyl esters bound to lipoproteins secreted by the small intestine can deliver vitamin A to peripheral organs under vitamin A sufficient conditions; 3) STRA6 plays a minimal role in modulating the JAK2/STAT5 signalling pathway in immune cells, and its upregulation after T cell activation has nothing to do with JAK2/STAT5 signaling; 4) We cannot exclude the possibility that STRA6 deletion might still affect certain T cell-mediated immune responses to some extent, but they have not been assessed in our experiments, or their magnitude was too small to be discerned by current assays; 5) Such up-regulation might be a parallel and irrelevant event during T-cell activation.

There is little systemic documentation on vitamin A sufficiency status in wild mammals in today's world. However, it is well-documented that vitamin A deficiency is prevalent in African and Southeast Asian populations, particularly affecting children and pregnant women, according to the World Health Organization [37], and such deficiency predisposes them to infectious diseases [38]. It is conceivable that, during evolution, mammals might have experienced vitamin A deficiencies in certain periods or regions in the world. Better cellular vitamin A transport will confer an evolutionary advantage to these animals with regard to but not restricted by their ability to cope with infectious diseases. If STAR6 is universally critical in all cell types for vitamin A uptake, its function should be revealed in immune responses in vitamin A deficiency. Experiments addressing this possibility are in progress.

STRA6 point mutations are found in some patients, with microphthalmia, anophthalmia, coloboma [7] and Matthew-Wood syndrome [referring to combinations of microphthalmia/anophthalmia, cardiac malformations, pulmonary dysgenesis, and diaphragmatic hernia; ref. 9]. In a study of 2 unrelated consanguineous families with malformation syndromes sharing anophthalmia and distinct eyebrows as common signs, homozygous mutations were identified in STRA6 [6]. Our STRA6 KO mice and those generated by Ruiz *et al.* [10] did not have dramatic phenotypes, such as a total absence of eyes, as seen in humans with STRA6 mutations.

Why cannot STRA6 KO in mice reproduce human disease phenotypes caused by STRA6 mutations? A simple explanation is that this is due to species differences. It is not unprecedented that gene mutations in mice and humans have very different phenotypes. For example, partial or complete loss of ABCA4 functions cause many blinding diseases in humans including retinitis pigmentosa, cone-rod dystrophy and Stargdardt macular dystrophy, but ABCA4 KO in mice does not cause blindness unless combined with a deletion of other genes such as RDH8 [39-41]. On the other hand, disease loci of microphthalmia and anophthalmia have been mapped to multiple chromosomes [42-45]. Patients with Matthew-Wood syndrome or malformation syndromes have quite large phenotype variations in terms of organ affliction and disease severity. Such observations suggest that these syndromes are not monogenic, and STRA6 mutation alone is not sufficient to evoke all such phenotypes. It could explain why no serious ophthalmic [13] or other organ malformations are apparent in STRA6 null mutation mice. If STRA6's major function is cellular vitamin A uptake, and human organ malformation syndromes are mainly caused by a lack of available intracellular vitamin A, it would support the notion that STRA6 only plays a minor role in cellular vitamin A uptake in vitamin A sufficiency, especially in organs other than the eyes. Unless other routes of cellular vitamin A uptake such as those mediated by RBPR2 or by retinyl esters bound to lipoproteins are simultaneously compromised, vitamin A in the cells of most, if not all, organs vitamin A contents will remain in the normal range, and the organs will develop and function normally in vitamin A sufficiency. However, significant phenotype might be revealed in vitamin A deficiency. This hypothesis is supported by results from RBP KO mice. These KO mice are

fertile and have no organ abnormality other than the vision phenotype [46-48], as is the case of STRA6 KO mice when fed with a vitamin A sufficient diet. However, they manifest severe systemic phenotype of embryonic lethality under a vitamin A deficient condition [49,50]. Consistently, in mouse embryo culture where is no retinyl ester pathway, RBP knockdown also causes severe developmental defects [51].

In summary, we conclude that, under normal dietary conditions, mouse lymphoid organ development, T-cell activation and differentiation, including T_{reg} cell development, and anti-LCMV responses, could proceed normally in the absence of STRA6 under vitamin A sufficient conditions.

REFERENCES

1. Bouillet P, Sapin V, Chazaud C, Messaddeq N, Décimo D, et al. (1997) Developmental expression pattern of STRA6, a retinoic acid-responsive gene encoding a new type of membrane protein. Mech Dev 63: 173-186.

2. Kawaguchi R, Yu J, Honda J, Hu J, Whitelegge J, et al. (2007) A membrane receptor for retinol binding protein mediates cellular uptake of vitamin Amin A. Science 315: 820-825.

3. Golczak M, Maeda A, Bereta G, Maeda T, Kiser PD, et al. (2008) Metabolic basis of visual cycle inhibition by retinoid and nonretinoid compounds in the vertebrate retina. J Biol Chem 283: 9543-9554.

4.Isken A, Golczak M, Oberhauser V, Hunzelmann S, Driever W, et al. (2008) RBP4 disrupts vitamin A uptake homeostasis in a STRA6-deficient animal model for Matthew-Wood syndrome. Cell Metab 7: 258-268.

5. Kawaguchi R, Yu J, Ter-Stepanian M, Zhong M, Cheng G, et al. (2011) Receptor-mediated cellular uptake mechanism that couples to intracellular storage. ACS Chem Biol 6: 1041-1051.

6. Pasutto F, Sticht H, Hammersen G, Gillessen-Kaesbach G, Fitzpatrick DR, et al. (2007) Mutations in STRA6 cause a broad spectrum of malformations including anophthalmia, congenital heart defects, diaphragmatic hernia, alveolar capillary dysplasia, lung hypoplasia, and mental retardation. Am J Hum Genet 80: 550-560.

7. Casey J, Kawaguchi R, Morrissey M, Sun H, McGettigan P, et al. (2011) First implication of STRA6 mutations in isolated anophthalmia, microphthalmia, and coloboma: a new dimension to the STRA6 phenotype. Hum Mutat 32: 1417-1426.

8. Ng W, Pasutto F, Bardakjian T, Wilson M, Watson G, et al. (2013) A puzzle over several decades: eye anomalies with FRAS1 and STRA6 mutations in the same family. Clin Genet 83: 162-168.

9. Chassaing N, Golzio C, Odent S, Lequeux L, Vigouroux A, et al. (2009) Phenotypic spectrum of STRA6 mutations: from Matthew-Wood syndrome to non-lethal anophthalmia. Hum Mutat 30: E673-681.

10. Ruiz A, Mark M, Jacobs H, Klopfenstein M, Hu J, et al. (2012) Retinoid content, visual responses, and ocular morphology are compromised in the retinas of mice lacking the retinol-binding protein receptor, STRA6. Invest Ophthalmol Vis Sci 53: 3027-3039.

11. Berry DC, Jin H, Majumdar A, Noy N (2011) Signaling by vitamin Amin A and retinol-binding protein regulates gene expression to inhibit insulin responses. Proc Natl Acad Sci USA 108: 4340-4345.

12. Cantorna MT, Nashold FE, Hayes CE (1994) In vitamin A deficiency multiple mechanisms establish a regulatory T helper cell imbalance with excess Th1 and insufficient Th2 function. J Immunol 152: 1515-1522.

13. Racke MK, Burnett D, Pak SH, Albert PS, Cannella B, et al. (1995) Retinoid treatment of experimental allergic encephalomyelitis. IL-4 production correlates with improved disease course. J Immunol 154: 450-458.

14. Stephensen CB, Rasooly R, Jiang X, Ceddia MA, Weaver CT, et al. (2002) Vitamin A enhances in vitro Th2 development via retinoid X receptor pathway. J Immunol 168: 4495-4503.

15. Mucida D, Park Y, Kim G, Turovskaya O, Scott I, et al. (2007) Reciprocal TH17 and regulatory T cell differentiation mediated by retinoic acid. Science 317: 256-260.

16. Benson MJ, Pino-Lagos K, Rosemblatt M, Noelle RJ (2007) All-trans retinoic acid mediates enhanced T reg cell growth, differentiation, and gut homing in the face of high levels of co-stimulation. J Exp Med 204: 1765-1774.

17. Sun CM, Hall JA, Blank RB, Bouladoux N, Oukka M, et al. (2007) Small intestine lamina propria dendritic cells promote de novo generation of Foxp3 T reg cells via retinoic acid. J Exp Med 204: 1775-1785.

18. Kang SG, Lim HW, Andrisani OM, Broxmeyer HE, Kim CH (2007) Vitamin Amin A metabolites induce gut-homing FoxP3+ regulatory T cells. J Immunol 179: 3724-3733.

19. Dong S, Tweardy DJ (2002) Interactions of STAT5b-RARalpha, a novel acute promyelocytic leukemia fusion protein, with retinoic acid receptor and STAT3 signaling pathways. Blood 99: 2637-2646.

20. Yao Z, Kanno Y, Kerenyi M, Stephens G, Durant L, et al. (2007) Nonredundant roles for Stat5a/b in directly regulating Foxp3. Blood 109: 4368-4375.

21. Blomhoff R, Green MH, Berg T, Norum KR (1990) Transport and storage of vitamin Amin A. Science 250: 399-404.

22. D'Ambrosio DN, Clugston RD, Blaner WS (2011) Vitamin Amin A metabolism: an update. Nutrients 3: 63-103.

23. Naylor HM, Newcomer ME (1999) The structure of human retinol-binding protein (RBP) with its carrier protein transthyretin reveals an interaction with the carboxy terminus of RBP. Biochemistry 38: 2647-2653.

24. Alapatt P, Guo F, Komanetsky SM, Wang S, Cai J, et al. (2013) Liver retinol transporter and receptor for serum retinol binding protein (RBP). J Biol Chem 288: 1250-1265.

25. Liu P, Jenkins NA, Copeland NG (2003) A highly efficient recombineering-based method for generating conditional knockout mutations. Genome Res 13: 476-484.

26. Nagy A, Rossant J, Nagy R, Abramow-Newerly W, Roder JC (1993) Derivation of completely cell culture-derived mice from early-passage embryonic stem cells. Proc Natl Acad Sci USA 90: 8424-8428.

27. Luo HY, Charpentier T, Wang XH, Qi SJ, Han B, et al. (2011) EFNB1 and EFNB2 proteins regulate thymocyte development, peripheral T cell differentiation and antiviral immune responses and are essential for IL-6 signaling J Biol Chem 286: 41135-41152.

28. Luo H, Qi SJ, Wu ZH, Han B, Wu JP (2011) EFNB1 and EFNB2 physically bind to IL-7Ra and retard its internalization from the cell surface. J Biol Chem 286: 44976-44987.

29. Yu G, Mao J, Wu Y, Luo H, Wu J (2006) EphrinB1 is critical in T-cell development J Biol Chem 281: 10222-10229.

30. Mao J, Qiao X, Luo, Wu J (2006) Transgenic Drak2 overexpression in mice leads to increased T cells apoptosis and compromised memory T cell development. J Biol Chem 281: 12587-12595.

31. Lacasse P, Denis J, Lapointe R, Leclerc D, Lamarre A (2008) Novel plant virus-based vaccine induces protective cytotoxic T-lymphocyte-mediated antiviral immunity through dendritic cell maturation. J Virol 82: 785-794.

32. Han B, Moore PA, Wu J, Luo H (2007) Overexpression of human decoy receptor 3 in mice results in a systemic lupus erythematosus-like syndrome. Arthritis Rheum 56: 3748-3758.

33. Yu G, Luo H, Wu Y, Wu J (2003) Mouse ephrinB3 augments T-cell responses to T-cell receptor ligation. J Biol Chem 278: 47209-47216.

34. Zhang J, Wang X, Fahmi H, Wojcik S, Fikes J, et al. (2009) Role of TL1A in the pathogenesis of rheumatoid arthritis. J Immunol 183: 5350-5357.

35. Quadro L, Hamberger L, Colantuoni V, Gottesman ME, Blaner WS (2003) Understanding the physiological role of retinol-binding protein in vitamin A metabolism using transgenic and knockout mouse models. Mol Aspects Med 24: 421-430.

36. Hall JA, Grainger JR, Spencer SP, Belkaid Y (2011) The role of retinoic acid in tolerance and immunity. Immunity 35: 13-22.

37.http://www.who.int/vmnis/vitamin Amina/data/database/countries/ en/index.html. Accessed 1 May 2013.

38. Sommer A (2008) Vitamin Amin a deficiency and clinical disease: an historical overview. J Nutr 138: 1835-1839.

39. Weng J, Mata NL, Azarian SM, Tzekov RT, Birch DG, et al. (1999) Insights into the function of Rim protein in photoreceptors and etiology of Stargardt's disease from the phenotype in abcr knockout mice. Cell 98: 13-23.

40. Maeda A, Golczak M, Maeda T, Palczewski K (2009) Limited roles of Rdh8, Rdh12, and Abca4 in all-trans-retinal clearance in mouse retina. Invest Ophthalmol Vis Sci 50: 5435-5443.

41. Maeda A, Maeda T, Golczak M, Palczewski K (2008) Retinopathy in mice induced by disrupted all-trans-retinal clearance. J Biol Chem 283: 26684-26693.

42. Bessant DA, Khaliq S, Hameed A, Anwar K, Mehdi SQ, et al. (1998) A locus for autosomal recessive congenital microphthalmia maps to chromosome 14q32. Am J Hum Genet 62: 1113-1116.

43. Graham CA, Redmond RM, Nevin NC (1991) X-linked clinical anophthalmos. Localization of the gene to Xq27-Xq28. Ophthalmic Paediatr Genet 12: 43-48.

44. Hmani-Aifa M, Ben Salem S, Benzina Z, Bouassida W, Messaoud R, et al. (2009) A genome-wide linkage scan in Tunisian families identifies a novel locus for non-syndromic posterior microphthalmia to chromosome 2q37.1. Hum Genet 126: 575-587.

45. Morlé L, Bozon M, Zech JC, Alloisio N, Raas-Rothschild A, et al. (2000) A locus for autosomal dominant colobomatous microphthalmia maps to chromosome 15q12-q15. Am J Hum Genet 67: 1592-1597.

46. Quadro L, Blaner WS, Salchow DJ, Vogel S, Piantedosi R, et al. (1999) Impaired retinal function and vitamin A availability in mice lacking retinol-binding protein. Embo J 18: 4633-4644.

47. Quadro L, Hamberger L, Colantuoni V, Gottesman ME, Blaner WS (2003) Understanding the physiological role of retinol-binding protein in vitamin A metabolism using transgenic and knockout mouse models. Mol Aspects Med 24: 421-430.

48. Quadro L, Gamble MV, Vogel S, Lima AA, Piantedosi R, et al. (2000) Retinol and retinol-binding protein: gut integrity and circulating immunoglobulins. J Infect Dis 182 Suppl 1: S97-S102.

49. Quadro L, Hamberger L, Gottesman ME, Colantuoni V, Ramakrishnan R, et al. (2004) Transplacental delivery of retinoid: the role of retinol-binding protein and lipoprotein retinyl ester. Am J Physiol Endocrinol Metab 286: E844-851.

50. Quadro L, Hamberger L, Gottesman ME, Wang F, Colantuoni V, et al. (2005) Pathways of vitamin A delivery to the embryo: insights from a new tunable model of embryonic vitamin A deficiency. Endocrinology 146: 4479-4490.

51. Bavik C, Ward SJ, Chambon P (1996) Developmental abnormalities in cultured mouse embryos deprived of retinoic by inhibition of yolk-sac retinol binding protein synthesis. Proc Natl Acad Sci U S A 93: 3110-3114.

FIGURE LEGENDS

Figure 1. STRA6 mRNA expression in organs and activated T cells

STRA6 mRNA in organs (A) and activated T cells (B) was measured by RT-qPCR. WT spleen T cells were cultured in wells coated with solid-phase anti-CD3 mAb and anti-CD28 mAb (0.5 μg/ml and 4 μg/ml, respectively, for coating) for the durations indicated. The cells were then harvested and their STRA6 mRNA levels measured by RT-qPCR. Samples were in triplicate for RT-qPCR, and means ± SD of ratios versus β-actin signals are reported. Experiments were conducted twice, and representative data are illustrated.

Figure 2. Generation of STRA6 KO mice

A. Targeting strategy for generating STRA6 KO mice

The red squares on the 5' and 3' sides of the mouse STRA6 WT genomic sequence represent the sequences serving as probes for genotyping by Southern blotting.

B. Genotyping of STRA6 mutant mice

Tail DNA was digested with XbaI, and analyzed by Southern blotting (top panel), with the 5' probe whose location is indicated in A. A 7.8-kb band representing the WT allele and a 5.2-kb band representing the recombinant allele are indicated by arrows. Similarly, tail DNA was digested with ScaI, and analyzed with the 3' probe (bottom panel). A 6.9-kb band representing the WT allele and a 4.3-kb band representing the recombinant allele are indicated by arrows.

C. Absence of STRA6 mRNA expression in STRA6 KO splenocytes

STRA6 mRNA levels from WT and KO splenocytes were analyzed by RT-qPCR. The RT-qPCR samples were in triplicate and the results are expressed as ratios of STRA6 versus β-actin mRNA signals with means ± SD indicated. The experiments were conducted twice and representative data of one experiment are shown.

D. Absence of STRA6 protein expression in KO thymocytes

WT and KO thymocytes were stained with goat anti-mouse STRA6 Ab, and analyzed by flow cytometry. The shaded area is the isotypic Ab staining control using WT thymocytes. The

thick line represents WT thymocytes stained with anti-STRA6 Ab, and the dotted line, KO thymocytes stained with anti-STRA6 Ab. The experiments were carried out three times and a representative histogram is shown.

Figure 3. STRA6 KO mice presented normal lymphoid organs and lymphocyte subpopulations

A. Weight and cellularity of WT and KO thymi and spleens

Mouse number (n) in each group is shown. No significant difference is detected in weight and cellularity between KO and WT organs (p>0.01, paired Student's t test).

B. CD4 and CD8 T-cell subpopulations in WT and KO spleens and LN

Splenocytes and LN cells were analyzed by 2-color flow cytometry for percentages of CD4 and CD8 T cells.

C. B cell populations in the spleen and LN of WT and KO mice

Splenocytes and LN cells were analyzed by 2-color flow cytometry for percentages of $CD19^+/B220^+$ B cells.

D and E. Normal thymocyte subpopulations and endogenous T_{reg} cells in KO thymi

CD4/CD8 double-negative, CD4/CD8 double-positive, CD4 single-positive and CD8 single-positive cells and $CD4^+CD8^-FoxP3^+$ T_{reg} cells in KO and WT thymi were analyzed by 3-color flow cytometry (D). $CD4^+CD25^+FoxP3^+$ T_{reg} cells in the WT and KO thymi were also analyzed by 3-color flow cytometry (E).

F and G. $CD4^+CD8^-FoxP3^+$ T_{reg} cells in KO and WT spleens and LN

$CD4^+CD8^-FoxP3^+$ T_{reg} cells in KO and WT spleens (F) and LN (G) were analyzed by 3-color flow cytometry.

The experiments in B through G were conducted more than 3 times, and representative histograms are presented. Percentages of relevant populations are indicated.

Figure 4. Normal activation and proliferation of KO T cells

A. Normal activation marker CD69 and CD25 expression on KO T cells

Total spleen cells were stimulated overnight by soluble anti-CD3 mAb (0.5 μg/ml). CD69 and CD25 expression on CD4 (left panel) and CD8 (right panel) T cells was measured by 3-color flow cytometry.

B. Normal proliferation of KO CD4 and CD8 cells upon TCR activation in vitro

Total spleen cells were loaded with CFSE and then stimulated with soluble anti-CD3 mAb (0.5 μg/ml). The cells were harvested after 72 h, and stained for CD4 and CD8; CFSE levels in these cells were analyzed by 3-color flow cytometry.

C. KO CD4 and CD8 cells present normal homeostatic expansion in vivo

Five million CFSE-loaded spleen cells were injected i.v. into sub-lethally irradiated (650 Rad) C57BL/6 recipients 5 h after the irradiation. On days 6, the CFSE fluorescence of CD4 and CD8 cells from the spleen and LN was analyzed by flow cytometry.

All experiments in this figure were conducted twice or more, and representative histograms are shown.

Figure 5. Normal differentiation of STRA6 KO CD4 cells in vitro

Naïve CD4 cells were cultured under conditions favouring Th1 (A), Th2 (B), Th17 (C) and T_{reg} (D) cell differentiation. Their intracellular cytokine or FoxP3 expression was quantified by flow cytometry on day 3 for Th1, Th17 and T_{reg} cells, and on day 5 for Th2 cells. Experiments were repeated more than 3 times, and representative histograms are shown.

Figure 6. Normal in vivo anti-LCMV immune responses of STRA6 KO mice

A. Spleen cell numbers on day 8 after LCMV infection

Means $\pm$ SD of absolute numbers of total splenocytes, $CD4^+$ cells, and $CD8^+$ cells in spleens of WT littermate control (n=4) and KO (n=4) mice on day 8 post-LCMV infection are presented.

B and C. LCMV-specific CD8 cells on day 8 post-LCMV infection

On day 8 post-infection, the absolute numbers of gp33, np396 and gp276 tetramer-positive CD8 T cells per spleen (B) and the percentage of gp33, np396 and gp276 tetramer-positive cells among CD8 cells (C) were measured by flow cytometry. Means ± SD of data from 4 pairs of WT littermate control and STRA6 KO mice are presented.

D and E. LCMV-specific TNF-α-producing CD4 and CD8 cells on day 8 post-LCMV infection

The absolute number of TNF-α-producing LCMV-specific CD4 cells (gp61-specific) and CD8 cells (gp33-specific) per spleen (D) and percentage (E) of these cells among total spleen cells of KO and WT mice on day 8 post-LCMV infection. Means ± SD of data from 4 pairs of STRA6 KO mice and WT littermate controls are shown.

F and G. Virus-specific IFN-γ-producing CD4 and CD8 cells on day 8 post-LCMV infection

The absolute number of TNF-α-producing LCMV-specific CD4 cells (gp61-specific) and CD8 cells (gp33-specific) per spleen (D) and percentage (E) of these cells among total spleen cells of KO and WT mice on day 8 post-LCMV infection. Means ± SD of data from 4 pairs of STRA6 KO mice and WT littermate controls are shown.

Figure 7. Glucose tolerance of KO and WT mice

WT (n=5) and KO (n=7) mice were fasted for 16 h, and then injected i.p. with D-glucose (2 mg/g body weight). Blood glucose was measured at different time points from the time of injection until 120 min. Means ± SD of glucose levels (mg/dL) are reported. No statistical significant difference is observed between the KO and WT groups (ANOVA).

Figure 8. Intracellular retinoid contents in lymphoid and other organs of STRA6 KO mice were comparable to those of WT mice

Retinoid (retinyl ester, A; retinol, B) contents (nmol/gram tissue or nmonl/ml serum) of the eyes, brain, kidney, spleen, thymus, spleen, thymus and sera from KO and WT mice were measured by HPLC. The mouse numbers (n) per grouop are indicated. The results are expressed as means + SD. The *p*-values are indicated when significant (Student's *t* test).

TABLES

Table 0.4 Antibodies and reagents for flow cytometry

Antibody	***Supplier***
PE-donkey anti-goat IgG	R & D Systems
APC-rat anti-mouse CD25 (clone PC61)	BD Biosciences
FITC-rat anti-mouse CD25 (clone 7D4)	BD Biosciences
PE-rat anti-mouse CD4 (clones GK1.5 and H129.19)	BD Biosciences
PerCP-rat anti-mouse CD4 (clone RM4-5)	BD Biosciences
biotin-rat anti mouse CD8b (clone 53-5.8)	BD Biosciences
APC-Cy7- anti-mouse B220 (clone RA3-6B2)	BD Biosciences
PE- or APC-hamster anti-mouse CD3ε (clone 145-2C11)	BD Biosciences
biotin- or FITC-rat anti-mouse CD44 (clone 1M7)	BD Biosciences
FITC- or PE-rat anti-mouse CD8α (clone 53-6.7)	BD Biosciences
APC-rat anti-mouse CD8α (clone H57-597)	BD Biosciences
PE-rat anti-mouse IL-17A	BD Biosciences
PE- and APC-rat anti-mouse IFN-γ	BD Biosciences
PE- and APC-rat anti-mouse IL4 mAbs	BD Biosciences
PerCP-streptavidin and 7-Amino-actinomycin D (7-AAD)	BD Biosciences
APC-Cy7-Streptavidin™	BioLegend
APC-rat anti-mouse TNF-α (clone MP6-XT22)	eBioscience (San Diego, CA)
FITC-rat anti-mouse IFN-γ (clone XMG1.2)	eBioscience
APC-rat anti-mouse IL17A (clone eBio17B7)	eBioscience
APC-rat anti mouse/rat Foxp3 (clone FJK-16s) mAbs	eBioscience
PE-Cy7-streptavidin	eBioscience
intracellular antigen fixation buffer	eBioscience
10X permeabilization buffer	eBioscience
APC-Cy™ PE-rat anti-mouse CD25 (clone PC61)	Cedarlane Laboratories Ltd (Burlington, Ontario, Canada)
Goat anti-mouse STRA6 Ab	Everest Biotech (Upper Heyford, Oxfordshire, UK)

Figure 0.8

Figure 1.

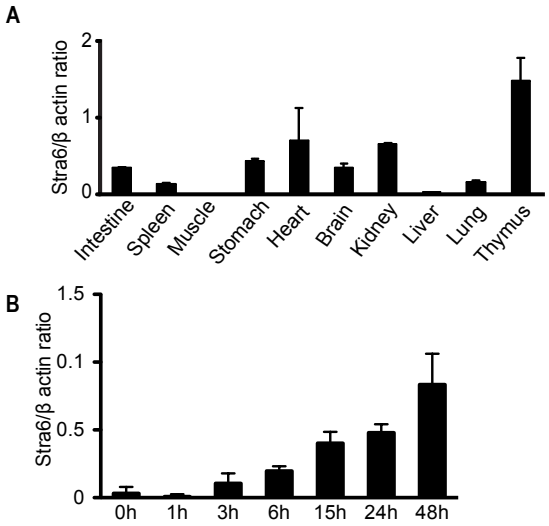

Figure 0.9

Figure 2.

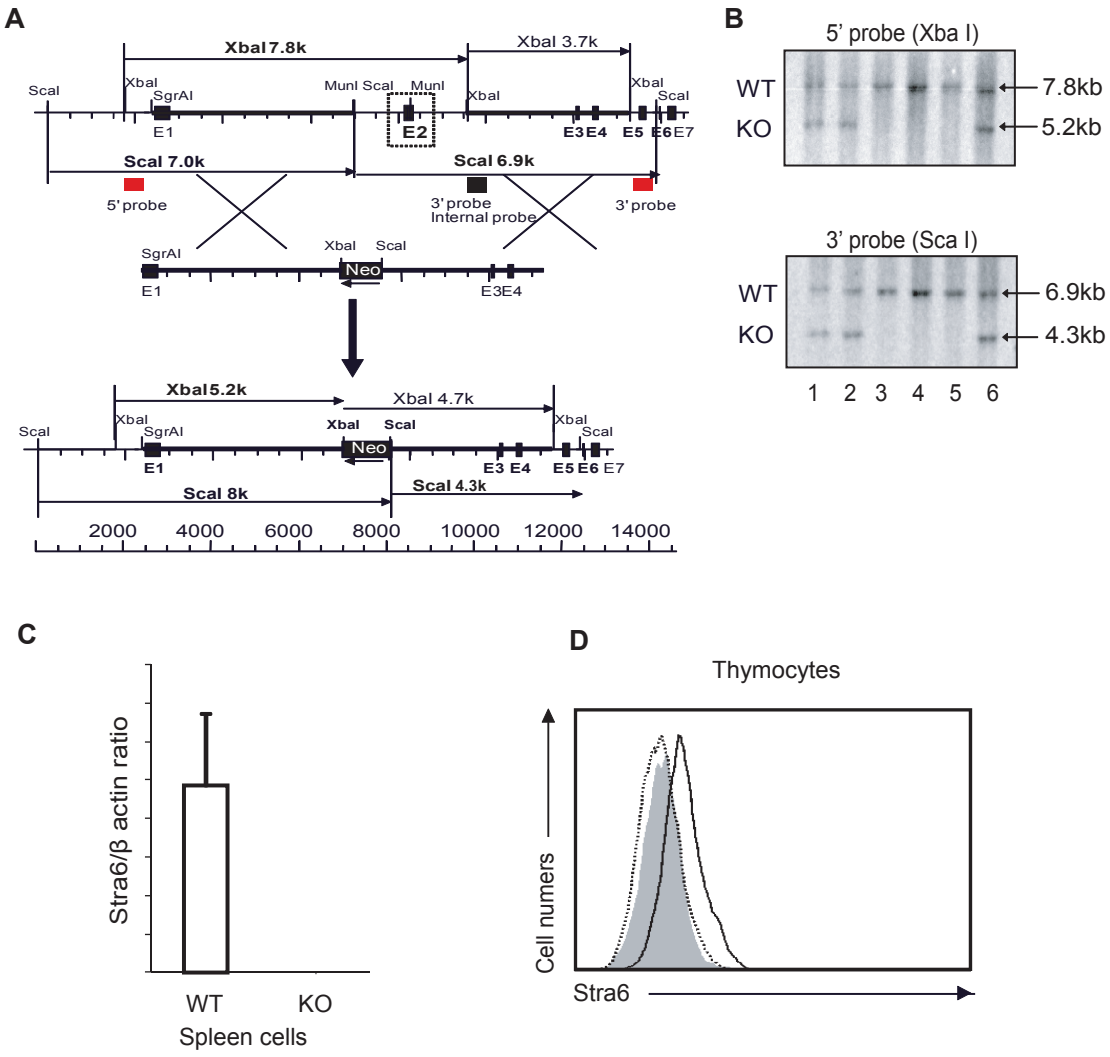

Figure 0.10

Figure 3.

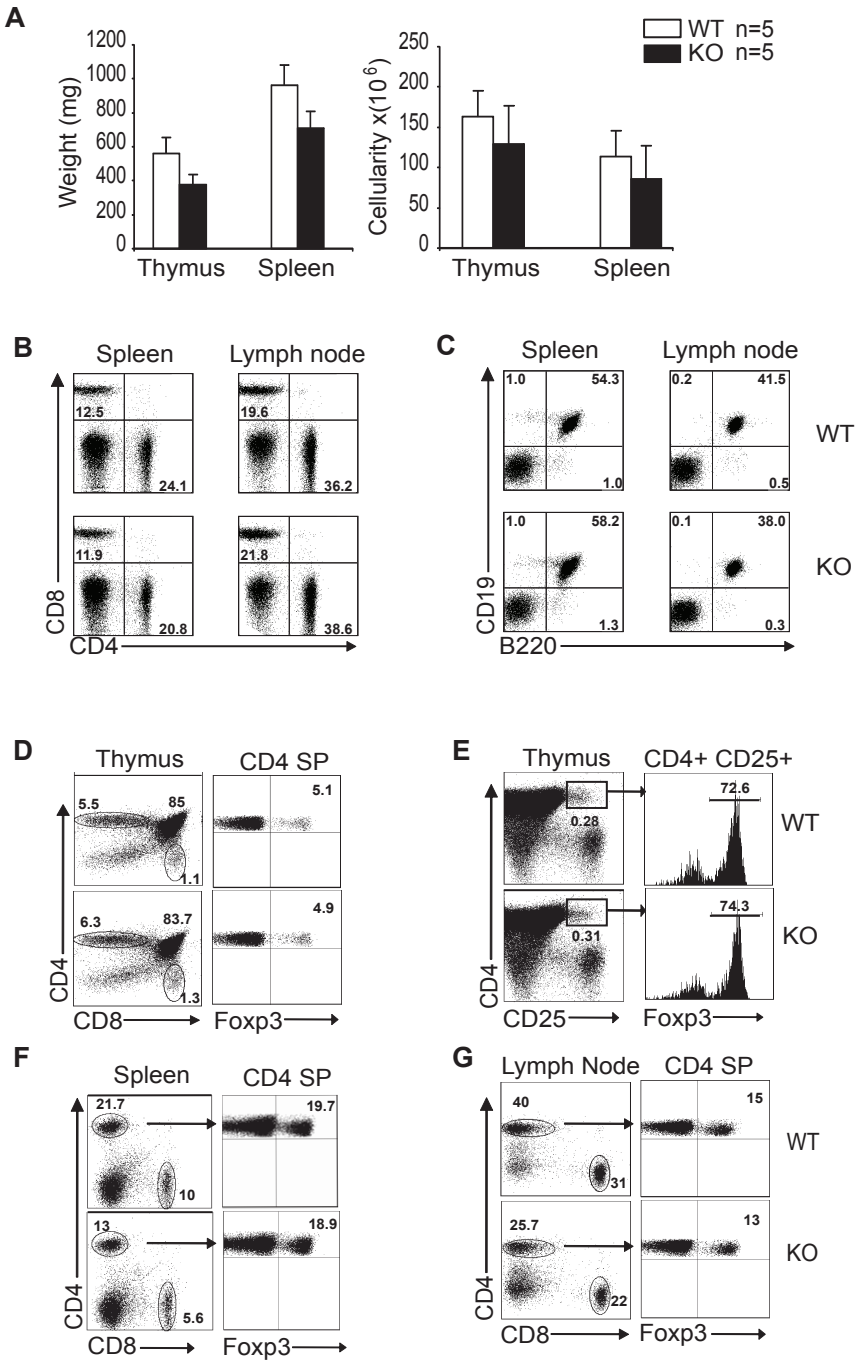

Figure 0.11

Figure 4.

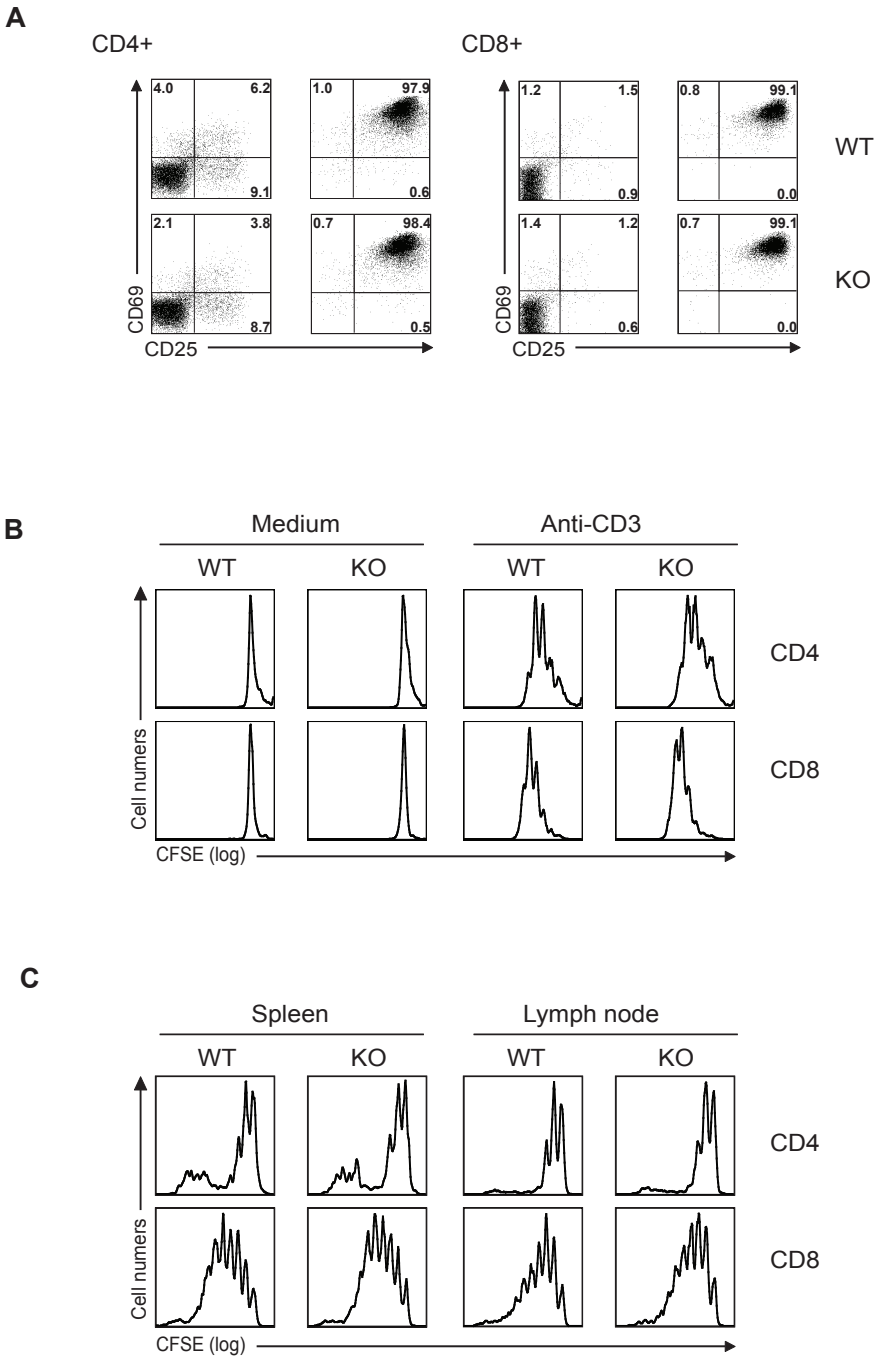

Figure 0.12

Figure 5.

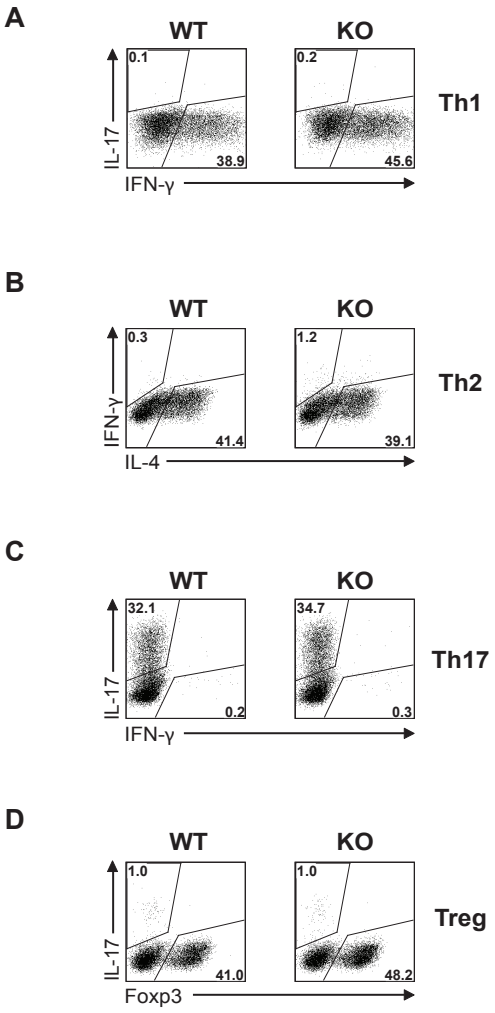

Figure 0.13

Figure 6.

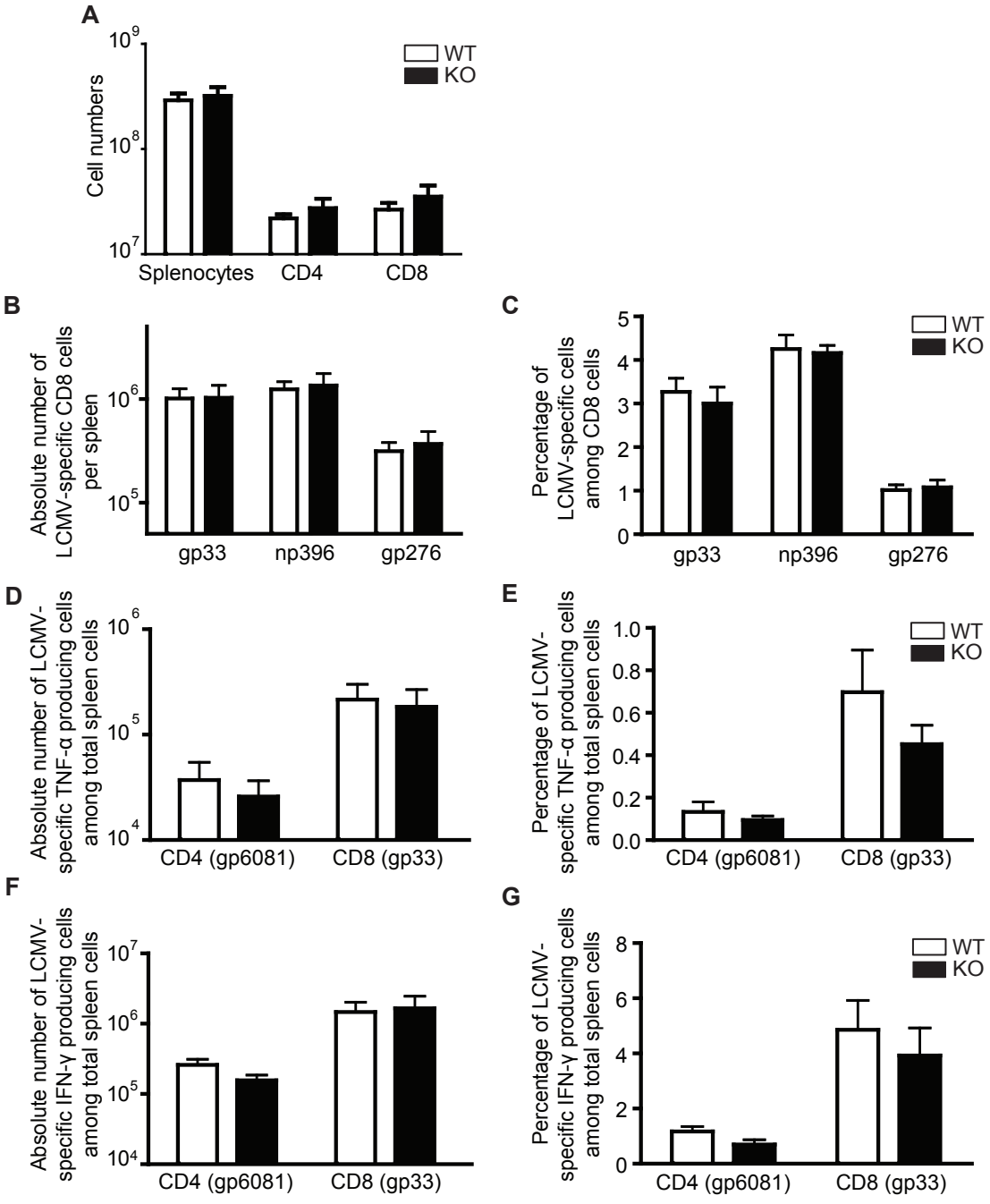

Figure 0.14

Figure 7.

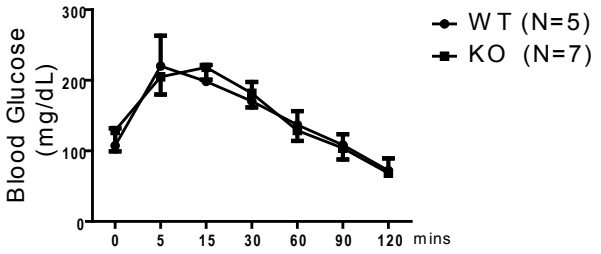

Figure 0.15

Figure 8.